Öppen

Report

Document ID	Version	Status	Reg no	Page
1439722	1.0	Godkänt		1 (186)
Author Jan Hernelind/5T Engineering AB			Date 2014-10-15	
Reviewed by			Reviewed date	
Approved by Jan Sarnet			Approved date 2014-11-24	

Detailed models for BWR-canisters for Earthquake induced rock shearing

Abstract

A number of analyses of earthquake induced rock shearing, based on detailed geometry descriptions of BWR inserts have been performed. The purpose was to obtain material for responses to questions posed by SSM in their review of SKB's licence application for a final repository for spent nuclear fuel at Forsmark. The shearing planes used in these analyses are located either at ¾ distances from the insert base or at the insert lid at the top of the insert. The obtained results show rather small differences in comparison to results from previous analyses which were based on a simplified geometry (Hernelind 2010).

Sammanfattning

Ett antal analyser av jordbävningsexiterad bergskjuvning har utförts med en detaljerad geometribeskrivning för BWR-insatser. Avsikten var att erhålla underlag för att besvara frågor ställda av SSM i deras granskning av SKB:s licensansökan för slutligt förvar av förbrukat kärnbränsle i Forsmark. Skjuvplanen som använts i dessa analyser är belägna vid ¾-avståndet från insatsens botten eller vid insatsens stållock vid toppen av insatsen. Resultaten visar relativt små skillnader mot de tidigare analyserna som baserades på en betydligt mer förenklad geometri (Hernelind 2010).

Svensk Kärnbränslehantering AB
Swedish Nuclear Fuel and Waste Management Co
PO Box 250, SE-101 24 Stockholm
Visiting address Blekholmstorget 30
Phone +46-8-459 84 00 Fax +46-8-579 386 10
www.skb.se
556175-2014 Seat Stockholm

Contents

1 Introduction and simulation strategy

1.1 Introduction

According to the design premises set out by SKB, see Table 1-1 (SKB 2010), the copper corrosion barrier should remain intact after a 5 cm shear movement at a velocity of 1 m/s for buffer material properties of a Ca-bentonite with saturated density of 2,050 kg/m^3, for all locations and angles of the shearing fracture in the deposition hole, and for temperatures down to 0°C. The insert should maintain its pressure-bearing properties to isostatic loads.

One important function of the buffer material in a deposition hole in a KBS-3 repository for spent nuclear fuel is to reduce the impact of rock movements on the canister. A severe case of rock movement is a fast, earthquake-induced shear that takes place along a fracture intersecting a deposition hole. The consequences of such a rock shear movement have been investigated earlier, both by laboratory tests (Börgesson et al. 2004), laboratory simulations in the scale 1:10 and finite element modelling (Börgesson et al. 1995, 2004, Börgesson and Hernelind 2006). Those investigations were focussed on a base case with a horizontal shear plane and Na-bentonite as buffer material. Also the influence of the shear angle was studied with 45 and 22.5 degrees inclination between the shear plane and the canister.

A sequence of analyses has previously been performed for earthquake induced rock shear. The outcome of these analyses is described by Börgesson and Hernelind (2006). A final, deterministic sequence of analyses, were summarized in Hernelind (2010) where the buffer material properties are based on Ca-bentonite instead of Na-bentonite as Na-bentonite is expected to be converted to Ca-bentonite under repository conditions. In that study, also the copper shell, insert (nodular cast iron) and insert lid (steel) material properties were based on at the time available experimental results.

The horizontal shear plane at ¾-distance from the insert base was identified as the most severe shear plane position for the insert according to previous studies (Hernelind 2010). However, for the copper shell, as for the insert lid and the centre fixing screw, shearing at the insert lid is more severe.

Previous analyses of earthquake induced rock shearing (Hernelind 2010) were based on geometries with several simplifications such as:

- The insert lid was modelled without some of its details (valve, holes for mounting the valve and for the fixing screw).
- The insert lid was modelled without the centre fixing screw (instead the insert lid was tied to the insert at the periphery).
- The washer between the screw and insert lid was not modelled.
- The steel channel tubes were tied to the insert and modelled without support plates.
- The base plate of the insert was modelled without screws, nuts and support plates derived from the fixing during the casting process.

Previous analyses were also based on a construction with nominal dimensions and thus didn't study any effect of allowable tolerances. Also, the initial position of the steel channel tube was assumed to be centred in the nodular cast iron insert.

The aim with this study is to investigate if the above mentioned assumptions are reasonable and whether they have any significant influences on the stress/strain levels and the corresponding conclusions regarding damage tolerance analysis and mechanical integrity.

In the present work, the geometry definition for the BWR canister is created based on CAD-drawings with as few simplifications as possible.

This report thus presents results for:

- Shearing at the ¾-distance between canister base and top for the cases of
  - Centrically placed channel tubes
    - Without washer between screw and insert lid
  - Eccentrically placed channel tubes based on allowable tolerances
  - Steel channel tubes welded to steel support plates
  - Channel tubes rotated such that the distance between a corner and the outer radius has minimum distance in the shearing direction. This will imply loss of symmetry and thus requires a full model. One case with centric and one case with eccentric location of the channel tubes are studied.
- Shearing at the insert lid (specifically to study the behaviour of the insert lid when this is modelled with a screw instead of welded to the top of the insert).

The obtained results based on the more detailed geometry are then compared with the corresponding results from previous analyses (Hernelind 2010).

1.2 Simulation strategy

The performed simulations are based on the same geometry and meshes used in previous analyses (Hernelind 2010) for the buffer (bentonite), and the copper shell. The insert and channel tubes are defined by all details in the drawings for BWR inserts. The channel tubes are connected by support plates welded to the channel tubes. The support plates are welded to the cast iron insert which also applies to the base plates and base screws. Otherwise, the channel tubes are constrained by contact conditions. All screw heads are simplified to a cylindrical shape and a few extremely small holes are removed (these holes doesn't exist in reality and have been removed). The insert lid is fixed by a screw in the centre – previous analyses used a tied constrain between the outer face and the insert top. The buffer material is Ca-bentonite with density 2,050 kg/m^3 for all analyses.
The default model is defined without considering tolerances and two models are defined by moving the steel channels (channel tubes) as much as possible (10 mm) in radial direction due to allowed tolerances (SKB 2010) with different directions of the prescribed shearing.
Table 1-1 shows job-names for all analyses described in this report. The comment "initial pre-stress" means that the screw has an initial condition and especially for cases including the washer most of the pre-stress in the screw is lost during the first equilibrium iteration. The comment "final pre-stress" means that the pre-stress in the screw is achieved after the first equilibrium iteration.

Table 1-1. Definition of simulation cases.

Case	Shear plane location	Comment
bwr_eccentric_lock	75%	Without considering tolerances.
bwr_eccentric_1	75%	The steel channels have been eccentrically positioned 20 mm (SKBdoc 1415152).
bwr_excentric_half	75%	The steel channels have been eccentrically positioned due to tolerances such as minimum distance occurs where the axial stress is in tension.
bwr_eccentric_lock	Insert lid	The steel channels have been positioned due to tolerances.
bwr_centric_rotated	75%	Full model where the cassettes are rotated having minimum distance between channel corner and insert outer radius
bwr_excentric_rotated	75%	Full model where the cassettes are rotated having minimum distance between channel corner and insert outer radius.
model6g_normal_quarter_2050ca3	75%	Previous BWR model - reference model (Hernelind 2010).

2 Meshes

The geometry used for the earthquake induced rock shear consists of the insert (made of nodular cast iron), the insert lid (made of steel) and the copper shell surrounded by buffer material (Ca-bentonite, density 2,050 kg/m^3). The geometry is based on CAD-geometries received from SKB, "Ritningsförteckning för kapselkomponenter" (SKBdoc 1203875, ver 1 for the reference model and ver 2 for the new detailed model) and should therefore correspond to the current design.

Due to symmetry only one half has been modelled. The mesh is then generated by 3-dimensional solid elements, mainly 8-noded hexahedral (most of them using full integration technique) and a few 6-noded wedge elements.

The model size is defined by about 126,000 elements and 160,000 nodes (total number of variables about 650,000).

When the channel tubes are rotated to have minimum distance between a channel tube corner and the outer radius of the insert the symmetry is lost and these cases require a full model and the model size increases to about 1,000,000 elements and 1,500,000 nodes (total number of variables is about 3,300,000).

The buffer has been partitioned at two different positions defining the rock shear perpendicular to the axis of the canister at the top of the insert lid and at ¾-distance from the insert base, Fig 2-1. Fig 2-2 shows details of the mesh at the top corner, Fig 2-3 details when the washer is included and finally Fig 2-4 shows details at the base.

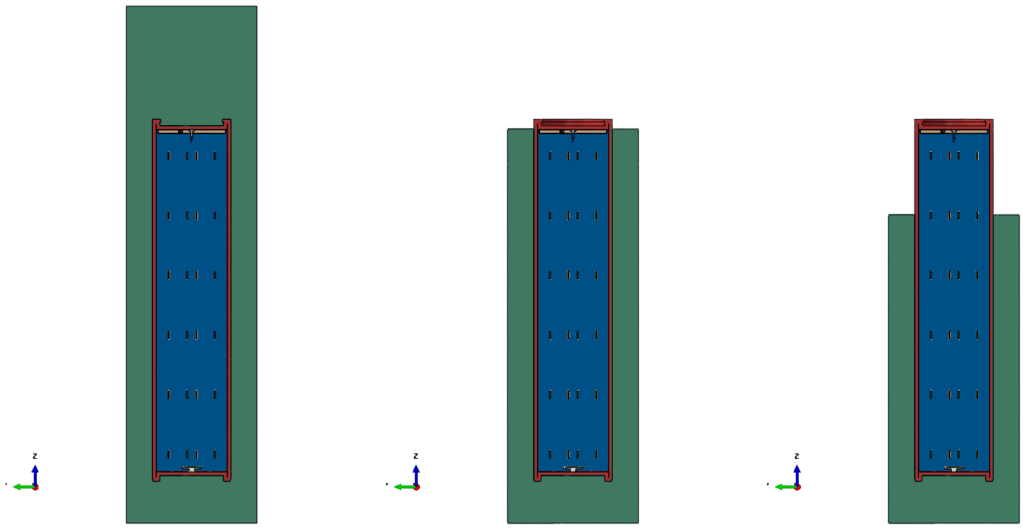

Figure 2-1. *From left to right plot of geometry for rock shear perpendicular to axis of canister, shearing plane at the insert lid and shearing plane at ¾-distance from the insert base.*

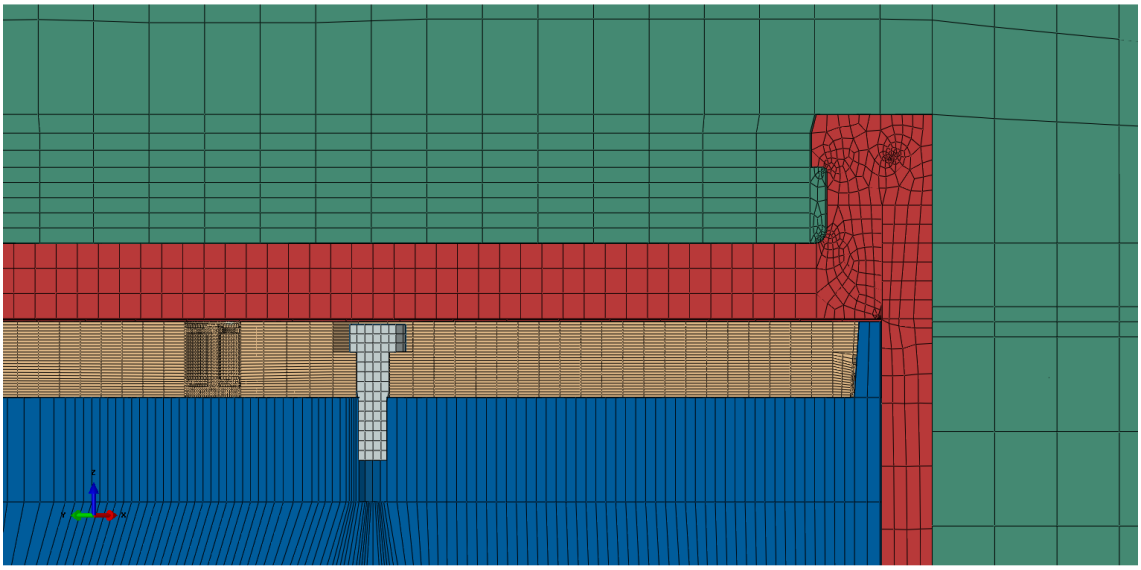

Figure 2-2. *Detail of upper corner showing bentonite (green), copper shell (red), insert lid (brown), inserts (blue) and screw (white).*

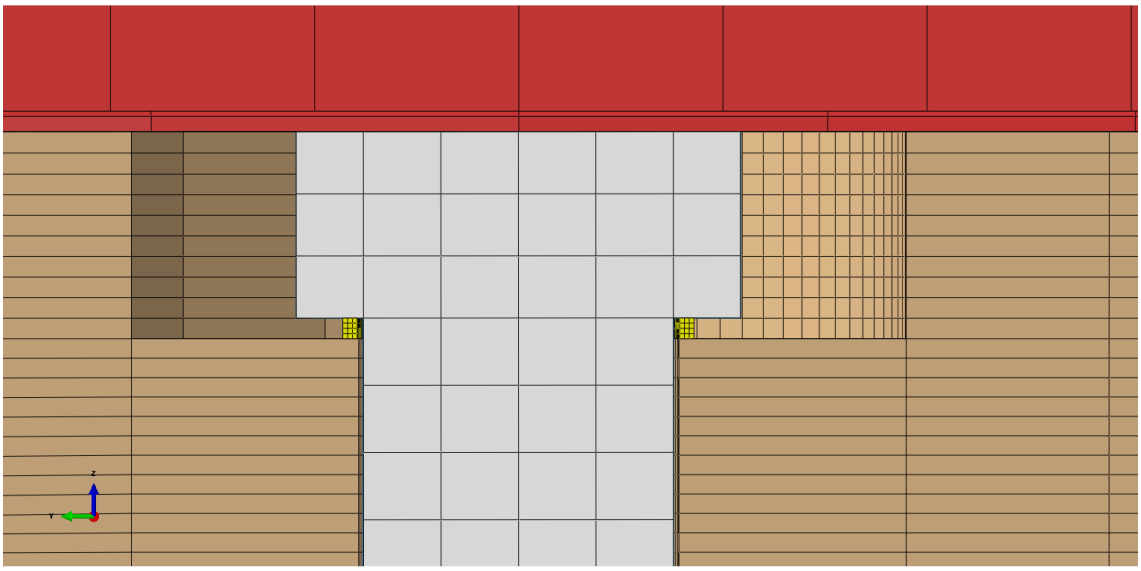

Figure 2-3. *Detail of screw (white) and washer (yellow) with copper shell (red), insert lid (brown).*

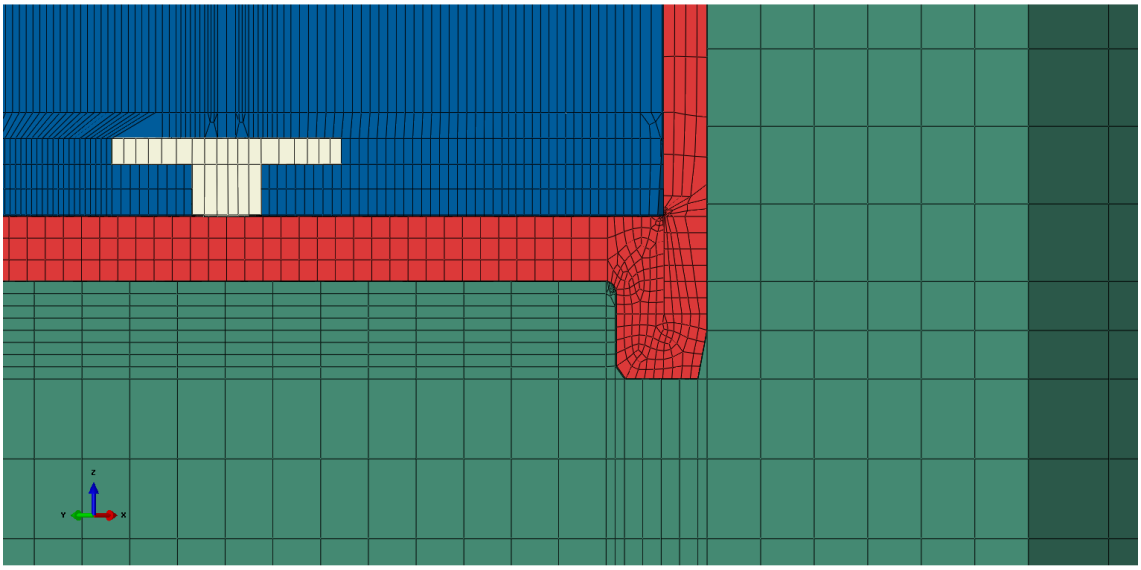

Figure 2-4. *Detail of base showing bentonite (green), copper shell (red), insert (blue) and steel channel screw (white).*

3 Geometry of parts

3.1 Deposition hole

The model of the deposition hole has a diameter of 1.75 m and a length of 6.9 m. The canister is placed about 0.5 m above the base and about 1.5 m below the top of the deposition hole. Buffer material (bentonite) surrounds the canister and will fill out the deposition hole. The rock shear is then simulated by prescribing boundary conditions at the buffer envelope.

3.2 Buffer (Ca-bentonite, density 2,050 kg/m^3)

The buffer has same geometry and mesh as in previous analyses (except for cases where the symmetry is lost) and is modelled with 3D solids, see Fig. 3-1.

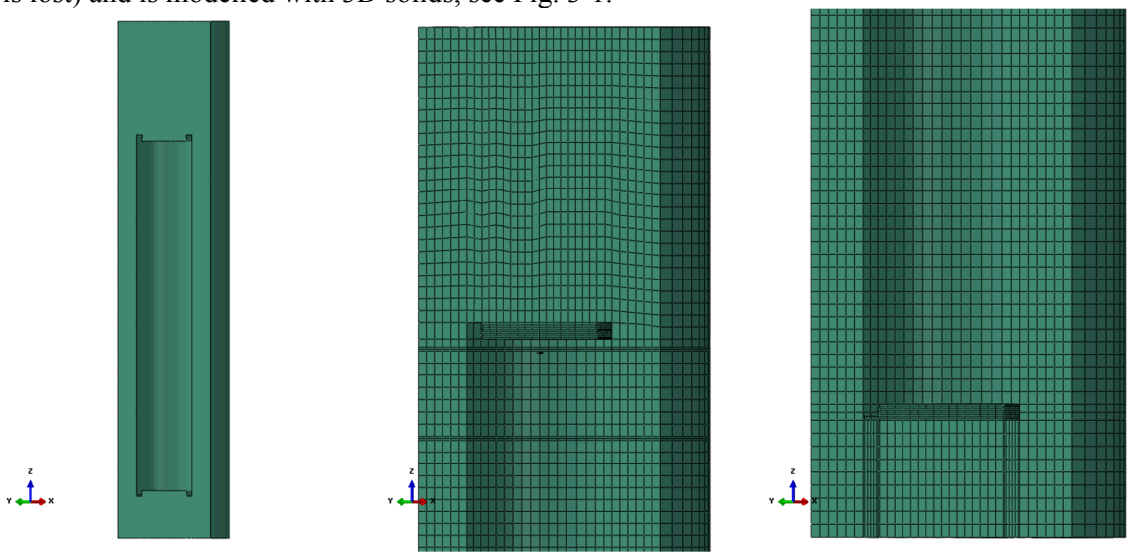

Figure 3-1. *Plot of buffer. Left – geometry, middle – mesh at the top, right – mesh at the base.*

3.3 Copper shell

The copper shell surrounds the insert and interacts with the buffer and the insert. The canister has been modelled rather accurately in order to catch “hot spots” where large strains and large strain gradients are expected, e.g. the fillets at the base and top (the copper lid). The lid is welded to the flange and will act as one part, see Figure 3-2.

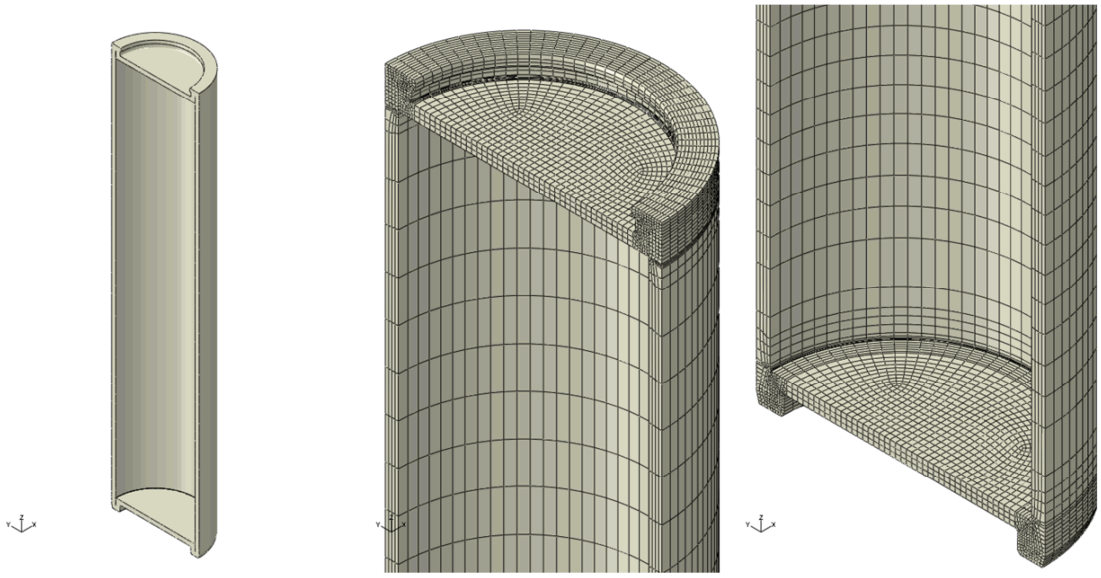

Figure 3-2. *Copper shell geometry (left), mesh top (mid) and mesh base (right).*

For cases not using symmetry the copper shell mesh has been slightly improved, see Figure 3-3.

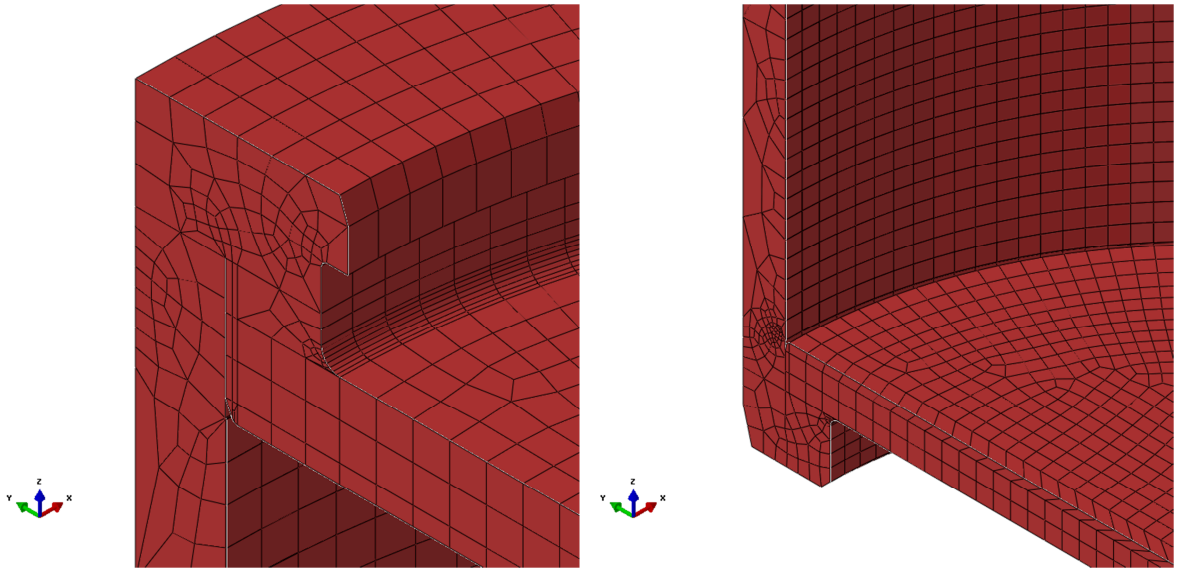

Figure 3-3. *Copper shell mesh for models without symmetry, top (left) and base (right).*

3.4 Insert (nodular cast iron)

The insert is made of nodular cast iron. The steel channel tubes with plates are placed inside the cast. One set-up is for BWR using nominal values and another where the tolerances have been included.

3.5 BWR-insert

The BWR-insert is modelled as a homogeneous part with 3D solids based on SKB drawings, see Figures 3-4 to 3-9 for models using symmetry. A few simplifications have been made:

- Screw head geometry is modified to a cylindrical shape.
- A few small cylindrical holes have been removed (these holes doesn't exist in reality and have been removed).
- Conical screw hole bottom modified to cylindrical shape.

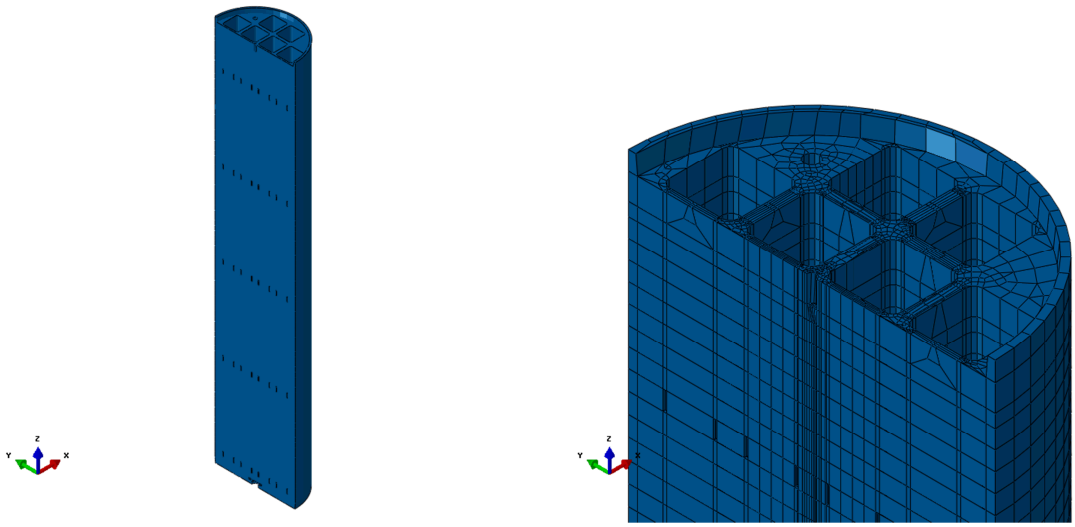

Figure 3-4. *Insert BWR geometry (left), and mesh (right) – top view.*

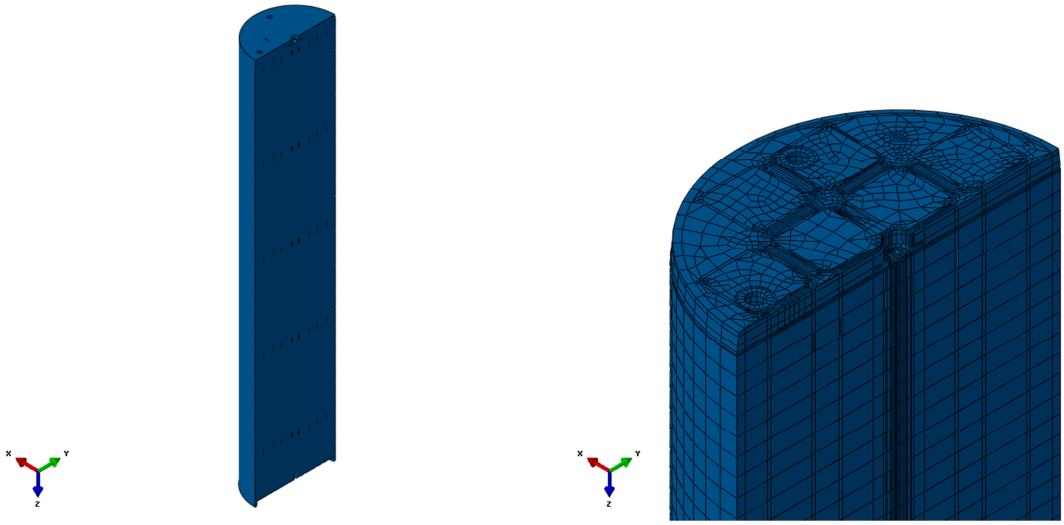

Figure 3-5. *Insert BWR geometry (left), and mesh (right) – base view.*

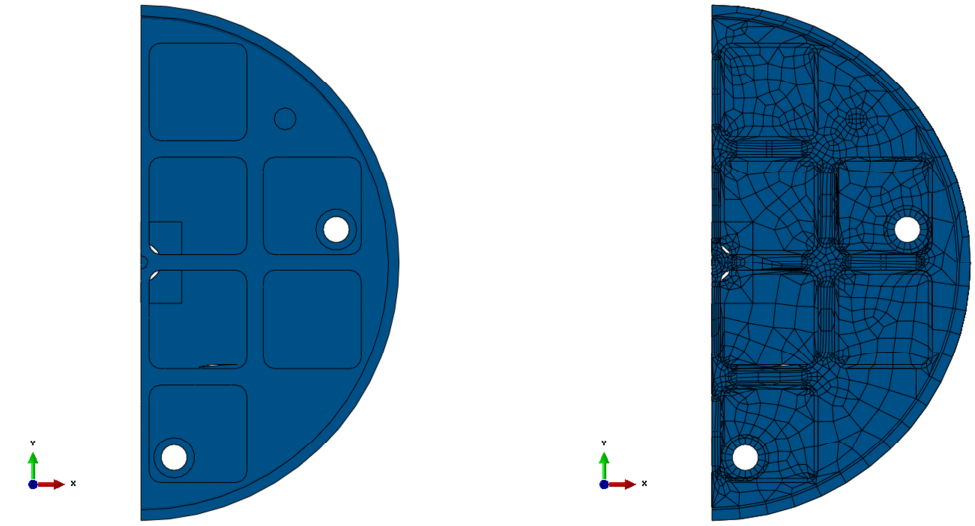

Figure 3-6. *Insert BWR geometry (left), and mesh (right) – top view. Symmetrically positioned channel tubes.*

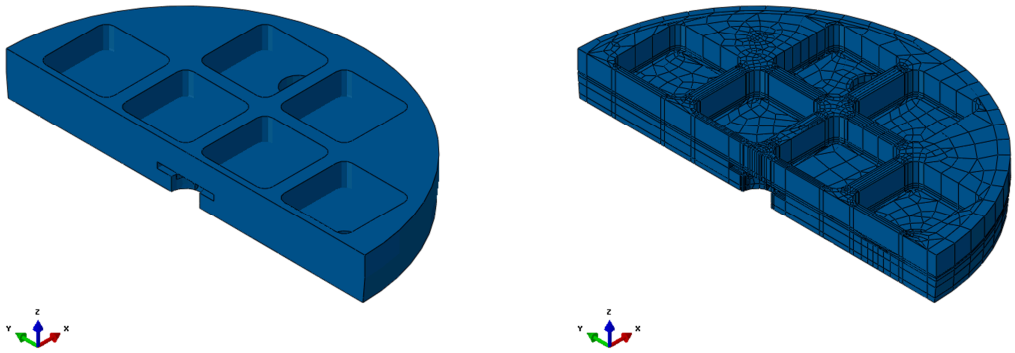

Figure 3-7. *Insert BWR geometry (left), and mesh (right) – base plate. Symmetrically positioned channel tubes.*

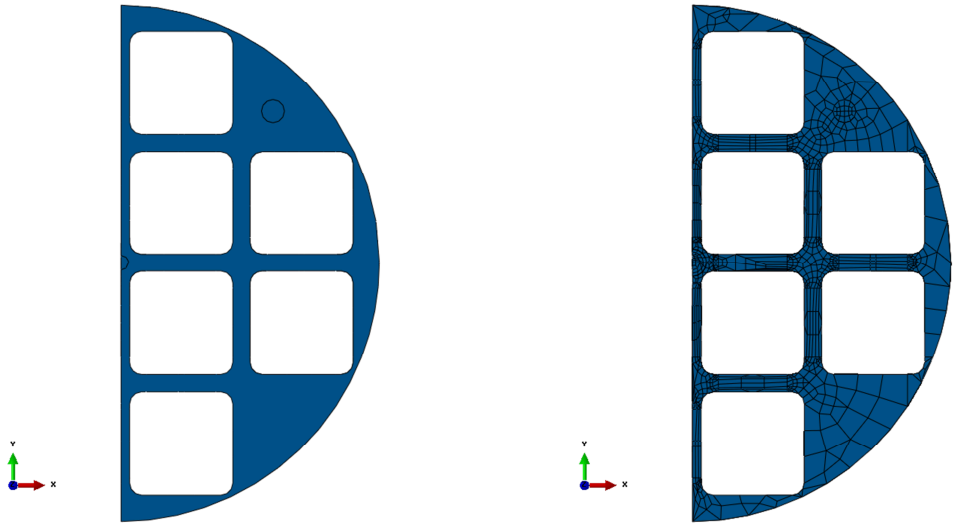

Figure 3-8. *Insert BWR geometry (left), and mesh (right) with centrically positioned channel tubes– top view showing the cross section.*

Figure 3-9 shows cases with eccentrically positioned channel tubes. One case with axial stress in compression in the neighbourhood of the corner having shortest distance to the insert outer radius (bwr_eccentric_1) and one case with axial stress in tension for the same region (bwr_excentric_half).

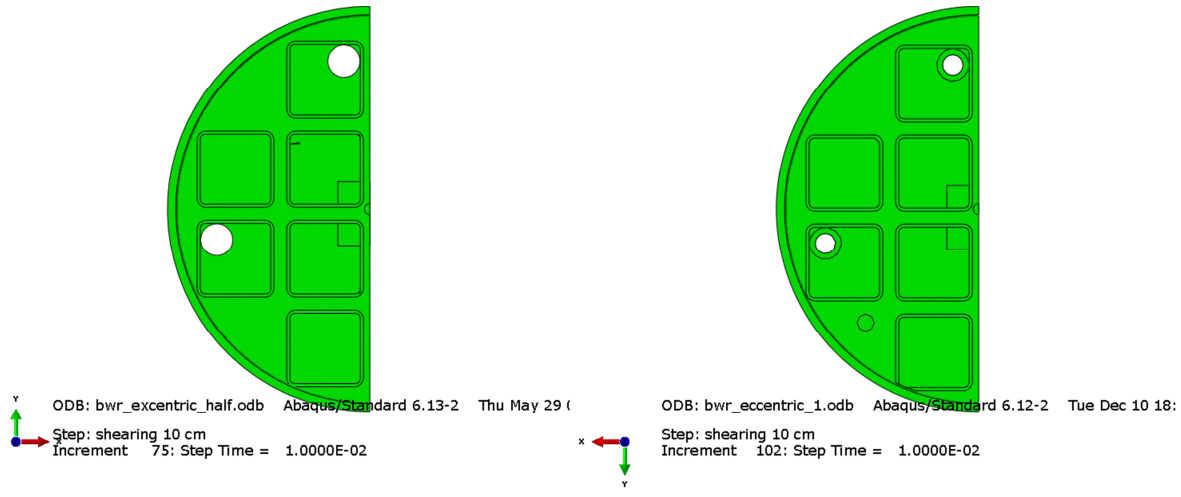

Figure 3-9. *Insert BWR geometry with eccentrically positioned channel tubes .Left plot with 10 mm eccentricity and right plot with 20 mm eccentricity (SKBdoc 1415152). Prescribed shearing in vertical direction.*

For models without symmetry (rotated channel tubes) the mesh has been improved, see Figures 3-10 – 3-12.

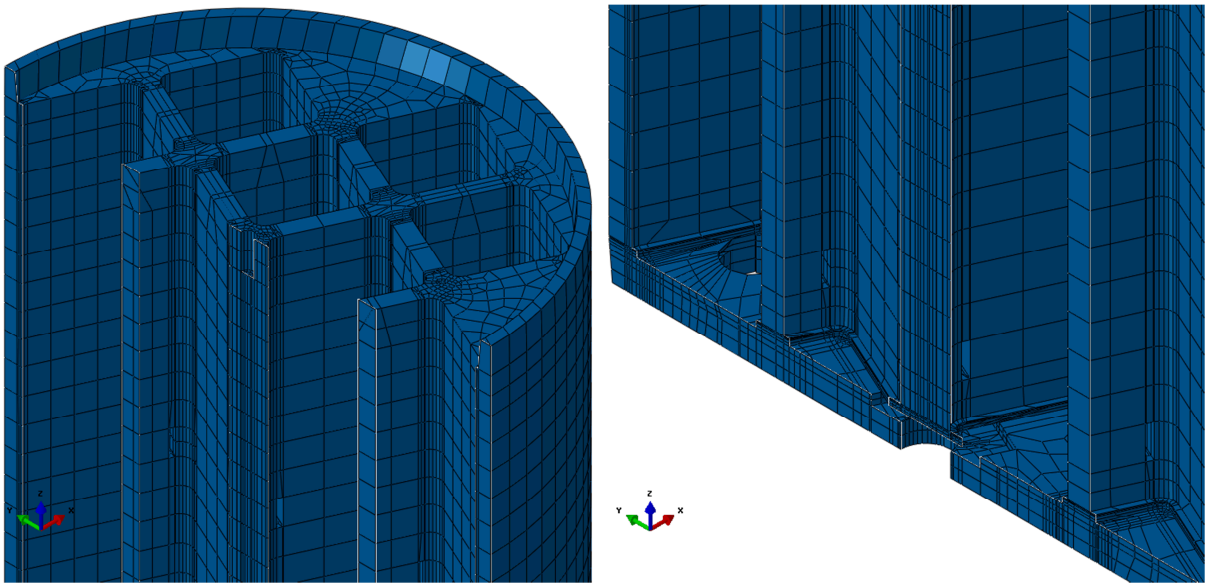

Figure 3-10. *Insert BWR mesh for cases without symmetry, top (right) and base (right).*

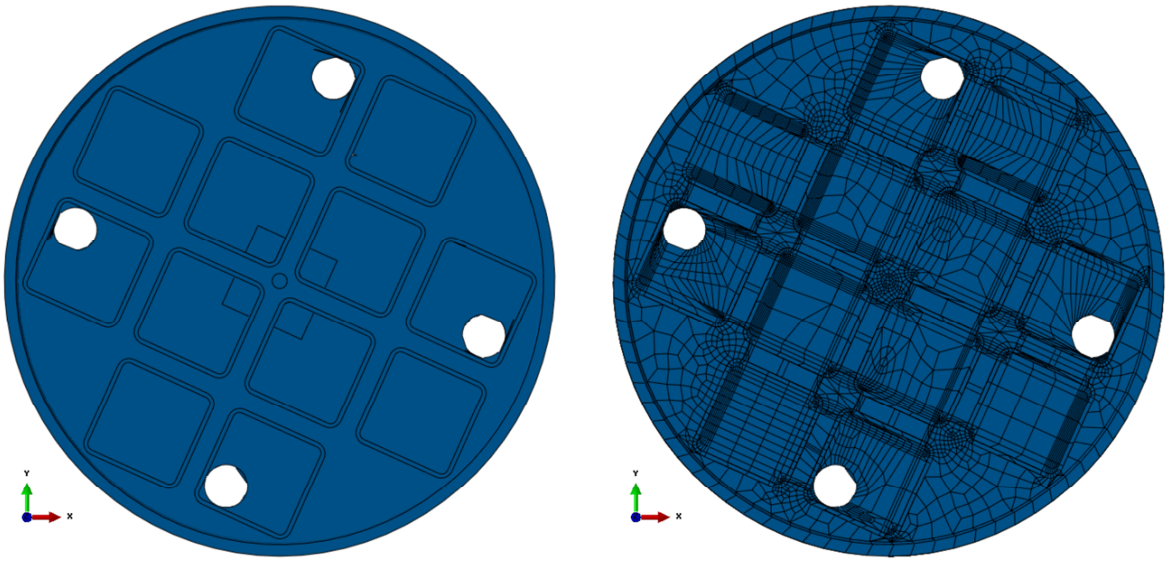

Figure 3-11. *Insert BWR geometry (left) and mesh (right) with rotated channel tubes– top view showing the cross section. Prescribed shearing in y-direction.*

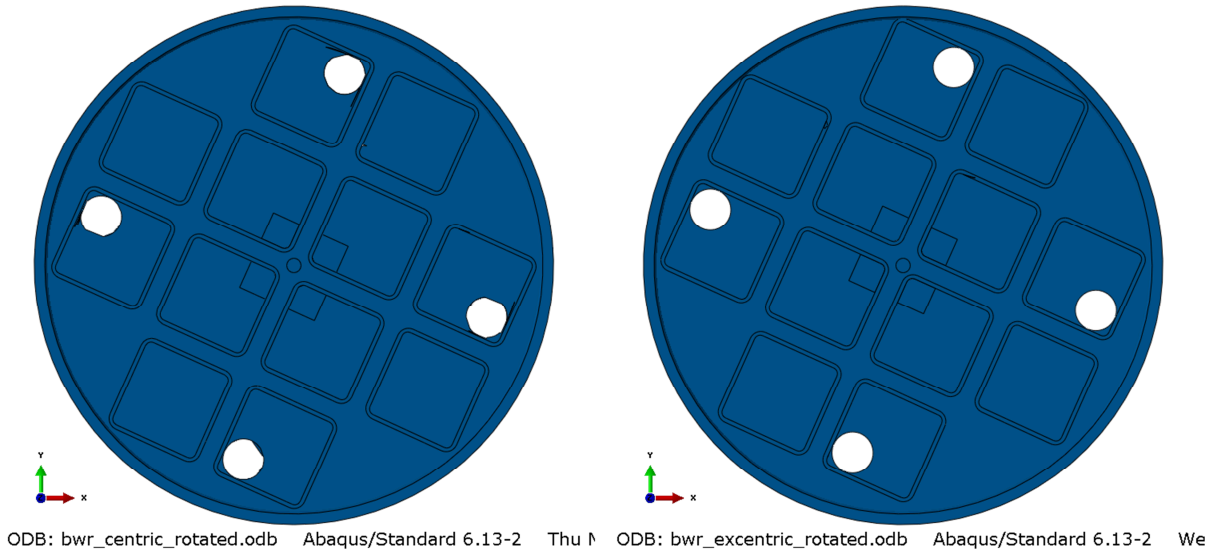

Figure 3-12. *Insert BWR geometry with symmetrically positioned channel tubes (left) and with eccentrically positioned channel tubes (right) – top view showing the cross section. Prescribed shearing in y-direction.*

3.6 Steel channel tubes (BWR)

The BWR steel channel tubes are connected by support plates which are tied to the insert (for models where the weld has not been modelled), see Figures 3-13 to 3-15.

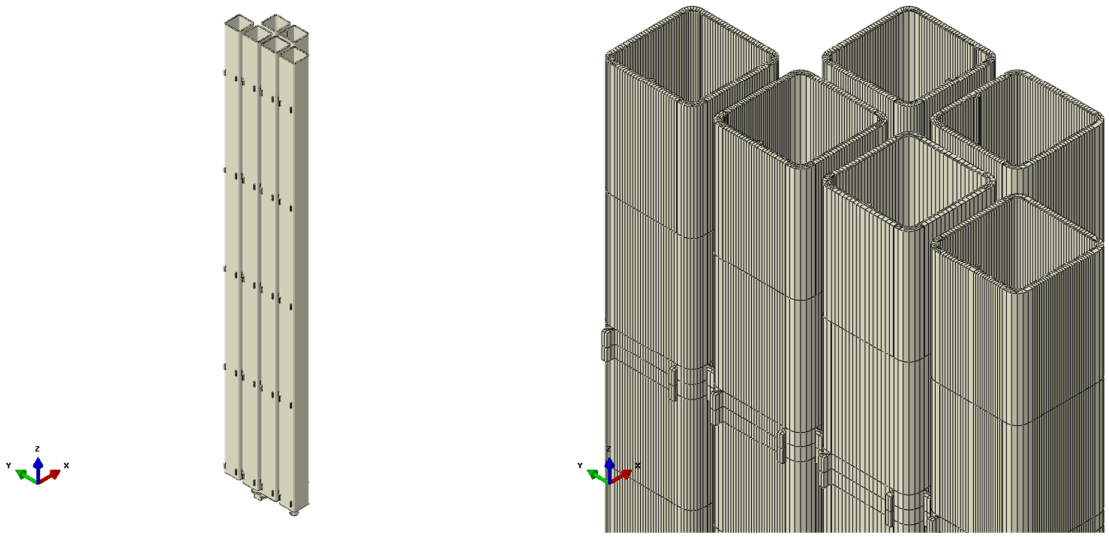

Figure 3-13. *Steel channel tubes geometry (left), and mesh (right) – top view. Symmetrically positioned channel tubes.*

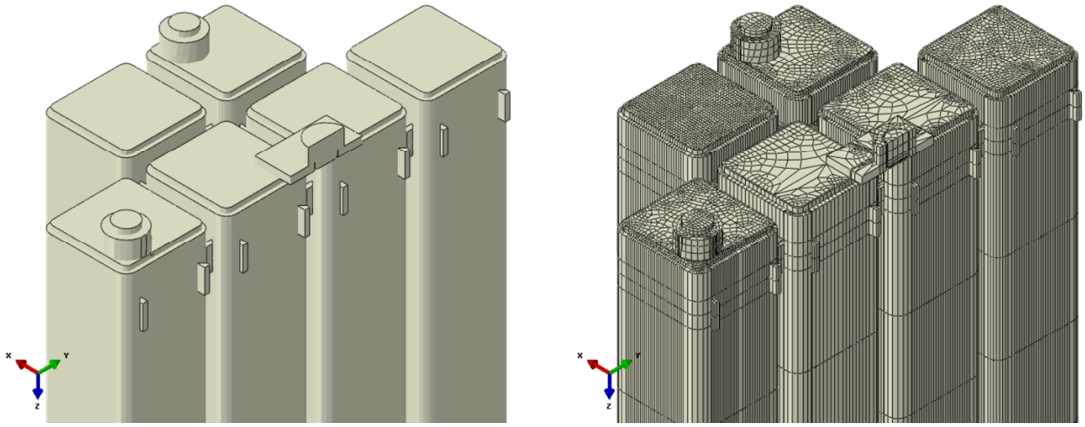

Figure 3-14. *Steel channel tubes geometry (left), and mesh (right) – base view. Symmetrically positioned channel tubes.*

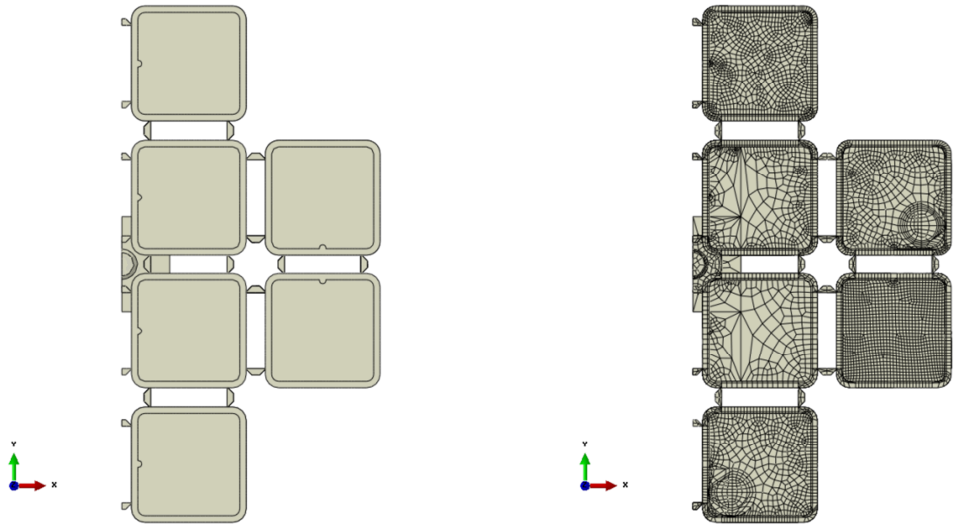

Figure 3-15. *Steel channel tubes geometry (left), and mesh (right) – base view showing also the support plates. Symmetrically positioned channel tubes.*

Figures 3-16 – 3-17 show cases with eccentrically positioned channel tubes. One case with axial stress in compression in the neighbourhood of the corner having shortest distance to the insert outer radius (bwr_eccentric_1, support plates without welds) and one case with axial stress in tension for the same region (bwr_excentric_half, support plates extended with welds).

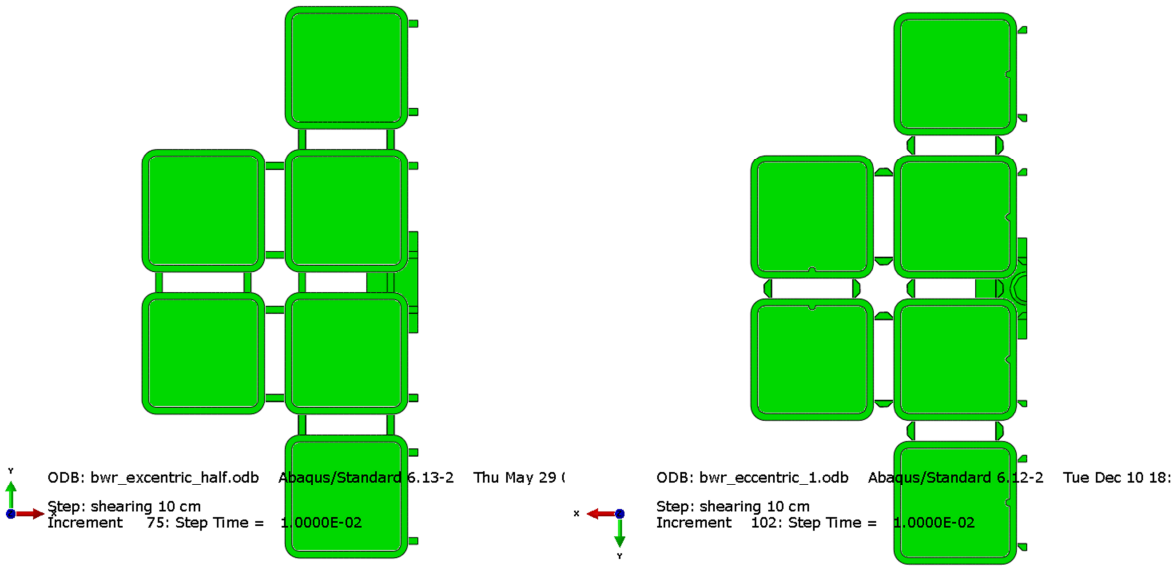

Figure 3-16. *Channel tubes geometry with eccentrically positioned channel tubes .Left plot with 10 mm eccentricity and right plot with 20 mm eccentricity (SKBdoc 1415152). Note how the support plates are modelled.*

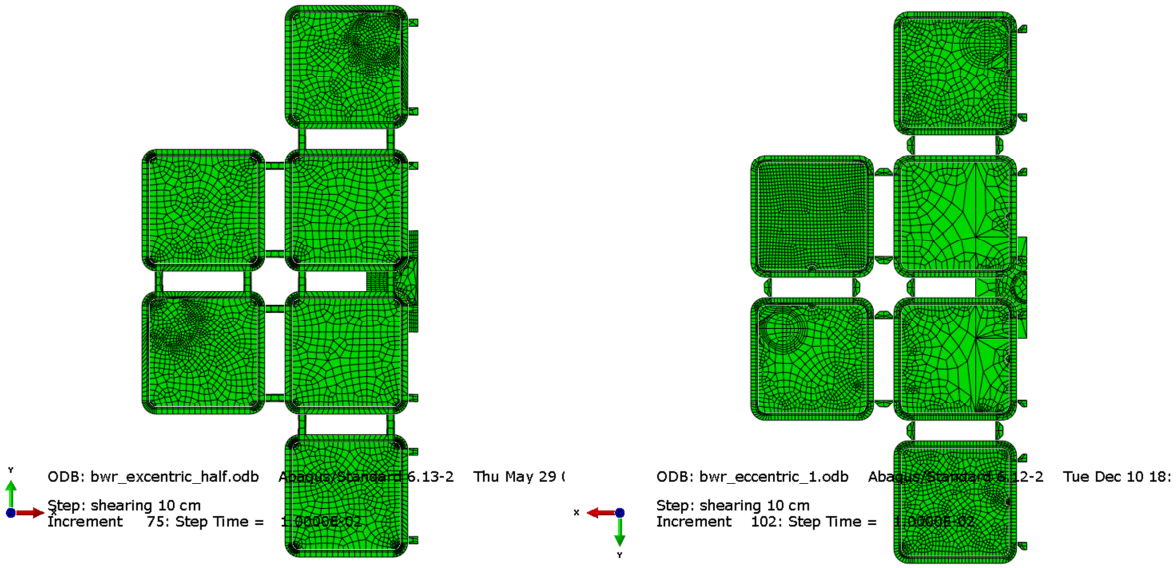

Figure 3-17. *Channel tubes geometry with eccentrically positioned channel tubes .Left plot with 10 mm eccentricity and right plot with 20 mm eccentricity (SKBdoc 1415152). Note how the support plates are modelled.*

For models without symmetry (rotated channel tubes) the mesh has been improved, see Figure 3-18 – 3-19. The welds for the support plates have been included by modifying the geometry for the plates, see Figure 3-20 where also the corner radius is shown.

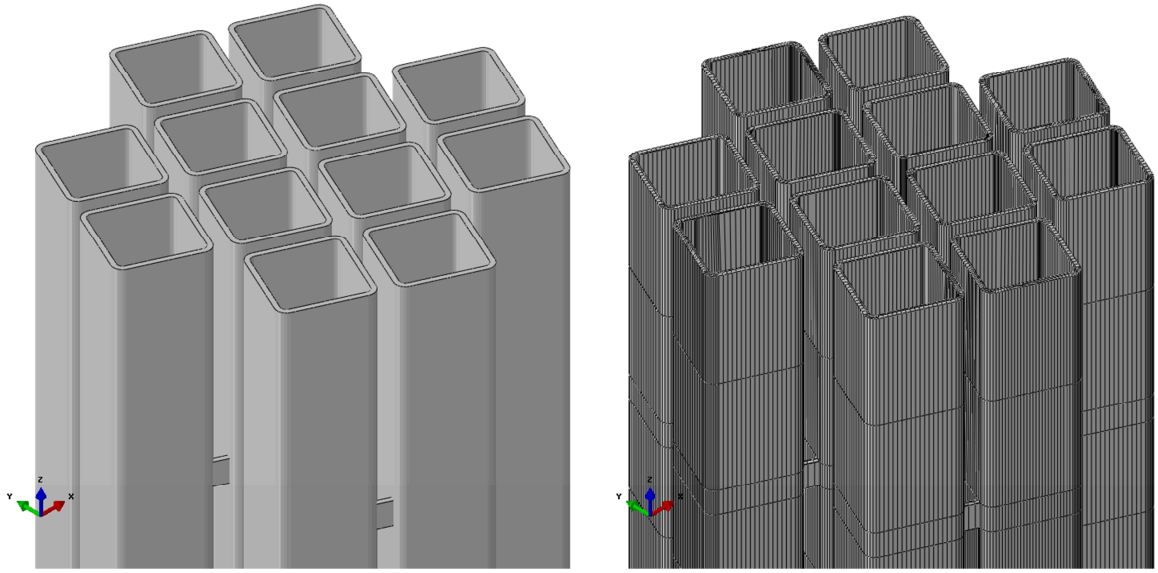

Figure 3-18. *Steel channel tubes geometry (left) and mesh (right).*

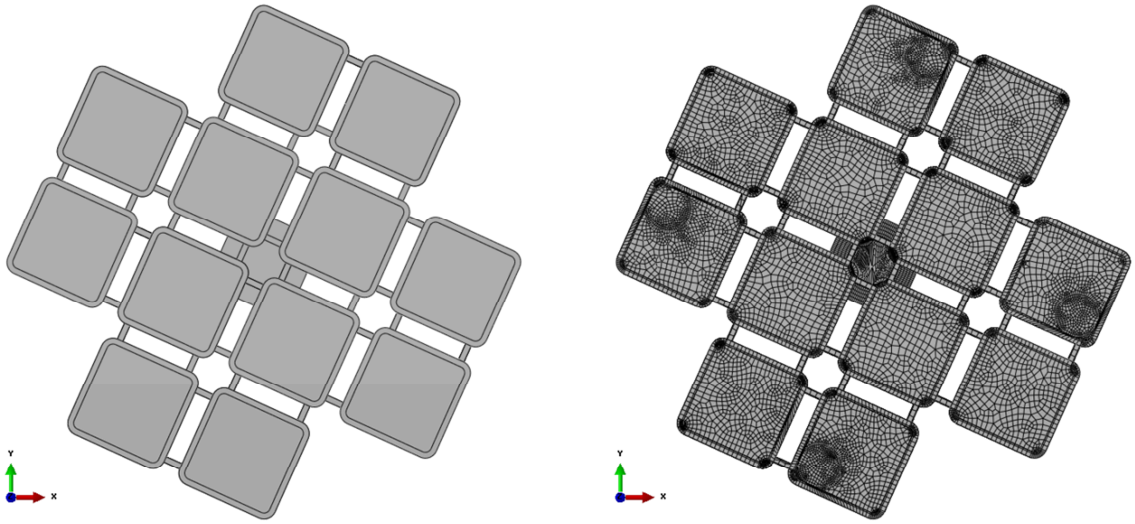

Figure 3-19. *Steel channel tubes geometry (left) and mesh (right) – top view showing also the support plates.*

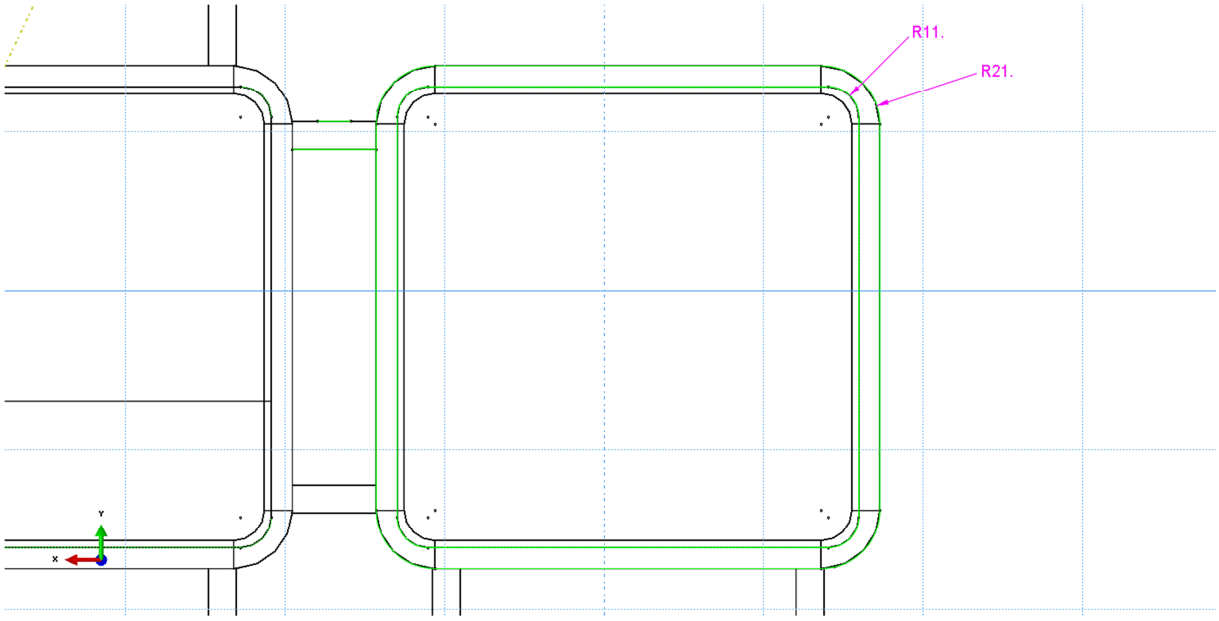

Figure 3-20. *Plot showing corner radius for the channel tubes. Also the modified geometry for the support plates with the weld are included could be noticed. Also note that the inner weld string from manufacturing of welded (shown at the CAD-drawing) tubes have been removed.*

3.7 Insert lid

The insert lid is made of steel and is modelled with 3D solids, see Figure 3-21. The surrounding gasket is not included which is assumed to have a minor effect on the stress distribution in the contact zone. Also a few details in the vent hole have been neglected since they hardly have any effect on the stiffness of the insert lid.

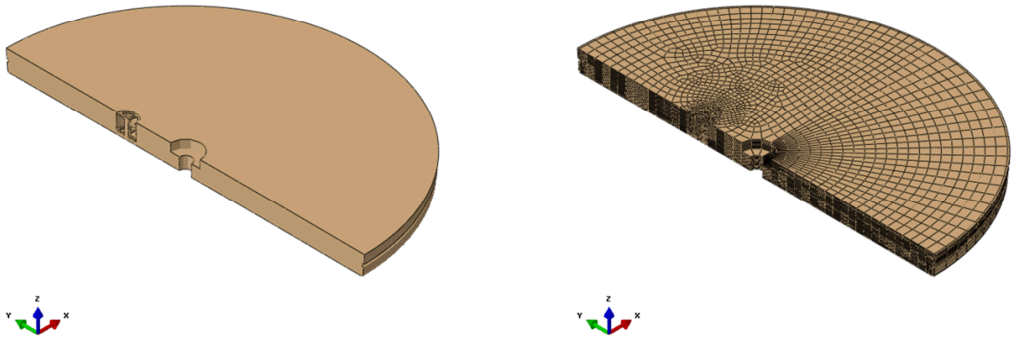

Figure 3-21. *Insert lid geometry (left) and mesh (right).*

For models without symmetry (rotated channel tubes) the mesh has been improved, see Figure 3-22.

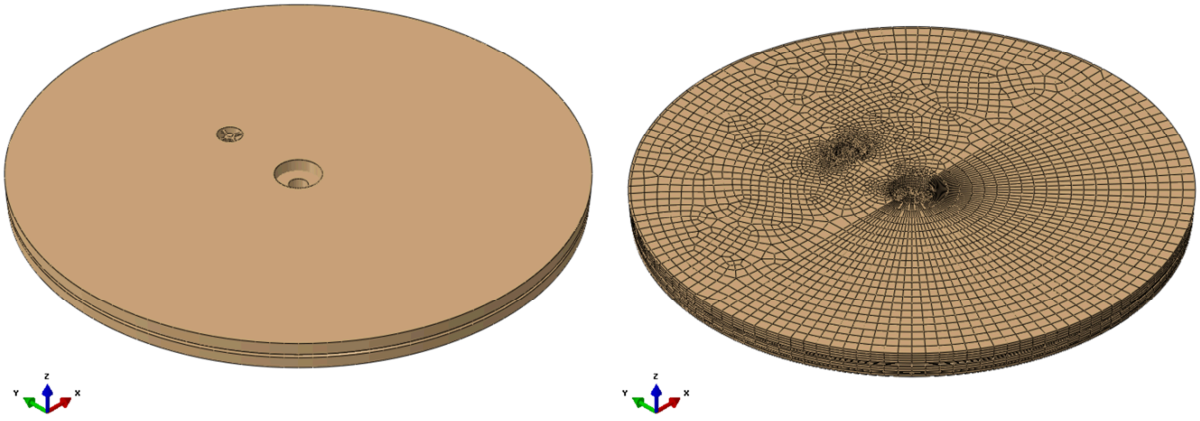

Figure 3-22. *Insert lid geometry (left) and mesh (right) for model s without symmetry.*

3.8 Washer

The washer is modelled with 3D solids, see Figure 3-23.

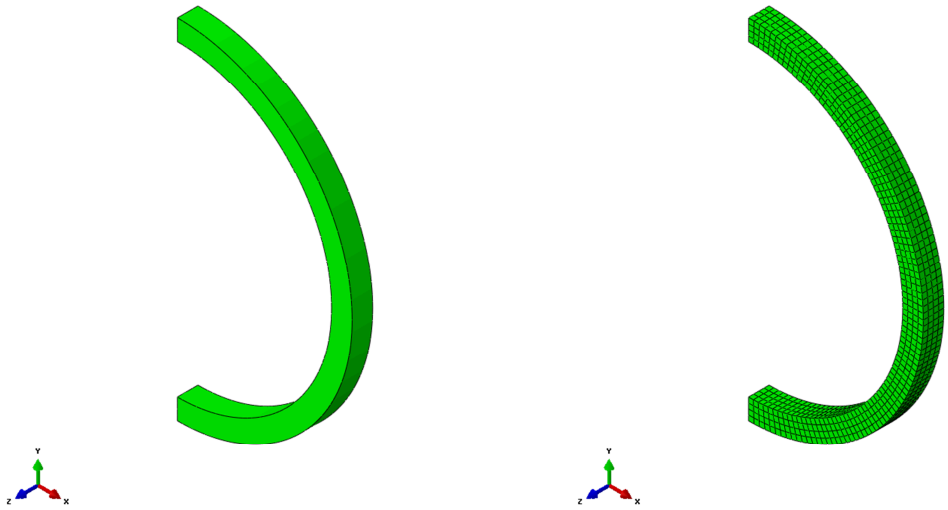

Figure 3-23. *Washer geometry (left), and mesh (right) – positioned between screw head and insert lid.*

3.9 Screw

The screw fixing the insert lid to the insert is modelled with 3D solids, see Figure 3-24.

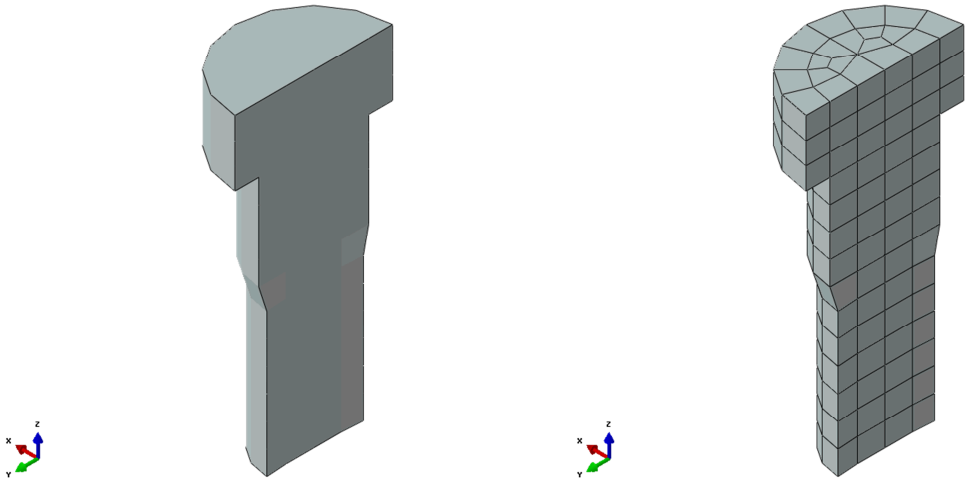

Figure 3-24. *Screw geometry (left), and mesh (right) – used to fix the insert lid to the insert.*

4 Material models

The finite element code ABAQUS version 6.12 (ABAQUS, 2013, Dassault Systèmes Simulia Corp.) was used for the calculations. The materials have been modelled as elastic-plastic with stress-strain properties that correspond to each material and the applied shear load induced strain rate, when applicable. The strains obtained from the simulations are below any necking and the material definitions thus cover the range of obtained results.

Note that in ABAQUS values outside the definition range will be constant with the last value defined.

4.1 Nodular cast iron (used by the insert)

The material model for the insert is based on a von Mises material model with elastic behaviour defined by Young's modulus and the Poisson's ratio and the plastic behaviour defined through yield surface (true stress) versus plastic strain (defined as logarithmic strain), see Table 4-1 and Figure 4-1 "Dragprovning av gjutjärn" (SKBdoc 1201865).

Data is available up to 15% plastic equivalent strain which covers the range of obtained results for the performed analyses.

The experiments were performed at 0^{o} C.

Table 4-1. True stress-true strain definition for BWR-insert.

Plastic strain (%)	Stress (MPa)			
	Strain rate=0	Strain rate=2×10^{-4}	Strain rate=0.5	Strain rate factor at strain rate=0.5
0	293	293	348	1.19
1	324	324	367	1.13
2	349	349	385	1.10
3	370	370	406	1.10
4	389	389	423	1.09
5	404	404	438	1.09
6	418	418	451	1.08
7	428	428	464	1.08
8	438	438	474	1.08
9	447	447	483	1.08
10	456	456	490	1.07
11	465	465	498	1.07
12	472	472	504	1.07
13	478	478	510	1.07
14	484	484	516	1.07
15	488	488	520	1.07

The strain rate dependency is defined by assuming that the yield surface is proportional to the strain rate factor (at the strain rate 0.5 1/s the factor 1.08 has been chosen and at strain rate 0 1/s the factor is 1.0).The instantaneous strain rate factor is then linearly interpolated between 1 and 1.08 using the instantaneous strain rate.

Furthermore, Young's modulus E = 166 GPa and Poisson's ratio $\nu = 0.32$ (Raiko et al. 2010).

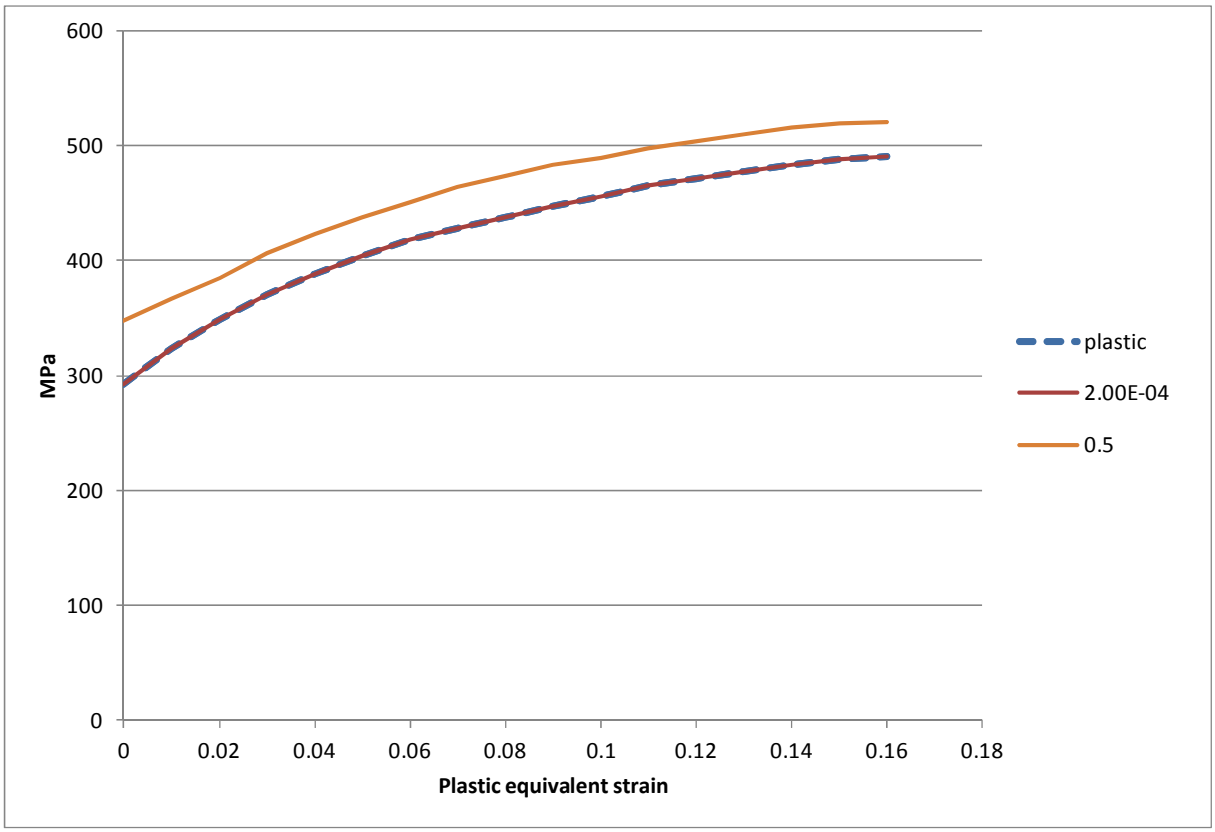

Figure 4-1. *Insert yield surface (nodular cast iron), true stress, [MPa] versus logarithmic plastic equivalent strain for different plastic strain rates. Note that the base (plastic) is defined to coincide with strain rate=2×10^{-4} [1/s].*

4.2 Steel (used by the channel tubes in the insert)

The material model for the channel tubes in the insert is based on a von Mises material model with elastic behaviour defined by Young's modulus and the Poisson's ratio. The plastic behaviour is defined through yield surface (true stress) versus plastic strain (using logarithmic strain).

The steel channel tubes are manufactured by steel S355J2H, for example Domex 355 MC B. SKB has earlier supplied test data for the yield point of their material, however no stress-strain data to be used in a plastic analysis. The stress-strain curve for Domex 355 MC B (SSABDirect 2008) can be scaled using the yield stress and tensile ultimate strength measured by SKB, *Re* = 412 MPa (yield stress) and *Rm* = 511MPa (ultimate stress). With this procedure a simplified stress-strain curve is obtained and described by Table 4-2 and Figure 4-2.

Table 4-2. Stress-strain definition for channel tubes used in the insert.

Strain (%)	Stress (MPa)	Log Strain (%)	True Stress (MPa)	Plastic equivalent strain (%)
0	0	0	0	0
0.196	412	0.196	412	0
15	509	14.3	587	14.0
20	511	18.5	613	18.2

Furthermore, Young's modulus E = 210 GPa and Poisson's ratio ν = 0.3 according to Raiko et al.(2010, Table 4-3).

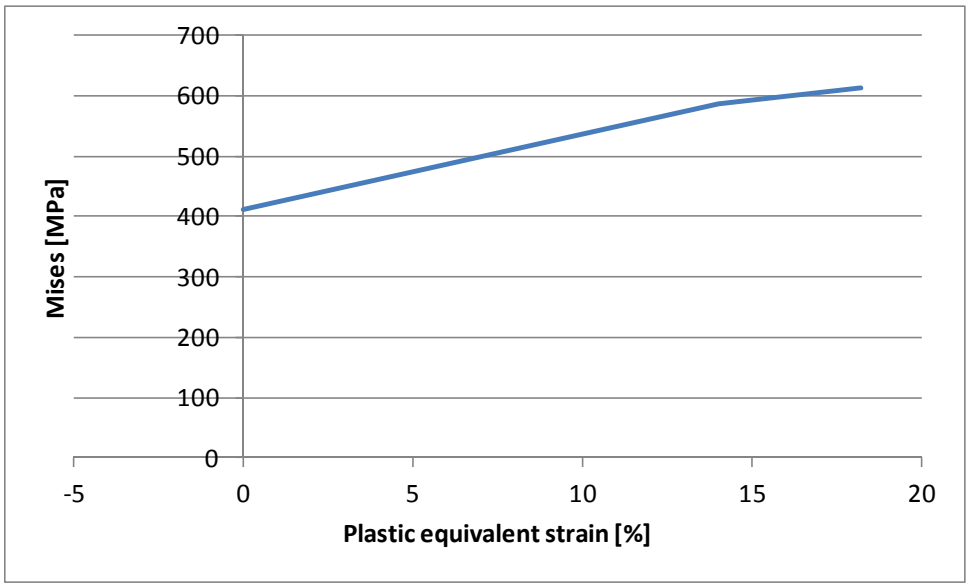

Figure 4-2. *Channel tube yield surface, true stress [MPa], as a function of the logarithmic plastic equivalent strain.*

The data with lowest value from the experiment has been chosen for the yield surface. However, the plasticity definition for the steel channel tubes has very minor influence on the overall results. Furthermore the obtained results from the performed analyses are within the range for available material data.

4.3 Steel (used by the insert lid, support plates, bottom plates and screws)

The material model for the insert lid is based on a von Mises material model with elastic behaviour defined by Young's modulus and the Poisson's ratio. The plastic behaviour is defined through yield surface (true stress) versus plastic strain (calculated as logarithmic strain).

Manufacturing drawings for the lid specify steel S355J2G3. Strain versus stress for steel Domex 355 MC B with *Re* = 389 MPa (yield stress) and *Rm* = 484 MPa (ultimate stress) can be found from SSABDirekt (2008). According to SS-EN 10025-2:2004, the material S355 with nominal thickness 40-63 mm has *Re* = 335 MPa (yield stress) and *Rm* = 470-630 MPa (ultimate stress). Scaling stress-strain curves for Domex 355 by the minimum values given in SS-EN 10025-2:2004 implies the simplified material definition (engineering data) shown in Table 4-3 and Figure 4-3.

Table 4-3. Stress-strain definition for the insert lid.

Strain (%)	Stress (MPa)	Log Strain (%)	True Stress (MPa)	Plastic equivalent strain (%)
0	0	0	0	0
0.1595	335	0.1593	335	0
15	470	13.98	540	13.7
20	470	18.2	564	17.9

Furthermore, Young's modulus E = 210 GPa and Poisson's ratio ν = 0.3 according to Raiko et al. (2010, Table 4-3).

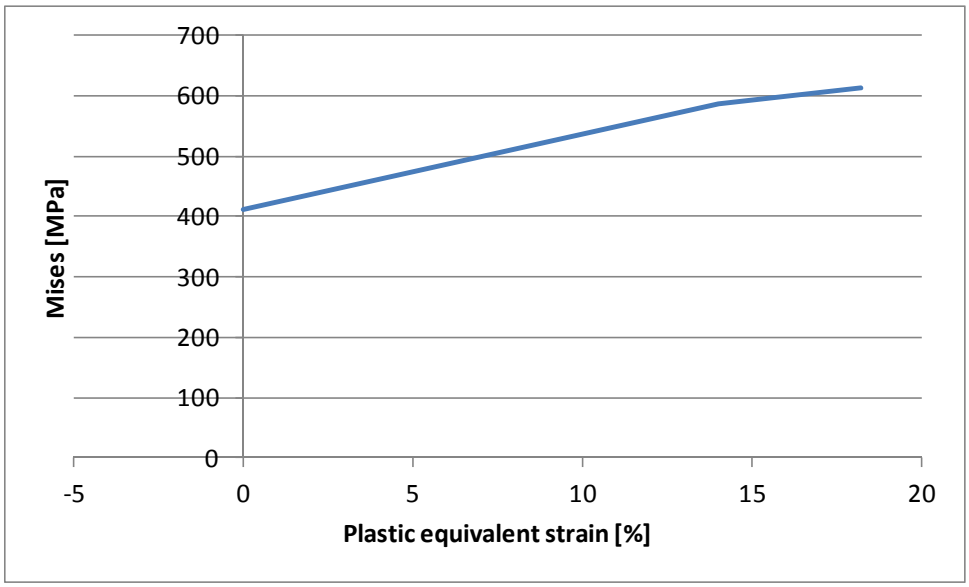

Figure 4-3. *Insert lid yield surface, true stress [MPa], as a function of the logarithmic plastic equivalent strain.*

The data with lowest value from the experiments (SS-EN 10025-2:2004) has been chosen for the yield surface. However, the plasticity definition for the insert lid has very minor influence on the overall results. Furthermore, the obtained results are within the range of available material data.

4.4 Bentonite model (used for the buffer)

The bentonite is modelled based on recent experiments, see Börgesson et al. (2010) and adapted to the actual density of the bentonite. The bentonite buffer is modelled using only total stresses that do not include the pore water pressure, the reason being the very fast compression and shear.

Two types of material models have been used in previous calculations. In the first calculations (Börgesson 1988) a total stress model that did not consider the pore water pressure was applied. In the later calculations (Börgesson 1992) the effective stress concept was applied. According to the effective stress concept the effective stress (the total stress minus the pore water pressure) is controlling the stress strain behaviour of a soil. A general experience regarding clays, which also is valid for swelling clays, is that the total stress concept is applicable for fast or undrained conditions while the effective stress is necessary to apply at drained processes that take place over longer times. The difference is mainly that the effective stress theory is required when there is time enough for the pore water to move in the clay and thus change the state of the clay.

The experience from the previous calculations was that the total stress approach, applied for the calculations of the model tests (Börgesson 1988), was well fitted for the fast shear movements used in these tests. The effective stress approach was motivated for the combined slow shear and creep studies made for the full-scale simulations (Börgesson 1992) but was also more complicated and more difficult to run.

Since the aim of this study e.g. is to study the effect of the fastest possible shear the conclusion is that the total stress approach is the best model for these calculations.

The most important properties of the bentonite for the rock shear are the stiffness and the shear strength. These properties vary with bentonite type, density and rate of strain. Ca-bentonite has higher shear strength than Na-bentonite and the shear strength increases with increasing density and strain

rate. Since it cannot be excluded that the Na-bentonite MX-80 will be ion-exchanged to Ca-bentonite the properties of Ca-bentonite is used in the modelling. The acceptable density at saturation of the buffer material is 1,950 kg/m^3 – 2,050 kg/m^3 which is covered by the models below.
The material model is in ABAQUS expressed with the von Mises stress σ_j that describes the "shear stress" in three dimensions according to Equation 4-1.

$$\sigma_j=(((\sigma_1- \sigma_3)^2 + (\sigma_1- \sigma_2)^2 + (\sigma_2- \sigma_3)^2)/2)^{1/2} \quad (4\text{-}1)$$

where

σ_1, σ_2 and σ_3 are the principal stress components.

The material model defines the relation between the stress and the strain and is partitioned in elastic and plastic parts. For details regarding definition of the shear strength and the influence of density, pressure and rate of shear, see Börgesson et al. (1995, 2004).

"Rate dependent elastic-plastic stress-strain relation

The elastic-plastic stress strain relations used for the three different densities are derived according to the description above in an identical way as the relations used in all previous calculations.

The bentonite is modelled as linear elastic combined with the von Mises plastic hardening - Table 4-4 shows the elastic constants. The plastic hardening curve is made a function of the strain rate of the material. The reason for the latter relation is that the shear strength of bentonite is rather sensitive to the strain rate. It increases with about 10% for every 10 times increase in strain rate.
Since the rock shear at an earthquake is very fast (1 m/s) the influence is strong and the resulting shear strength will be different at different parts of the buffer. Figure 4-4 shows the material model. The stress-strain relation is plotted at different strain rates.

Table 4-4. Elastic material data for the bentonite buffer Na converted to Ca.

Density (kg/m^3)/Swelling pressure (MPa)	Elastic part	
	E **(MPa)**	**ν**
Low - 1950/5.3	243	0.49
Mean - 2000/8	307	0.49
High - 2050/12.3	462	0.49

The experiments (Börgeson et al. 2010) show that also Young's modulus *E* is dependent on strain rate but in the calculations this has been neglected and a representative stiffness has been chosen (sensitivity analyses did show minor changes of the results when varying Young's modulus between maximum and minimum values achieved from the experiments).

From the performed analyses it's obvious that the bentonite gets plastic strains outside the defined range for material data. However, other studies, "Earthquake induced rock shear through a deposition hole – Part 2. Additional calculations of the influence of inhomogeneous buffer on the stresses in the canister." (SKBDoc 1407337) shows that it doesn't affect the results significantly.

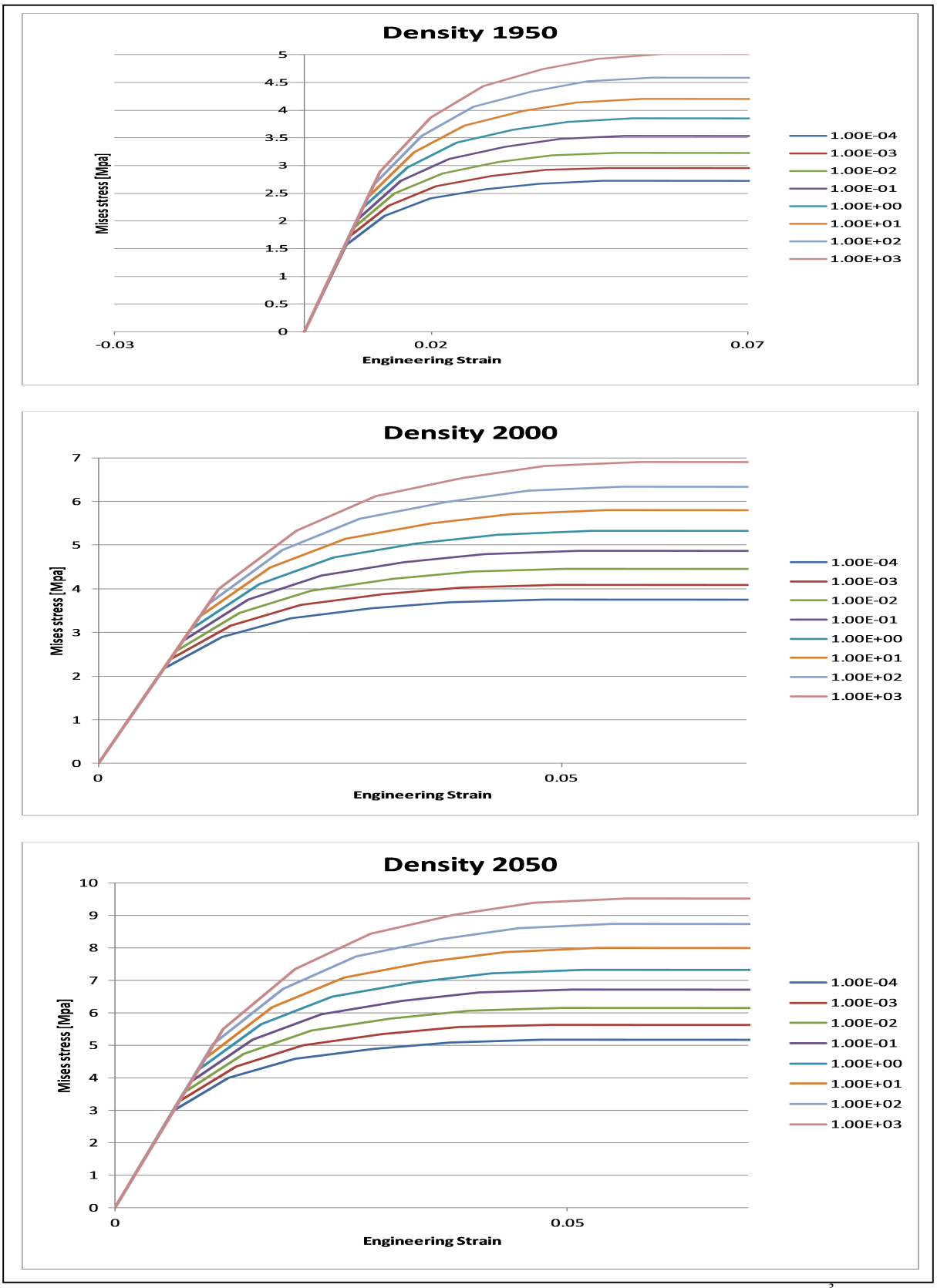

Figure 4-4. *Plot of material definition for the bentonite buffer for different densities [kg/m^3] and strain rates [1/s]. Mises stress [MPa] versus engineering strain.*

4.5 Copper material model (used by copper shell and washer)

4.5.1 Kimab material

The material model used for copper for most of the global analyses is described below.
The stress-strain properties of the copper in the copper shell were investigated by the Corrosion and metals research institute Swerea Kimab and the results are then represented by a creep material model developed by Rolf Sandström, see Sandström and Andersson (2008), Jin and Sandström (2008) and Sandström et al. (2009).

The material model for the short duration rock shear analysis, used for all analyses in this study and also in previous studies for short duration rock shear analyses (Hernelind 2010) and "Global simulation of copper canister – final deposition" (SKBdoc 1339902), is based on a simplified elastic-plastic material model, see Table 4-5, using data from the creep model assuming a strain rate of 5×10^{-3}/s which is considered as conservative.

The flow curve data has been calculated from Sandström et al. (2009) wherein eq.(17) has been used together with the parameter values defined in the corresponding Table 4-2, as well as $m = 3.06$, $\alpha = 0.19$, $\omega = 14.66$.

The copper model data is shown in Figure 4-5. Data is available up to 50% and covers the range of obtained results.

Table 4-5. Elastic-plastic material data for the copper at strain rate 5×10^{-3}/s.

Elastic part		Plastic part: von Mises stress σ_j (MPa) at the following plastic strains (ε_p)					
E (MPa)	ν	0	0.10	0.20	0.30	0.40	0.50
$1.2\cdot10^5$	0.308	72	178	235	269	288	300

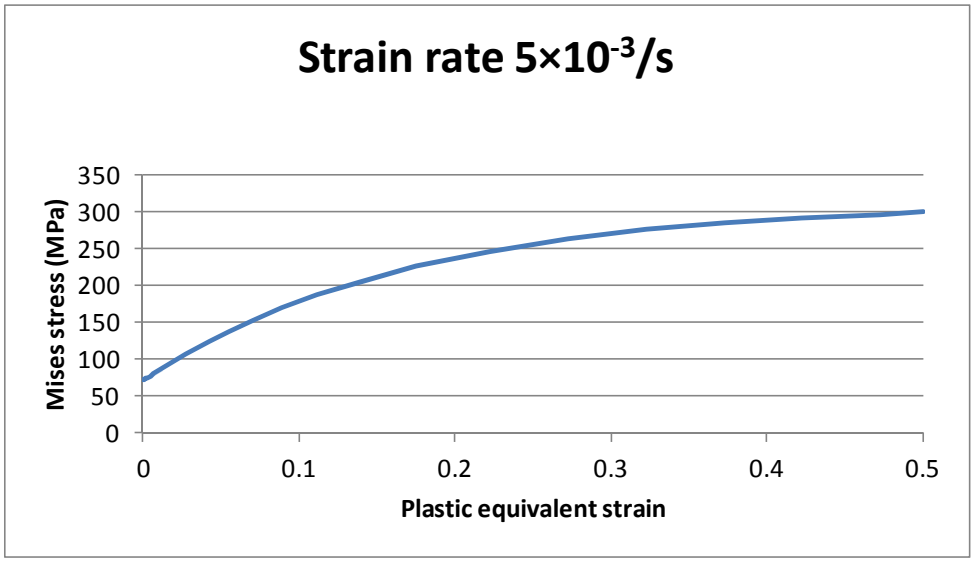

Figure 4-5. *Copper shell yield surface, true stress, [MPa] as a function of the logarithmic plastic equivalent strain.*

5 Contact definitions

All the boundaries of the buffer, the copper shell, the insert and the insert lid interact through contact surfaces allowing finite sliding. All contact surfaces have friction at sliding with no cohesion and the friction coefficient 0.1, i.e. the friction angle (ϕ) is 5.7˚ and the cohesion (c) is 0 kPa.

The contact is released when the contact pressure is lost.

Contact pairs between support plates and the insert are tied together (tied means that the surfaces are constrained together and will not allow for opening/closing or sliding) which is assumed to be a reasonable assumption since the gravity and the pre-stress in the screw implies pressure in the axial direction.

The interaction between the buffer and the rock (not modelled) is assumed to be tied through prescribed boundary conditions and will not allow for opening/closing or sliding.

6 Initial conditions

Initial conditions are defined as:

- Temperature for all nodes in the model as 300 K (only used when the copper material is defined by a creep material model which has not been done in this study). The temperature is assumed not to change during the analysis.

- The fixing screw between the insert lid and the insert has an initial stress in the axial direction corresponding to yield stress in the screw.

- Total pressure for the buffer (17.3 MPa) based on the swelling pressure (12.3 MPa for bentonite with density 2,050 kg/m^3) plus 500 meter water pressure (5 MPa) when using elastic-plastic material model without pore pressure (the repository is located 500 meter below the surface for the Forsmark site). Since the canister deforms when the initial stresses are applied, the calculated magnitude of the swelling pressure will decrease. For that reason the initial condition for pressure is given as 40.2 MPa based on the obtained pressure (about 17.3 MPa) after equilibrium iterations. At the start of rock shearing simulation the pressure on the outer surface of the copper shell thus is about 17.3 MPa. Another observation is that the calculated swelling pressure will vary both in the axial and radial direction which means that it's not possible to have the correct swelling pressure without using elements with pore pressure as a degree of freedom (ABAQUS have those elements but the material model is tuned to total stresses (pore pressure + effective pressure) and not effective stresses (effective stress for soils corresponds to mean stress).

7 Boundary conditions

Symmetry conditions have been specified for the symmetry plane (displacements in the normal direction to the symmetry plane prescribed to zero), see Fig 7-1 for models using symmetry (model6g_normal_quarter_2050ca3, bwr_eccentric_lock, bwr_eccentric_1, bwr_excentric_half, bwr_eccentric_lock).
The surrounding rock has been simulated by prescribing the corresponding displacements at the outer surface of the buffer and depends also on type of simulation.

For models without symmetry, boundary conditions are prescribed only at the outer surface of the buffer.

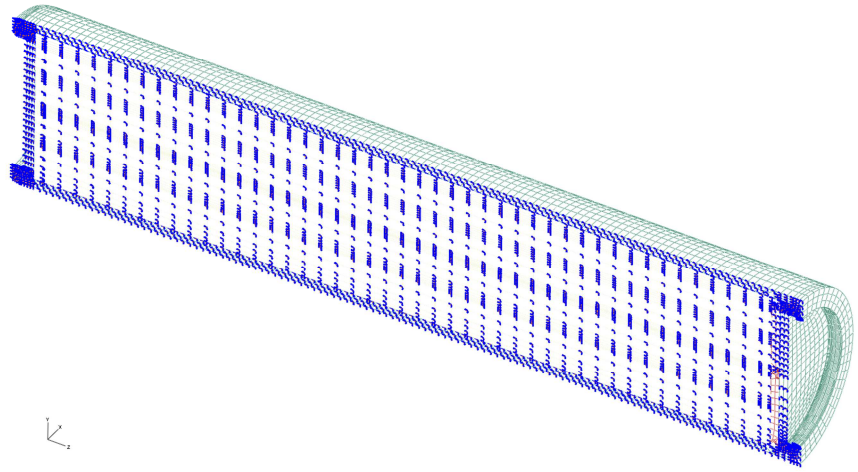

Figure 7-1. *Prescribed symmetry conditions.*

8 Calculations

8.1 General

Previous analyses for Earthquake induced rock shearing (Hernelind 2010) have been based on geometries having several simplifications as:

- Insert lid modelled without some details (valve, holes for mounting the valve and for the fixing screw).
- Insert lid without the centre fixing screw (instead the insert lid was tied to the insert at the periphery).
- The washer between the screw and insert lid was not modelled.
- Steel channel tubes tied to the insert and modelled without support plates.
- Base plate of the insert was modelled without screws, nuts and support plates derived from the fixing during the casting process.

Previous analyses (Hernelind 2010) also assumed a construction based on nominal measures and thus didn't study any effect of allowable tolerances and also the initial position of the steel channel tubes was assumed to be centred in the nodular cast iron insert.
The aim with this study is to check if the above mentioned assumptions are reasonable and not have significant influences on the stress/strain levels and corresponding conclusions regarding damage tolerance analysis and mechanical integrity.
The geometry definition for the BWR canister is therefore created based on CAD-drawings with as few simplifications as possible.

The obtained results are compared with previous analyses (Hernelind 2010) when Ca-bentonite with density 2,050 kg/m^3 is used for the buffer. Two horizontal shear planes, one at 75% of the insert height from the base and one at the insert lid.

8.1.1 Rock shear calculation cases

The reference case for BWR is based on Na-bentonite converted to Ca-bentonite with density 2,050 kg/m^3. Two cases of rock shear positions perpendicular to the axis of the canister have been analyzed (see also Table 1-1):

- at 75% of the height from the insert base
- at top of the insert lid

8.1.2 Analysis approach

The numerical calculations are performed using the FE-code ABAQUS version 6.12 (ABAQUS, 2013, Dassault Systèmes Simulia Corp.) assuming non-linear geometry and material definitions. This means that all non-linearities defined by the input will be considered such as large displacements, large deformations, non-linear interactions (contact) and non-linear materials. All non-linear contributions will be used when forming the equations to be solved for each equilibrium iteration. Short term analysis is based on quasi-static response but the results will depend on the time used for the simulation since rate-dependent material data is used. The code will choose suitable time-increments for the loading based on (in most cases) default convergence tolerances.

8.2 Short term analyses

The short term analyses (with 1 m/s as shearing velocity the time for 1 cm shearing is 0.01 second) consist of three steps where the shearing is prescribed by boundary conditions.

In the first step initial stresses corresponding to the swelling pressure (12.3 MPa for bentonite with density 2,050 kg/m^3) plus 5 MPa hydrostatic pressure (the deposition is made about 500 meters below the surface) in the bentonite is applied, see also in chapter "Initial conditions".

In the second step 5 cm is used for the shearing magnitude and finally the third step defines additional 5 cm shearing.

The results are shown in Appendix 1-4 and 6 for the BWR insert. Appendix 5 contains some comparisons between all cases after 8 cm shearing showing rather similar global responses. Appendix 7 contains comparisons for the last converged solutions.

9 Results for rock shear

For each analysis a large amount of results are available and to have an indication only a few values are reported. When stress components are plotted S22 corresponds to normal stress in y-direction (lateral) and S33 corresponds to normal stress in z-direction (axial).

Contour plots are based on element values extrapolated to nodal points and then contributions from different elements are averaged (the threshold value for averaging has been chosen to 100% which implies that averaging always is performed regardless of how much difference it is between the nodal values calculated for each element). Another extreme alternative is to define the threshold value to 0% which implies that averaging never is performed – this alternative will show greatest values but will often result in non-smooth contour plots. For a perfect mesh the choice of averaging doesn't matter but for the models used in this report where focus is on global results there exist regions where the choice has a significant effect (especially where the geometry has some kind of discontinuity).

The Table values are taken from the contour plots and often from regions with locally bad mesh (or bad geometry) but nevertheless the values can be used for comparison purposes. It should be noted that the results are useful on the global level but if more detailed results are requested close to singularities (or regions having large gradients of stresses and strains) a submodel analysis is recommended as a following study.

The insert should withstand a shearing magnitude of 5 cm but results are also shown for 10 cm shearing.

9.1 Comparison with previous analyses for the BWR insert

As reference case the horizontal shear plane at ¾-distance from the insert base have been chosen since this case experience the highest stresses/strains for the insert. Figures 9-1 to 9-15 show the outcome at 5 cm shearing (comparison at last converged result, see Appendix 7) for the BWR insert with symmetrically positioned channel tubes for detailed BWR-model (bwr_eccentric_lock) and the reference model (model6g_normal_quarter_2050ca3).
Figures 9-16 to 9-21 compare the results for centrically (bwr_eccentric_lock) and eccentrically (bwr_eccentric_1 with 20 mm eccentricity) positioned channel tubes when one symmetry plane is used.
One observation is that even though the global response is similar for the two models the peak values differ more substantially. Some of this difference comes from geometry modelling difficulties due to extremely many details have been included.
Significant differences are observed for the insert lid which is expected due to different modelling of the interaction with the insert - insert lid fixing screw which only exists for the detailed model and also the peripheral connection which is a tied connection for the reference model and contact pairs (simulating opening/closing) for the detailed model.

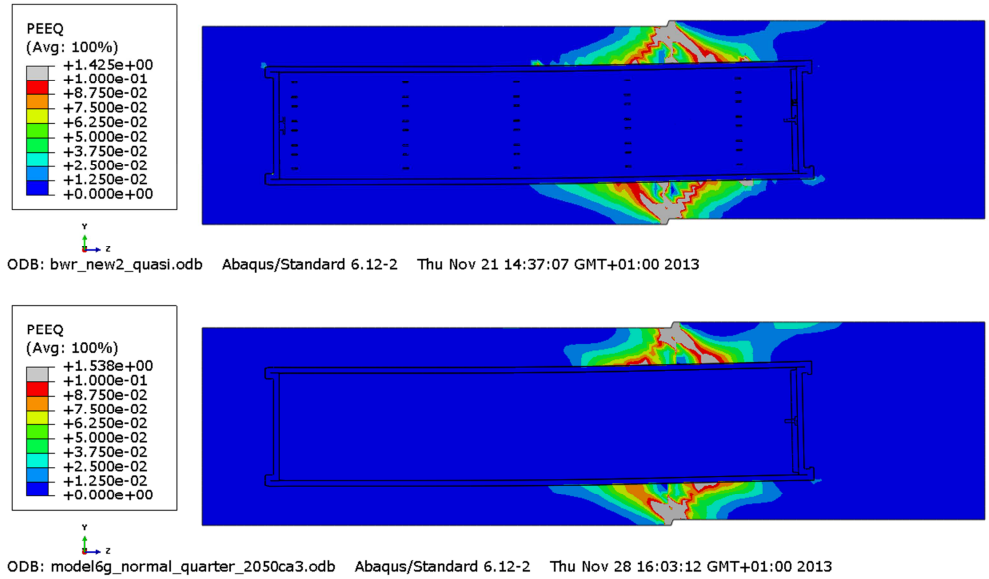

Figure 9-1. *Plot showing equivalent plastic strain (PEEQ) after 5 cm shearing for detailed BWR model (upper) and the reference BWR model (lower). Symmetrically positioned channel tubes.*

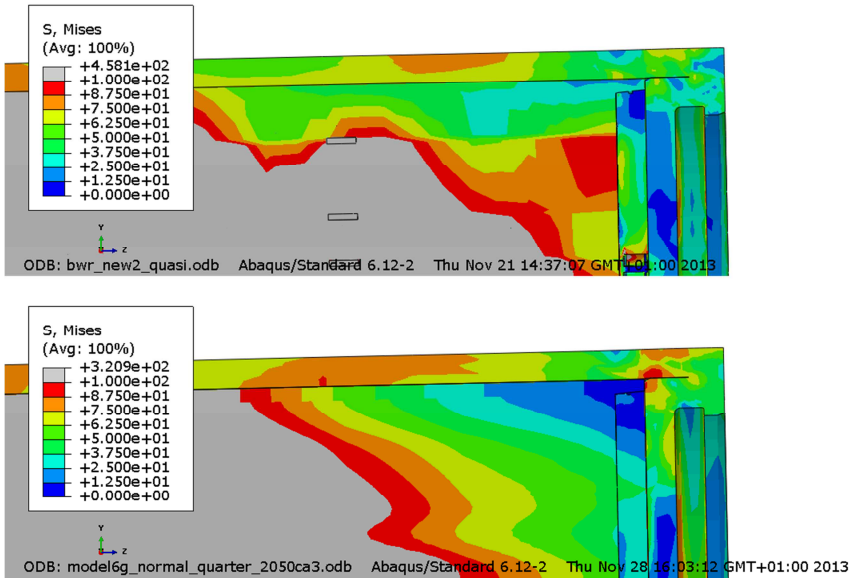

Figure 9-2. *Plot showing Mises stress at the left top corner after 5 cm shearing for detailed BWR model (upper) and the reference BWR model (lower). Symmetrically positioned channel tubes.*

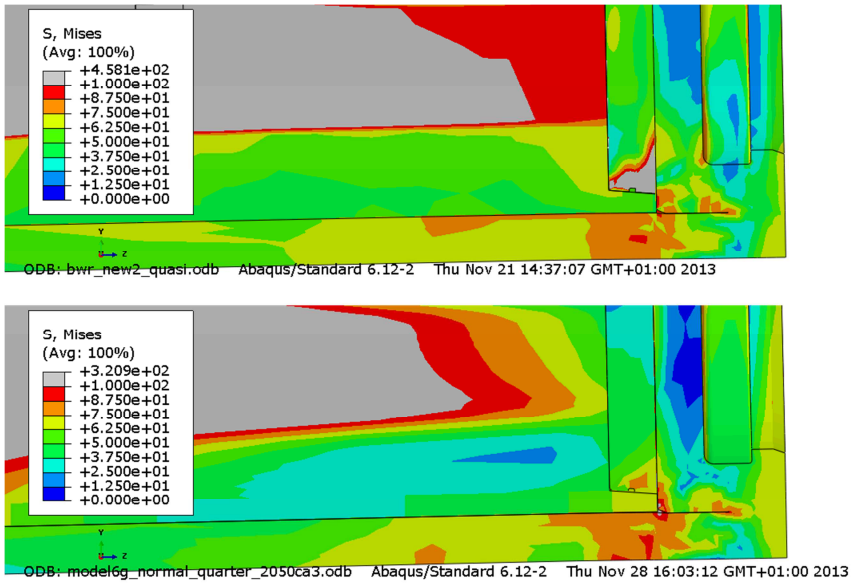

Figure 9-3. *Plot showing Mises stress at the right top corner after 5 cm shearing for detailed BWR model (upper) and the reference BWR model (lower). Symmetrically positioned channel tubes.*

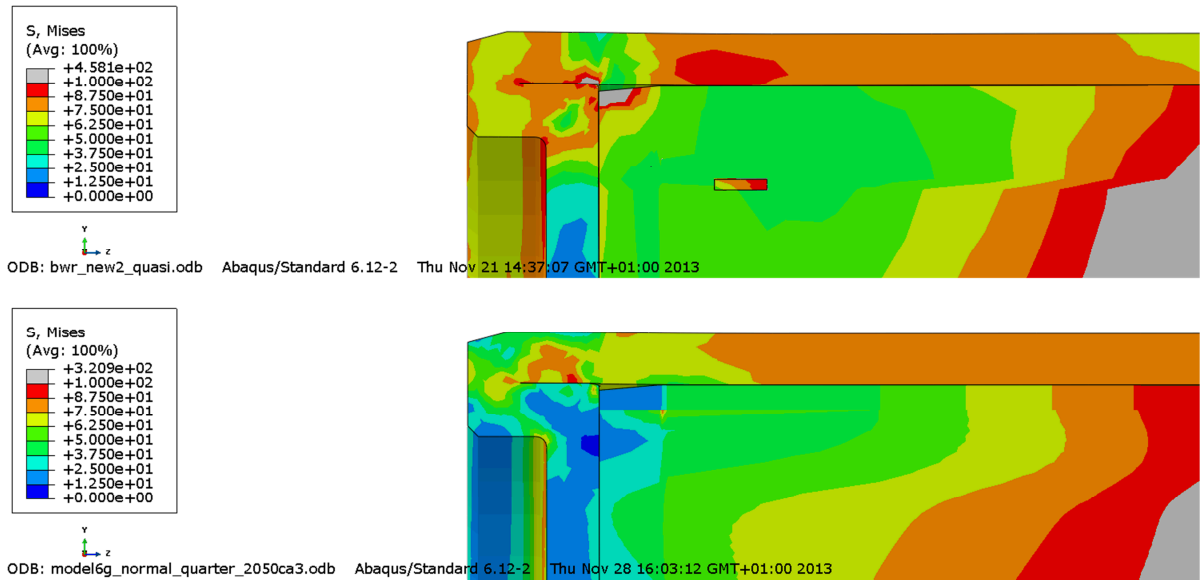

Figure 9-4. *Plot showing Mises stress at the left bottom corner after 5 cm shearing for detailed BWR model (upper) and the reference BWR model (lower). Symmetrically positioned channel tubes.*

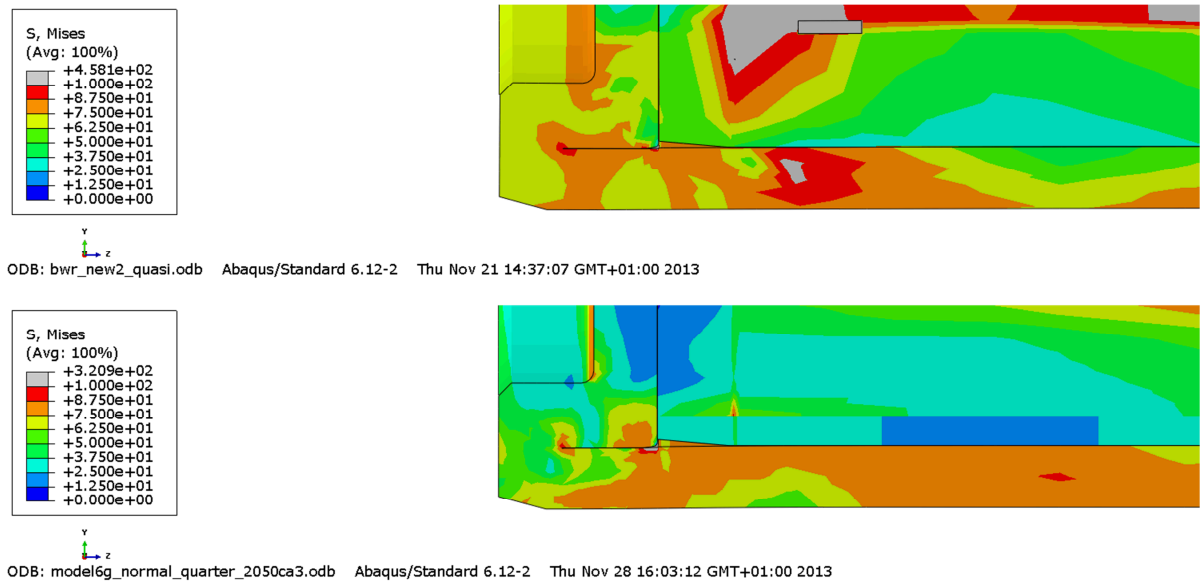

Figure 9-5. *Plot showing Mises stress at the right top corner after 5 cm shearing for detailed BWR model (upper) and the reference BWR model (lower). Symmetrically positioned channel tubes.*

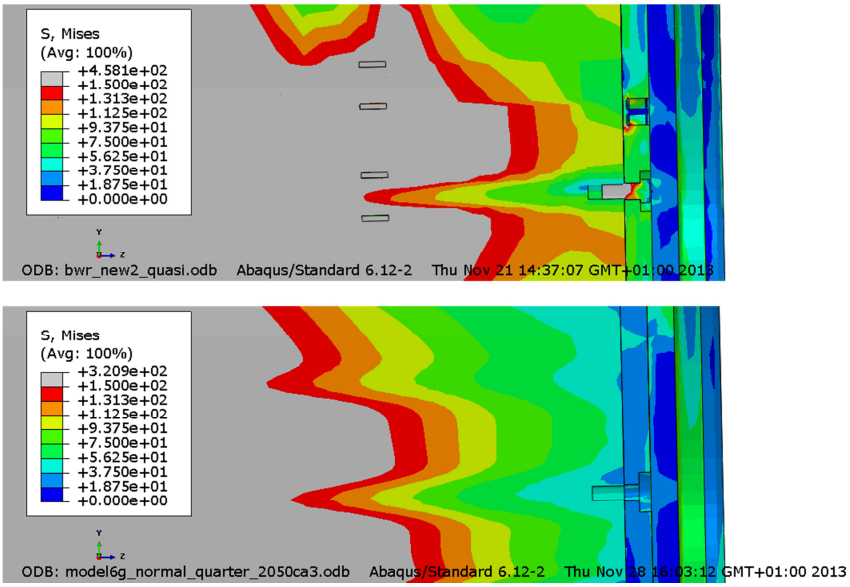

Figure 9-6. *Plot showing Mises stress at the top close to the screw after 6 cm shearing for detailed BWR model (upper) and the reference BWR model (lower). Symmetrically positioned channel tubes.*

9.1.1 Copper shell

Figures 9-7 to 9-8 show rather small differences between the detailed BWR-model (bwr_eccentric_lock) and the reference model (model6g_normal_quarter_2050ca3) for the copper shell. Highest values are for the reference model even though the global response shows higher values for the detailed BWR-model. The global values are acceptable and the local peak values occur in areas mainly in compression and where the model has discontinuities.

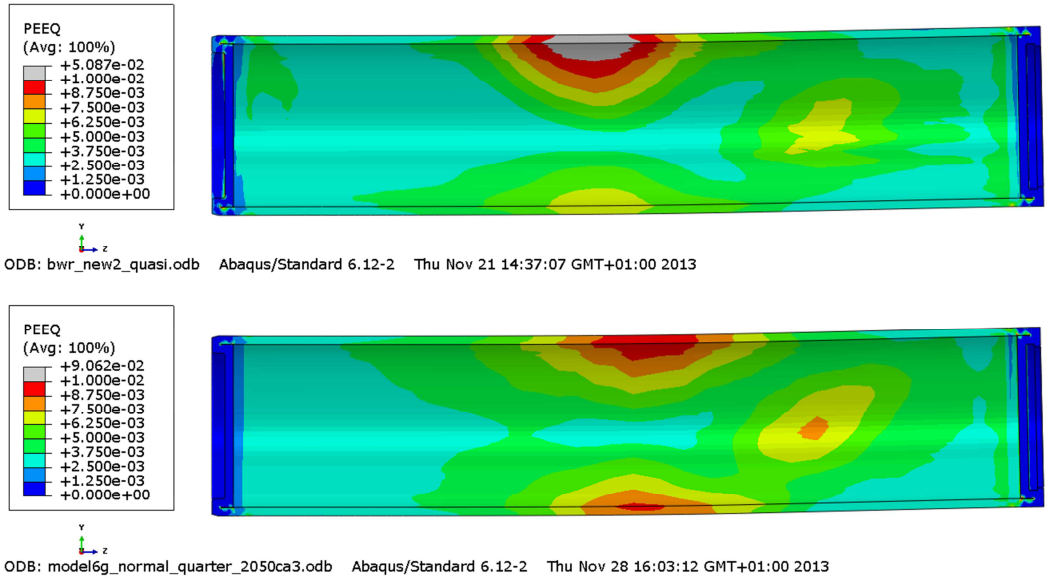

Figure 9-7. *Plot showing equivalent plastic strain (PEEQ) for the copper shell after 5 cm shearing for detailed BWR model (upper) and the reference BWR model (lower). Symmetrically positioned channel tubes.*

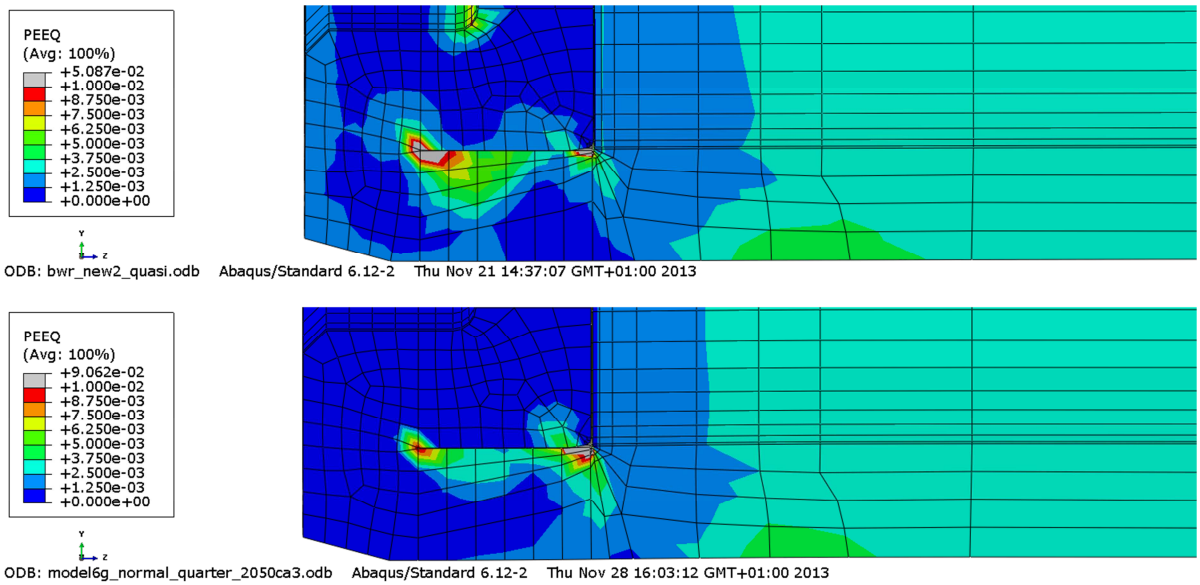

Figure 9-8. *Plot showing equivalent plastic strain (PEEQ) for the copper shell after 5 cm shearing for detailed BWR model (upper) and the reference BWR model (lower). Symmetrically positioned channel tubes.*

9.1.2 Nodular cast iron insert

Figures 9-9 and 9-13 show similar results for detailed BWR-model (bwr_eccentric_lock) and the reference model (model6g_normal_quarter_2050ca3) for the equivalent plastic strain except at the corner radius for the steel channel tubes.

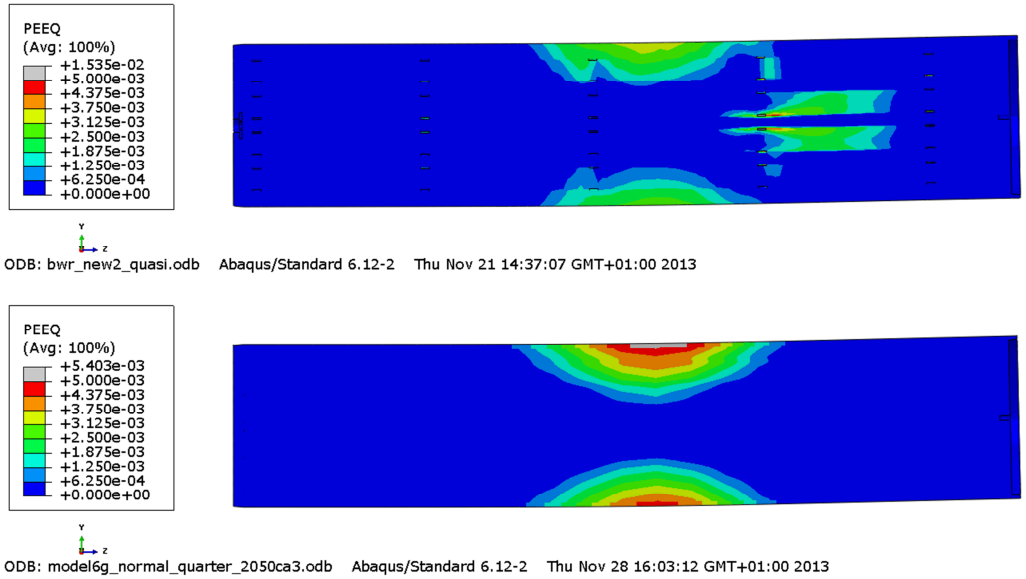

Figure 9-9. *Plots showing plastic equivalent strain (PEEQ) for the insert after 5 cm shearing for detailed BWR model (upper) and the reference BWR model (lower). Symmetrically positioned channel tubes.*

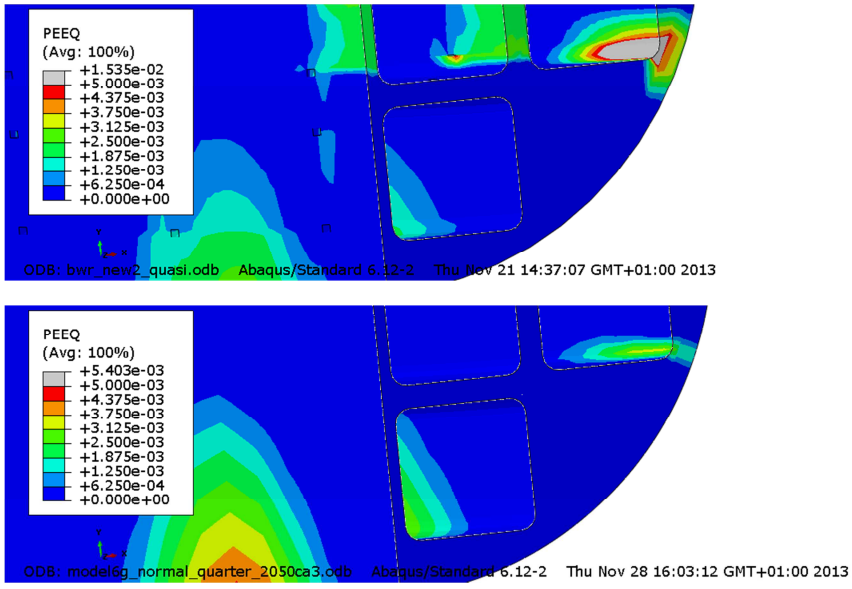

Figure 9-10. *Plots showing plastic equivalent strain (PEEQ) for the insert after 5 cm shearing for detailed BWR model (upper) and the reference BWR model (lower). Symmetrically positioned channel tubes.*

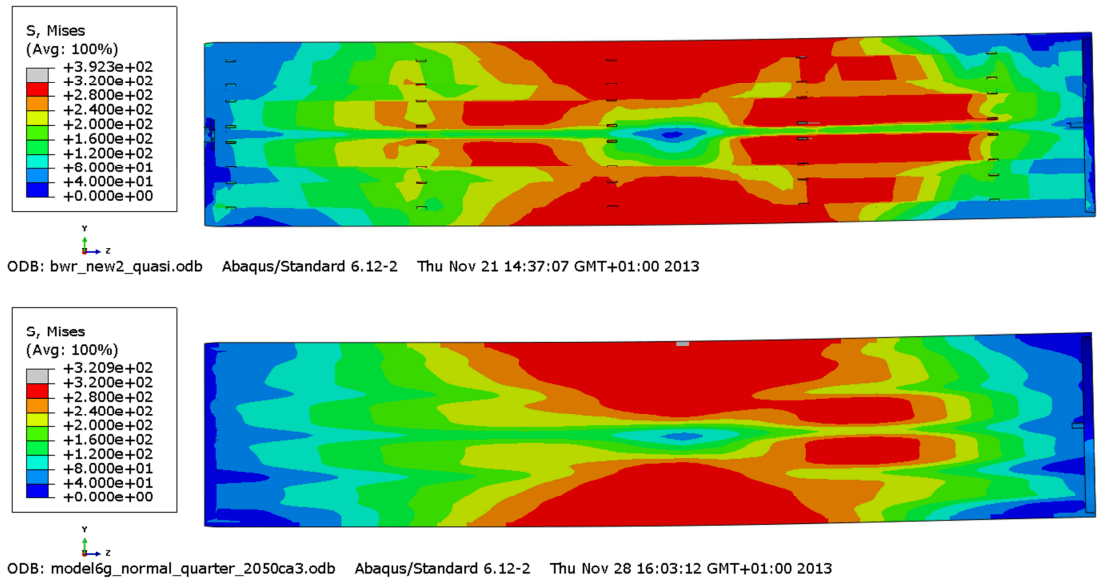

Figure 9-11. *Plots showing Mises stress for the insert after 5 cm shearing for detailed BWR model (upper) and the reference BWR model (lower). Symmetrically positioned channel tubes.*

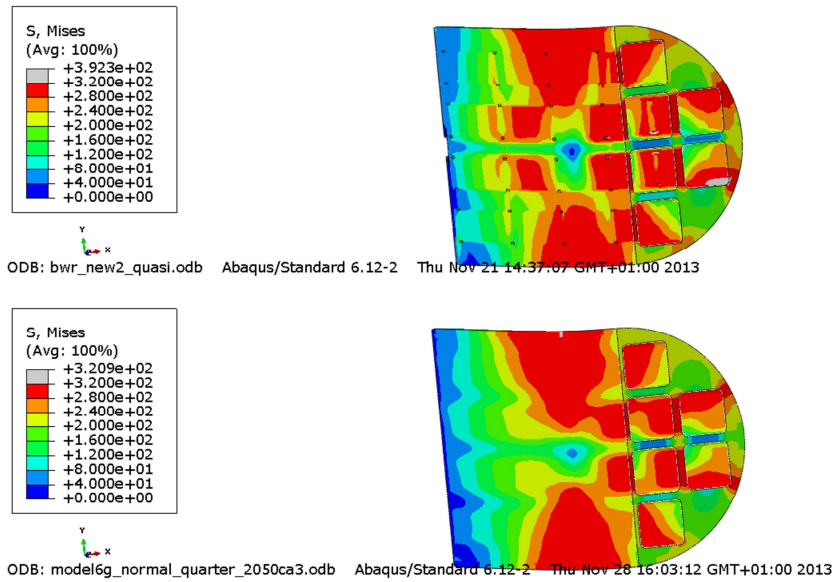

Figure 9-12. *Plots showing Mises stress for the insert after 5 cm shearing for detailed BWR model (upper) and the reference BWR model (lower). Symmetrically positioned channel tubes.*

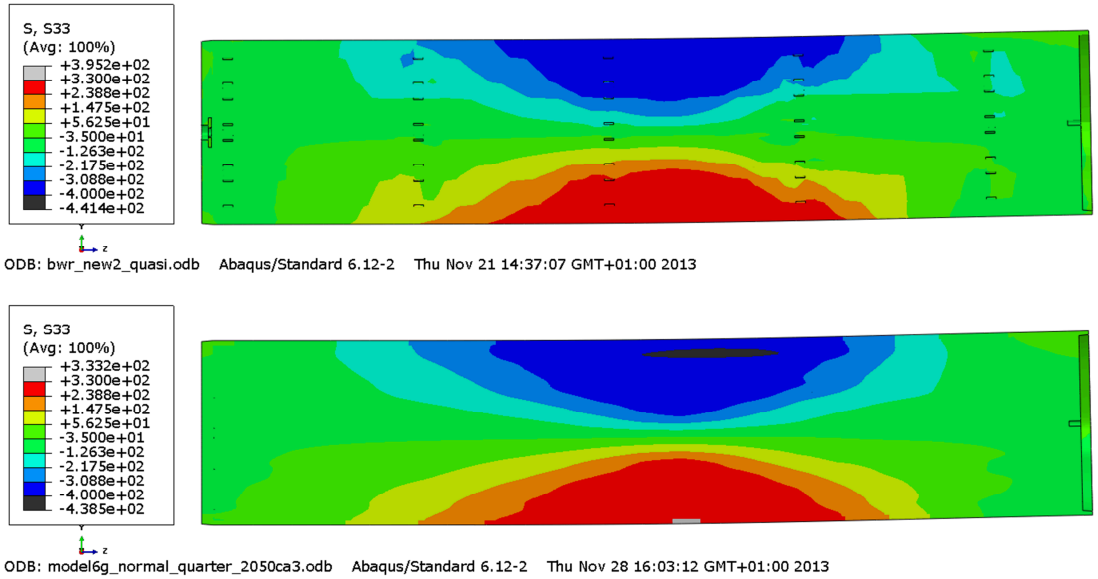

Figure 9-13. *Plots showing axial stress (S33) for the insert after 5 cm shearing for detailed BWR model (upper) and the reference BWR model (lower). Symmetrically positioned channel tubes.*

9.1.3 Steel channel tubes

Figures 9-14 to 9-15 show differences between the detailed BWR-model (bwr_eccentric_lock) and the reference model (model6g_normal_quarter_2050ca3). One observation is that the global stress level is lower for the detailed model even though the maximum value is higher. The reason for the decreased stress level could be explained by the support plates which increase the bending stiffness.

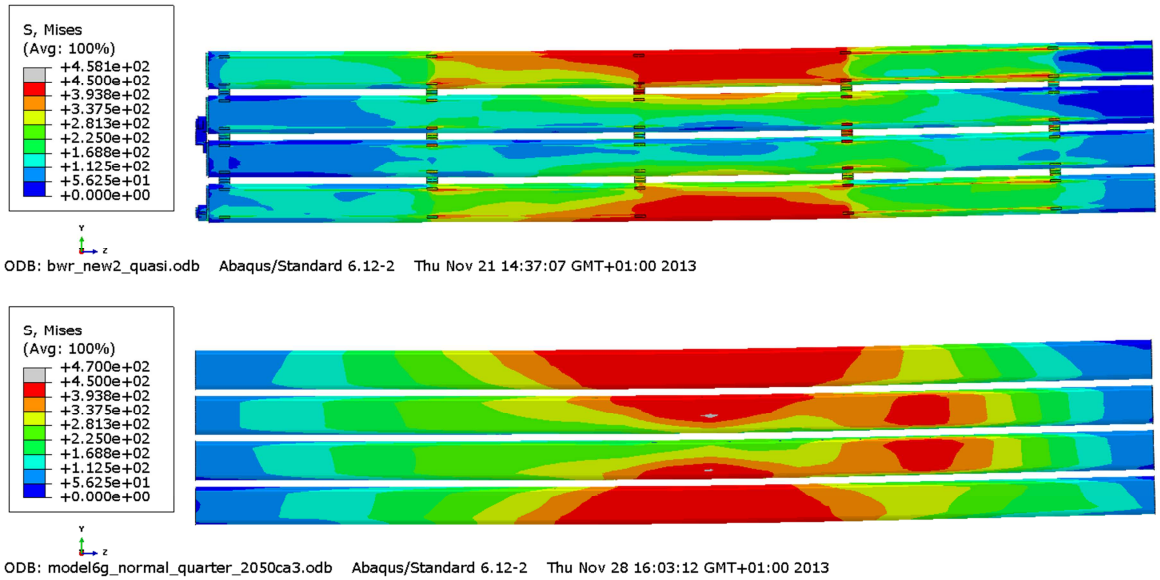

Figure 9-14. *Plots showing Mises stress for the steel channel tubes after 5 cm shearing for detailed BWR model (upper) and the reference BWR model (lower). Symmetrically positioned channel tubes.*

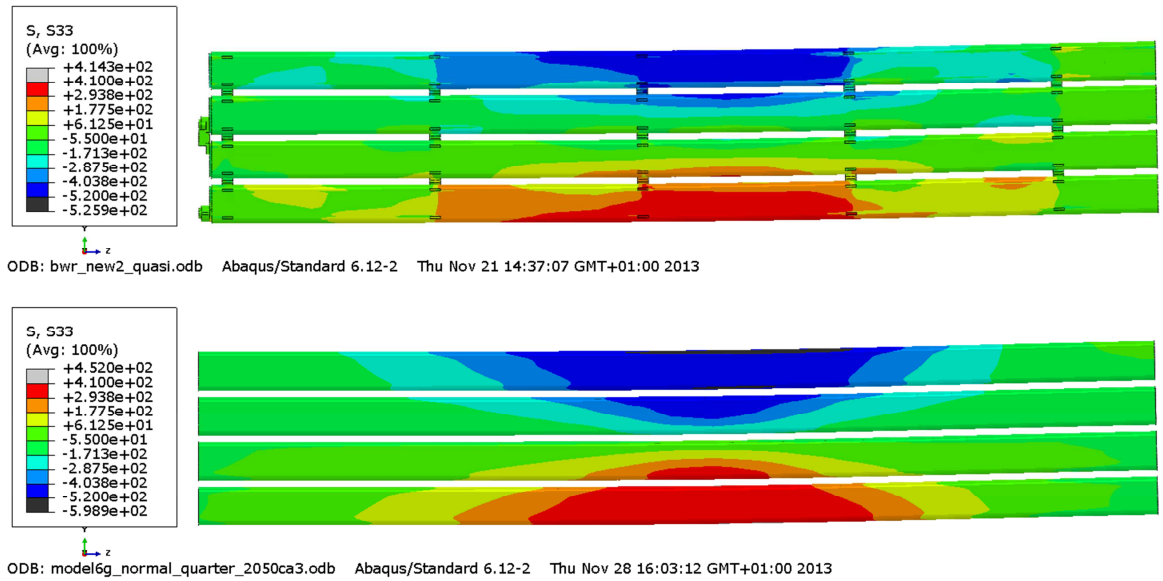

Figure 9-15. *Plots showing axial stress (S33) for the steel channel tubes after 5 cm shearing for detailed BWR model (upper) and the reference BWR model (lower). Symmetrically positioned channel tubes.*

9.2 Eccentric positioning of the steel channel tubes for the BWR insert. Symmetrically positioned channel tubes.

The reference case is based on nominal dimensions but the drawings also define allowable tolerances. One case of interest is when the tolerances imply that the steel channel tubes are placed as most eccentric as possible assuming symmetrically positioned channel tubes. Two cases are studied, see

Figure 3-9:

- The first case (bwr_eccentric_1) has the eccentricity defined such that the shortest distance between one corner of the channel tube and the outer radius of the insert is an a region with compressive stresses (by mistake this case has an eccentricity of 20 mm instead of the 10 mm based on tolerances, see (SKBdoc 1415152)).
- The second case (bwr_excentric_half) has the eccentricity defined such that the shortest distance between one corner of the channel tube and the outer radius of the insert is in a region with tensile stresses (this case has an eccentricity of 10 mm). Also the mesh is improved (with less number of bad elements) for this case.

Figures 9-16 to 9-21 compare results using the detailed model for centric and eccentric positioning of the steel channel tubes when a horizontal shearing is applied at ¾-distance from the insert base for the first case at 5 cm shearing.
Figure 9-16 shows positioning of steel channel tubes with and without tolerances. Figures 9-17 to 9-18 show comparison of the Mises stress and equivalent plastic strain (PEEQ) where a slightly increase could be observed when eccentric positioning. The peak value for Mises stress increases from 458 to 468 MPa and plastic equivalent strain increases from 5.0 to 5.1%. However, visual inspection of the plots shows very similar contours. Figures 9-19 - 9-20 shows similar observation for the steel channel tubes. The peak value for axial stress (S33) decreases from 414 to 406 MPa. The largest difference is for the equivalent plastic strain (PEEQ), 1.5 respectively 2.7%, at the corner radius of the insert for the thinnest wall thickness, Figure 9-21.
Note! Even though the eccentricity is modelled as 20 mm instead of the correct value of 10 mm the increase of equivalent plastic strain is rather small.

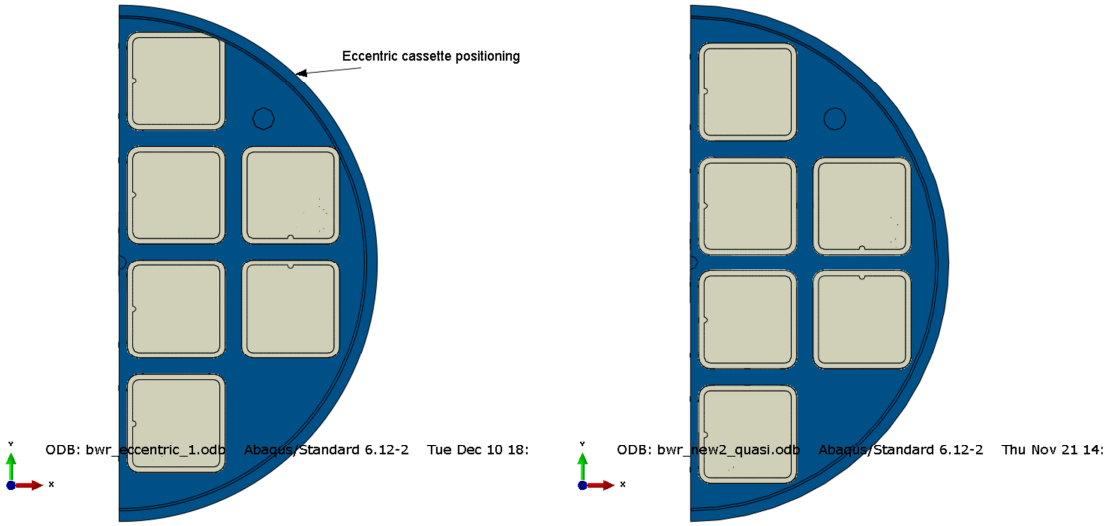

Figure 9-16 *Plots showing positioning of steel channel tubes, first case eccentric (left) and centric (right).*

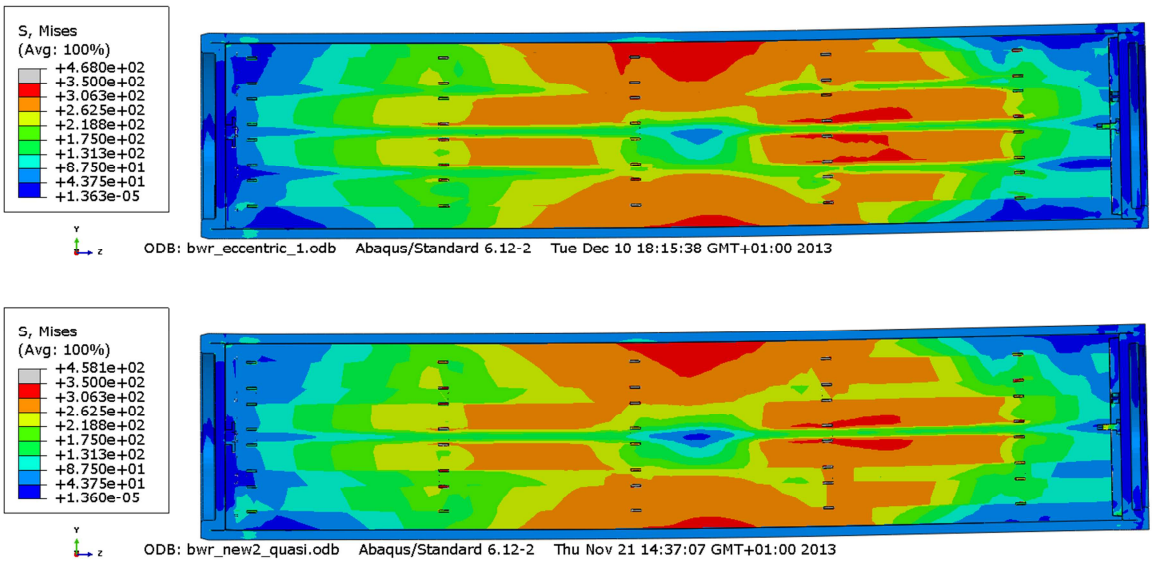

Figure 9-17 *Plots showing Mises stress after 5 cm shearing for first case eccentric BWR model (upper) and the centric BWR model (lower).*

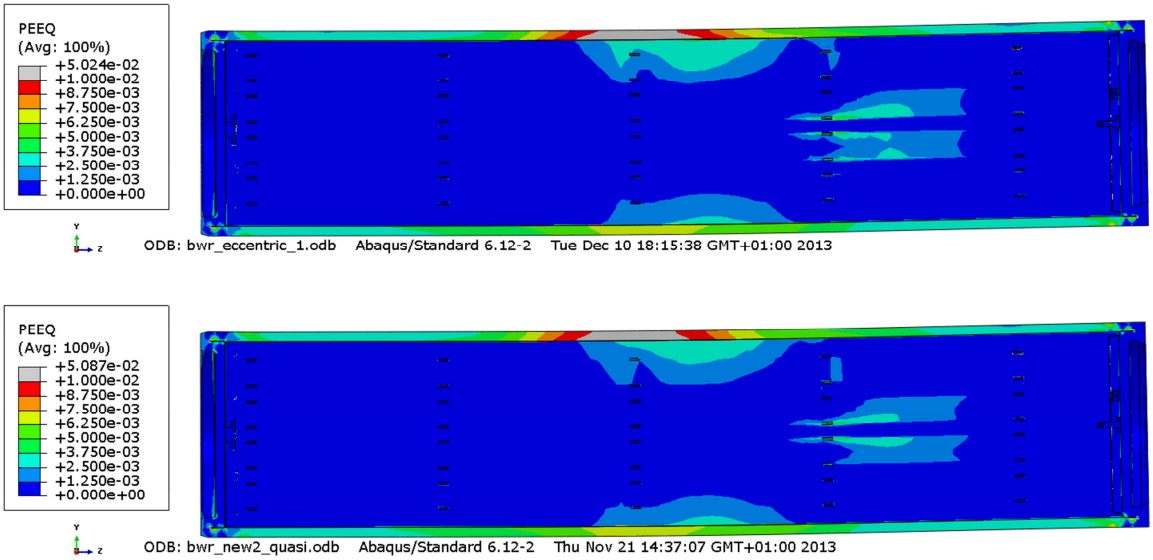

Figure 9-18 *Plots showing equivalent plastic strain (PEEQ) after 5 cm shearing for first case eccentric BWR model (upper) and the centric BWR model (lower).*

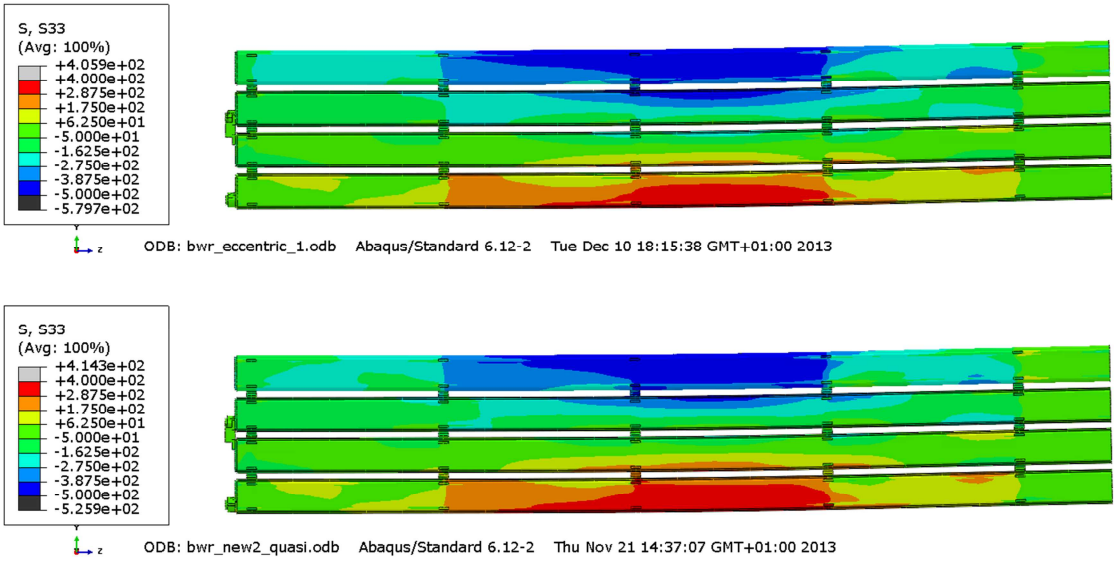

Figure 9-19 *Plots showing axial stress for the steel channel tubes after 5 cm shearing for first case eccentric BWR model (upper) and the centric BWR model (lower).*

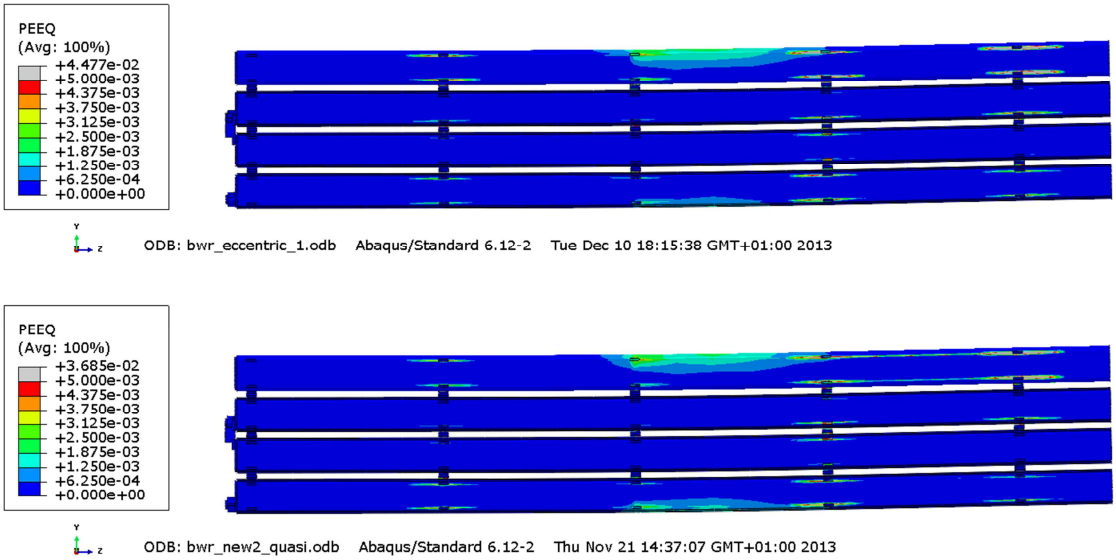

Figure 9-20 *Plots showing equivalent plastic strain (PEEQ) for the steel channel tubes after 5 cm shearing for first case eccentric BWR model (upper) and the centric BWR model (lower).*

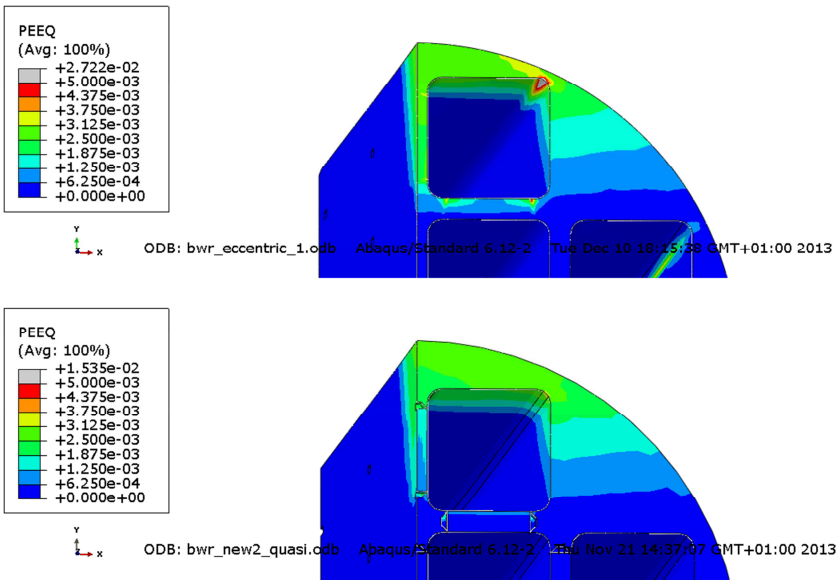

Figure 9-21 *Plots showing equivalent plastic strain (PEEQ) for the insert after 5 cm shearing for first case eccentric BWR model (upper) and the centric BWR model (lower).*

Figures 9-22 – 9-36 compare results for the first (bwr_eccentric_1 with 20 mm eccentricity and shearing such that the region with shortest distance between shell corner node and outer surface of the insert has compressive axial stress) and second case (bwr_eccentric_half with 10 mm eccentricity and shearing such that the region with shortest distance between shell corner node and outer surface of the insert has axial stress in tension) for eccentricity definitions after 5 cm shearing (Appendix 7 shows comparison after 10 cm shearing).

Figure 9-22 shows small difference between the axial stresses for the two cases which also imply similar results for the plastic equivalent strain (PEEQ), see Figure 9-23. For both cases the highest values for PEEQ occurs in the region with compressive stresses probably because the contribution to compressive stresses from the initial hydrostatic pressure. Figure 9-24 shows that the peak values for PEEQ occur at the second row of channel tubes and not where the distance between the channel tube corner and insert outer radius has its minimum.

Figures 9-26 – 9-28 shows results for the channel tubes. Also for the channel tubes the stresses (axial and Mises) shows higher values for the second case and lower magnitude for plastic equivalent strain. Figures 9-29 – 9-30 shows results for the insert lid and the screw. Figure 9-30 shows that there are small plastic strains in the screw.

Figure 9-31 show the plastic equivalent strain in the buffer and also the shearing direction is visible. Figures 9-32 – 9-36 show plastic equivalent strains for the two cases with small differences except at the fillets where the second model has an improved mesh picking up the strains more accurate.

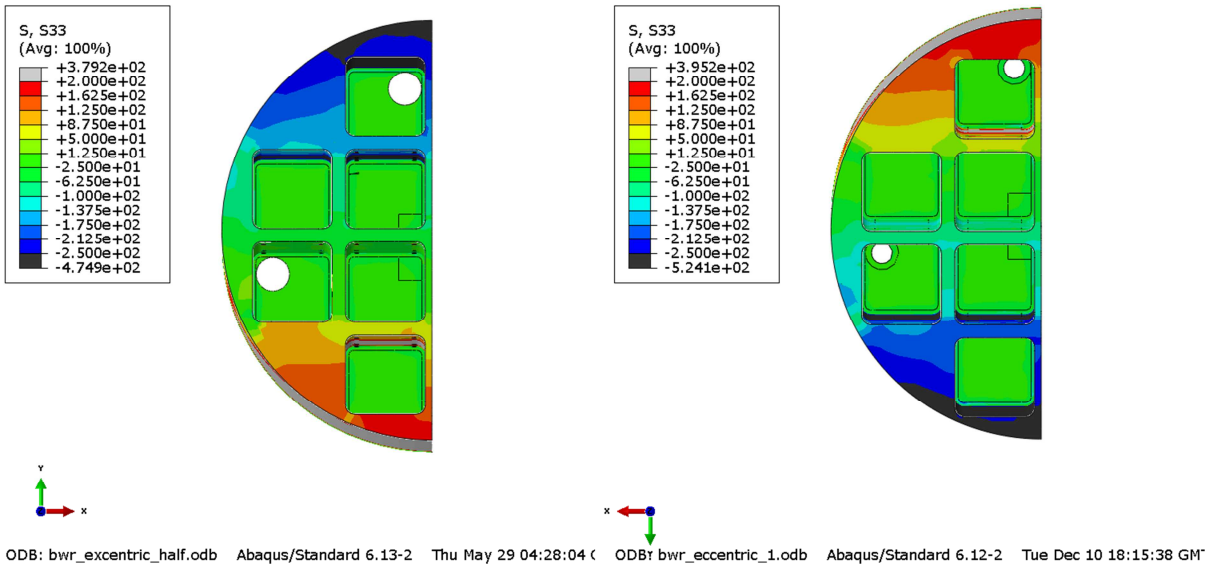

Figure 9-22 *Plots showing axial stress (S33 [MPa]) for the insert after 5 cm shearing for first (right) and second (left) case eccentric BWR model. Note the sign difference for the axial stress.*

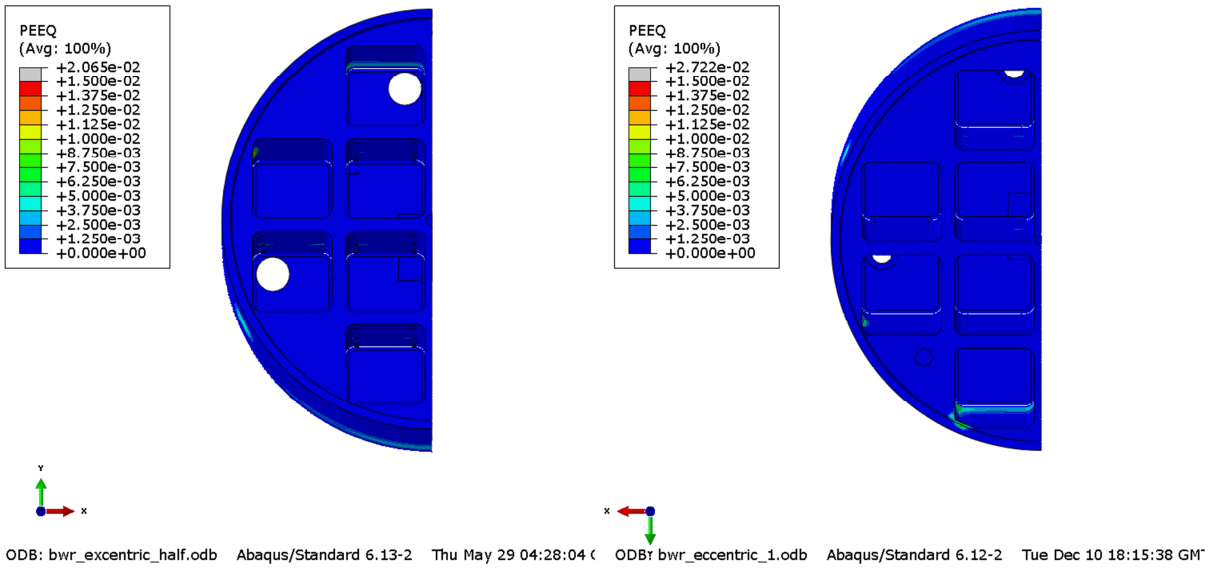

Figure 9-23 *Plots showing plastic equivalent strain (PEEQ) for the insert after 5 cm shearing for first (right) and second (left) case eccentric BWR model.*

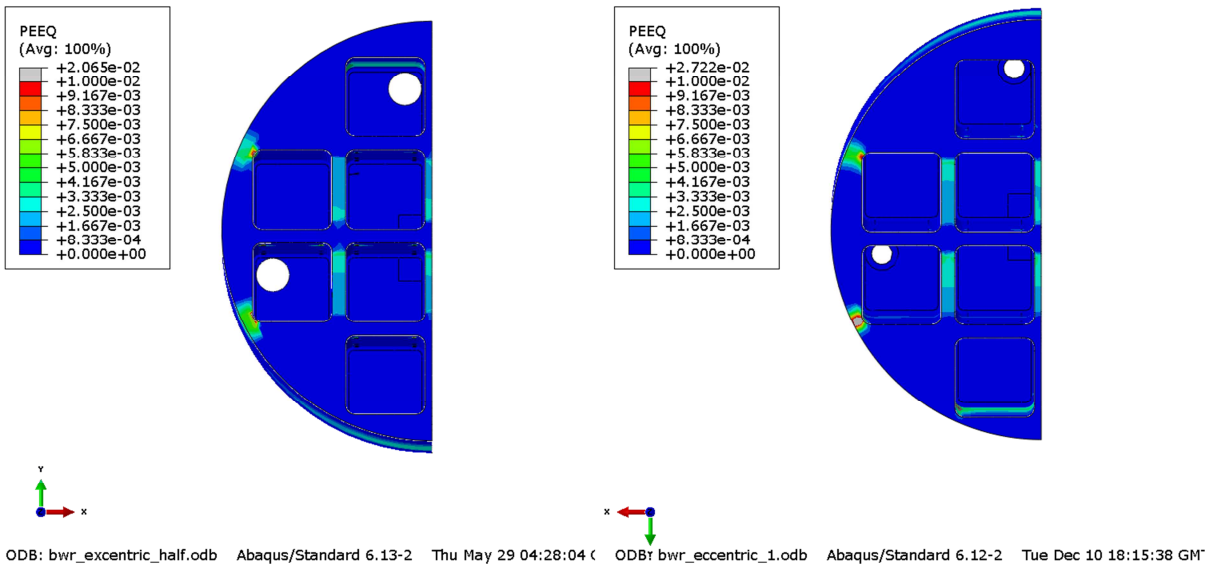

Figure 9-24 *Plots showing plastic equivalent strain (PEEQ) for the insert after 5 cm shearing for first (right) and second (left) case eccentric BWR model. Section at the highest magnitude of PEEQ.*

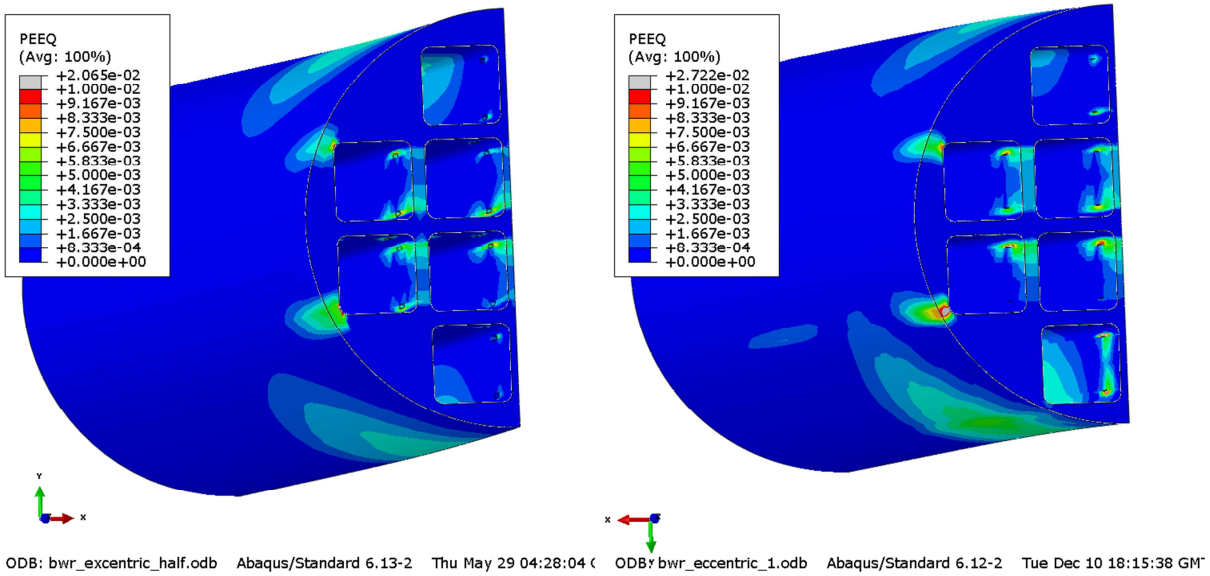

Figure 9-25 *Plots showing plastic equivalent strain (PEEQ) for the insert after 5 cm shearing for first (right) and second (left) case eccentric BWR model. Section at the highest magnitude of PEEQ.*

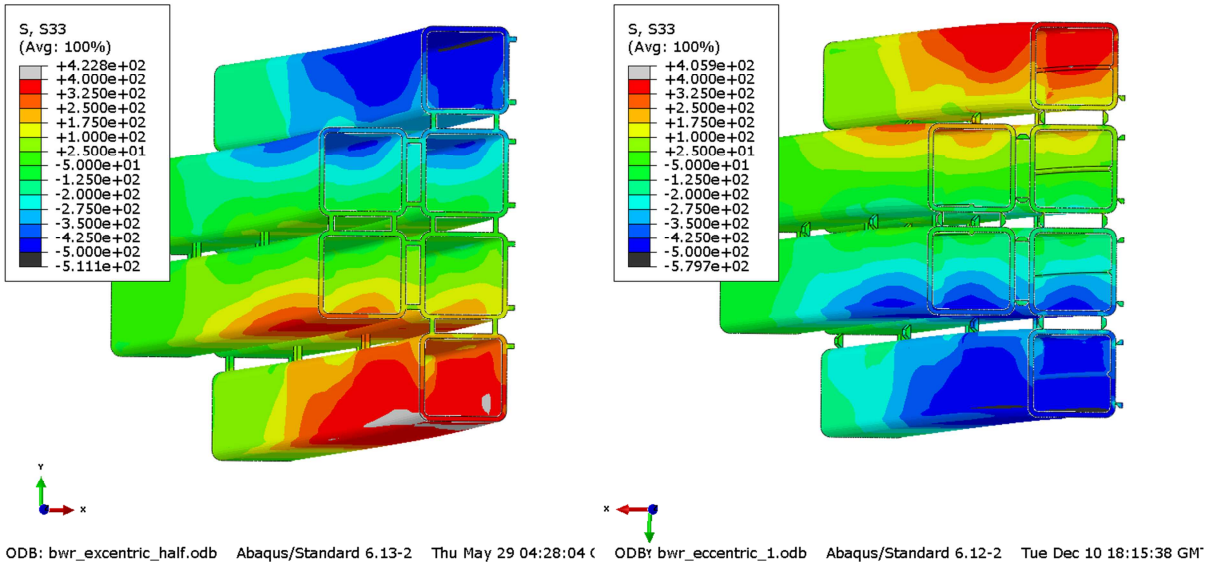

Figure 9-26 *Plots showing axial stress (S33 [MPa]) for the channel tubes after 5 cm shearing for first (right) and second (left) case eccentric BWR model.*

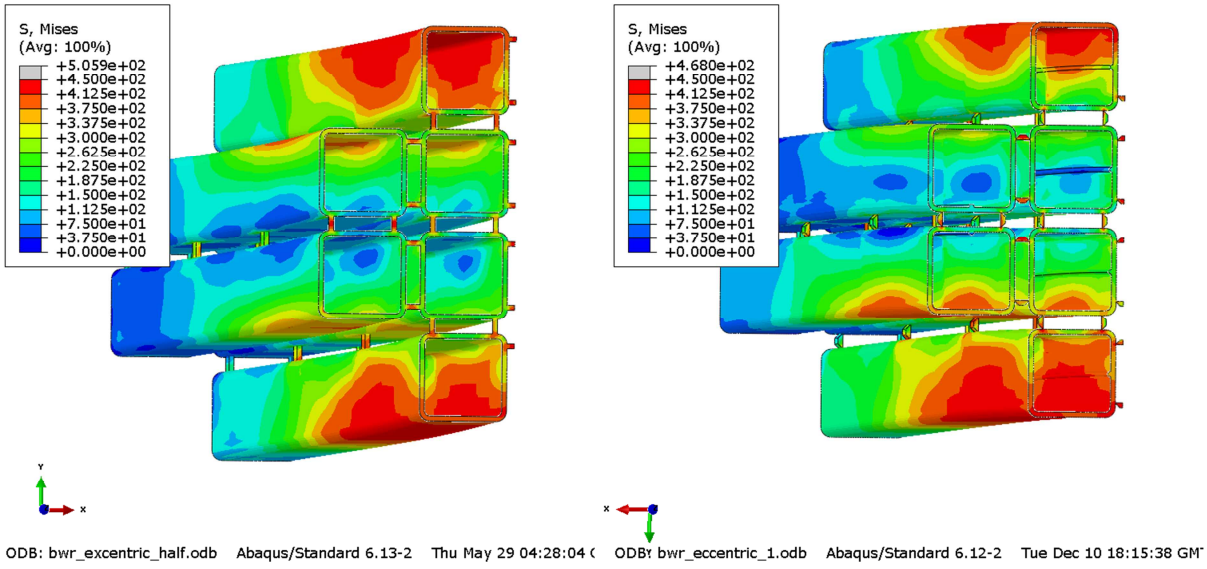

Figure 9-27 *Plots showing Mises stress [MPa] for the insert after 5 cm shearing for first (right) and second (left) case eccentric BWR model.*

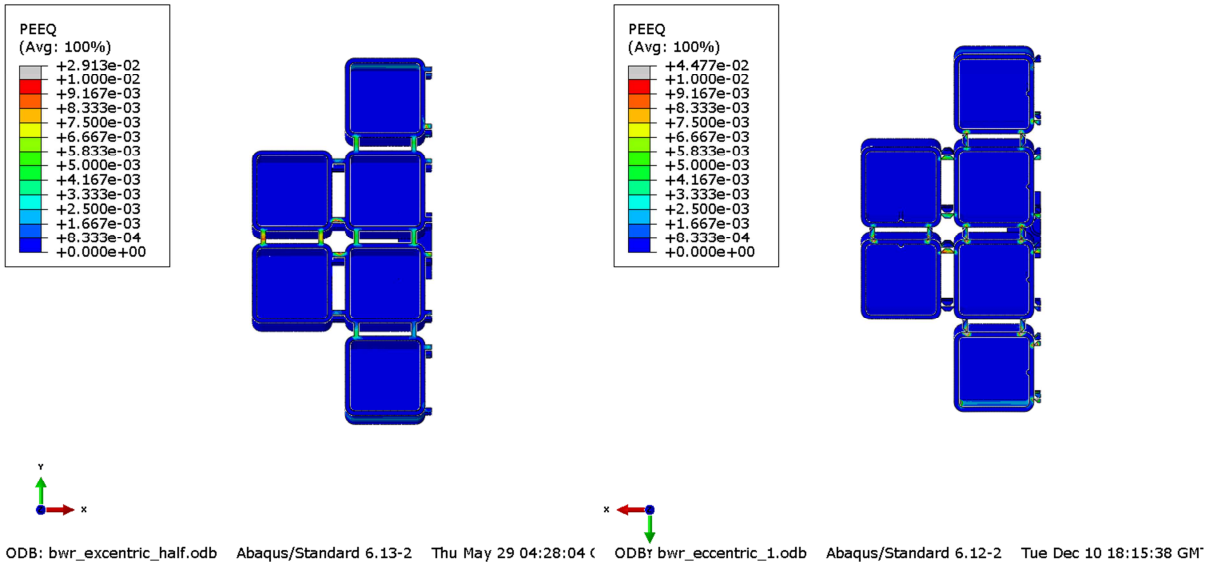

Figure 9-28 *Plots showing plastic equivalent strain (PEEQ) for the channels after 5 cm shearing for first (right) and second (left) case eccentric BWR model.*

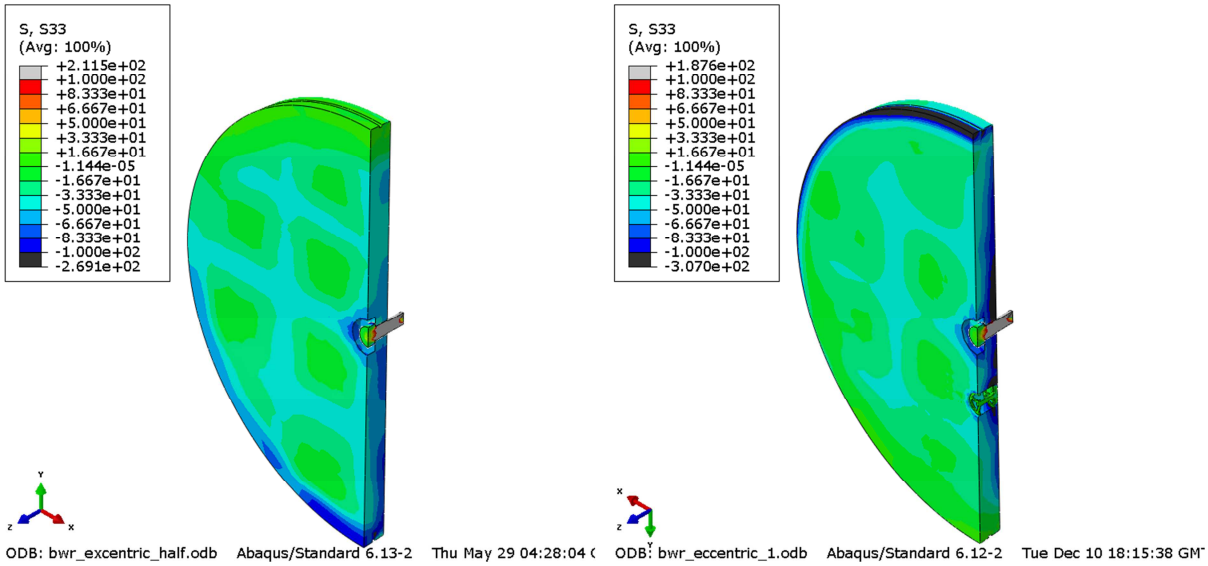

Figure 9-29 *Plots showing axial stress (S33 [MPa]) for the insert after 5 cm shearing for first (right) and second (left) case eccentric BWR model.*

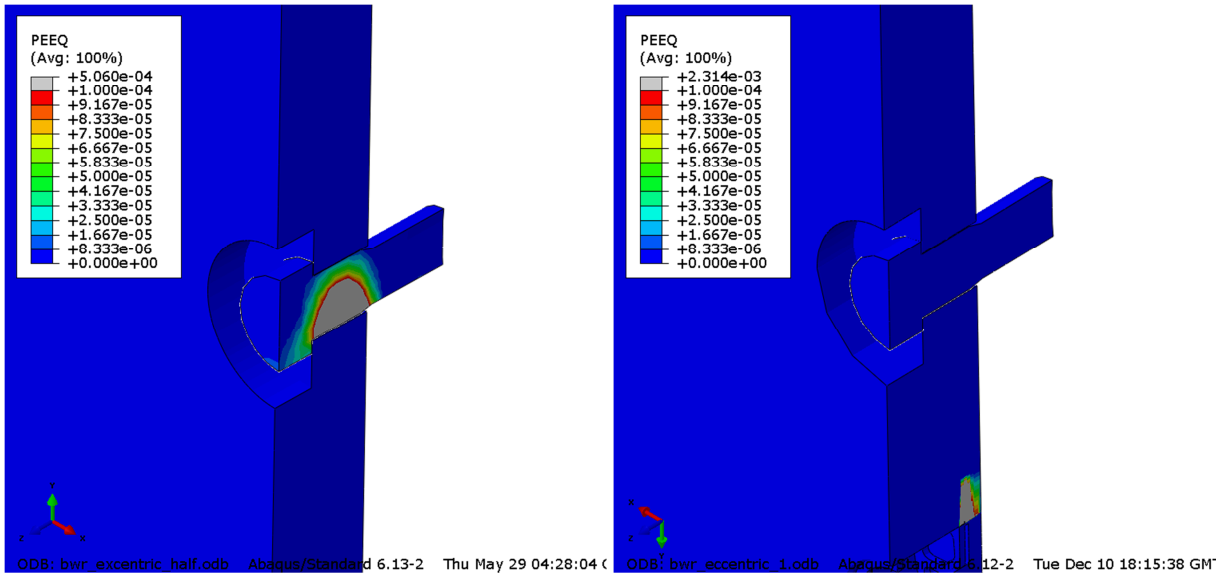

Figure 9-30 *Plots showing plastic equivalent strain (PEEQ) for the insert lid and centre screw after 5 cm shearing for first (right) and second (left) case eccentric BWR model.*

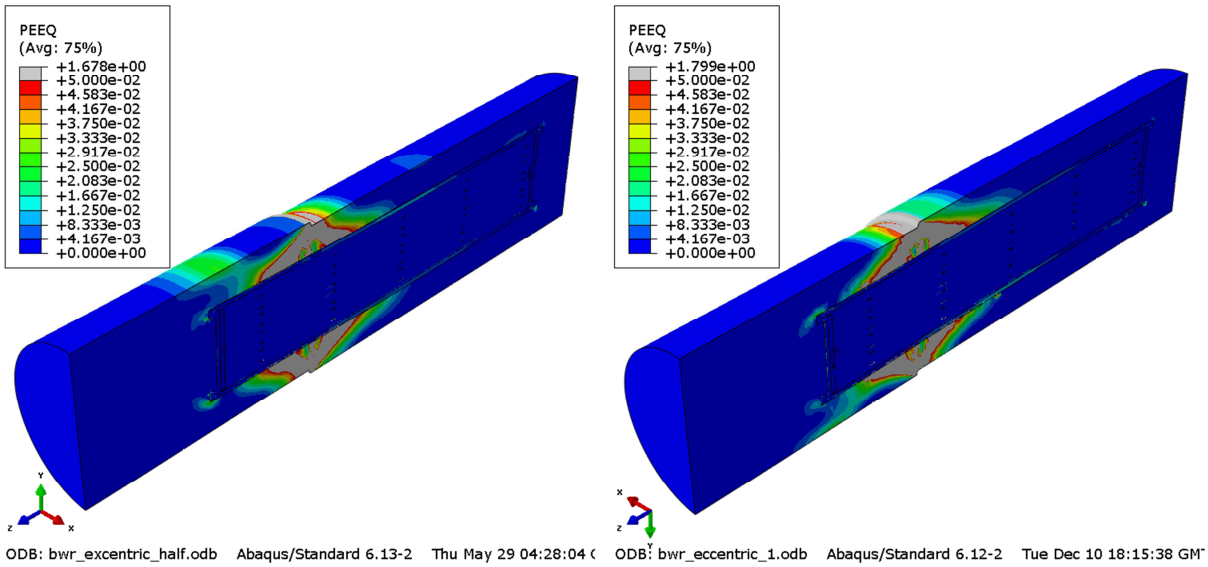

Figure 9-31 *Plots showing plastic equivalent strain (PEEQ) for the buffer after 5 cm shearing for first (right) and second (left) case eccentric BWR model.*

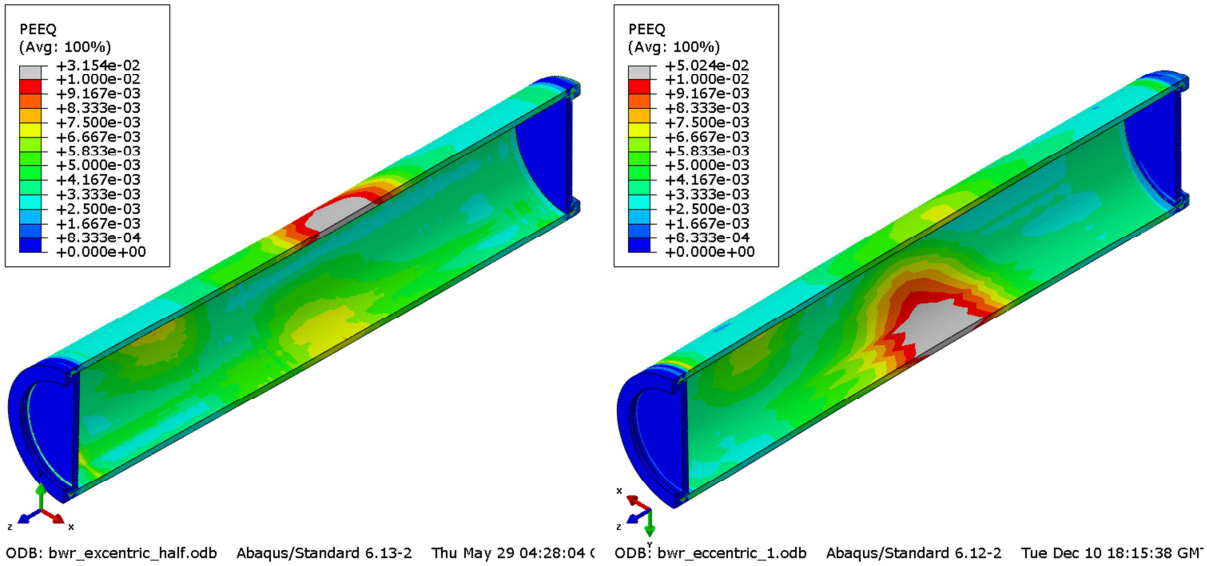

Figure 9-32 *Plots showing plastic equivalent strain (PEEQ) for the copper shell after 5 cm shearing for first (right) and second (left) case eccentric BWR model.*

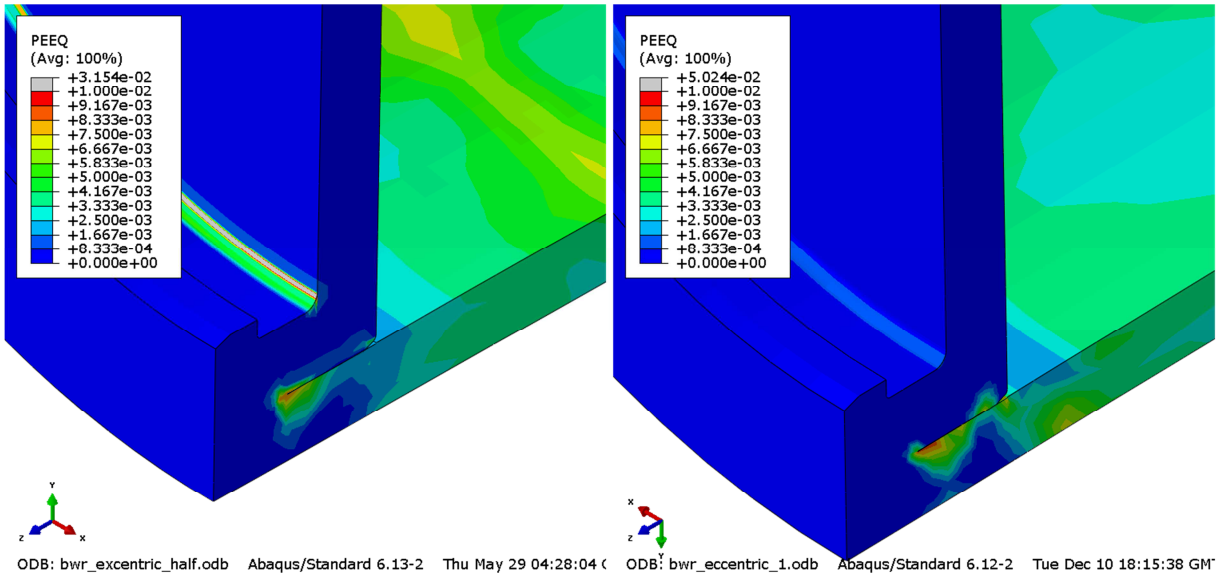

Figure 9-33 *Plots showing plastic equivalent strain (PEEQ) for the copper shell left top after 5 cm shearing for first (right) and second (left) cases eccentric BWR model.*

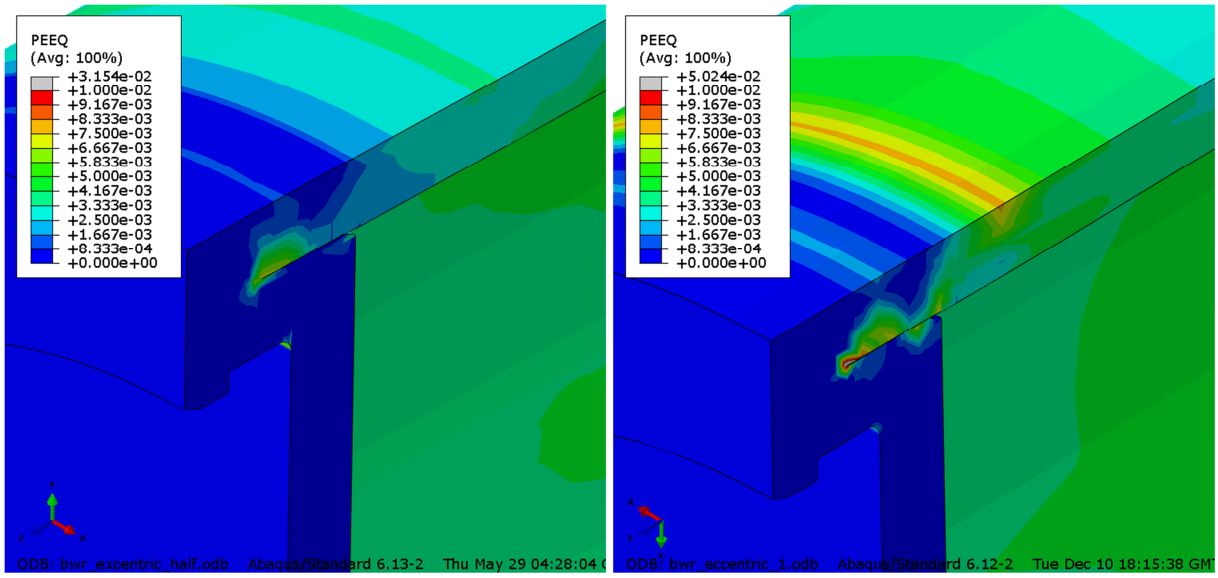

Figure 9-34 *Plots showing plastic equivalent strain (PEEQ) for the copper shell right top after 5 cm shearing for first (right) and second (left) cases eccentric BWR model.*

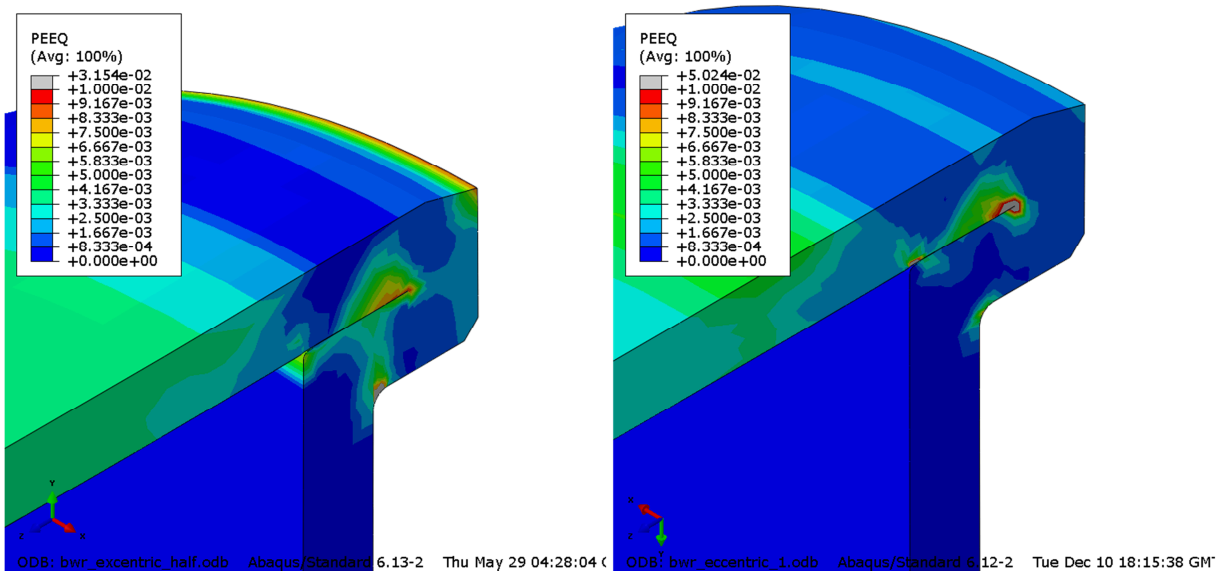

Figure 9-35 *Plots showing plastic equivalent strain (PEEQ) for the copper shell right bottom after 5 cm shearing for first (right) and second (left) case eccentric BWR model.*

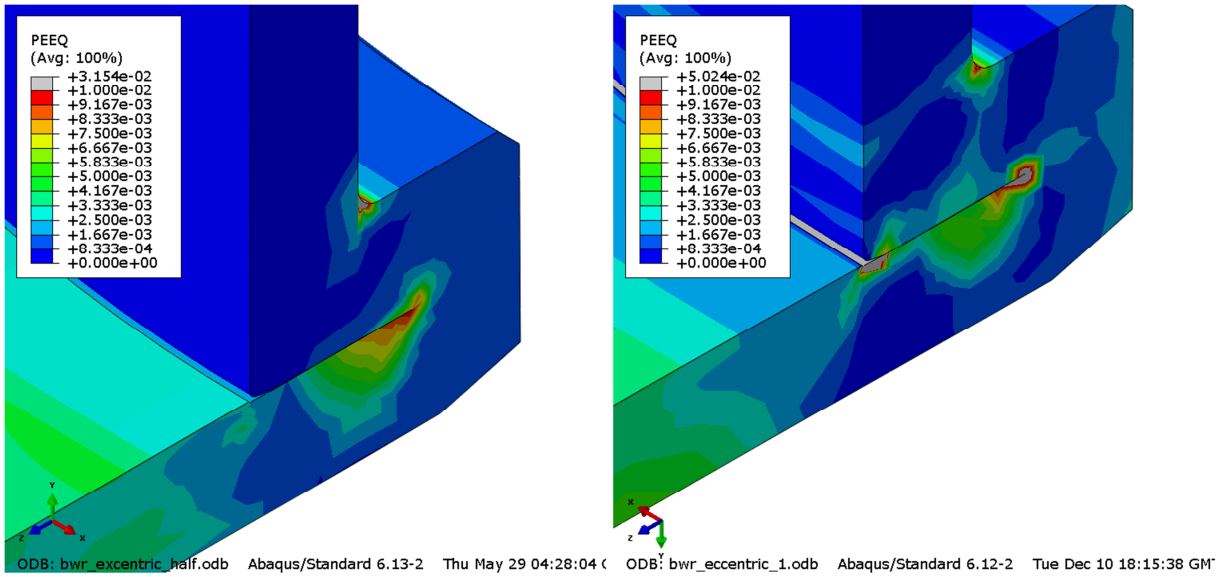

Figure 9-36 *Plots showing plastic equivalent strain (PEEQ) for the copper shell left bottom after 5 cm shearing for first (right) and second (left) cases eccentric BWR model.*

9.3 Steel channel tubes rotated for the BWR insert. Symmetrically and eccentrically positioned channel tubes.

Most analyses have been performed defining the shearing direction such that one symmetry plane exist which makes the analyses less demanding. However, there is a risk that defining the shearing direction to coincide with the direction where the distance between channel tube corner and the insert outer radius is shortest could imply larger stresses/strains. This could e.g. be achieved by rotating the channel tubes to have the shortest distance to the insert outer radius in the global y-direction. Two cases are studied:

- First (bwr_centric_rotated) case with the channel tubes positioned centric to the insert.
- Second case (bwr_eccentric_rotated) with the channel tubes positioned eccentrically (10 mm eccentricity).

Figures 9-37 – 9-47 shows comparison of results for these two cases after 5 cm shearing (Appendix 7 show results after 9 cm shearing).

The obtained results for stresses and strains show small differences between the two cases even though there are some findings:

- Maximum global stresses and strains are used by bending of the insert.
- Eccentric positioned channel tubes moves the bending axis which means that stresses/strains increase in the region with axial tensile stresses and decrease in the region with axial compressive stresses when comparing with centric positioned channel tubes, see e.g. Figures 9-38 – 9-39.
- Maximum plastic equivalent strain is however caused by shearing stress and occurs close to the bending axis.
- For the copper shell there are six regions with similar magnitude of maximum plastic equivalent strain (fillets at top and base, welds at top and base and also top and base of the outer shell), see Figures 9-43 – 9-47. However, the maximum magnitude of PEEQ is rather low 3.4% for the eccentric positioned channel tubes and 2.8% for the centric positioned channel tubes.

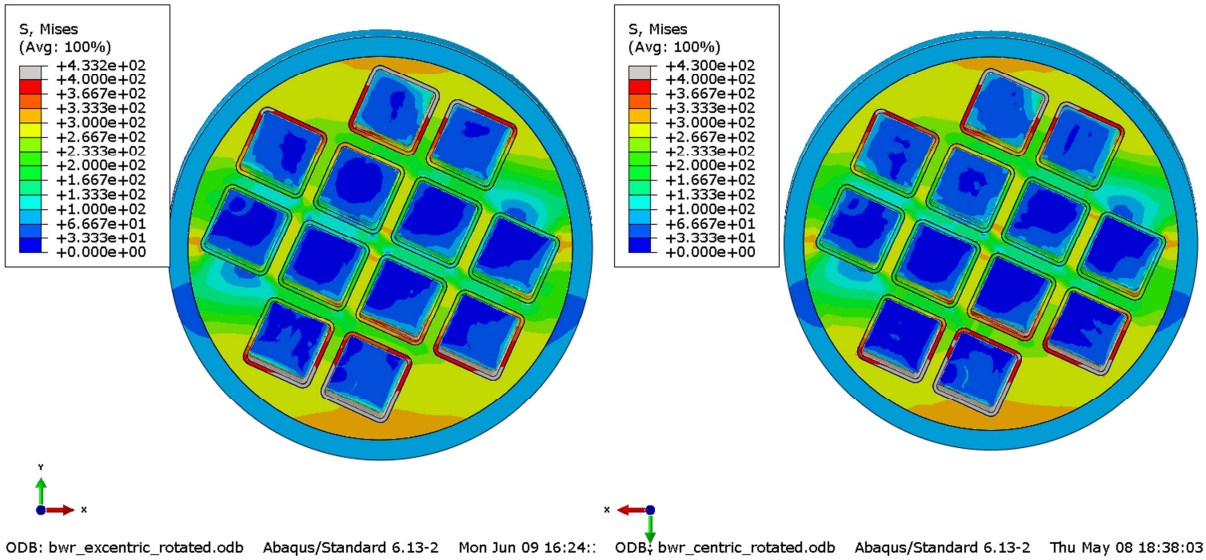

Figure 9-37 *Plots showing Mises stress [MPa] for the insert after 5 cm shearing with rotated channel tubes for eccentric(left) and centric (right) BWR model.*

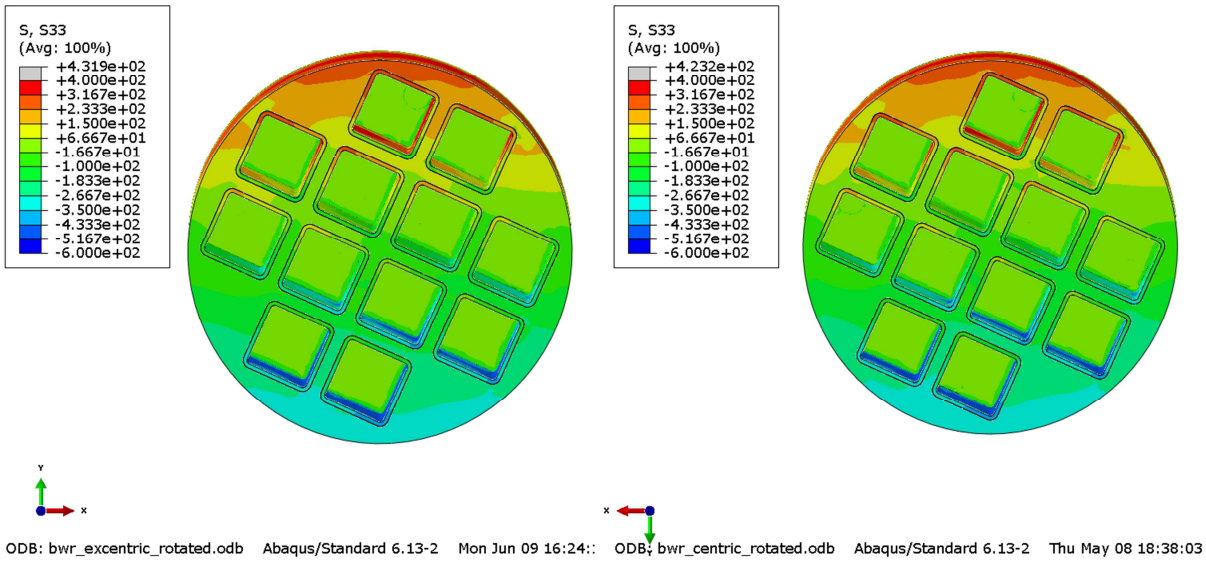

Figure 9-38 *Plots showing axial stress, S33, [MPa] for the insert after 5 cm shearing with rotated channel tubes for eccentric(left) and centric (right) BWR model.*

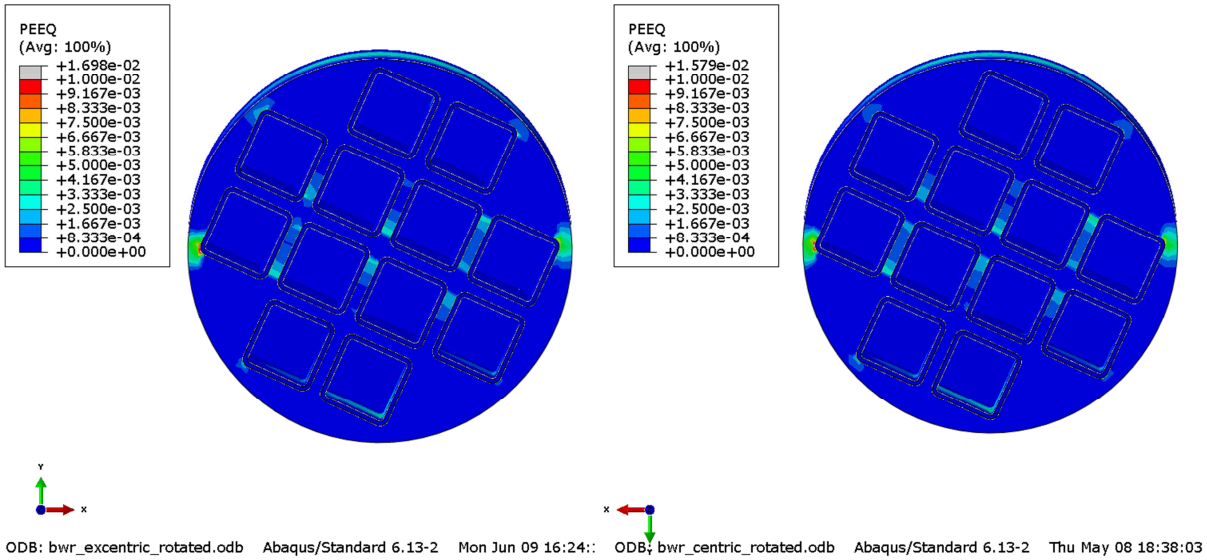

Figure 9-39 *Plots showing plastic equivalent strain (PEEQ)] for the insert after 5 cm shearing with rotated channel tubes for eccentric (left) and centric (right) BWR model.*

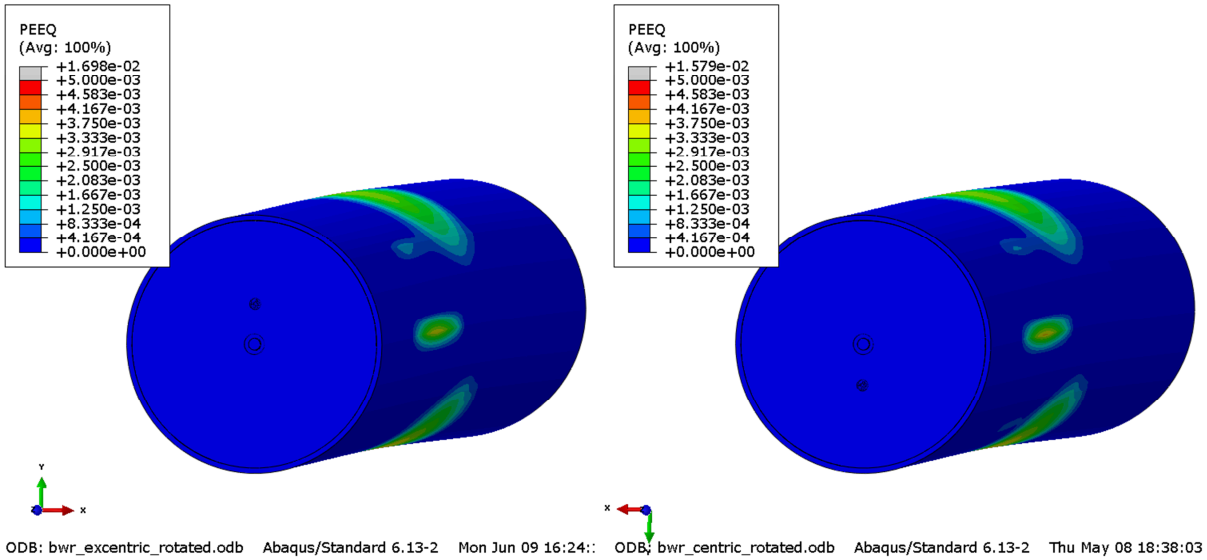

Figure 9-40 *Plots showing plastic equivalent strain (PEEQ) for the insert after 5 cm shearing with rotated channel tubes for eccentric (left) and centric (right) BWR model.*

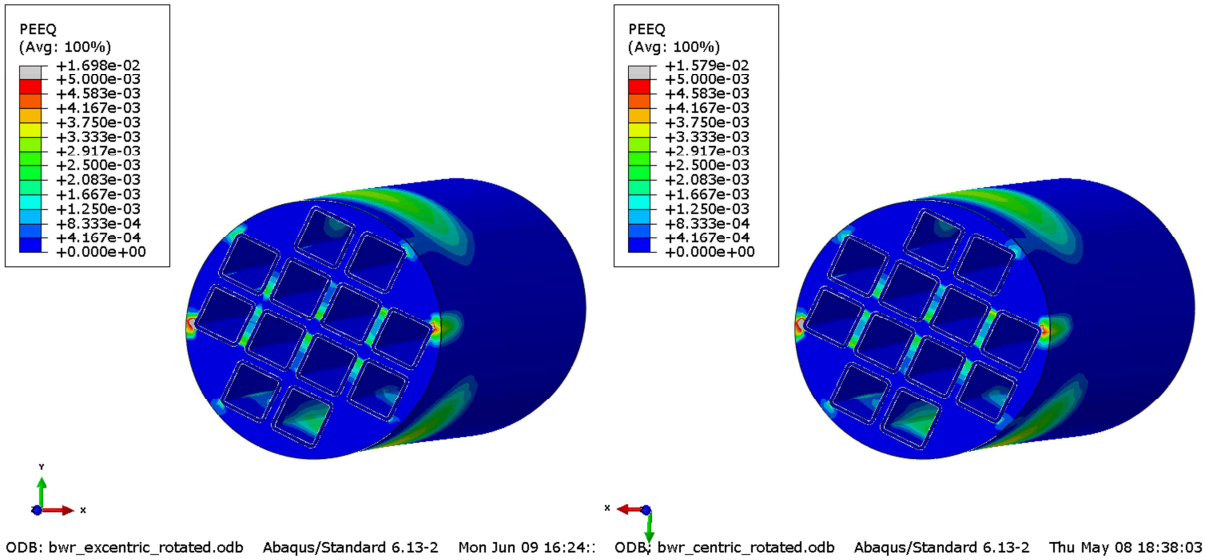

Figure 9-41 *Plots showing plastic equivalent strain (PEEQ) for the insert section with maximum magnitude after 5 cm shearing with rotated channel tubes for eccentric (left) and centric (right) BWR model.*

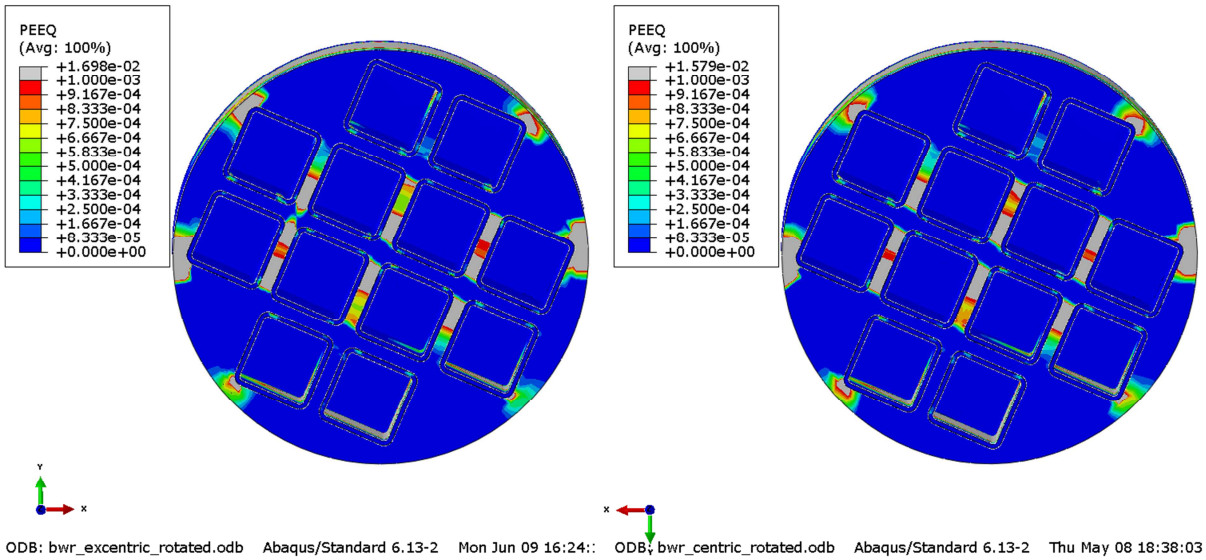

Figure 9-42 *Plots showing plastic equivalent strain (PEEQ) for the insert section with maximum magnitude after 5 cm shearing with rotated channel tubes for eccentric (left) and centric (right) BWR model.*

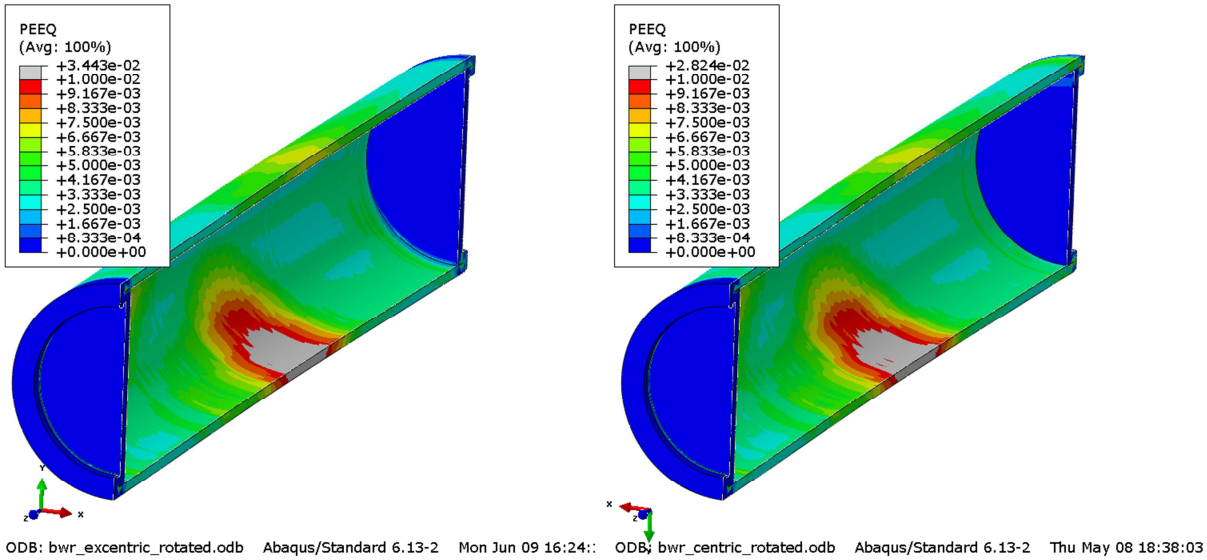

Figure 9-43 *Plots showing plastic equivalent strain (PEEQ) for the copper shell after 5 cm shearing with rotated channel tubes for eccentric (left) and centric (right) BWR model.*

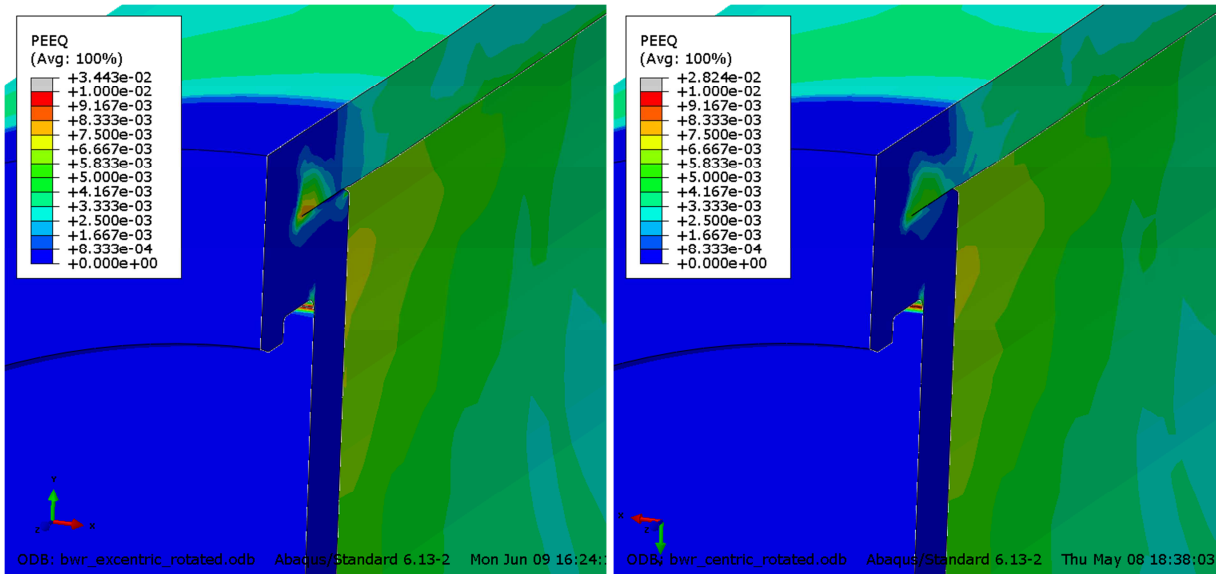

Figure 9-44 *Plots showing plastic equivalent strain (PEEQ) for the copper shell top upper corner after 5 cm shearing with rotated channel tubes for eccentric (left) and centric (right) BWR model.*

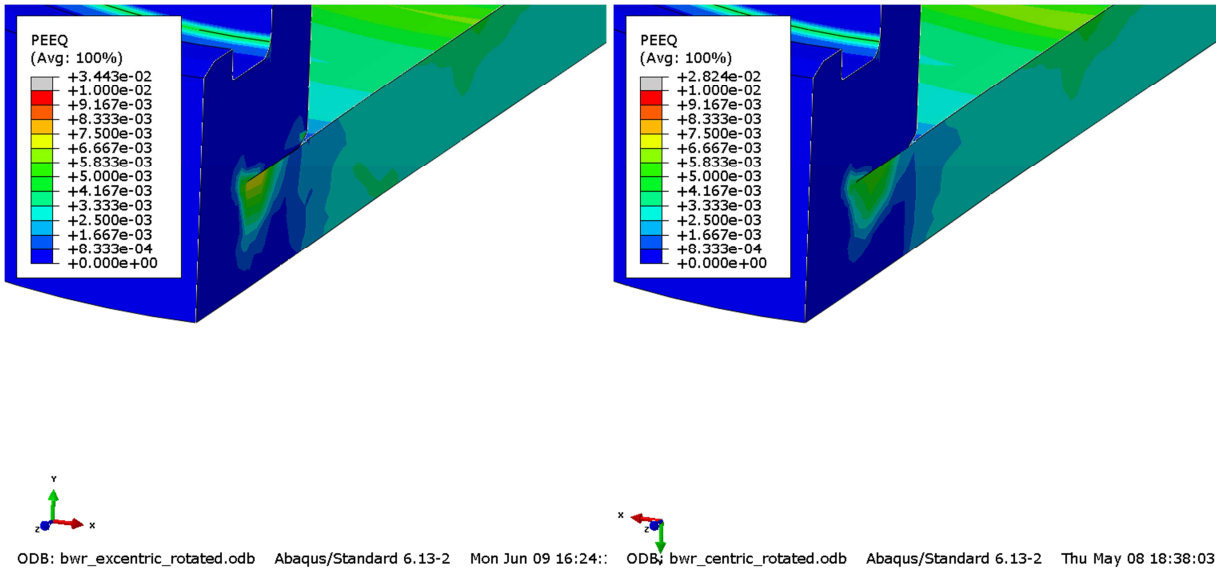

Figure 9-45 *Plots showing plastic equivalent strain (PEEQ) for the copper shell top lower corner after 5 cm shearing with rotated channel tubes for eccentric (left) and centric (right) BWR model.*

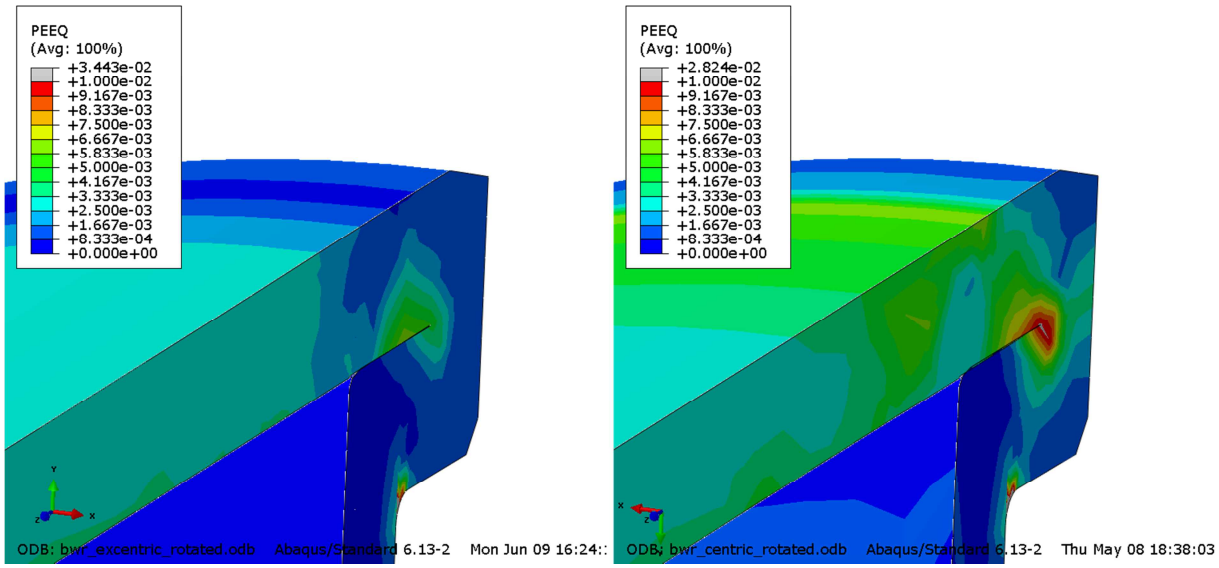

Figure 9-46 *Plots showing plastic equivalent strain (PEEQ) for the copper shell bottom upper corner after 5 cm shearing with rotated channel tubes for eccentric (left) and centric (right) BWR model.*

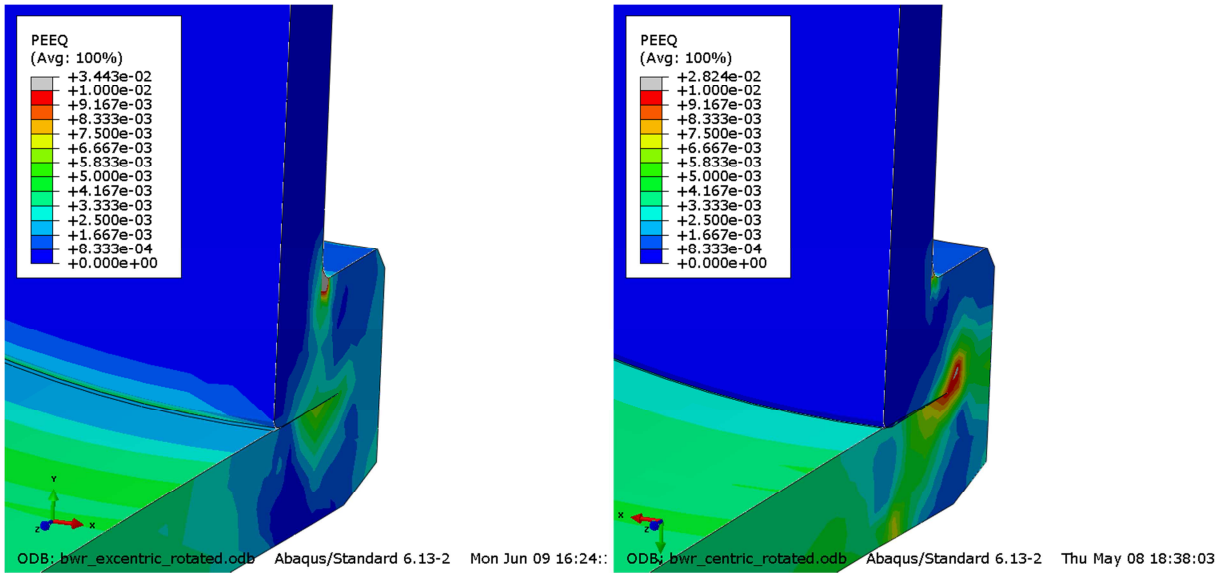

Figure 9-47 *Plots showing plastic equivalent strain (PEEQ) for the copper shell bottom lower corner after 5 cm shearing with rotated channel tubes for eccentric (left) and centric (right) BWR model.*

The rather high increase of stress and strain for the insert lid is explained by how the contact is modelled between the insert lid and the insert, see Figures 9-48 – 9-49. Figure 9-49 shows Mises stress when the elements with plasticity in the insert lid have been removed.

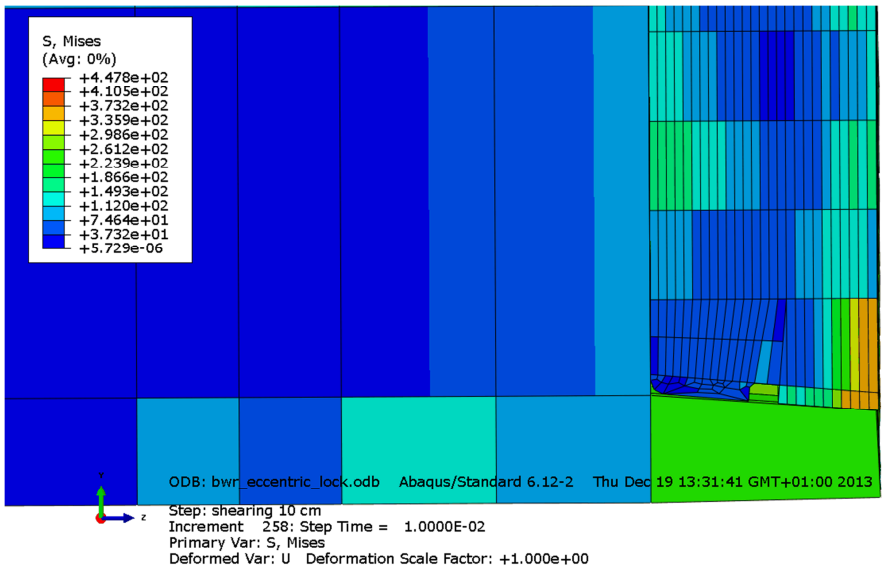

Figure 9-48 *Plots showing Mises stress in the insert lid and the insert at the upper lower corner. Note that the contact is lost at the top when shearing (6 cm) at the insert lid.*

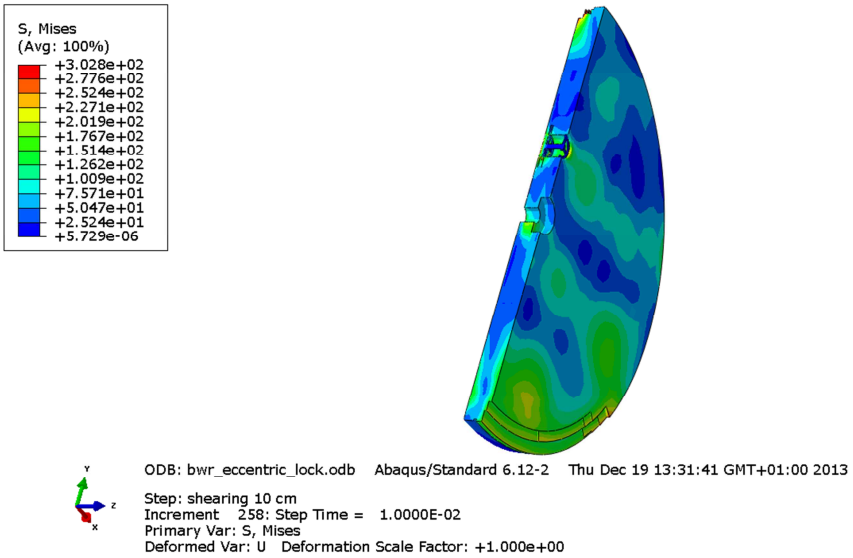

Figure 9-49 *Plots showing Mises stress in the insert lid when shearing (6 cm) at the insert lid. Elements with plasticity have been removed.*

9.4 Tables summarising results for the BWR-insert analyses

Below the obtained results are summarized in Tables 9-1 to 9-12. The tables show maximum values for Mises stress, PEEQ (plastic equivalent strain) and for the insert and channel tubes also maximum and minimum axial stress (S33). These values are not always representative since the extreme values could be caused by badly shaped elements or discontinuities in the geometry and furthermore the values are taken from the corresponding contour plots which are based on extrapolated values. However, the values together with contour plots can still be used for comparison purposes. Also note that the material definition only is satisfied at the integration points and e.g. if the yield surface has been reached then the Mises stress is defined from PEEQ at the integration points.

Tables 9-1 to 9-6 show the results for the BWR-insert for 5 and 8 cm shearing at ¾-distance from the insert base. The highest value for Mises stress in the insert occurs for the eccentric case, Table 9-1 and 9-2, even though that analysis stopped already at 6 cm shearing. The plastic strains are also higher for the detailed model mostly related to discontinuities close to the connection with the support plates (the weld has not been included which will increase stresses/strains).

Table 9-1. Maximum Mises stress [MPa] for BWR-insert with shearing of 5 cm at ¾-distance.

Model name	Copper shell	Insert	Channel tubes	Insert lid	Screw
Reference (Herenelind 2010) – model6g_normal_quarter_2050ca3	201	321	470	103	-
bwr_eccentric_lock	153	392	458	340	301
bwr_eccentric_1	152	401	468	270	291
bwr_excentric_half	112	396	506	307	332
bwr_centric_rotated	109	360	430	239	335
bwr_eccentric_rotated	116	365	433	223	335

Table 9-2. Maximum Mises stress [MPa] for BWR-insert with shearing of 8 cm at ¾-distance.

Model name	Copper shell	Insert	Channel tubes	Insert lid	Screw
Reference (Hernelind 2010) – model6g_normal_quarter_2050ca3	199	341	606	122	-
bwr_eccentric_lock	172	413	506	344	306
bwr_eccentric_1 (6 cm)	157	417	483	258	296
bwr_excentric_half	120	432	496	325	335
bwr_centric_rotated	119	396	465	245	336
bwr_eccentric_rotated	126	414	470	229	336

Table 9-3. Maximum PEEQ (plastic equivalent strain) [%] for BWR-insert with shearing of 5 cm at ¾-distance.

Model name	Copper shell	Insert	Channel tubes	Insert lid	Screw
Reference (Hernelind 2010) – model6g_normal_quarter_2050ca3	9.1	0.54	0.88	0	-
bwr_eccentric_lock	5.1	1.5	3.7	0.35	0.001
bwr_eccentric_1	5	2.7	4.5	0.23	0
bwr_excentric_half	3.15	2.1	2.9	0.05	0.03
bwr_centric_rotated	2.8	1.4	1.6	0	0.03
bwr_eccentric_rotated	3.4	1.6	1.7	0.03	0.03

Table 9-4. Maximum PEEQ (plastic equivalent strain) [%] for BWR-insert with shearing of 8 cm at ¾-distance.

Model name	Copper shell	Insert	Channel tubes	Insert lid	Screw
Reference (Hernelind 2010) – model6g_normal_quarter_2050ca3	9.1	1.2	2.2	0	
bwr_eccentric_lock	6.0	3.8	7.5	0.68	0.0015
bwr_eccentric_1 (6 cm)	5.5	4.1	5.7	0.23	0
bwr_excentric_half	3.8	3.9	6.7	0.08	0.03
bwr_centric_rotated	3.7	3.1	4.2	0	0.04
bwr_eccentric_rotated	4.3	3.9	4.7	0.06	0.03

Table 9-5. Axial stress, S33 [MPa] for BWR-insert with shearing of 5 cm at ¾-distance.

Model name	Insert		Channel tubes	
	maximum	minimum	maximum	minimum
Reference (Hernelind 2010) – model6g_normal_quarter_2050ca3	333	-439	452	-599
bwr_eccentric_lock	395	-441	414	-526
bwr_eccentric_1	395	-524	406	-580
bwr_excentric_half	379	-475	423	-511
bwr_centric_rotated	366	-448	423	-520
bwr_eccentric_rotated	380	-444	432	-515

Table 9-6. Axial stress, S33 [MPa] for BWR-insert with shearing of 8 cm at ¾-distance.

Model name	Insert		Channel tubes	
	maximum	minimum	maximum	minimum
Reference (Hernelind 2010) – model6g_normal_quarter_2050ca3	351	-463	463	-617
bwr_eccentric_lock	451	-501	430	-593
bwr_eccentric_1 (6 cm)	438	-569	415	-613
bwr_excentric_half	434	-524	440	-528
bwr_centric_rotated	390	-483	447	-553
bwr_eccentric_rotated	405	-473	447	-535

When shearing at the insert lid the most significant finding is the increase of stresses and strains for the insert lid when using the detailed model, Tables 9-7 to 9-12. The insert lid shows locally some small plasticity and is judged to not cause any severe damage. The rather high increase of stress and strain is explained by how the contact is modelled between the insert lid and the insert, see Figures 9-48 – 9-49.

The axial stress shows as expected lower values, Tables 9-5, 9-6 and 9-9, when shearing at the insert lid compared to shearing at ¾-distance from the base.

Table 9-7. Maximum Mises stress [MPa] for BWR-insert with shearing of 5 cm at insert lid.

Model name	Copper shell	Insert	Channel tubes	Insert lid	Screw
Reference (SKBdoc 1339902) – N34b_finer_1sekm_normal_quasi_model6	183	178	322	160	-
bwr_eccentric_lock	216	355	425	350	341

Table 9-8. Maximum Mises stress [MPa] for BWR-insert with shearing of 6 cm at insert lid.

Model name	Copper shell	Insert	Channel tubes	Insert lid	Screw
Reference (SKBdoc 1339902) – N34b_finer_1sekm_normal_quasi_model6	187	201	349	169	-
bwr_eccentric_lock	227	365	427	355	349

Table 9-9. Maximum PEEQ (plastic equivalent strain) [%] for BWR-insert with shearing of 5 cm at insert lid.

Model name	Copper shell	Insert	Channel tubes	Insert lid	Screw
Reference (SKBdoc 1339902) – N34b_finer_1sekm_normal_quasi_model6	9	0	0	0	-
bwr_eccentric_lock	15.5	1.1	1.1	0.98	0.42

Table 9-10. Maximum PEEQ (plastic equivalent strain) [%] for BWR-insert with shearing of 6 cm at insert lid.

Model name	Copper shell	Insert	Channel tubes	Insert lid	Screw
Reference (SKBdoc 1339902) – N34b_finer_1sekm_normal_quasi_model6	11	0	0	0	-
bwr_eccentric_lock	17	1.4	1.3	1.3	0.93

Table 9-11. Axial stress, S33 [MPa] for BWR-insert with shearing of 5 cm at insert lid.

Model name	Insert		Channel tubes	
	maximum	minimum	maximum	Minimum
Reference (SKBdoc 1339902) – N34b_finer_1sekm_normal_quasi_model6	89	-184	85	-253
bwr_eccentric_lock	382	-266	82	-237

Table 9-12. Axial stress, S33 [MPa] for BWR-insert with shearing of 6 cm at insert lid.

Model name	Insert		Channel tubes	
	maximum	minimum	maximum	minimum
Reference (SKBdoc 1339902) – N34b_finer_1sekm_normal_quasi_model6	202	-198	99	-270
bwr_eccentric_lock	389	-272	91	-255

10 Uncertainties

The obtained results are based on several assumptions regarding loads and material properties. Also the discretization in the computer model will affect the results. Some of these influencing factors are addressed below:

- All experiments used for material calibration have a spread which will imply a range for the properties defining each material model.

- Material properties for bentonite and nodular cast iron depends on hydrostatic pressure but in this study the material definitions are based on Mises plasticity theory using tensile properties except for the bentonite where typical tests are triaxial compression and oedometer tests. Same assumptions have been used for material properties as in previous analyses, e.g. Hernelind (2010).

- Swelling pressure for the bentonite will affect the material stiffness. The experimental results have a spread in the results and the used data should be conservative in the sense that the obtained stress and strain magnitudes are overestimated.

- Element mesh is rather fine but nevertheless it is too coarse in some regions, especially at the welds and regions with geometric discontinuities. A more refined mesh will probably increase the maximum stress and strain levels. Fortunately, the use of non-linear material properties (such as plasticity) will decrease the sensitivity on the used mesh. The used mesh has been judged to be accurate enough for evaluation of expected stress and strain magnitudes. If more detailed results are required one possibility is to create submodels with boundary conditions from the reported global analyzes.

11 Evaluation and conclusions

The results obtained from the rock shear analyses could be summarized as follows.

- General findings
    - The maximum plastic strain in the copper shell, 15.5%, occurs in fillets (besides regions containing singularities) for the case bwr_eccentric_lock at 5 cm shearing.
    - The maximum plastic strains in the insert result from bending, case bwr_eccentric_1 at 6 cm shearing. However, the magnitude is small (4.1%) compared to ultimate strains (>6.3%) and is considered not to threaten the mechanical integrity. At 5 cm shearing the magnitude of PEEQ is 2.7%.
    - The maximum principal stress in the insert, 511 MPa, mainly comes from bending of the shell, case bwr_eccentric_1 at 6 cm shearing (463 MPa at 5 cm shearing) – the level depends mainly on material properties for the insert (and dimensions) and the stiffness of the buffer.
    - The maximum plastic strain in the steel tubes, 7.5%, occurs at the corners of a specific steel tube, Figure A5-6. However, the magnitude is small compared to ultimate strains (>16%) and is considered not to cause any failure.
    - Strain rate effects for bentonite, copper and iron will affect the results. Strain rate dependency is included for the buffer and the cast iron. The copper shell will have the strain rate effect included when the creep model is used but in this study all analyzes have been performed by using Mises plasticity theory.
    - The nodular cast iron material has pressure dependent properties but data from tensile tests has been used which is considered to be pessimistic.
- Effect on modelling steel tubes with support plates and contact surfaces
    - The approach used for connecting the steel tubes to the insert (tied connection) in previous analyses (Hernelind 2010) imply very similar results as when modelling the connection with steel plates welded to the steel tubes. E.g. the axial stress (S33) differ less than 1% at 5 cm shearing for the insert outer surface compared with the reference case (Hernelind 2010), Figure 11-1. The peak values for S33 and Mises stress differ more where the support plates between the steel tubes are tied to the insert. Another finding is that the channel tubes have decreased stress magnitudes due to increased stiffness when including the support plates.

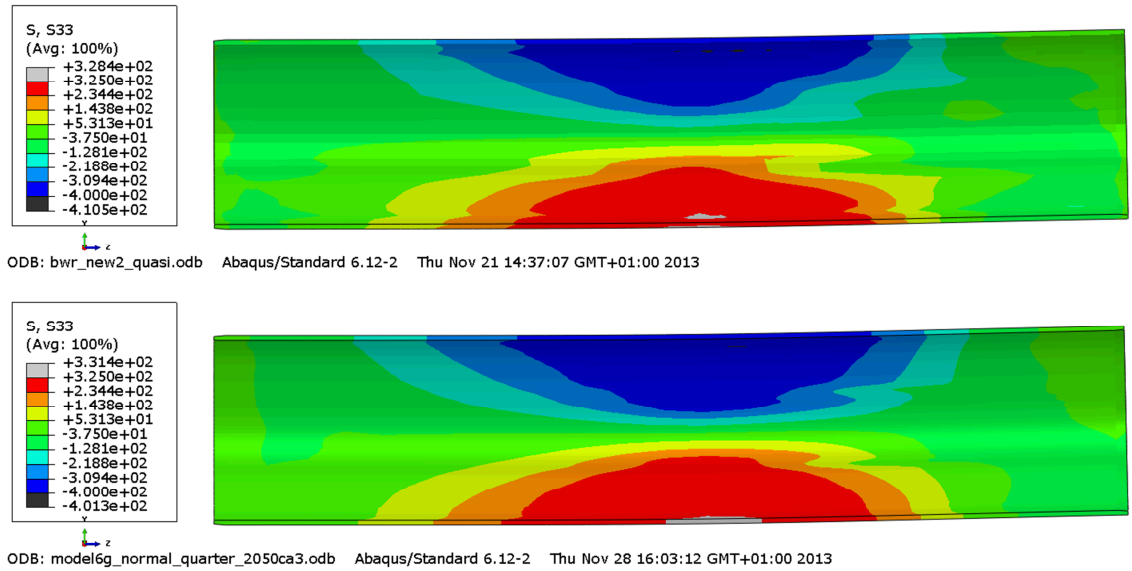

Figure 11-1. *Plots axial stress (S33) [MPa] for the insert outer surface after 5 cm shearing for detailed BWR model (upper) and the reference BWR model (lower). Symmetrically positioned channel tubes.*

- Effect of modelling the insert lid with a fixing screw in the centre
    - Modelling the insert lid with a fixing screw in the centre will change the stress distribution in the insert lid ends as well at the peripheral insert top but the strain/strain-level is still not considered to cause any severe damage. The stresses in the insert lid are in the elastic range except for a small region close to the contact with the insert – small equivalent plastic strains less than 0.01. Also the screw shows stresses in the elastic range except locally close to the contact with the insert lid. Low pre-stress in the screw implies slip between screw head and insert lid - the screw takes the load by almost pure elastic shear stresses. High pre-stress in the screw prevents slip and the screw takes the load by bending causing some plasticity (equivalent plastic strain less than 0.005). Using a washer distributes the contact stresses more smoothly but doesn't change the conclusions above.
- Effect of including small details
    - Neglecting small details (screw holes, steel tube bottom plates, screws and nuts) does not cause any visible stress concentrations (except for the support plates). The Mises stress is in the elastic range at the insert base and steel tubes base (containing plates, screws and nuts) which is also the case for the insert top (containing a small screw hole). However, the mesh is not fine enough to have the correct stress distribution. A sub-model based on the obtained global displacement solution could be used to obtain more accurate results for these regions.
- Effect of manufacturing tolerances
    - Considering tolerances when creating the model increases stresses/strains in regions where the wall thickness have been reduced but the magnitude for stress/strain will not cause any failure. At the corner where the wall thickness is smallest the equivalent plastic strain (PEEQ) increases at most from 1.5% to 2.7%, comparing bwr_eccentric_lock with bwr_eccentric_1.
- Effect of changed direction of shearing (rotated channel tubes), 8 cm shearing.

- Eccentric positioned channel tubes has slightly higher magnitude of PEEQ compared to centric positioned channel tubes for the insert (3.9% respectively 3.1%) and occurs in the region with compressive axial stress.

- For the channel tubes the corresponding values for PEEQ are 4.7% respectively 4.2%.

- For the copper shell the corresponding values for PEEQ are 4.3% respectively 3.7%.

The plastic equivalent strains are low for all cases and occurs at localized regions, except for the insert when shearing at ¾-distance from the base where the highest strain of 4.1% at 6 cm shearing and 2.7% at 5 cm shearing is found. However, also this strain level is considered to be low and will not break the insert.

The insert lid have for most cases a pure elastic response and when plastic strains occur (as most about 6%), they are very localized and will not cause any failure.

Maximum equivalent plastic strain in the copper shell, 15.5%, is found at a geometric discontinuity and is much localized. This strain level is not considered to cause any failure of the copper shell.

The used material definitions are valid for the strain levels obtained in the reported analyses and the strains are all far below any necking (or softening of the material when looking at engineering stresses/strains).

References

ABAQUS, 2013. Version 6.12.1. Dassault Systèmes Simulia Corp.

Börgesson L, 1988. Modelling of buffer material behaviour. Some examples of material models and performance calculations. SKB TR-88-29, Svensk Kärnbränslehantering AB.

Börgesson L, 1992. Interaction between rock, bentonite buffer and canister. FEM calculations of some mechanical effects on the canister in different disposal concepts. SKB TR-92-30, Svensk Kärnbränslehantering AB.

Börgesson L, Hernelind J, 2006. Earthquake induced rock shear through a deposition hole. Influence of shear plane inclination and location as well as buffer properties on the damage caused to the canister. SKB TR-06-43, Svensk Kärnbränslehantering AB.

Börgesson L, Johannesson L-E, Sandén T, Hernelind J, 1995. Modeling of the physical behavior of water saturated clay barriers. Laboratory tests, material models and finite element application. SKB TR 95-20, Svensk Kärnbränslehantering AB.

Börgesson L, Johannesson L-E, Hernelind J, 2004. Earthquake induced rock shear through a deposition hole. Effect on the canister and the buffer. SKB TR-04-02, Svensk Kärnbränslehantering AB.

Börgesson L, Dueck A, Johannesson L-E, 2010. Material model for shear of the buffer – evaluation of laboratory test results. SKB TR-10-31, Svensk Kärnbränslehantering AB.

Hernelind J, 2010. Modelling and analysis of canister and buffer for earthquake induced rock shear and glacial load. SKB TR-10-34, Svensk Kärnbränslehantering AB.

Jin L-Z, Sandström R, 2008. Creep of copper canisters in power-law breakdown. Computational Materials Science 43, 403–416.

Raiko H, Sandström R, Rydén H, Johansson M, 2010. Design analysis report for the canister. SKB TR-10-28, Svensk Kärnbränslehantering AB.

Sandström R, Andersson H C M, 2008. Creep in phosphorus alloyed copper during power-law breakdown. Journal of Nuclear Materials 372, 76–88.

Sandström R, Hallgren J, Burman G, 2009. Stress strain flow curves for Cu-OFP. SKB R-09-14, Svensk Kärnbränslehantering AB.

SKB, 2010. Design, production and initial state of the canister. SKB TR-10-14, Stockholm: Svensk Kärnbränslehantering AB.

SSABDirekt, 2008. Steelfacts Domex 355 MC. Available at http://www.ssabdirect.com. [19 September 2008].

SS-EN 10025-2:2004. Varmvalsade konstruktionsstål – Del 2: Tekniska leveransbestämmelser för olegerade stål (Hot rolled products of structural steels - Part 2: Technical delivery conditions for non-alloy structural steels). Stockholm: Swedish Standards Institute.

Unpublished documents

SKBdoc id, version	Title	Issuer, year
1201865 ver 1.0	Dragprovning av gjutjärn. (In Swedish.)	KTH, 2009
1203875 ver 1.0	Ritningsförteckning för kapselkomponenter. (In Swedish.)	SKB, 2009
1203875 ver 2.0	Ritningsförteckning för kapselkomponenter. (In Swedish.)	SKB, 2014
1339902 ver 1.0	Global simulation of copper canister – final deposition	SKB, 2013
1407337 ver 1.0	Earthquake induced rock shear through a deposition hole – Part 2. Additional calculations of the influence of inhomogeneous buffer on the stresses in the canister.	Clay Technology/ 5T Engineering, 2013
1415152 ver 2.0	Detailed models for PWR- and BWR-canisters for Earthquake induced rock shearing	5T Engineering, 2014

Appendix 1 – Plots for bwr_eccentric_lock

Plots showing deformed geometry as contour plots for all parts at shearing magnitude 5 and 8 cm for case bwr_eccentric_lock (horizontal shearing at ¾ distance from insert base). The view shows the symmetry plane and all deformations are scaled by a factor of two. Note! The analysis failed to converge for shearing displacement > 8 cm.

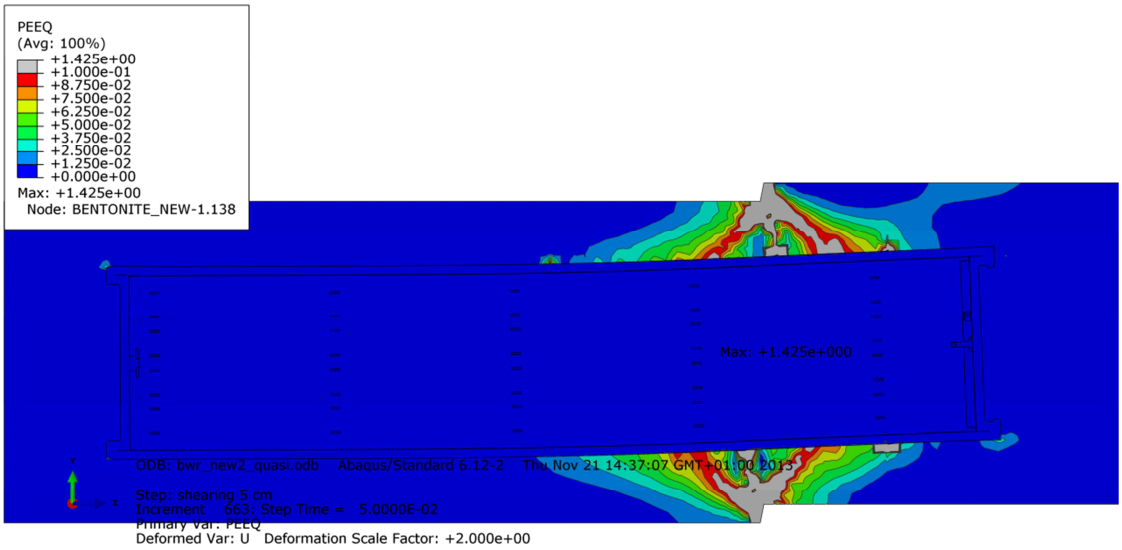

Figure A1-1 *Plot showing equivalent plastic strain (PEEQ) after 5 cm shearing.*

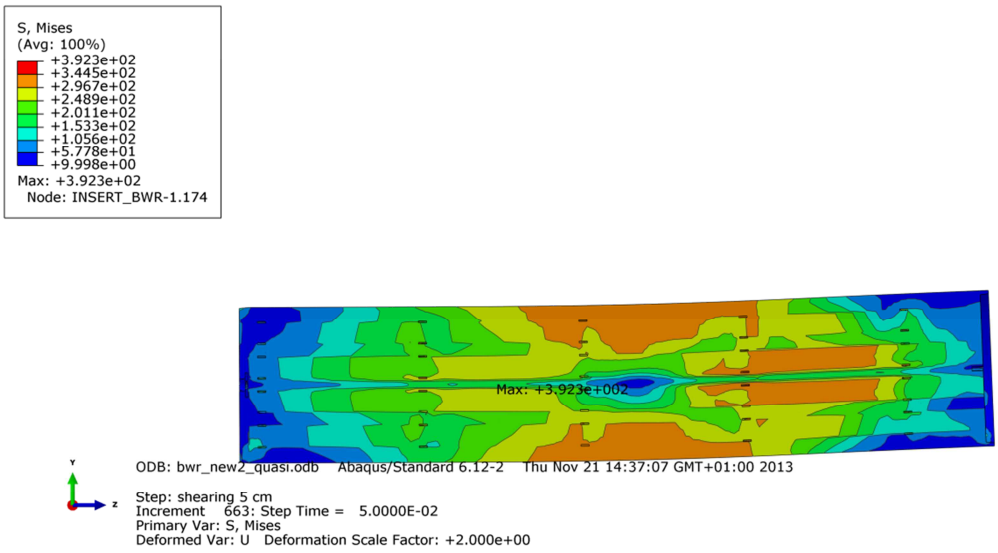

Figure A1-2 *Plot showing Mises stress [MPa] for the insert after 5 cm shearing.*

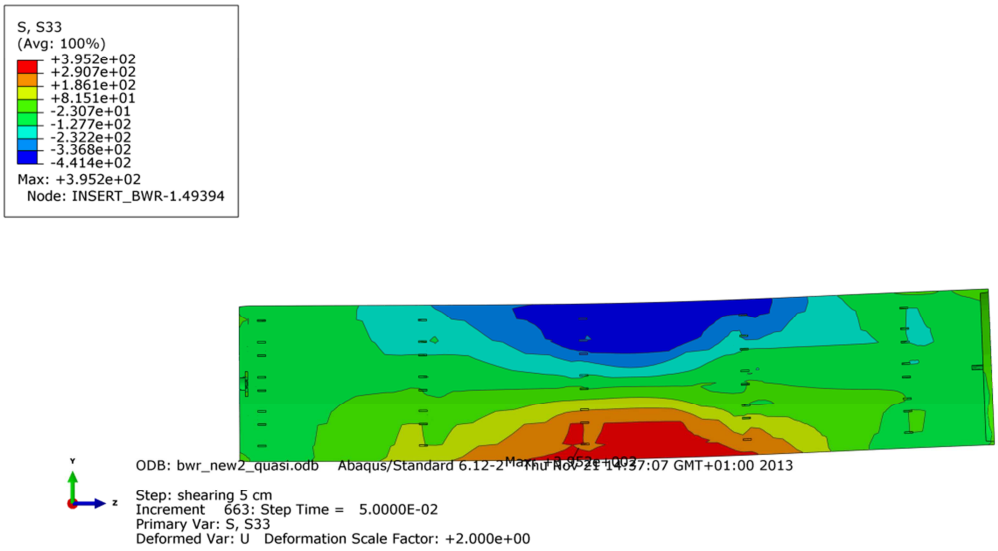

Figure A1-3 *Plot showing axial stress [MPa] for the insert after 5 cm shearing.*

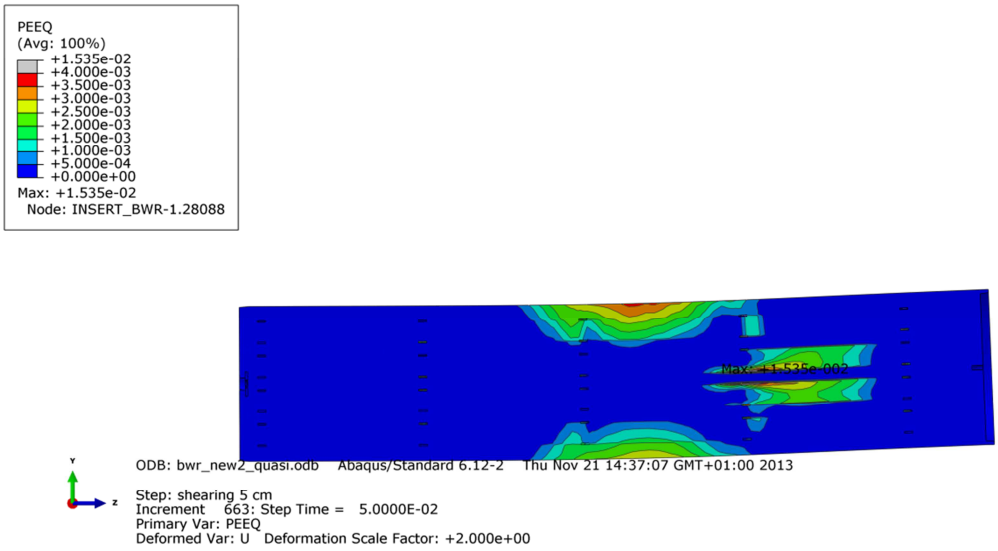

Figure A1-4 *Plot showing equivalent plastic strain (PEEQ) for the insert after 5 cm shearing.*

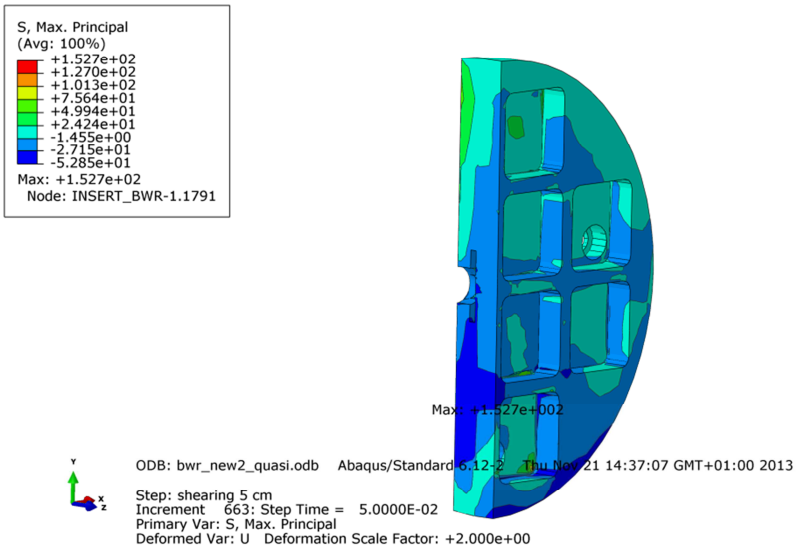

Figure A1-5 *Plot showing maximum principal stress [MPa] for the insert base after 5 cm shearing.*

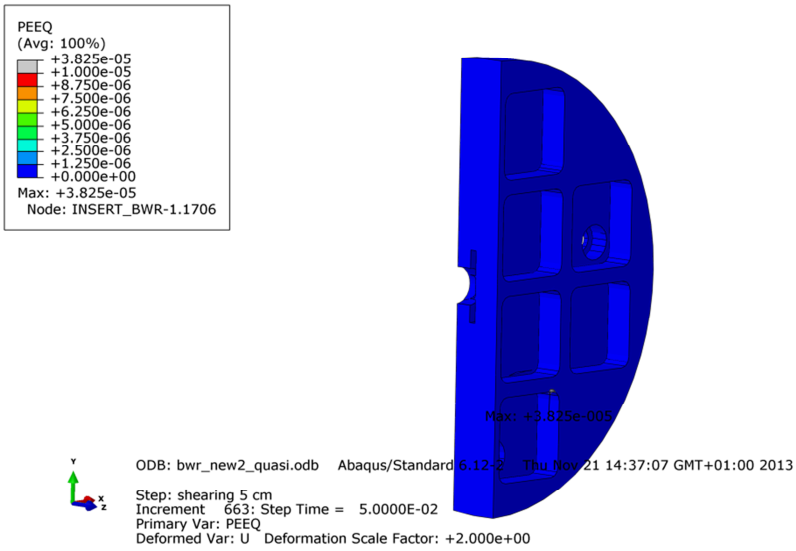

Figure A1-6 *Plot showing equivalent plastic strain (PEEQ) for the insert base after 5 cm shearing.*

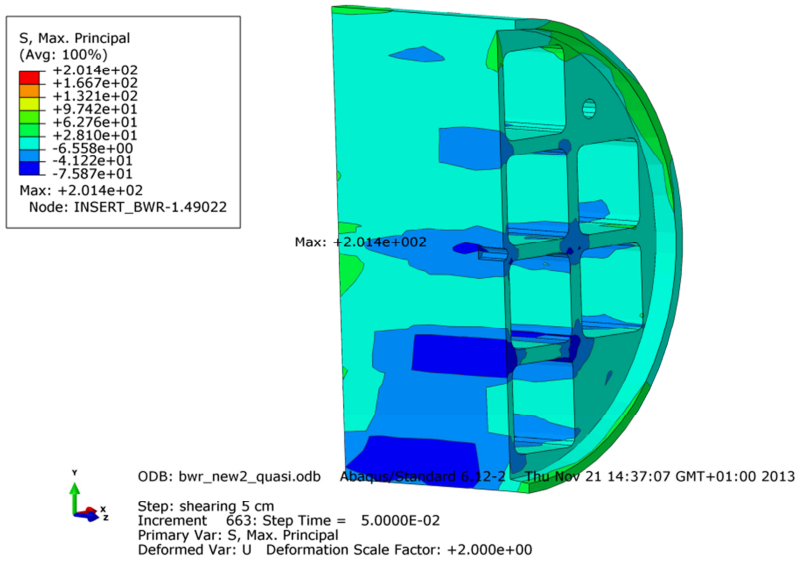

Figure A1-7 *Plot showing maximum principal stress [MPa] for the insert top after 5 cm shearing.*

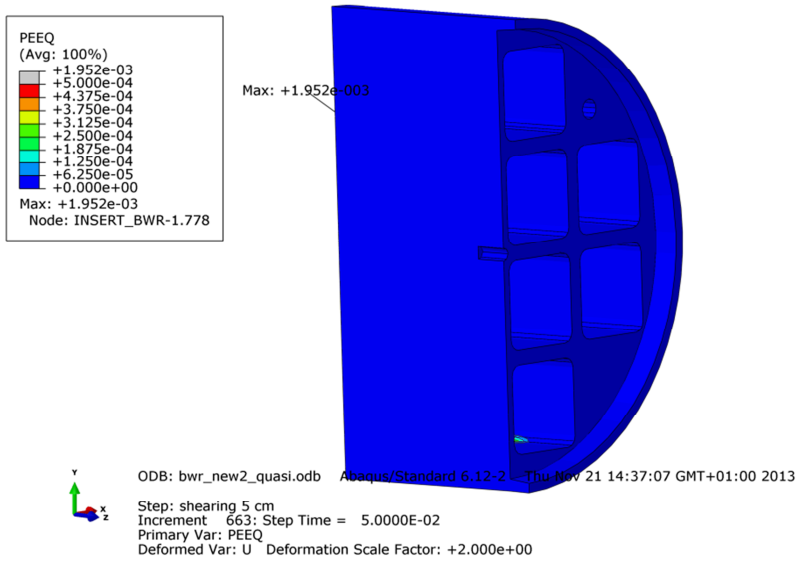

Figure A1-8 *Plot showing equivalent plastic strain (PEEQ) for the insert top after 5 cm shearing.*

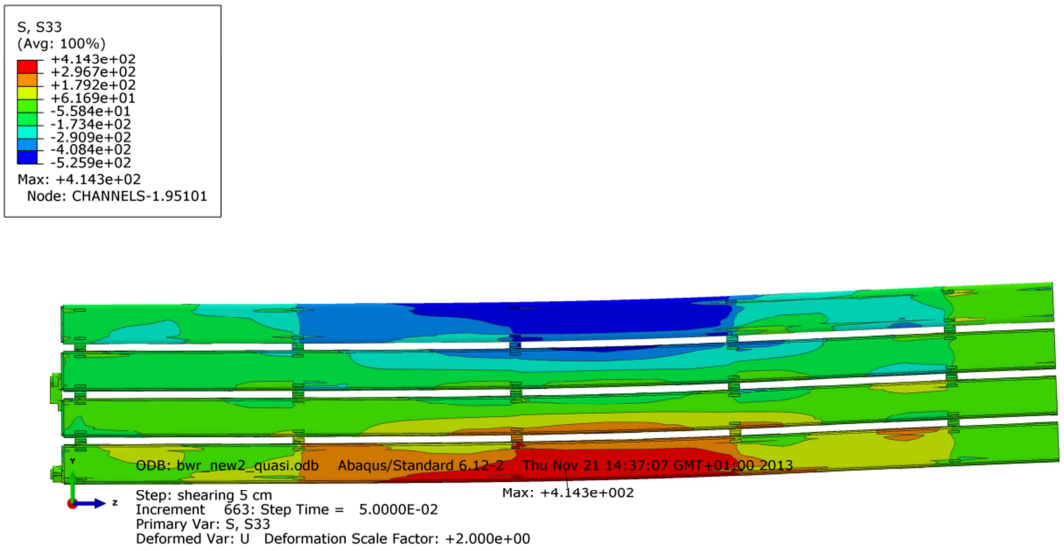

Figure A1-9 *Plot showing axial stress [MPa] for the steel channel tubes after 5 cm shearing.*

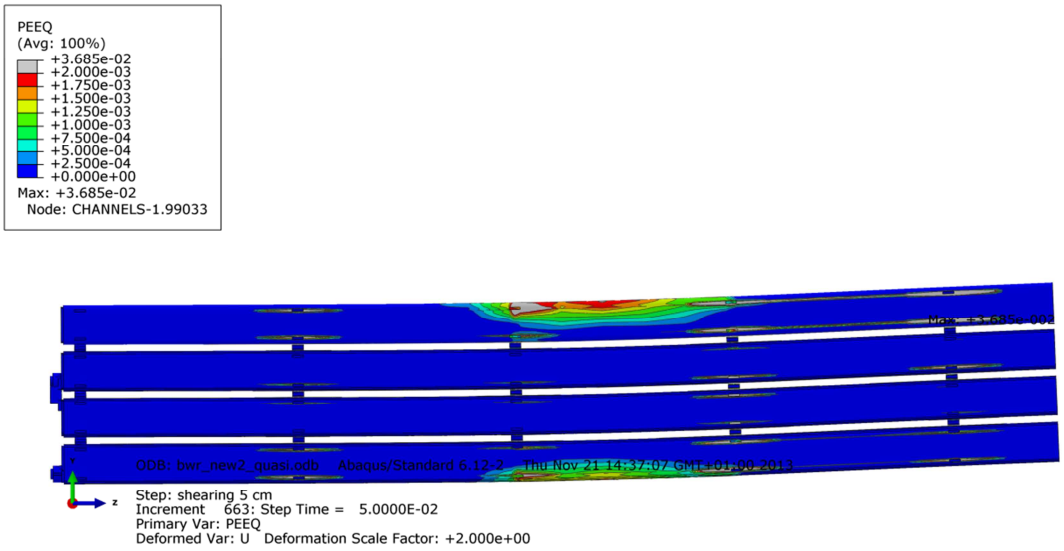

Figure A1-10 *Plot showing equivalent plastic strain (PEEQ) for the steel channel tubes after 5 cm shearing.*

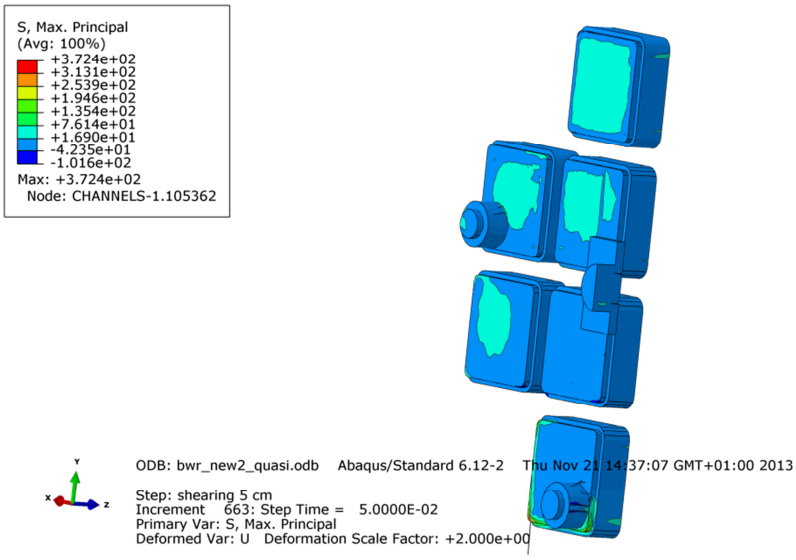

Figure A1-11 *Plot showing maximum principal stress [MPa] for the steel channel tubes base plates after 5 cm shearing.*

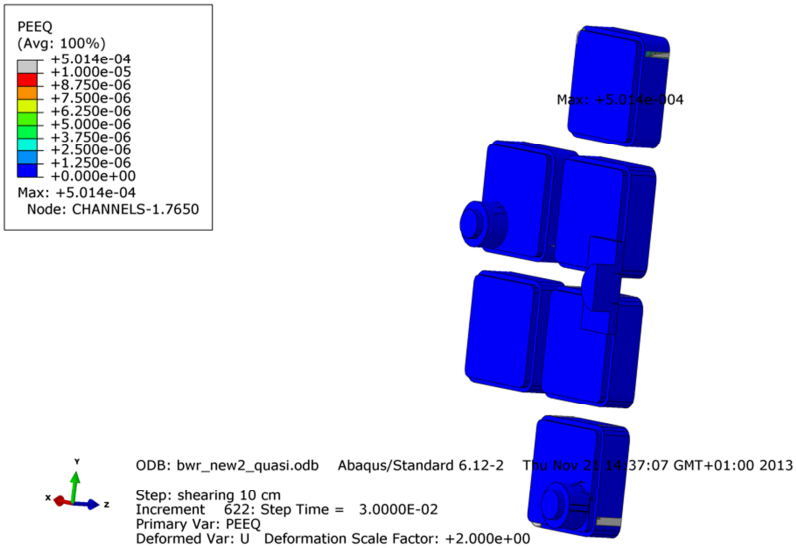

Figure A1-12 *Plot showing equivalent plastic strain (PEEQ) for the steel channel tubes base plates after 5 cm shearing.*

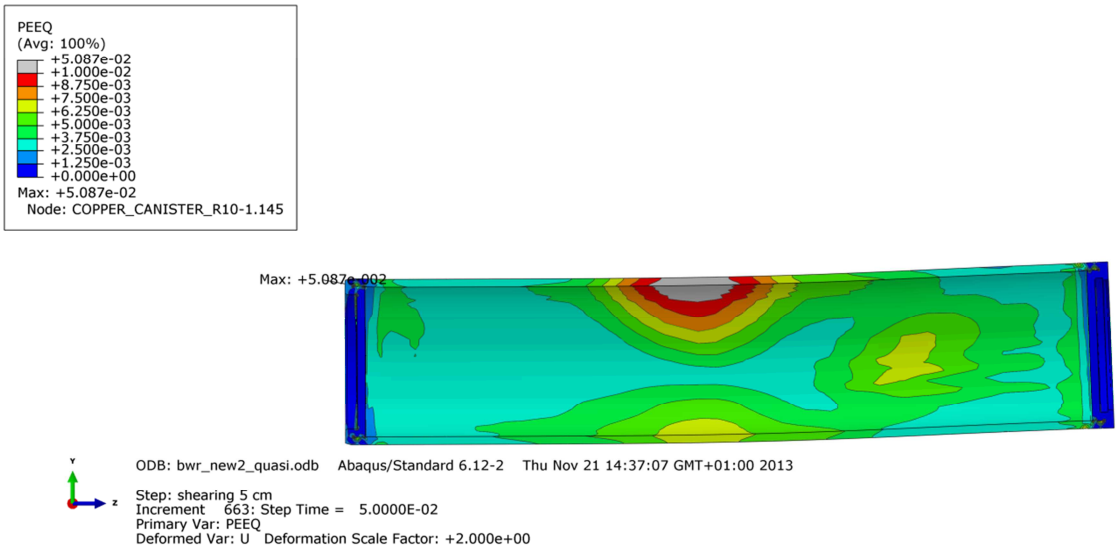

Figure A1-13 *Plot showing equivalent plastic strain (PEEQ) for the copper shell after 5 cm shearing.*

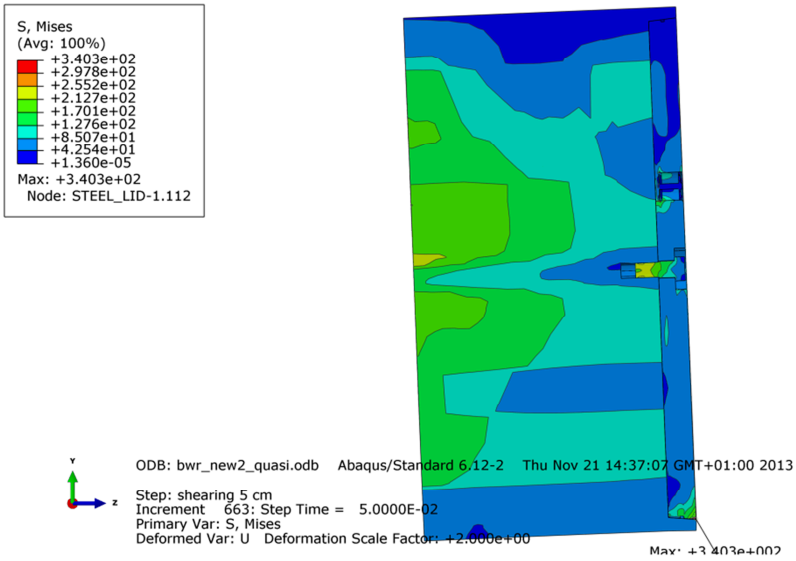

Figure A1-14 *Plot showing Mises stress [MPa] close to the insert lid fixing screw after 5 cm shearing.*

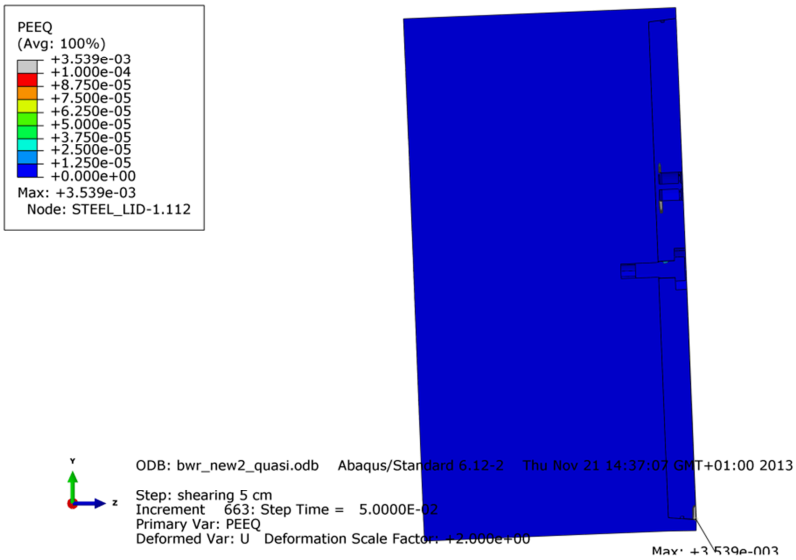

Figure A1-15 *Plot showing equivalent plastic strain (PEEQ) close to the insert lid fixing screw after 5 cm shearing.*

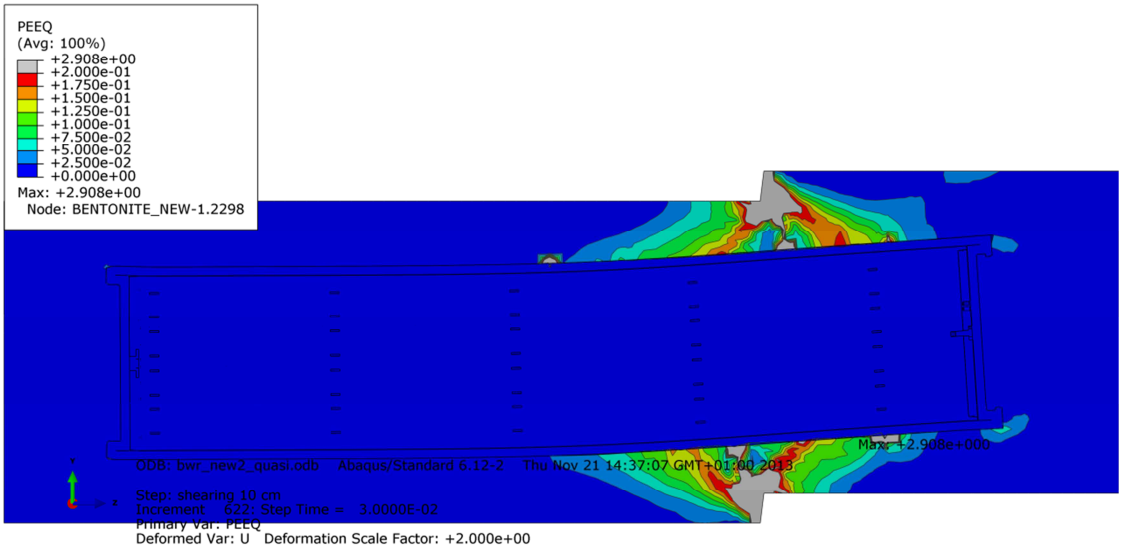

Figure A1-16 *Plot showing equivalent plastic strain (PEEQ) after 8 cm shearing.*

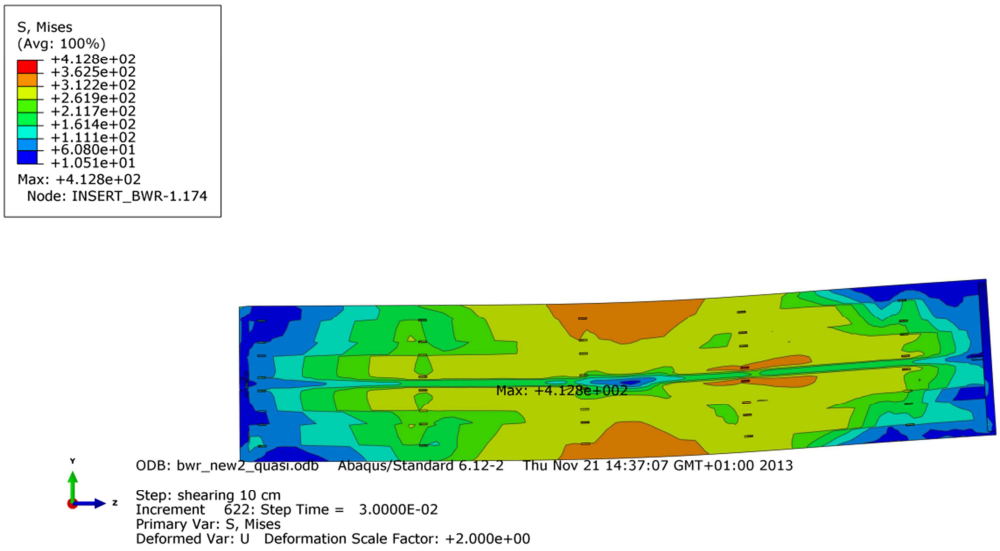

Figure A1-17 *Plot showing Mises stress [MPa] for the insert after 8 cm shearing.*

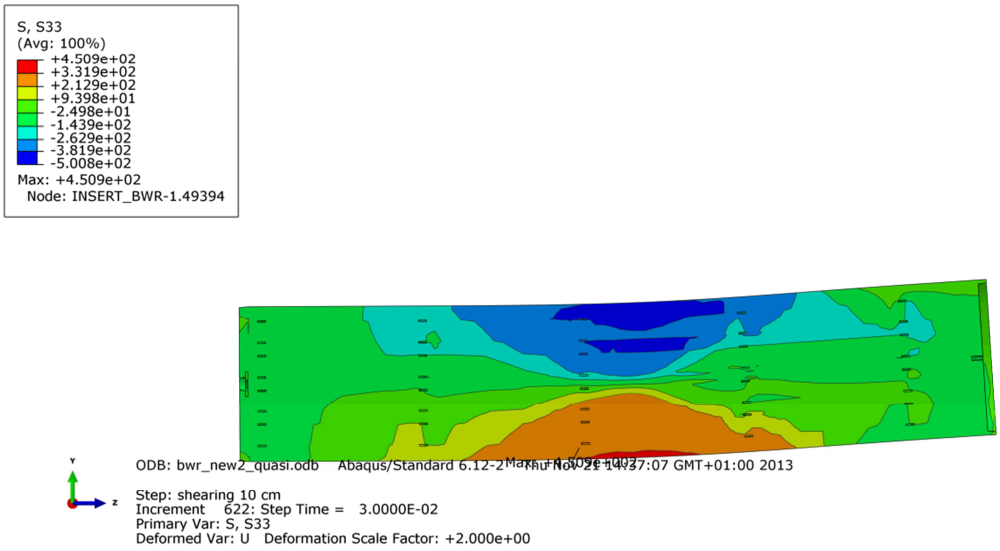

Figure A1-18 *Plot showing axial stress [MPa] for the insert after 8 cm shearing.*

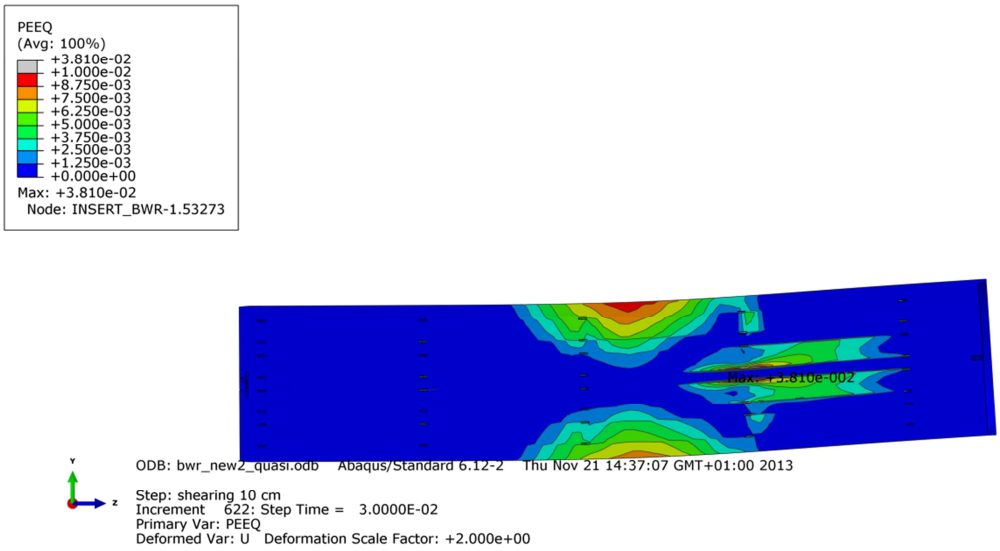

Figure A1-19 *Plot showing equivalent plastic strain (PEEQ) for the insert after 8 cm shearing.*

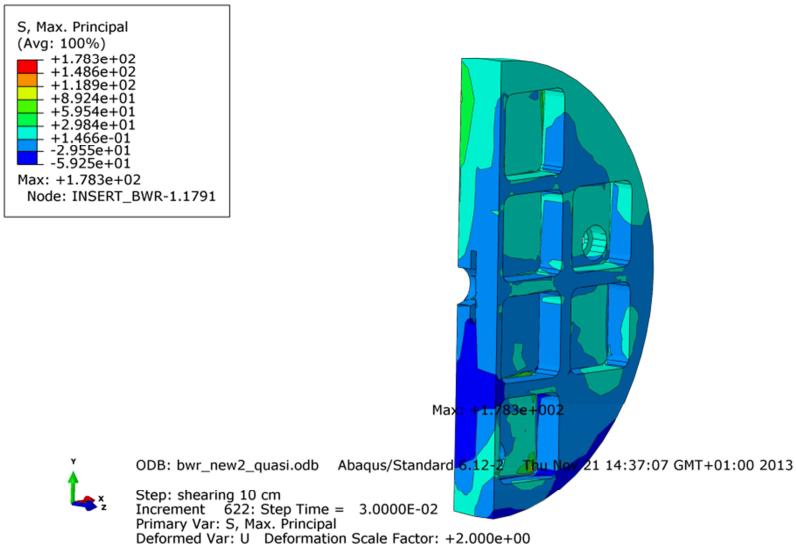

Figure A1-20 *Plot showing maximum principal stress [MPa] for the insert base after 8 cm shearing.*

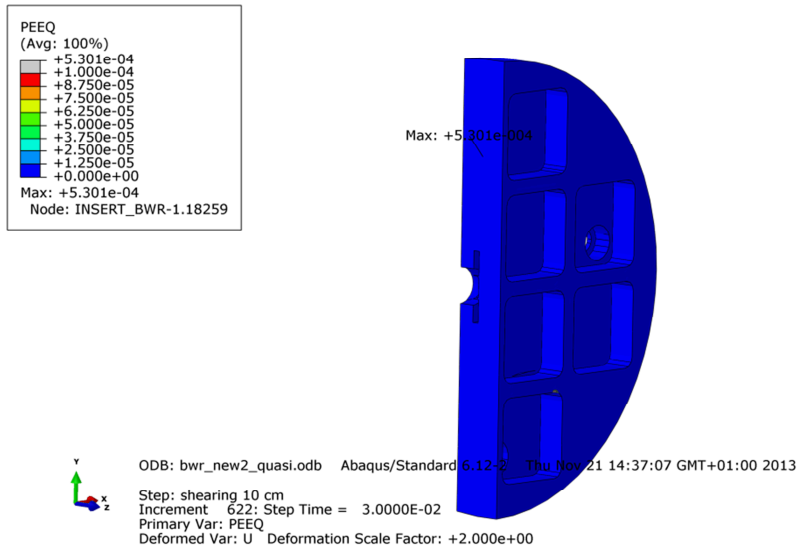

Figure A1-21 *Plot showing equivalent plastic strain (PEEQ) for the insert base after 8 cm shearing.*

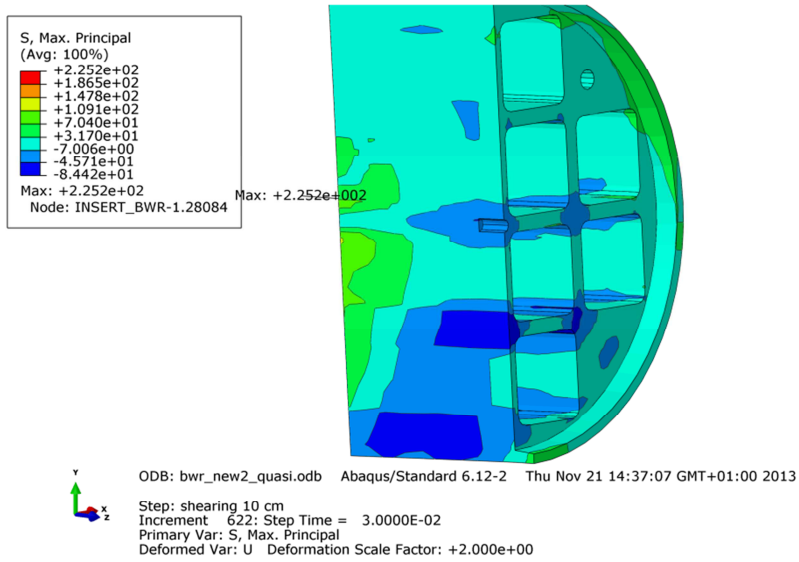

Figure A1-22 *Plot showing maximum principal stress [MPa] for the insert top after 8 cm shearing.*

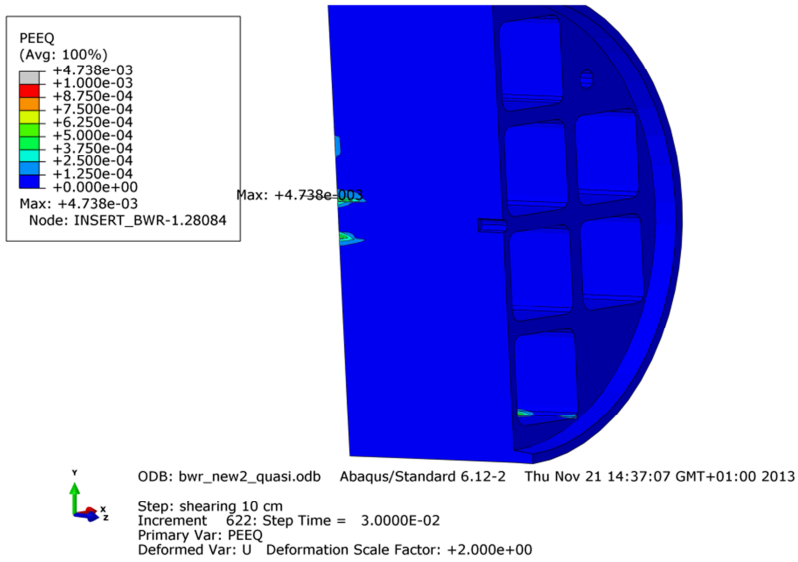

Figure A1-23 *Plot showing equivalent plastic strain (PEEQ) for the insert top after 8 cm shearing.*

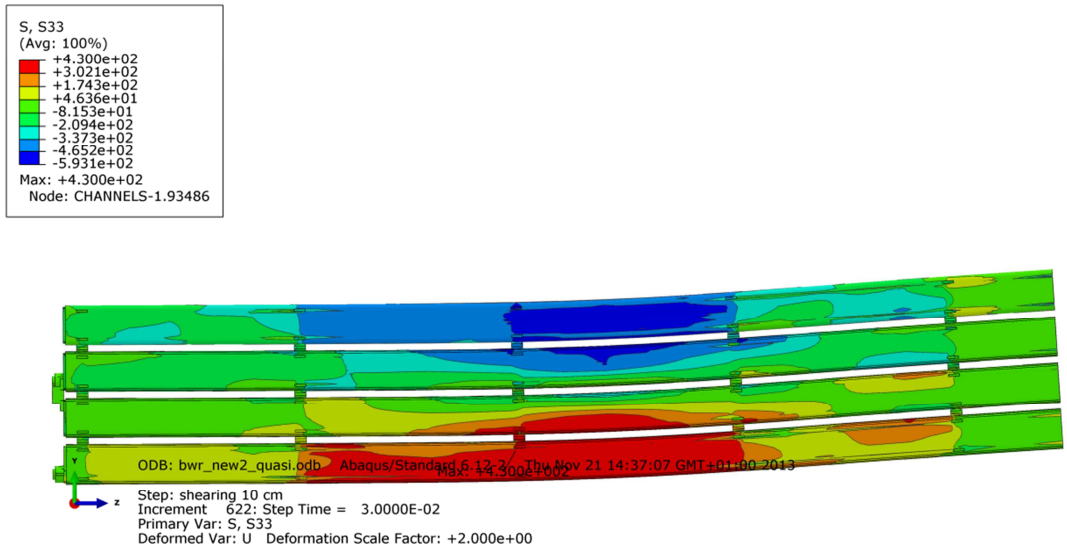

Figure A1-24 *Plot showing axial stress [MPa] for the steel channel tubes after 8 cm shearing.*

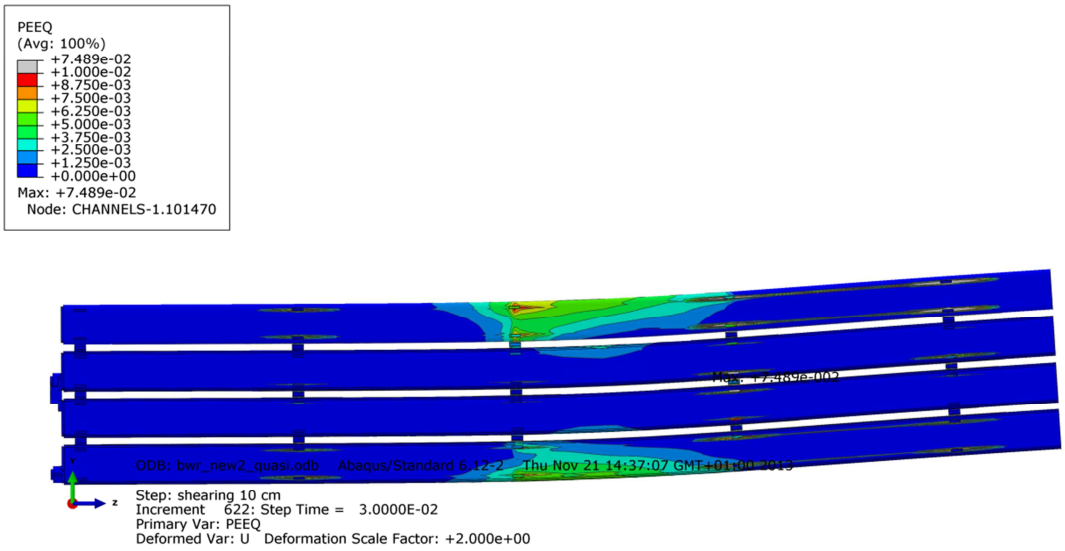

Figure A1-25 *Plot showing equivalent plastic strain (PEEQ) for the steel channel tubes after 8 cm shearing.*

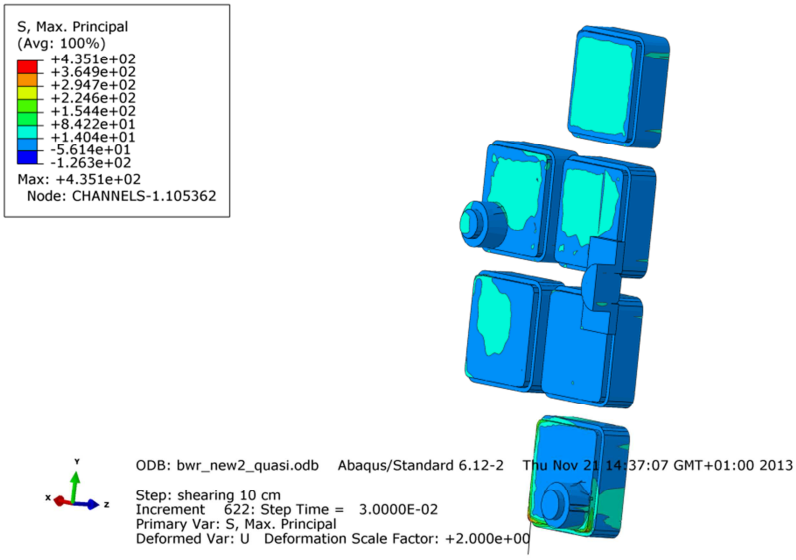

Figure A1-26 *Plot showing maximum principal stress [MPa] for the steel channel tubes base plates after 8 cm shearing.*

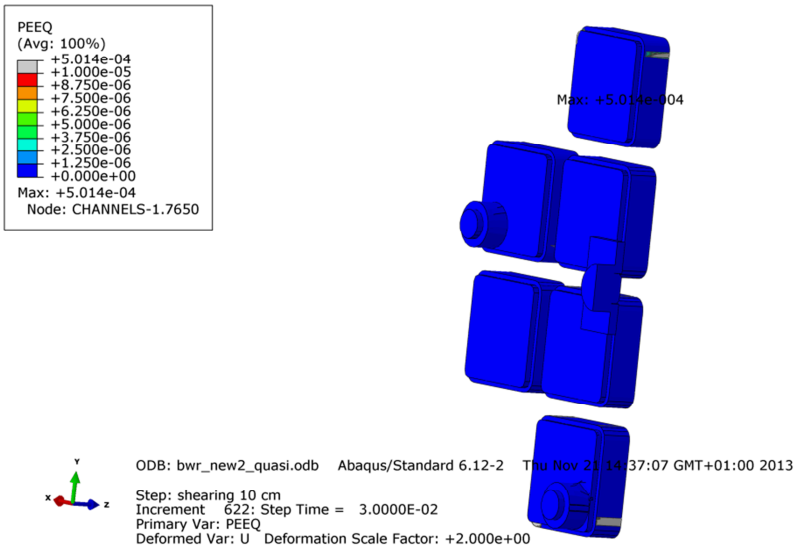

Figure A1-27 *Plot showing equivalent plastic strain (PEEQ) for the steel channel tubes base plates after 8 cm shearing.*

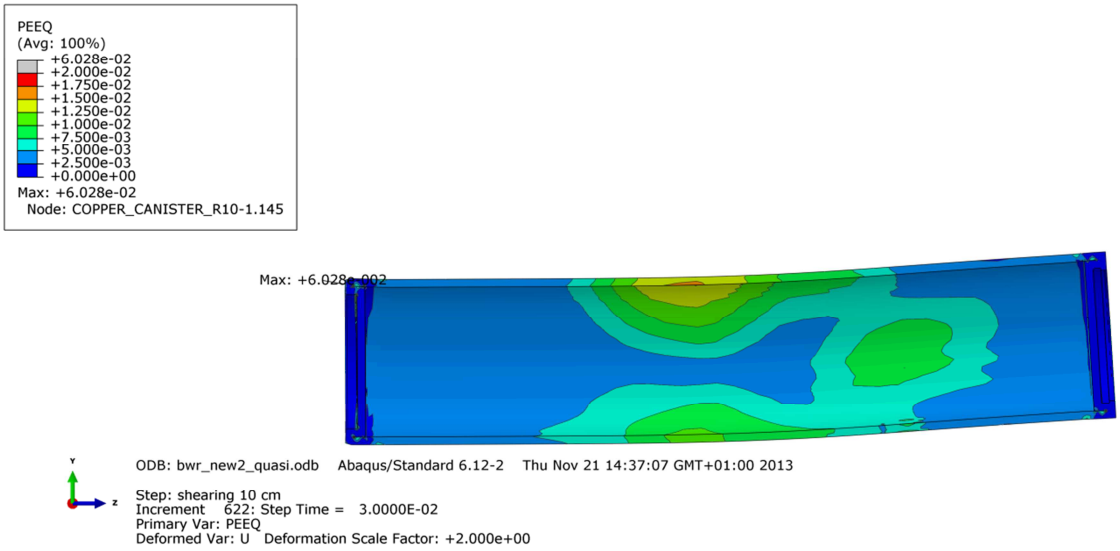

Figure A1-28 *Plot showing equivalent plastic strain (PEEQ) for the copper shell after 8 cm shearing.*

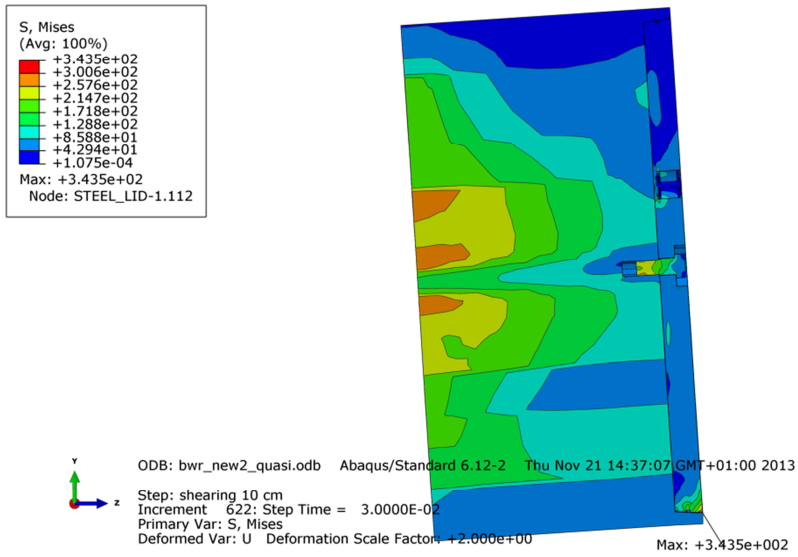

Figure A1-29 *Plot showing Mises stress [MPa] close to the insert lid fixing screw after 8 cm shearing.*

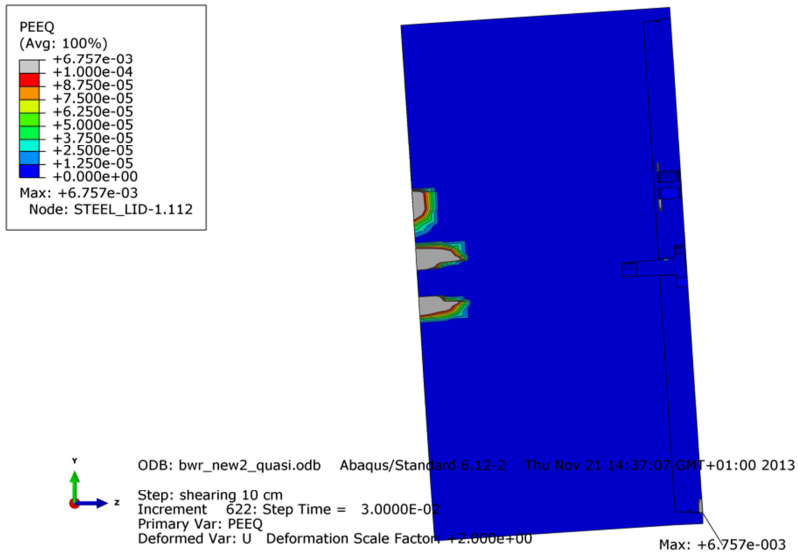

Figure A1-30 *Plot showing equivalent plastic strain (PEEQ) close to the insert lid fixing screw after 8 cm shearing.*

Appendix 2 – Plots for bwr_excentric_half

Plots showing deformed geometry as contour plots for all parts at shearing magnitude 5 and 10 cm for case bwr_excentric_half (horizontal shearing at ¾-distance from the insert base). The view shows the symmetry plane and all deformations are scaled by a factor of two.

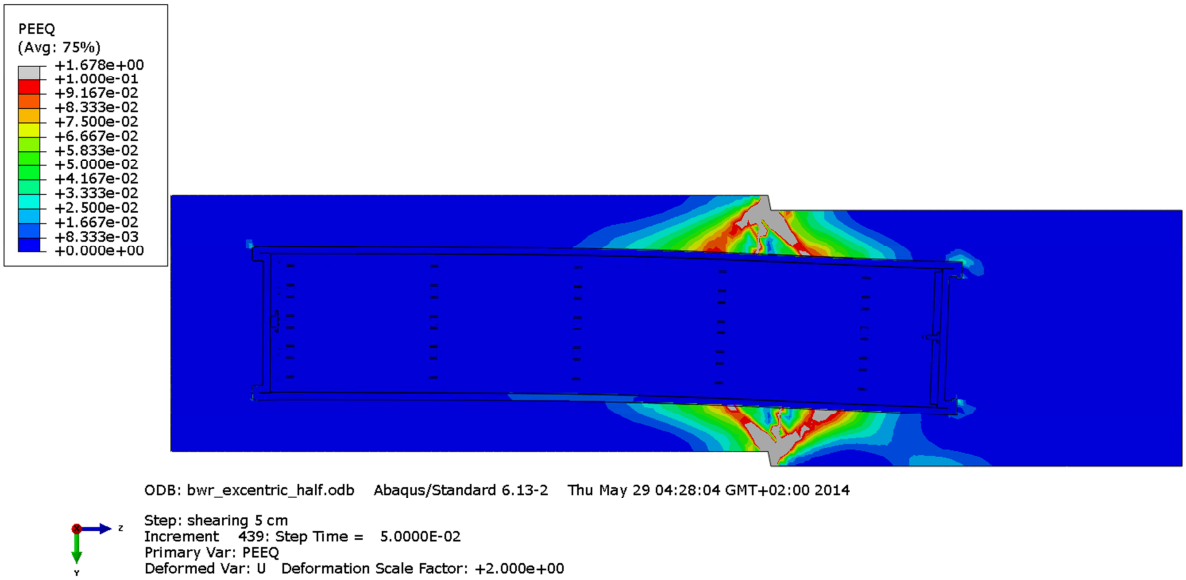

Figure A2-1 *Plot showing equivalent plastic strain (PEEQ) after 5 cm shearing.*

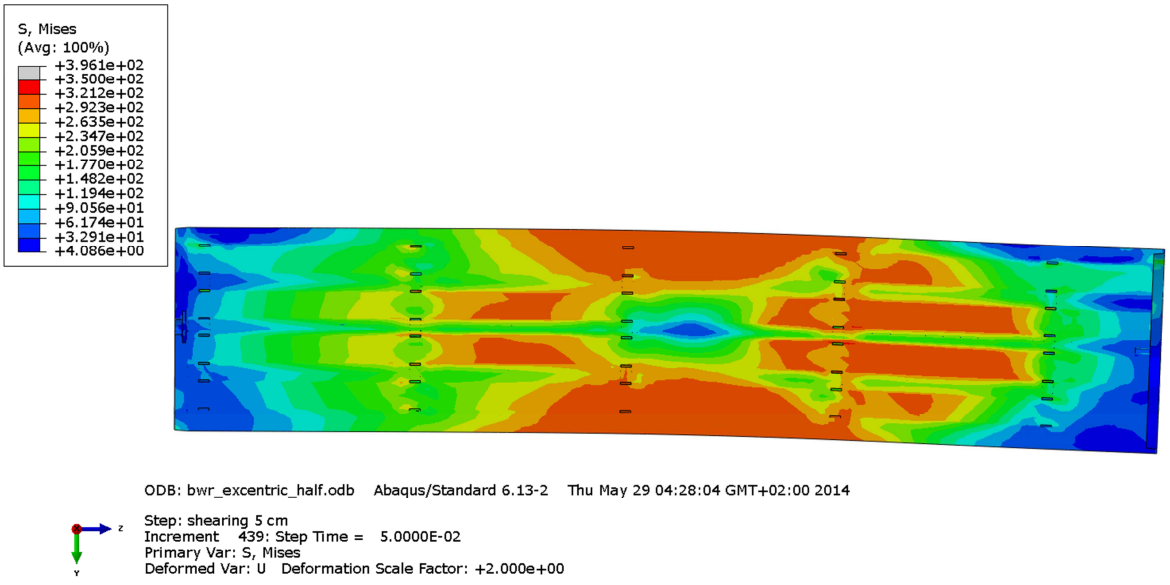

Figure A2-2 *Plot showing Mises stress [MPa] for the insert after 5 cm shearing.*

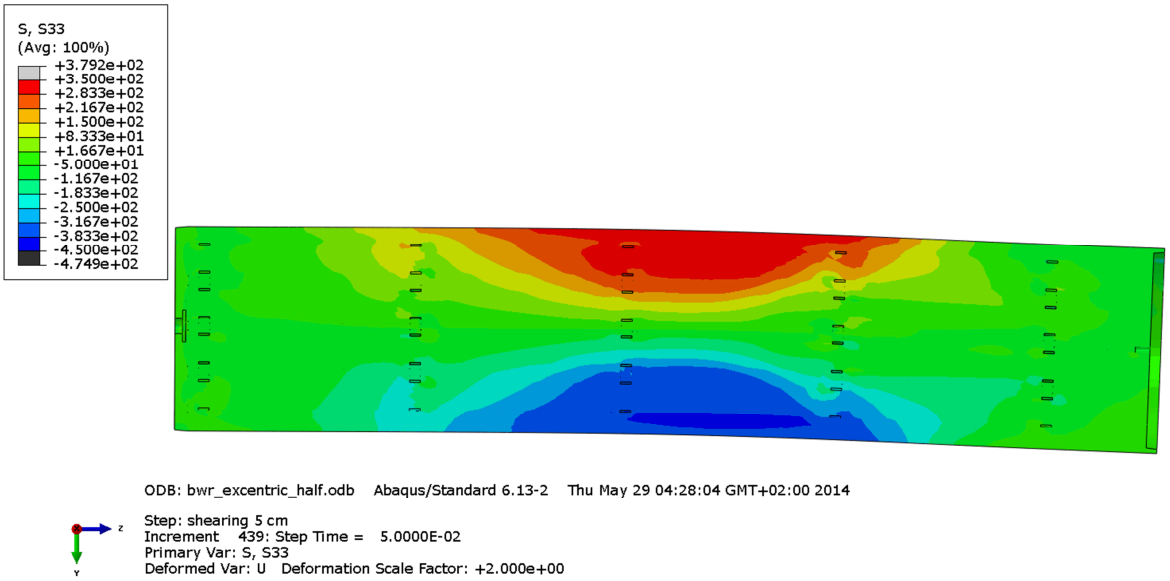

Figure A2-3 *Plot showing axial stress [MPa] for the insert after 5 cm shearing.*

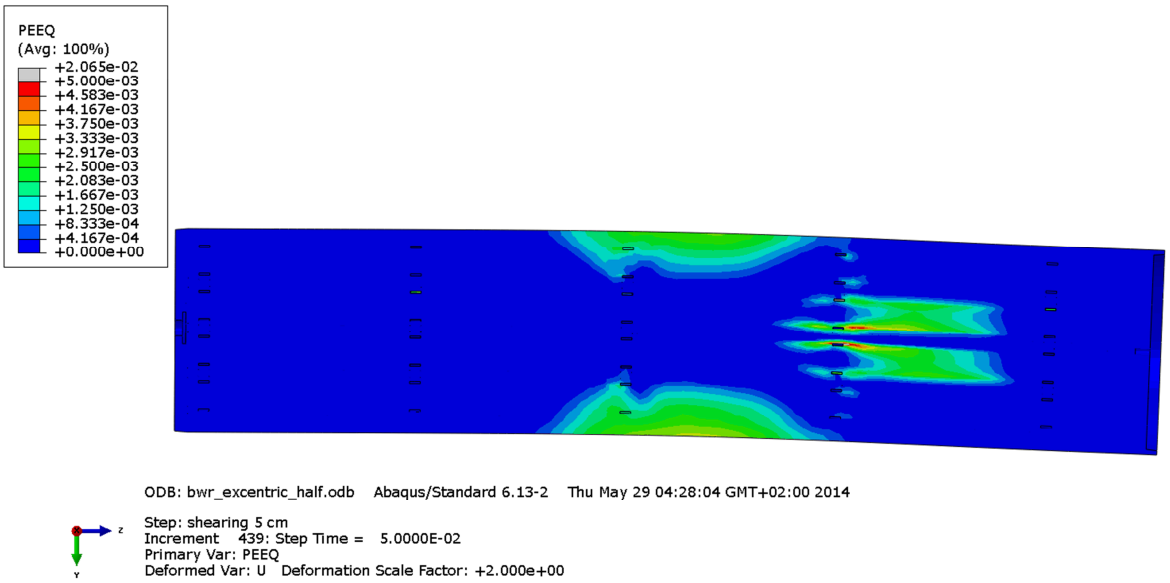

Figure A2-4 *Plot showing equivalent plastic strain (PEEQ) for the insert after 5 cm shearing.*

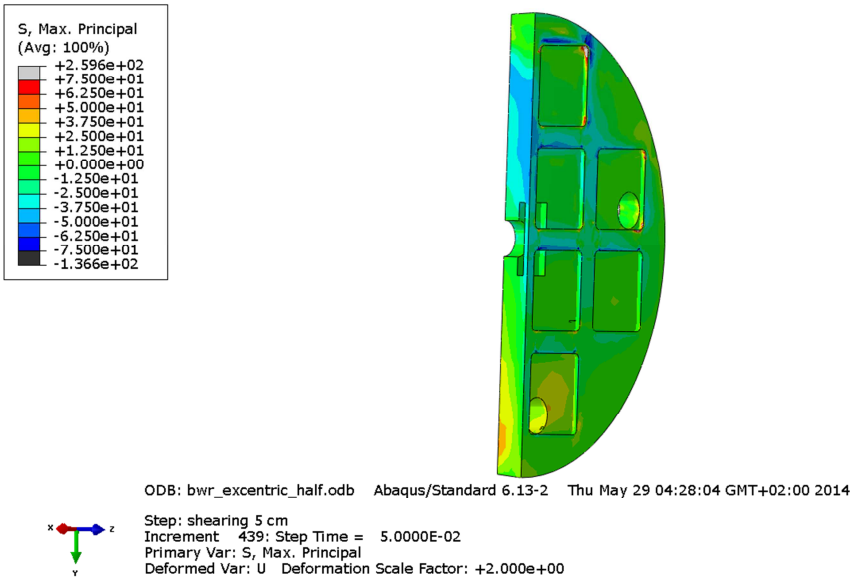

Figure A2-5 *Plot showing maximum principal stress [MPa] for the insert base after 5 cm shearing.*

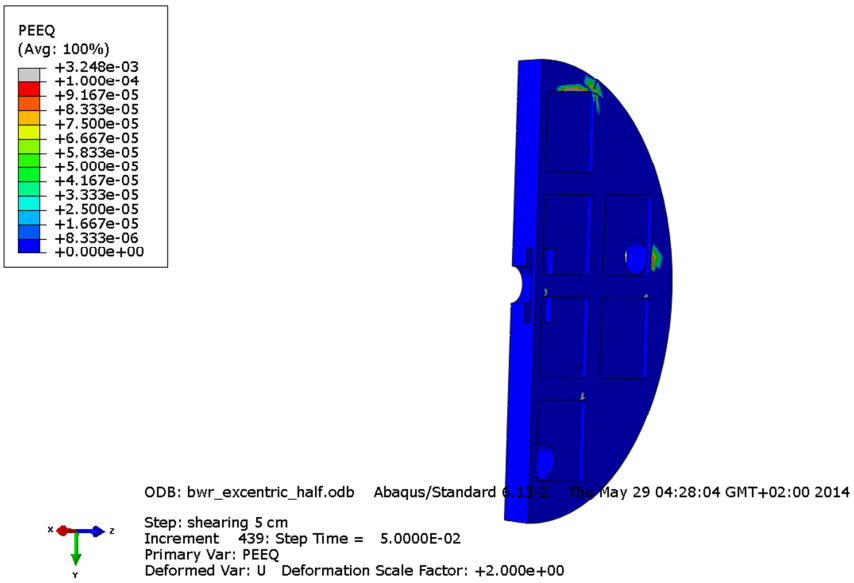

Figure A2-6 *Plot showing equivalent plastic strain (PEEQ) for the insert base after 5 cm shearing.*

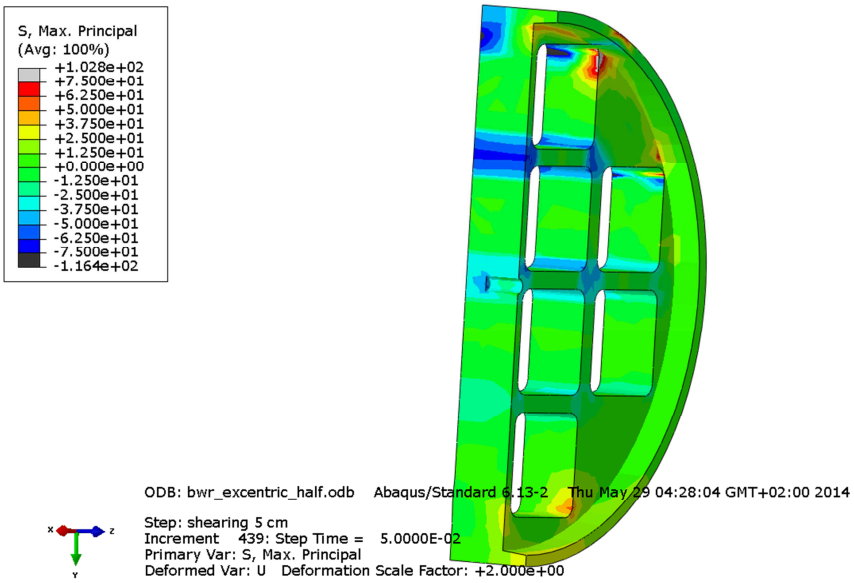

Figure A2-7 *Plot showing maximum principal stress [MPa] for the insert top after 5 cm shearing.*

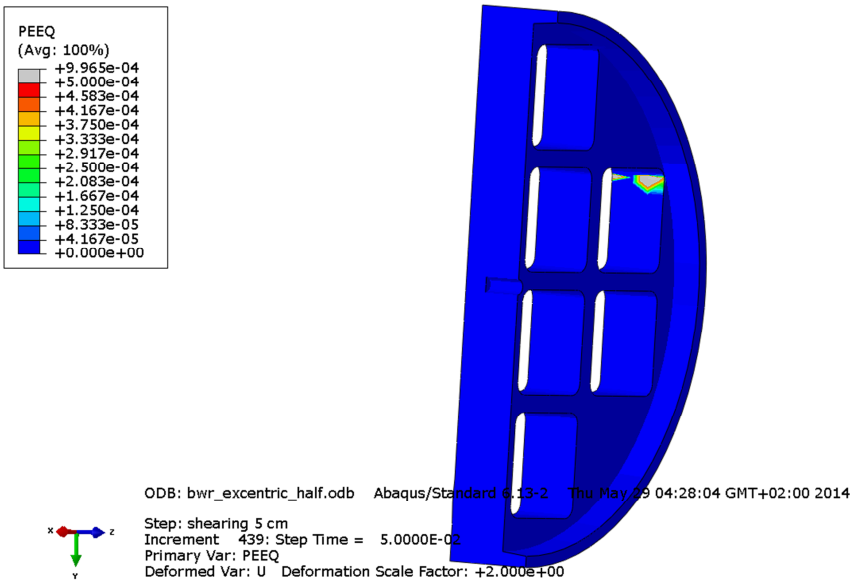

Figure A2-8 *Plot showing equivalent plastic strain (PEEQ) for the insert top after 5 cm shearing.*

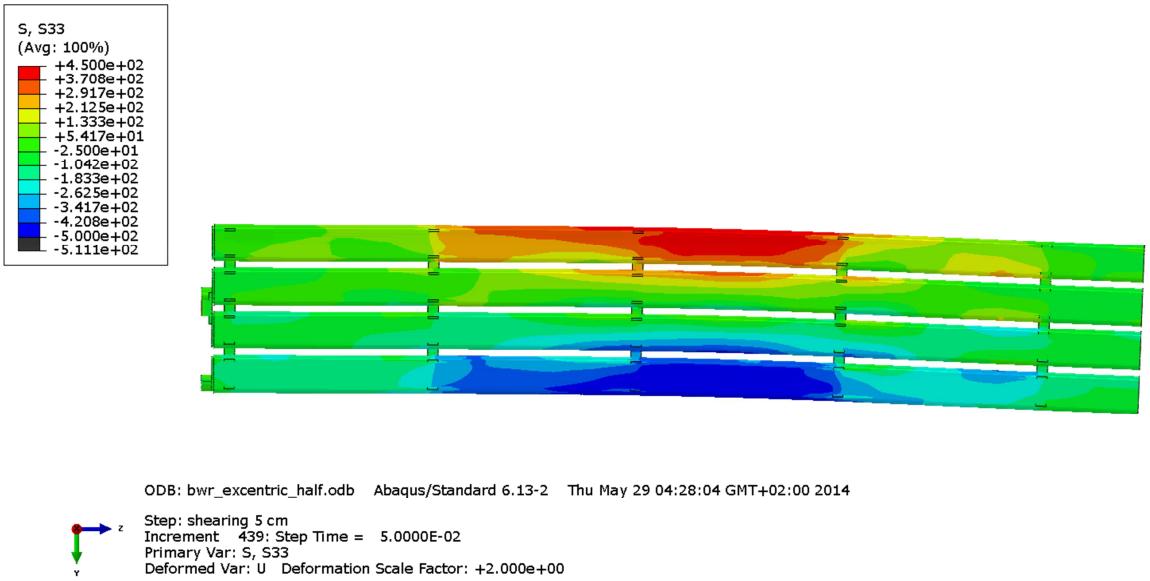

Figure A2-9 *Plot showing axial stress [MPa] for the steel channel tubes after 5 cm shearing.*

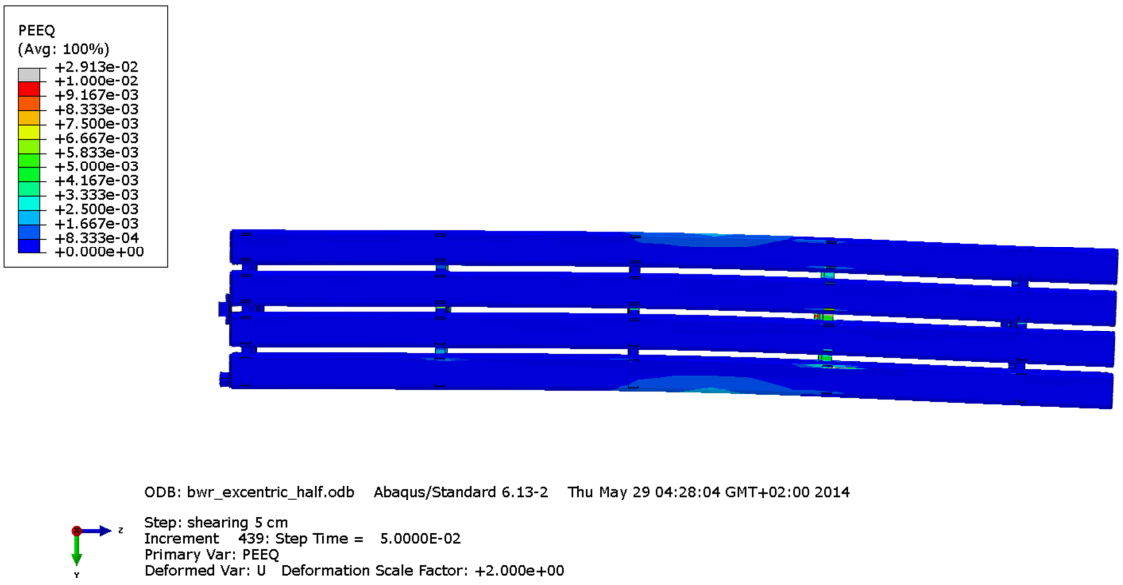

Figure A2-10 *Plot showing equivalent plastic strain (PEEQ) for the steel channel tubes after 5 cm shearing.*

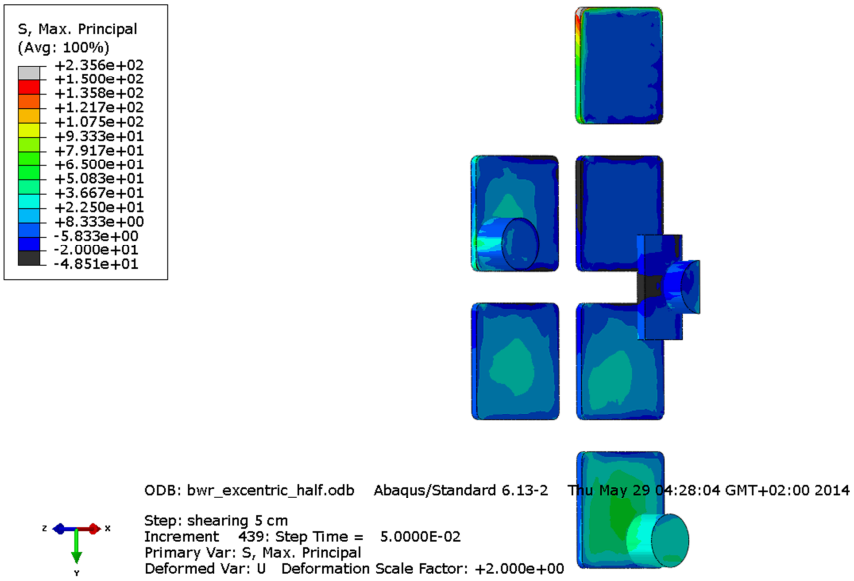

Figure A2-11 *Plot showing maximum principal stress [MPa] for the steel channel tubes base plates after 5 cm shearing.*

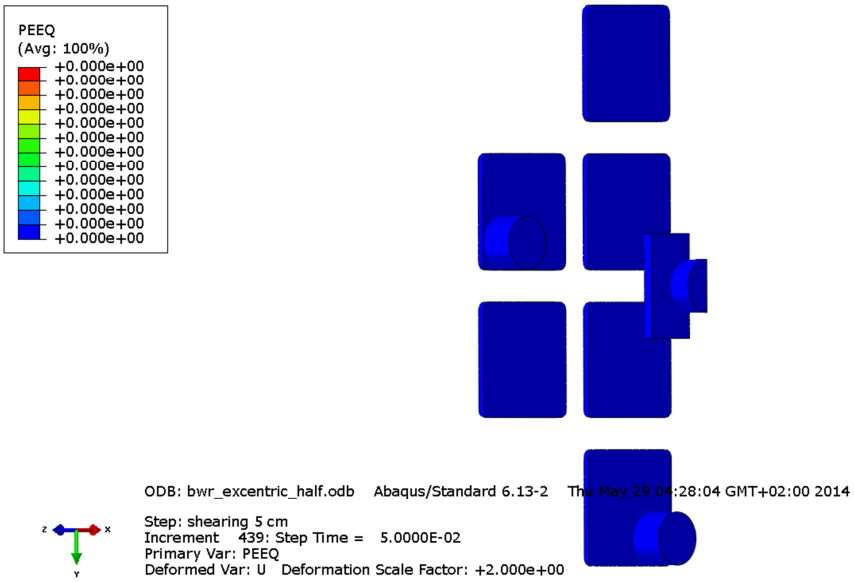

Figure A2-12 *Plot showing equivalent plastic strain (PEEQ) for the steel channel tubes base plates after 5 cm shearing.*

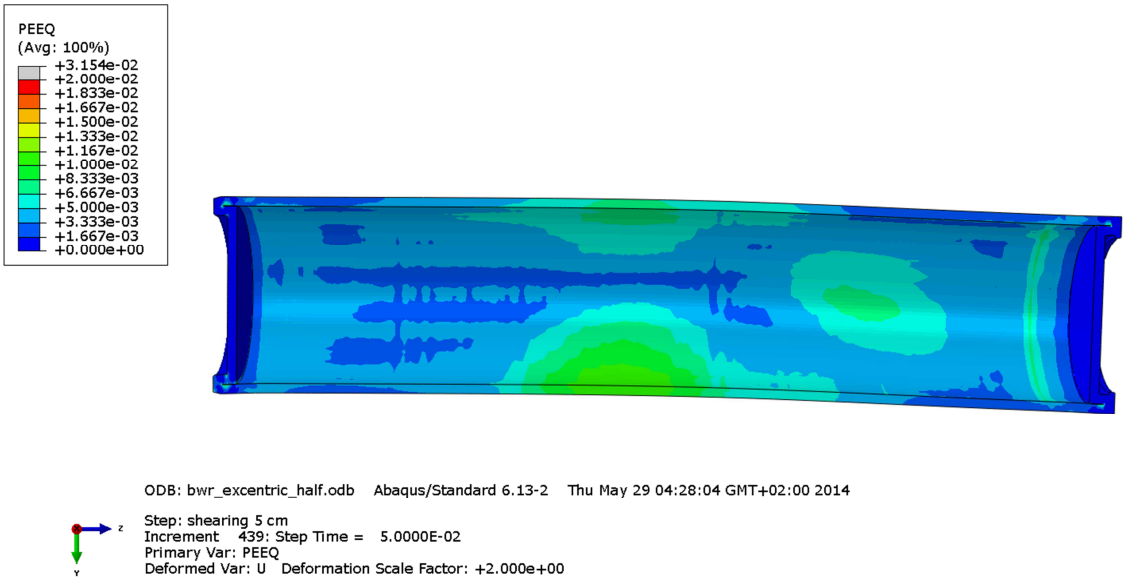

Figure A2-13 *Plot showing equivalent plastic strain (PEEQ) for the steel copper shell after 5 cm shearing.*

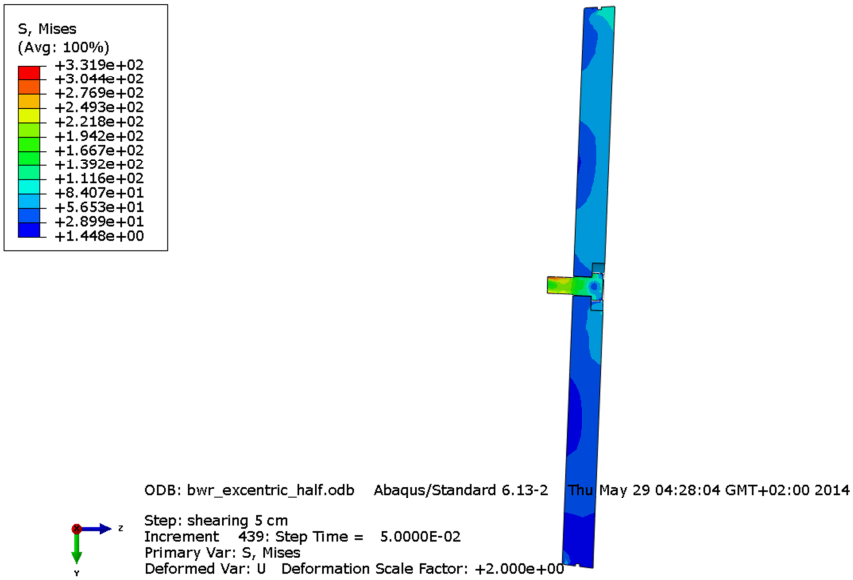

Figure A2-14 *Plot showing Mises stress [MPa] close to the insert lid fixing screw after 5 cm shearing.*

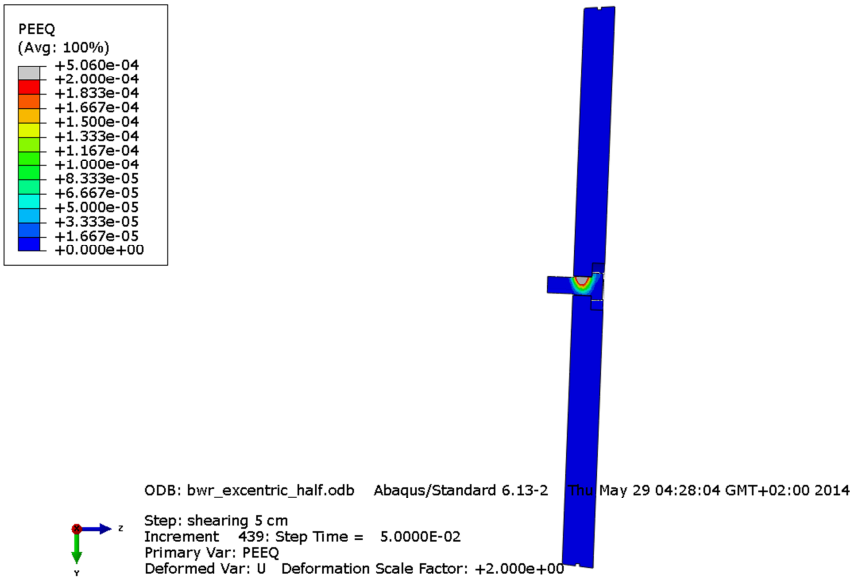

Figure A2-15 *Plot showing equivalent plastic strain (PEEQ) close to the insert lid fixing screw after 5 cm shearing.*

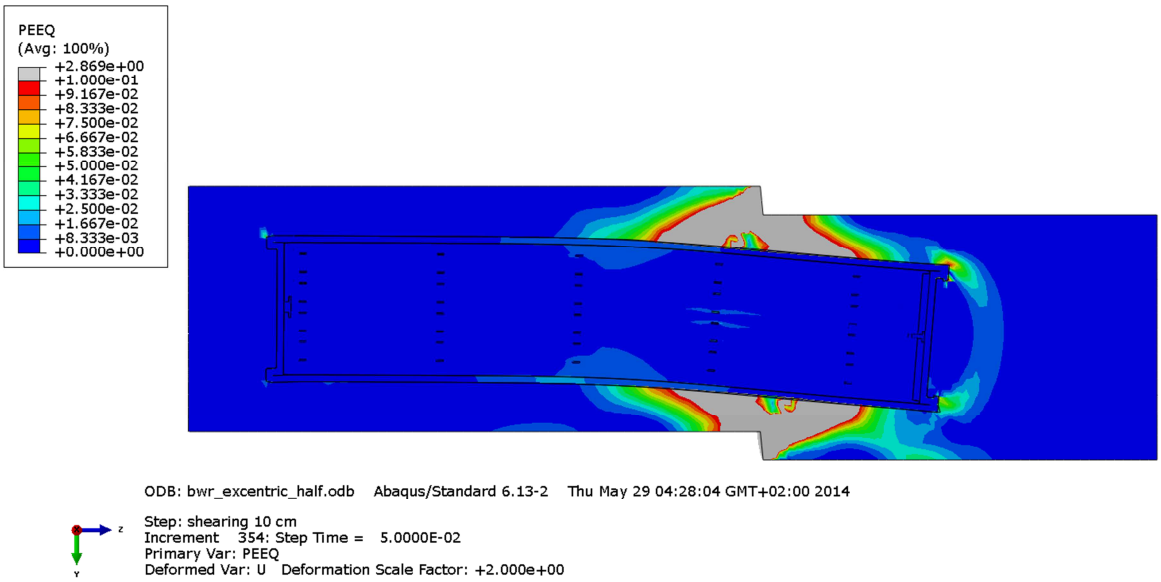

Figure A2-16 *Plot showing equivalent plastic strain (PEEQ) after 10 cm shearing.*

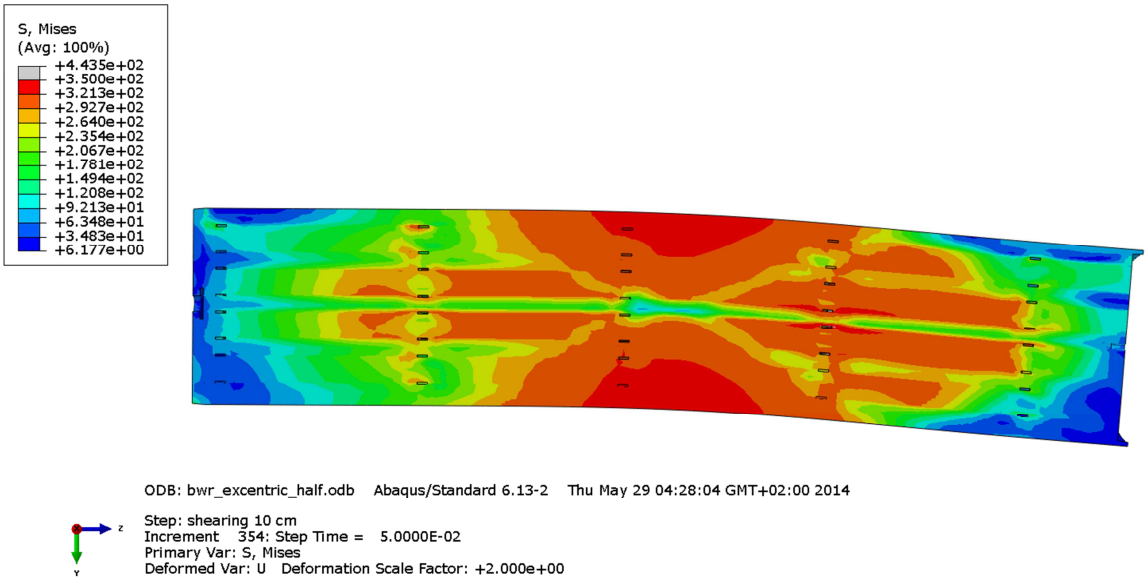

Figure A2-17 *Plot showing Mises stress [MPa] for the insert after 10 cm shearing.*

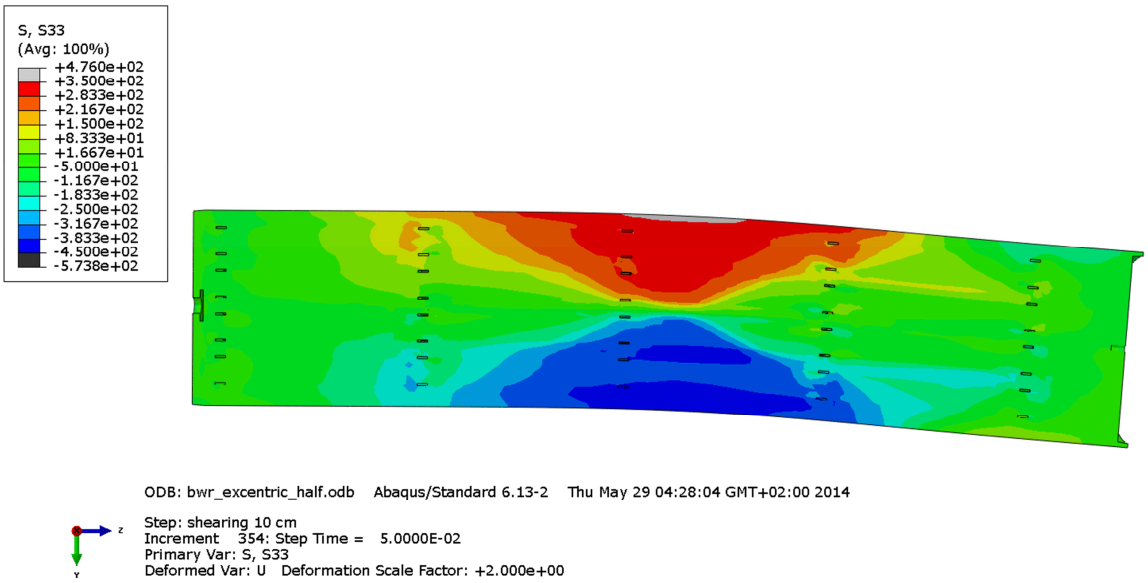

Figure A2-18 *Plot showing axial stress [MPa] for the insert after 10 cm shearing.*

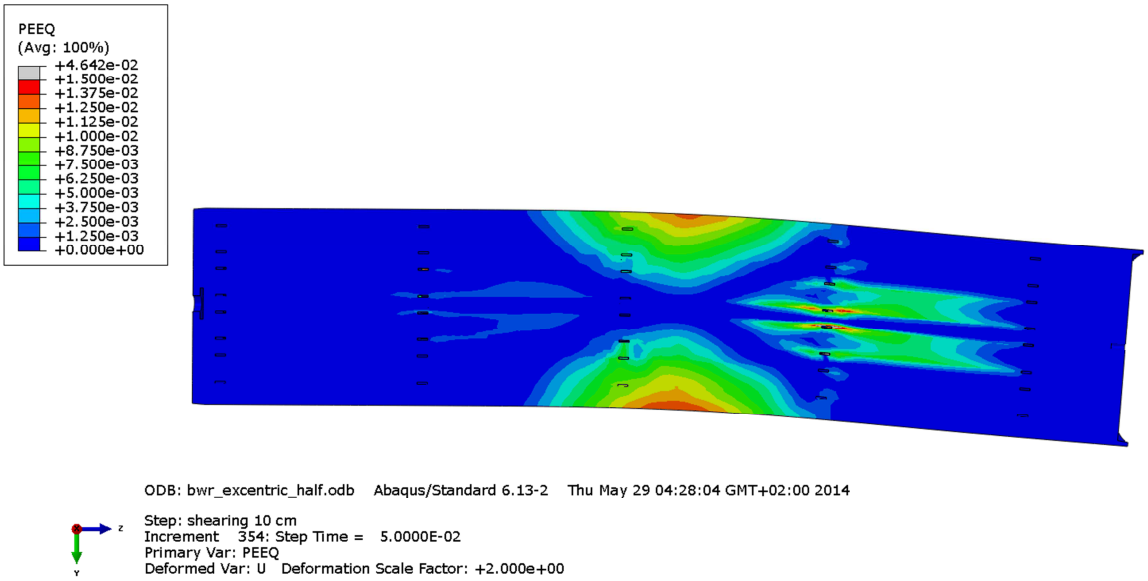

Figure A2-19 *Plot showing equivalent plastic strain (PEEQ) for the insert after 10 cm shearing.*

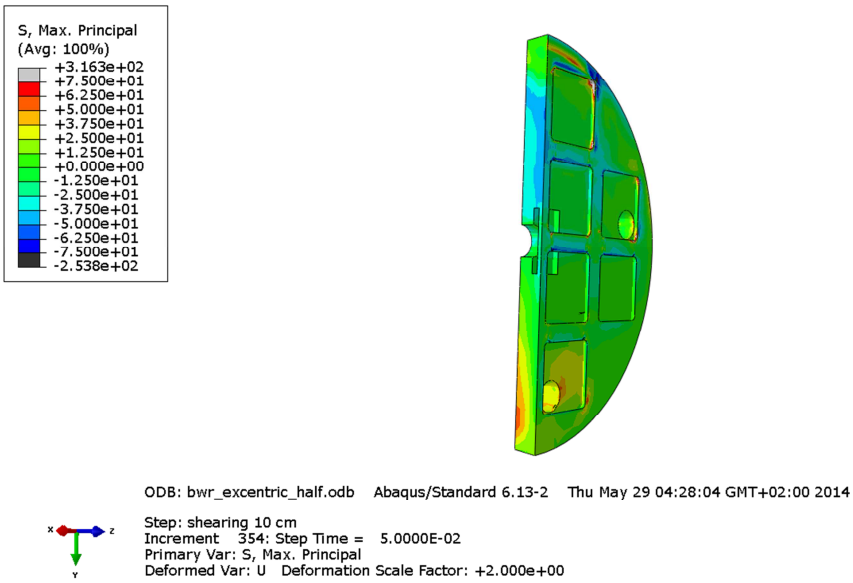

Figure A2-20 *Plot showing maximum principal stress [MPa] for the insert base after 10 cm shearing.*

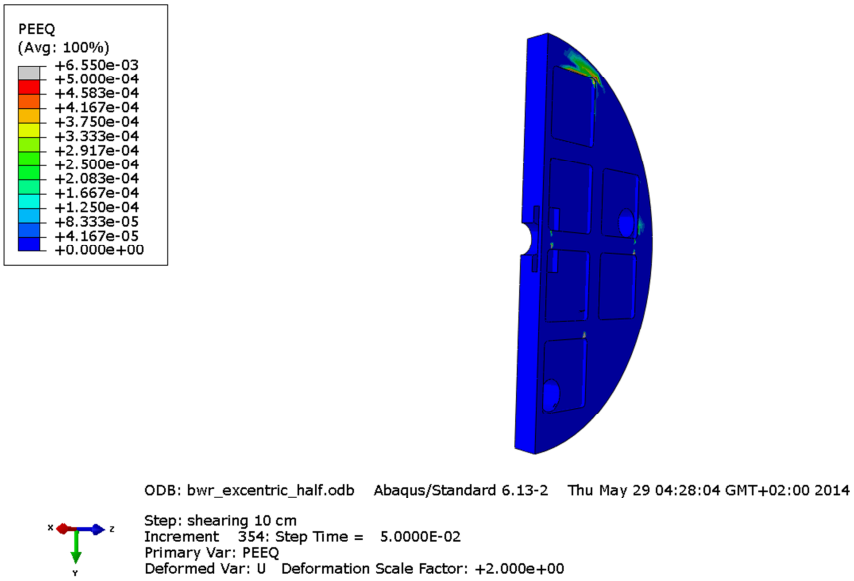

Figure A2-21 *Plot showing equivalent plastic strain (PEEQ) for the insert base after 10 cm shearing.*

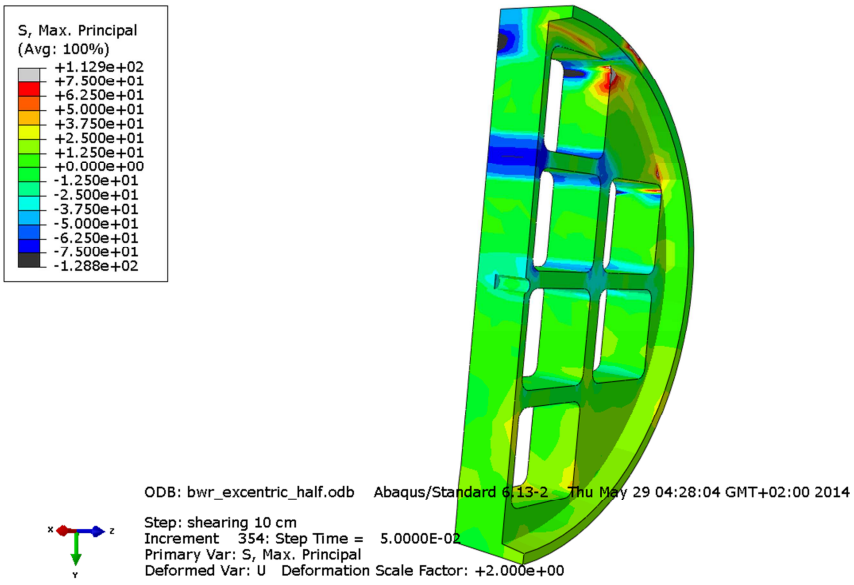

Figure A2-22 *Plot showing maximum principal stress [MPa] for the insert top after 10 cm shearing.*

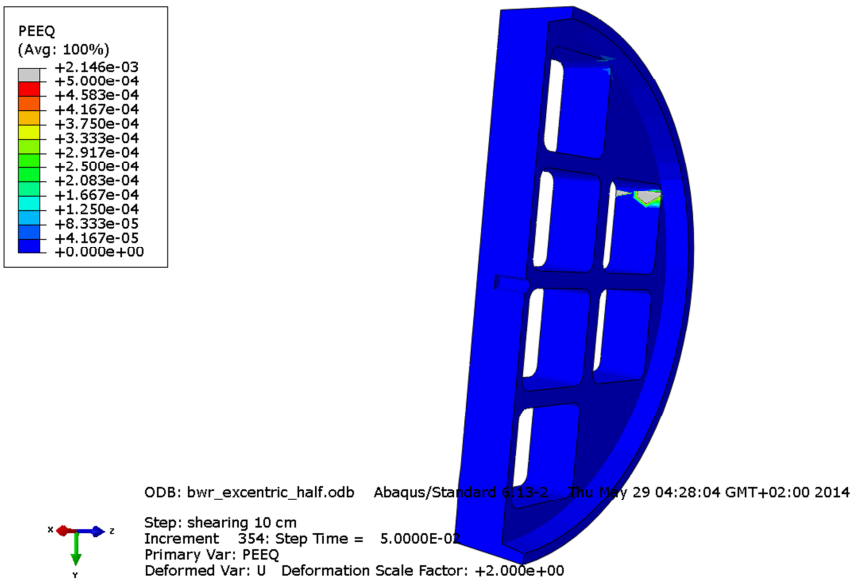

Figure A2-23 *Plot showing equivalent plastic strain (PEEQ) for the insert top after 10 cm shearing.*

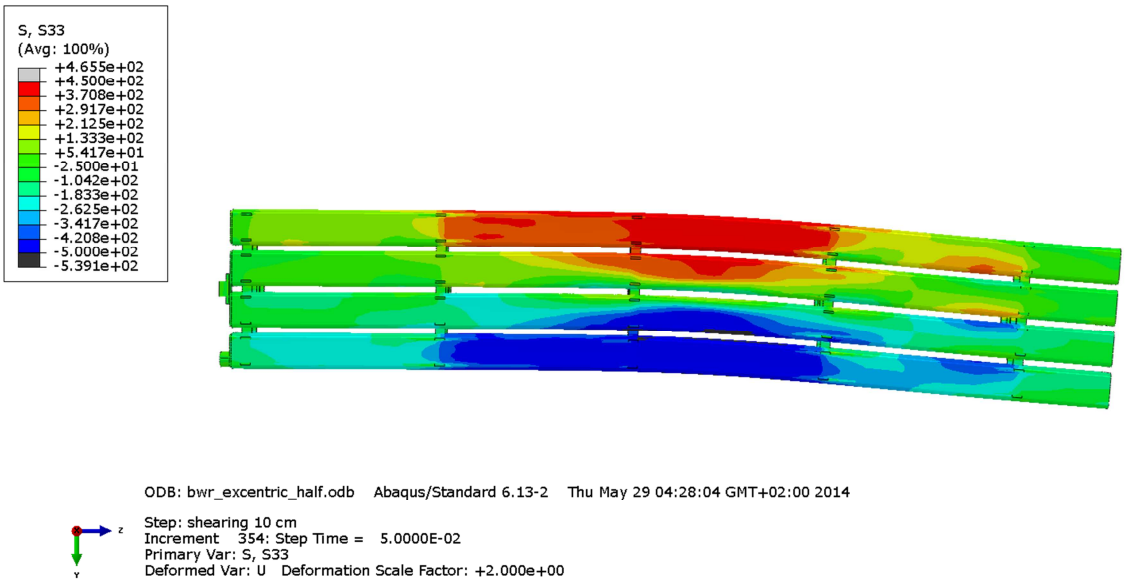

Figure A2-24 *Plot showing axial stress [MPa] for the steel channel tubes after 10 cm shearing.*

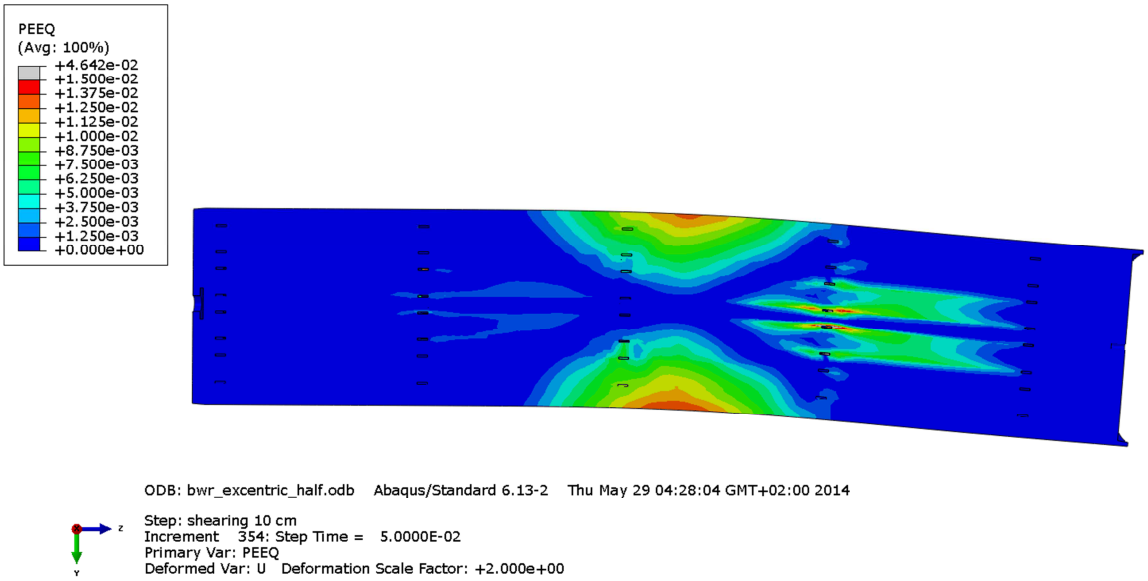

Figure A2-25 *Plot showing equivalent plastic strain (PEEQ) for the steel channel tubes after 10 cm shearing.*

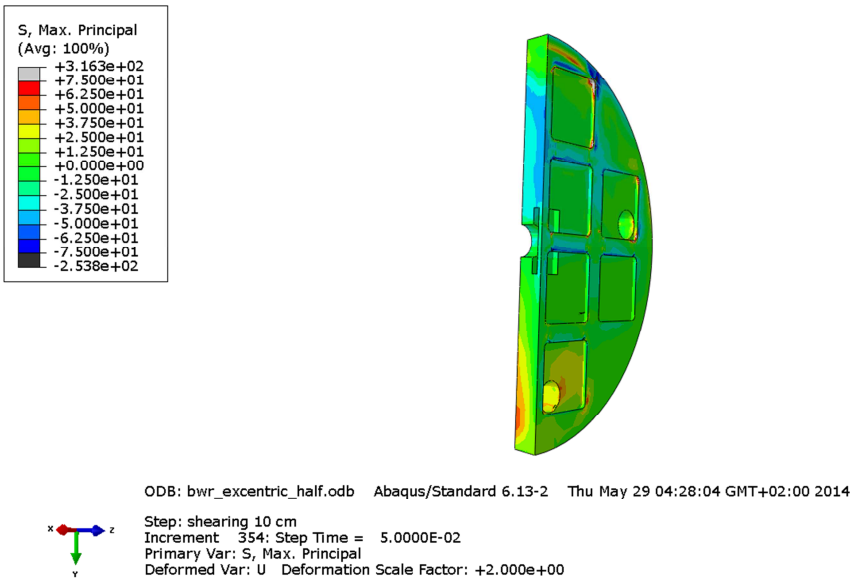

Figure A2-26 *Plot showing maximum principal stress [MPa] for the steel channel tubes base plates after 10 cm shearing.*

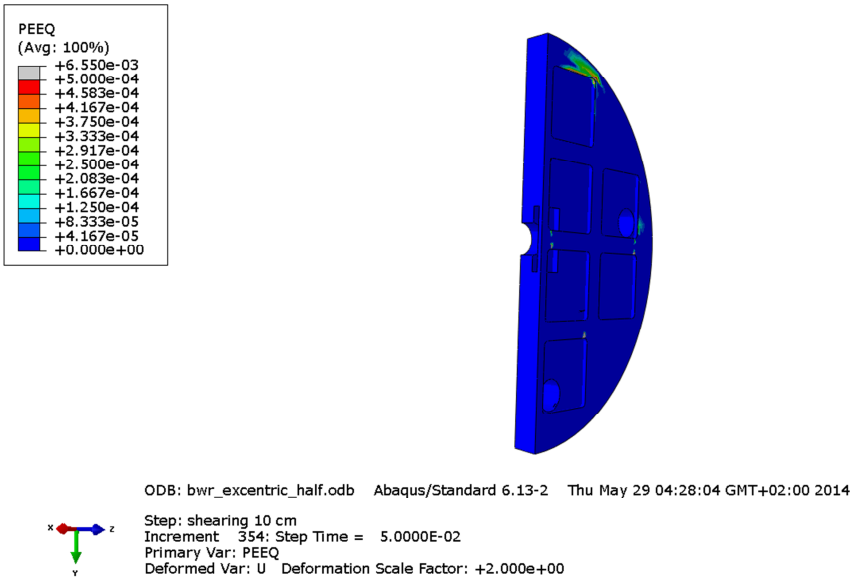

Figure A2-27 *Plot showing equivalent plastic strain (PEEQ) for the steel channel tubes base plates after 10 cm shearing.*

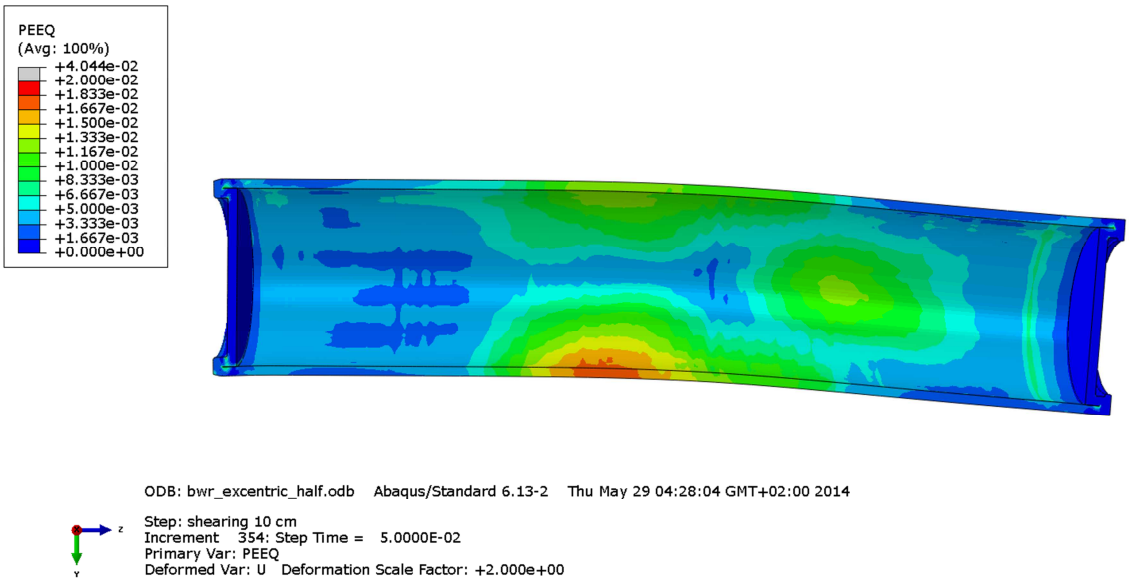

Figure A2-28 *Plot showing equivalent plastic strain (PEEQ) for the copper shell after 10 cm shearing.*

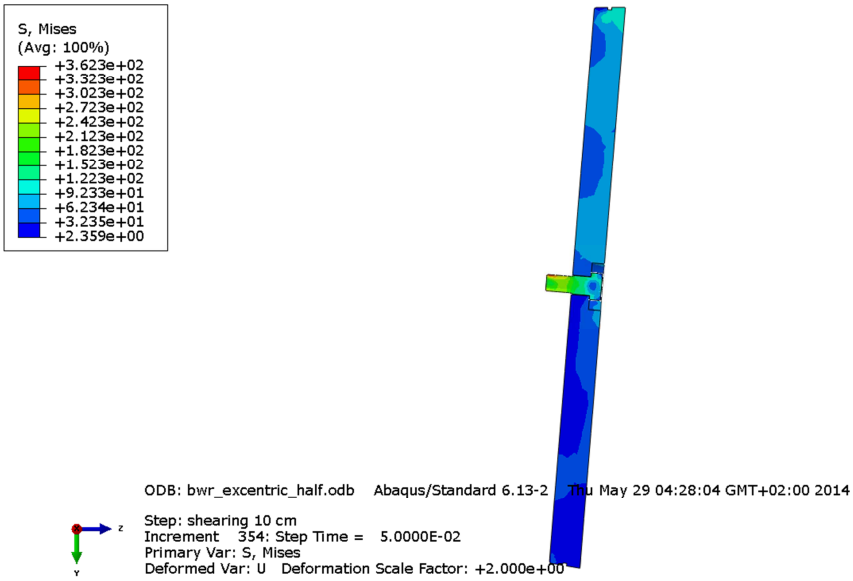

Figure A2-29 *Plot showing Mises stress [MPa] close to the insert lid fixing screw after 10 cm shearing.*

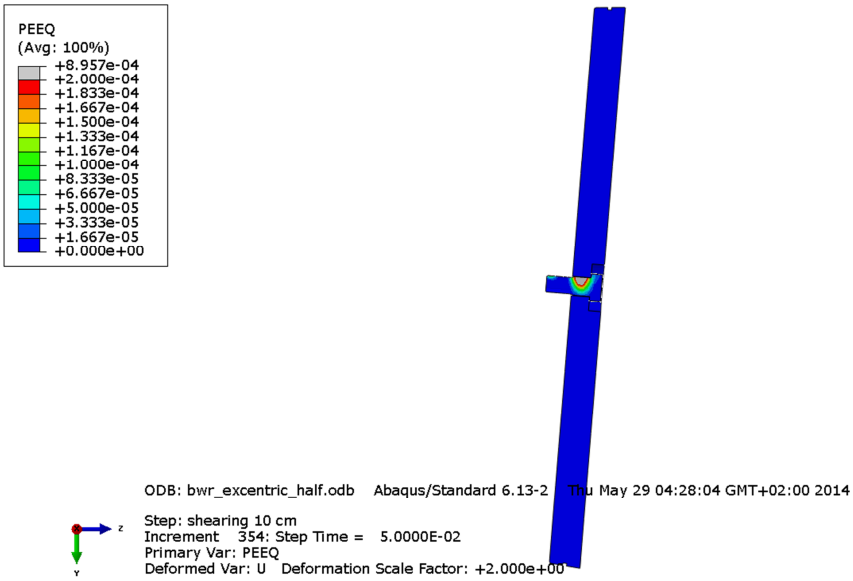

Figure A2-30 *Plot showing equivalent plastic strain (PEEQ) close to the insert lid fixing screw after 10 cm shearing.*

Appendix 3 – Plots for bwr_centric_rotated

Plots showing deformed geometry as contour plots for all parts at shearing magnitude 5 and 9 cm for case bwr_centric_rotated (horizontal shearing at ¾ distance from insert base when the cassettes are rotated to have minimum distance between the cassette corner and the insert outer radius). The view shows the symmetry plane and all deformations are scaled by a factor of two. Note! The analysis failed to converge for shearing displacement > 9 cm. The plots are shown for a vertical cut through the centre of the canister.

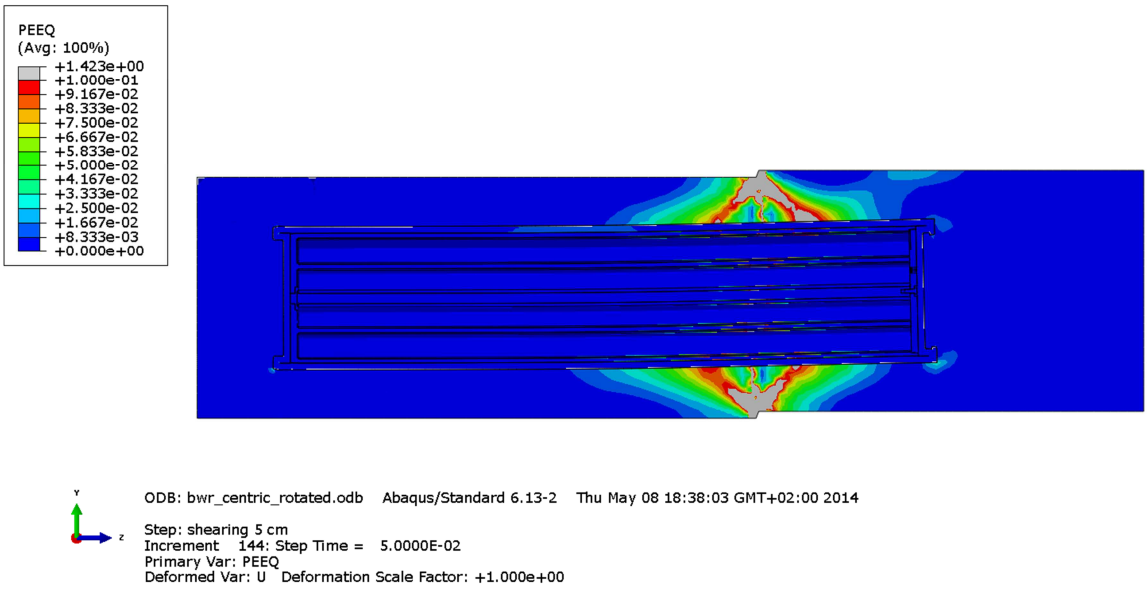

Figure A3-1 *Plot showing equivalent plastic strain (PEEQ) after 5 cm shearing.*

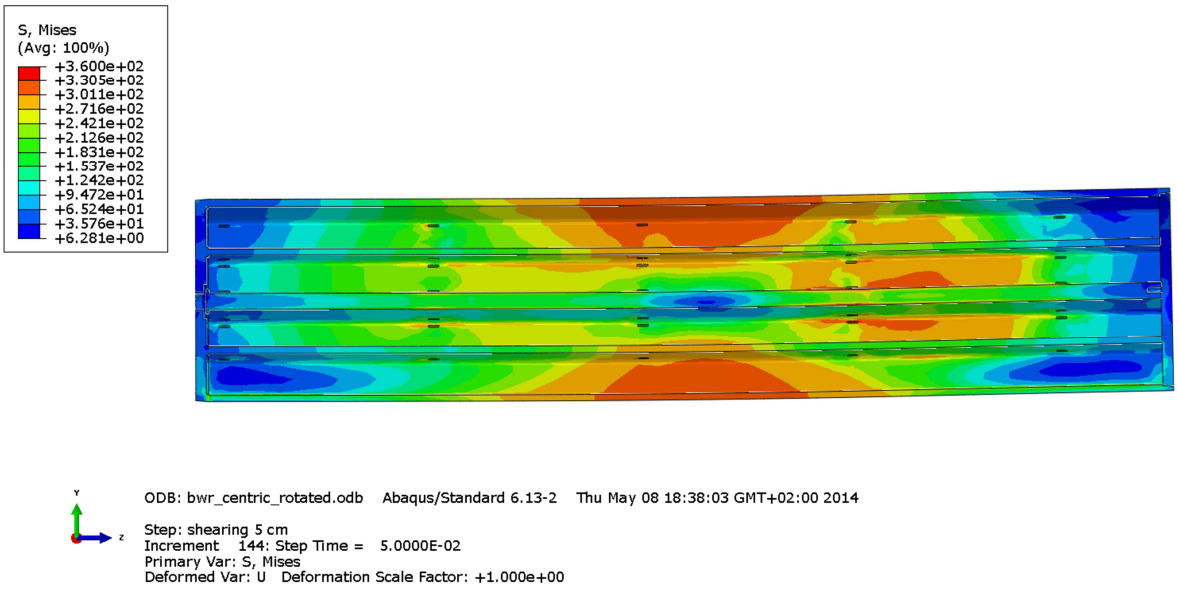

Figure A3-2 *Plot showing Mises stress [MPa] for the insert after 5 cm shearing.*

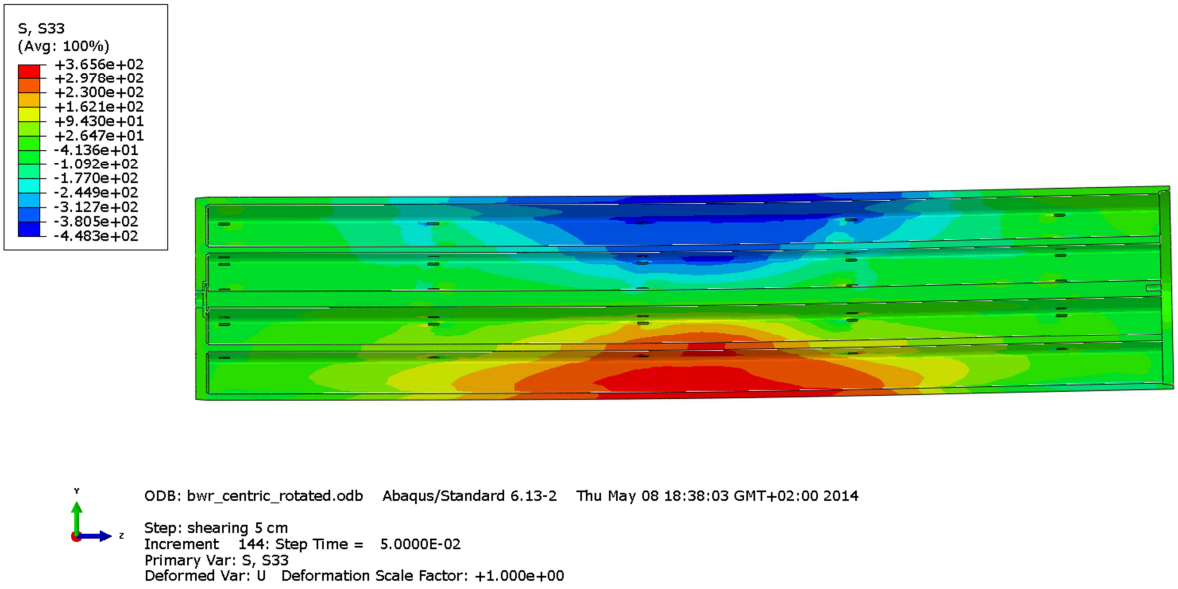

Figure A3-3 *Plot showing axial stress [MPa] for the insert after 5 cm shearing.*

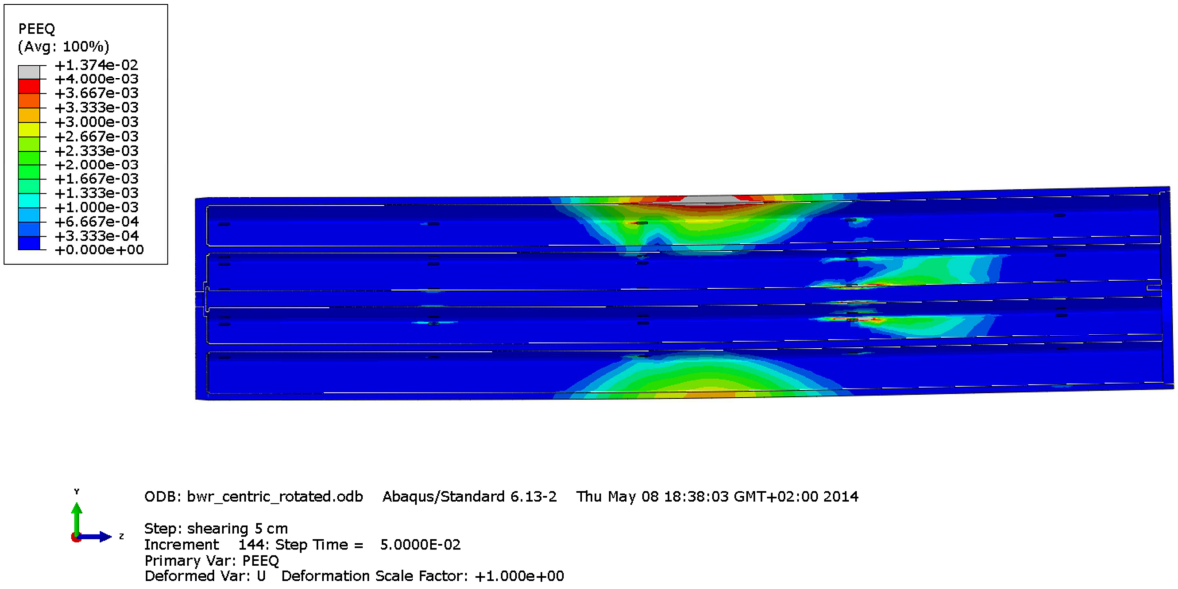

Figure A3-4 *Plot showing equivalent plastic strain (PEEQ) for the insert after 5 cm shearing.*

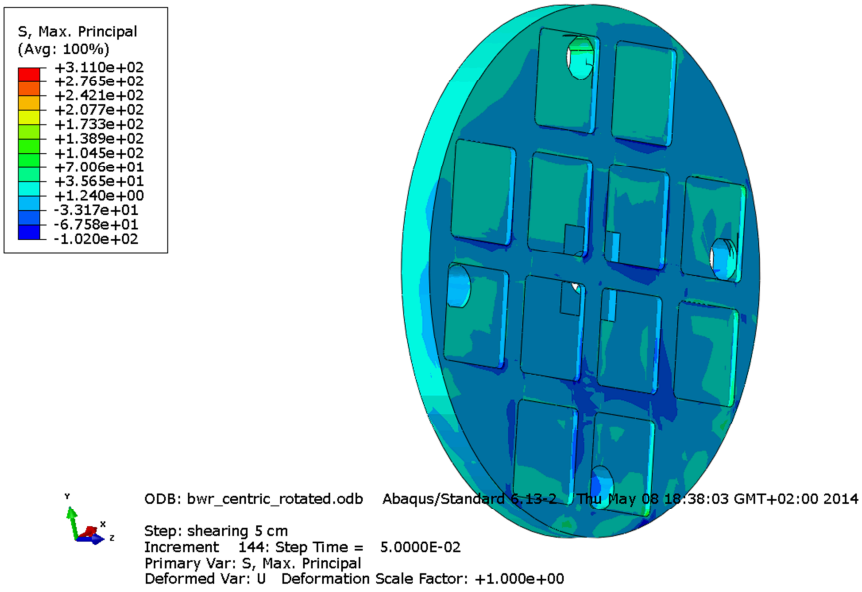

Figure A3-5 *Plot showing maximum principal stress [MPa] for the insert base after 5 cm shearing.*

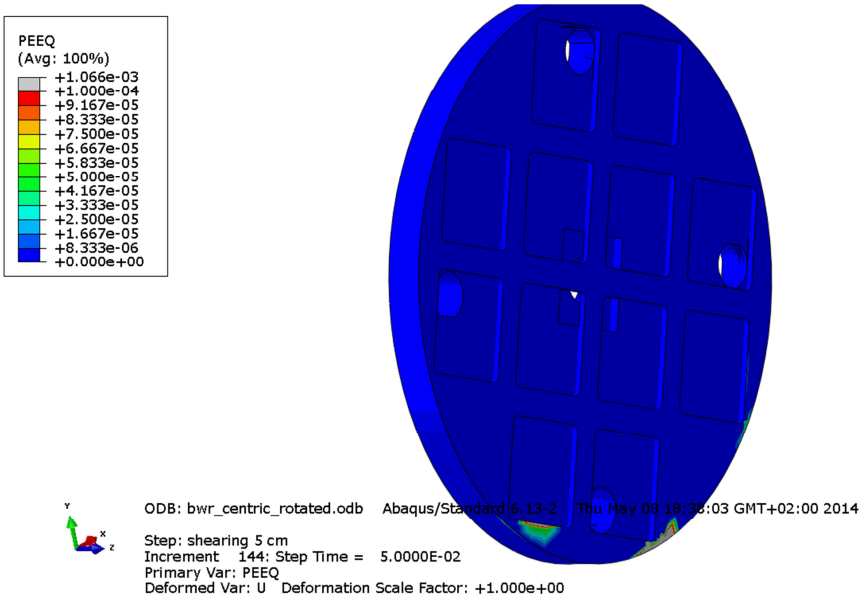

Figure A3-6 *Plot showing equivalent plastic strain (PEEQ) for the insert base after 5 cm shearing.*

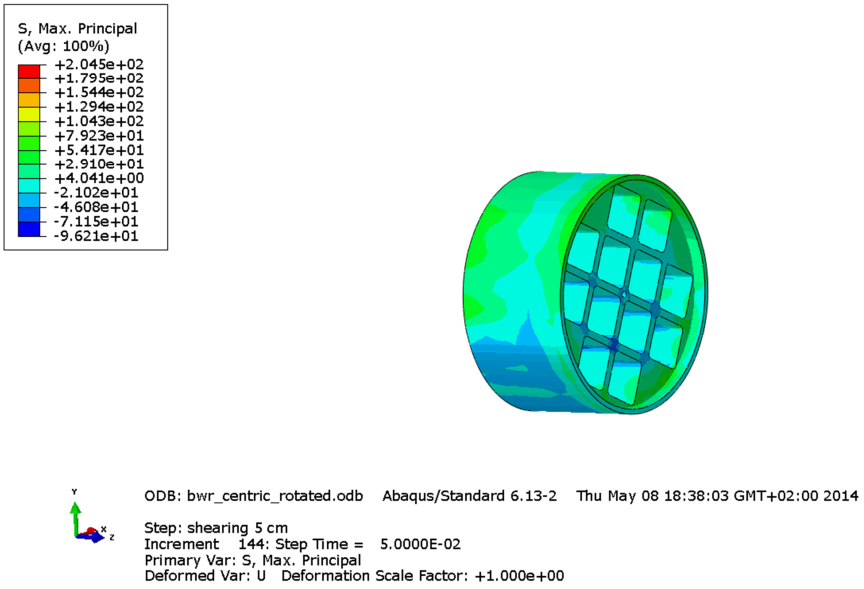

Figure A3-7 *Plot showing maximum principal stress [MPa] for the insert top after 5 cm shearing.*

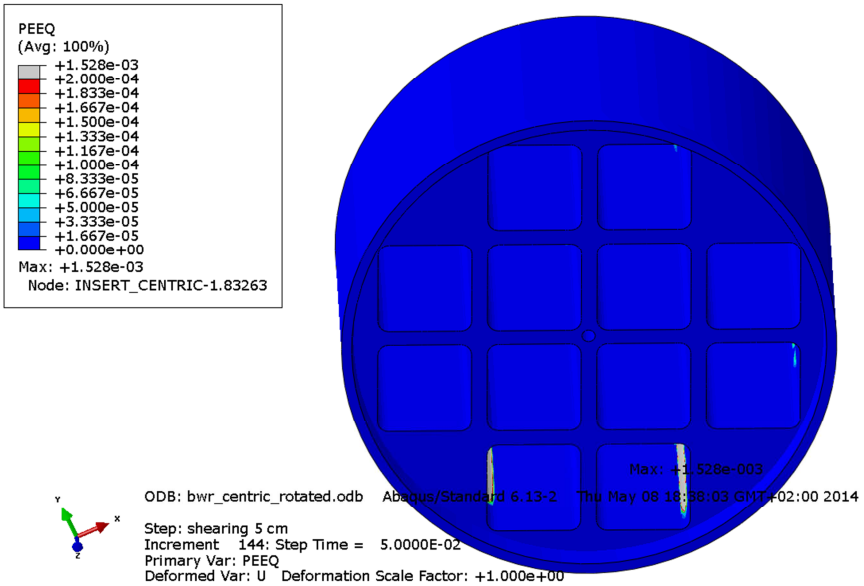

Figure A3-8 *Plot showing equivalent plastic strain (PEEQ) for the insert top after 5 cm shearing.*

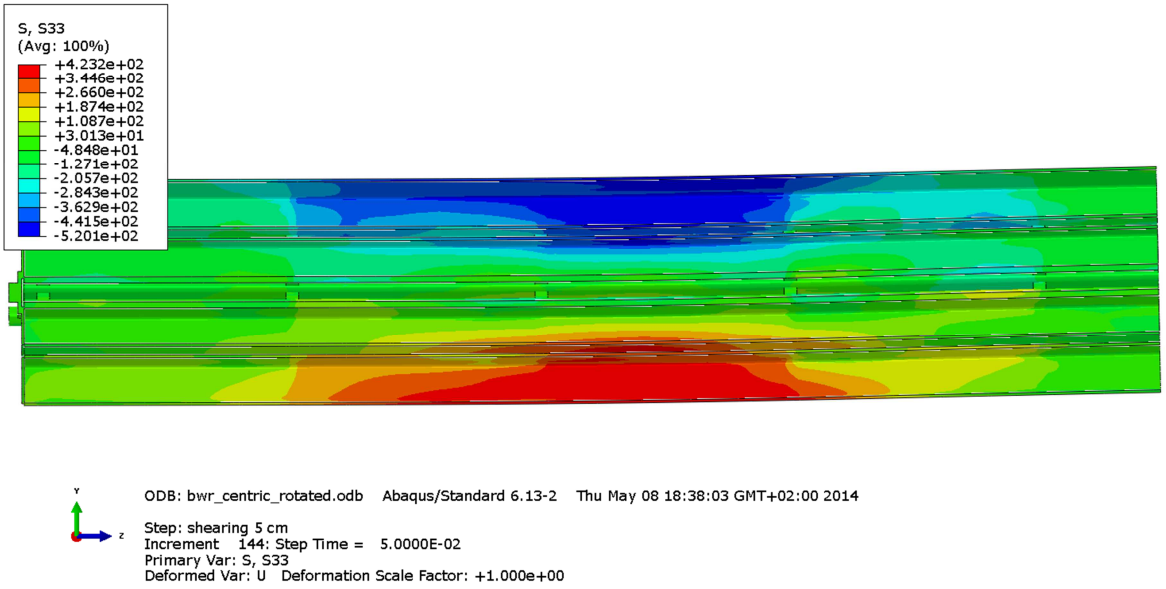

Figure A3-9 *Plot showing axial stress [MPa] for the steel channel tubes after 5 cm shearing.*

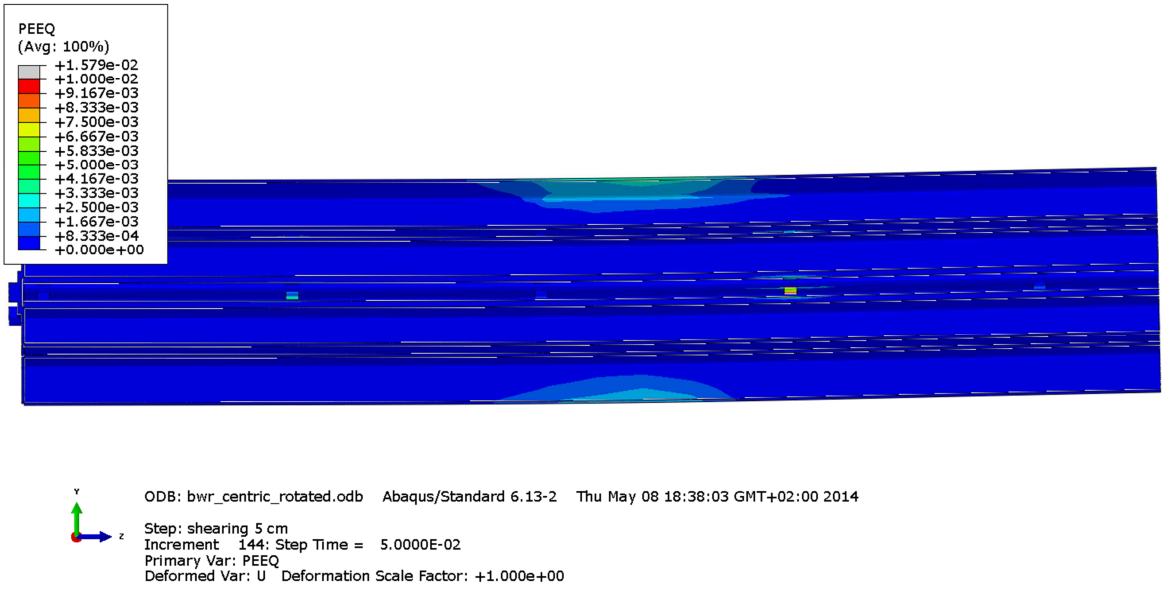

Figure A3-10 *Plot showing equivalent plastic strain (PEEQ) for the steel channel tubes after 5 cm shearing.*

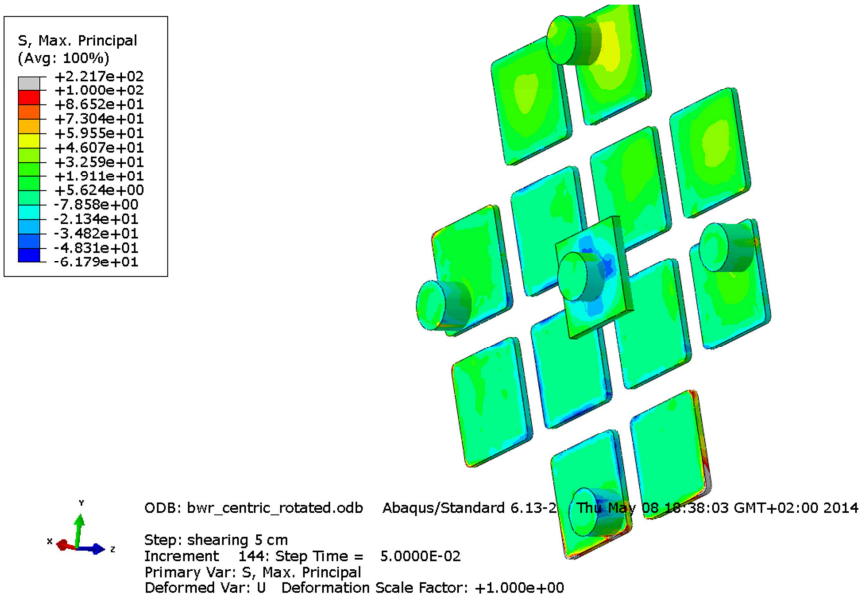

Figure A3-11 *Plot showing maximum principal stress [MPa] for the steel channel tubes base plates after 5 cm shearing.*

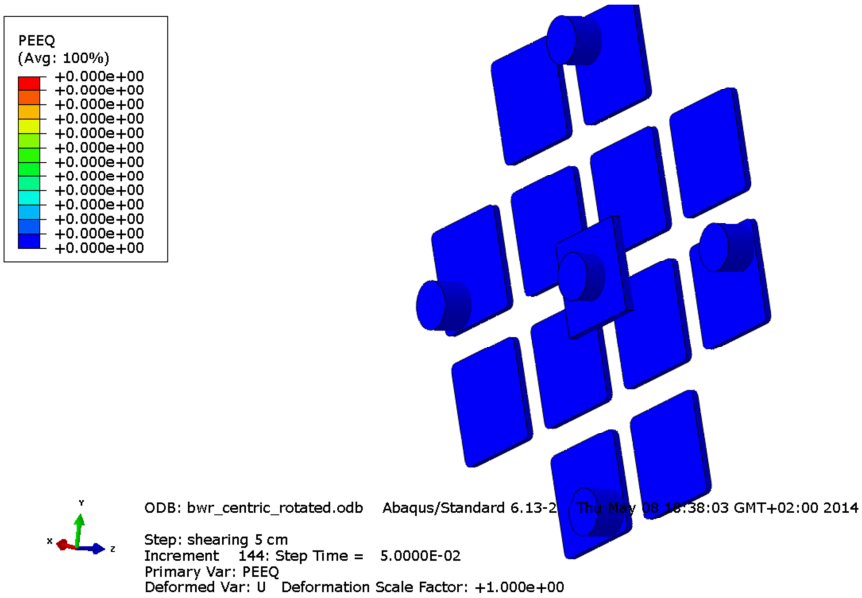

Figure A3-12 *Plot showing equivalent plastic strain (PEEQ) for the steel channel tubes base plates after 5 cm shearing.*

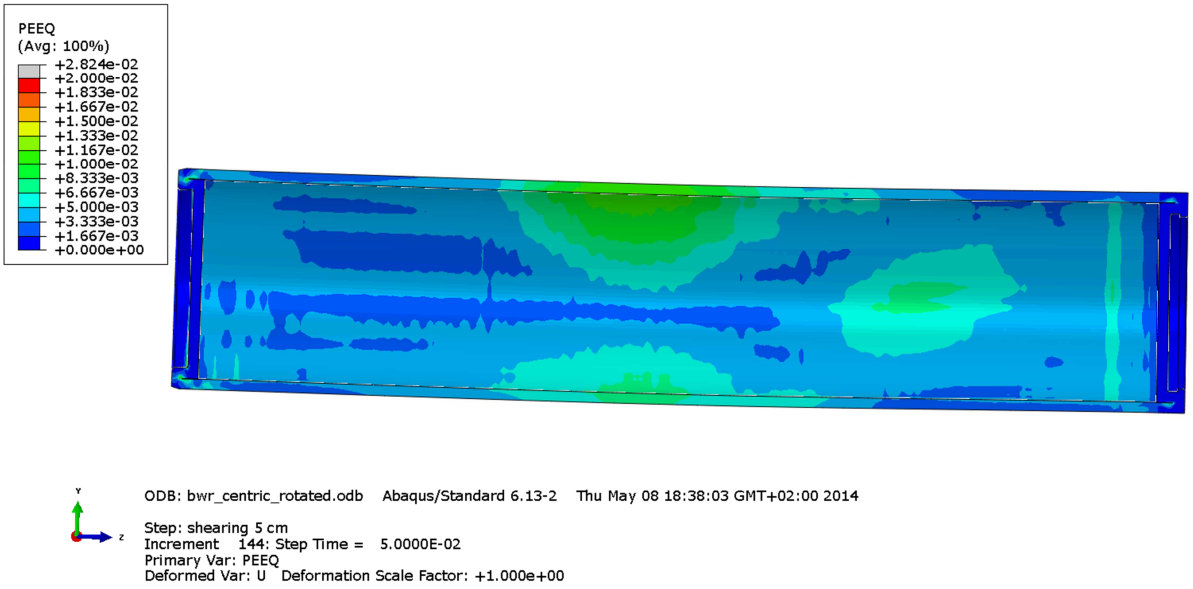

Figure A3-13 *Plot showing equivalent plastic strain (PEEQ) for the copper shell after 5 cm shearing.*

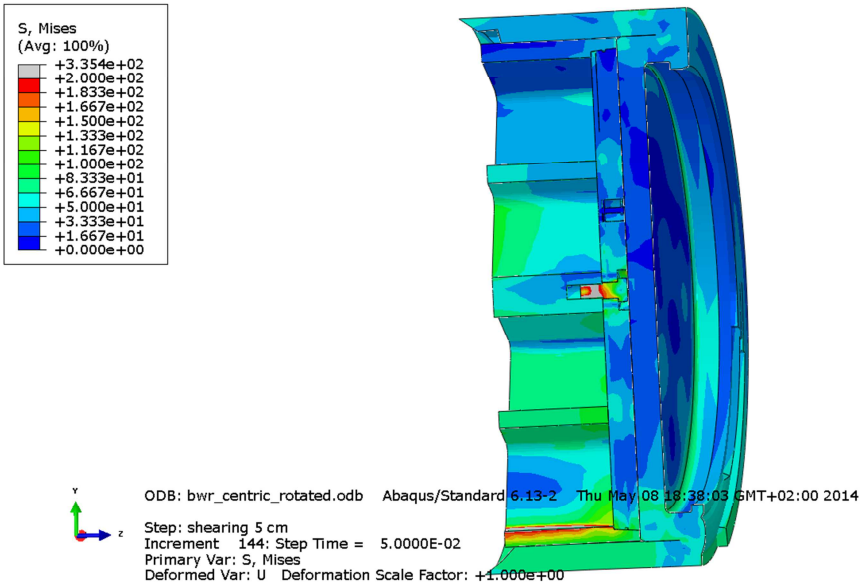

Figure A3-14 *Plot showing Mises stress [MPa] close to the insert lid fixing screw after 5 cm shearing.*

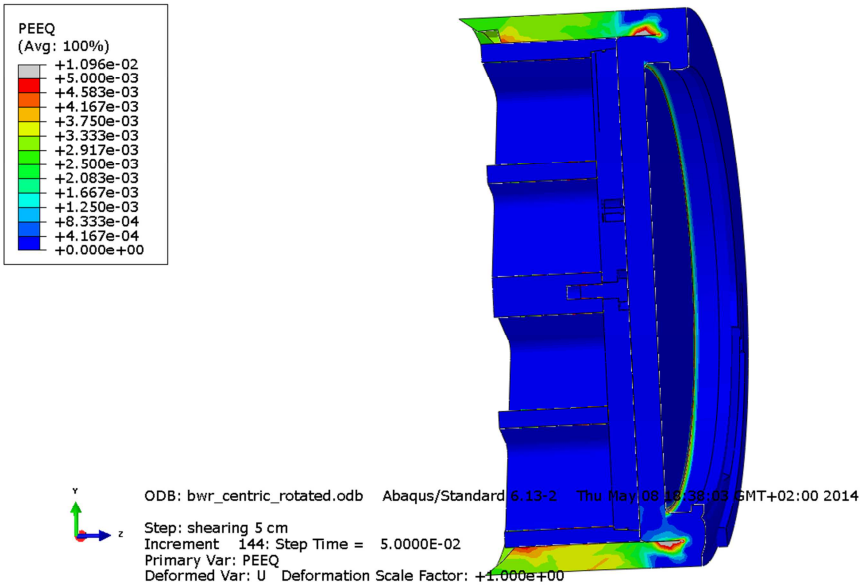

Figure A3-15 *Plot showing equivalent plastic strain (PEEQ) close to the insert lid fixing screw after 5 cm shearing.*

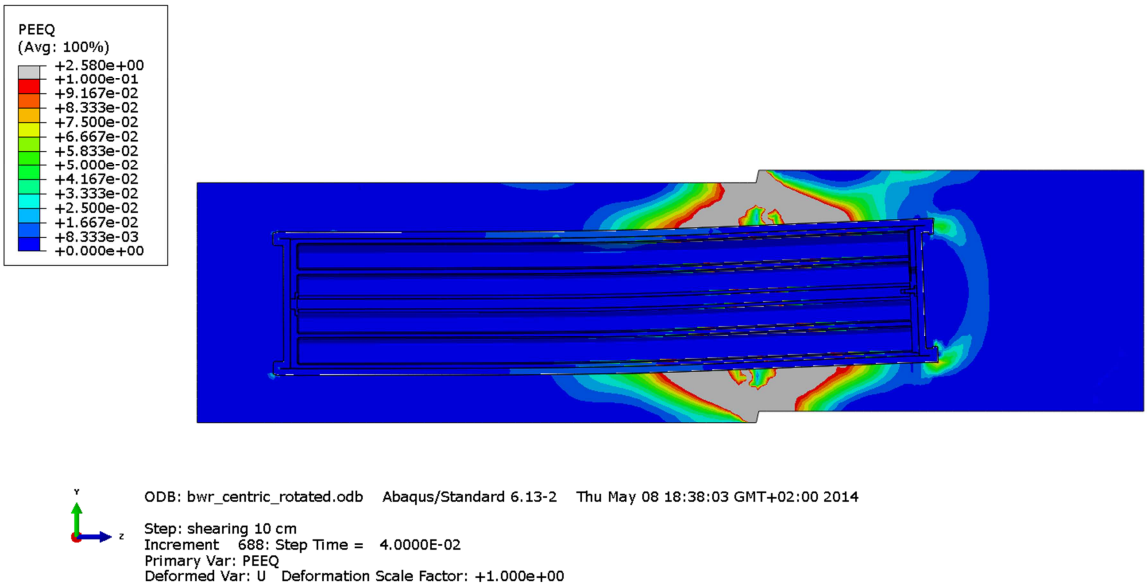

Figure A3-16 *Plot showing equivalent plastic strain (PEEQ) after 9 cm shearing.*

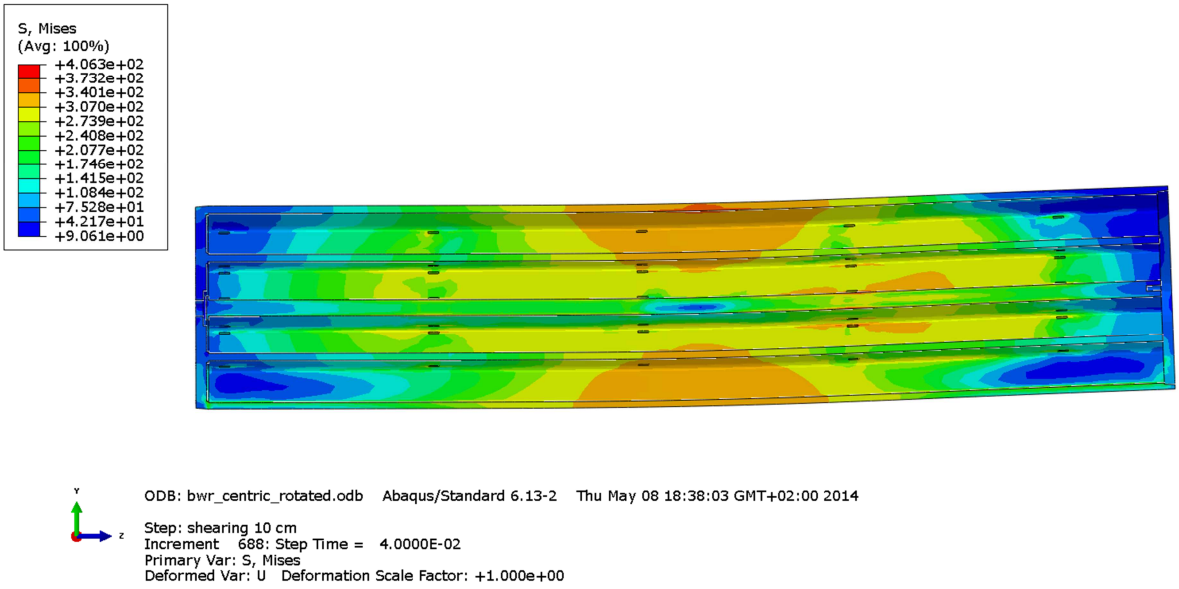

Figure A3-17 *Plot showing Mises stress [MPa] for the insert after 9 cm shearing.*

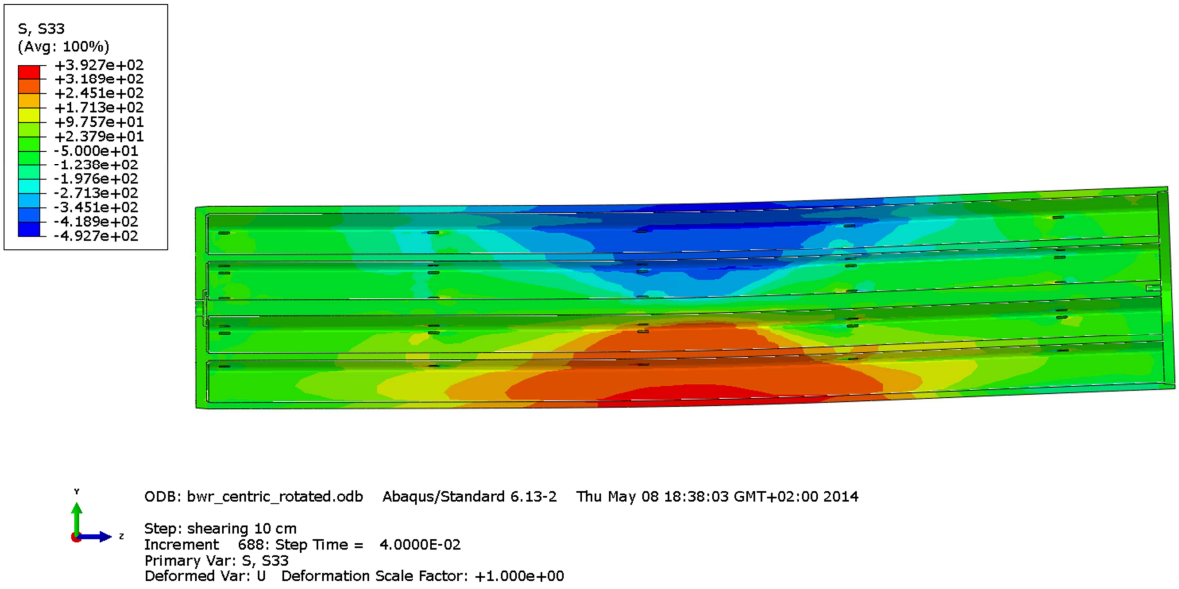

Figure A3-18 *Plot showing axial stress [MPa] for the insert after 9 cm shearing.*

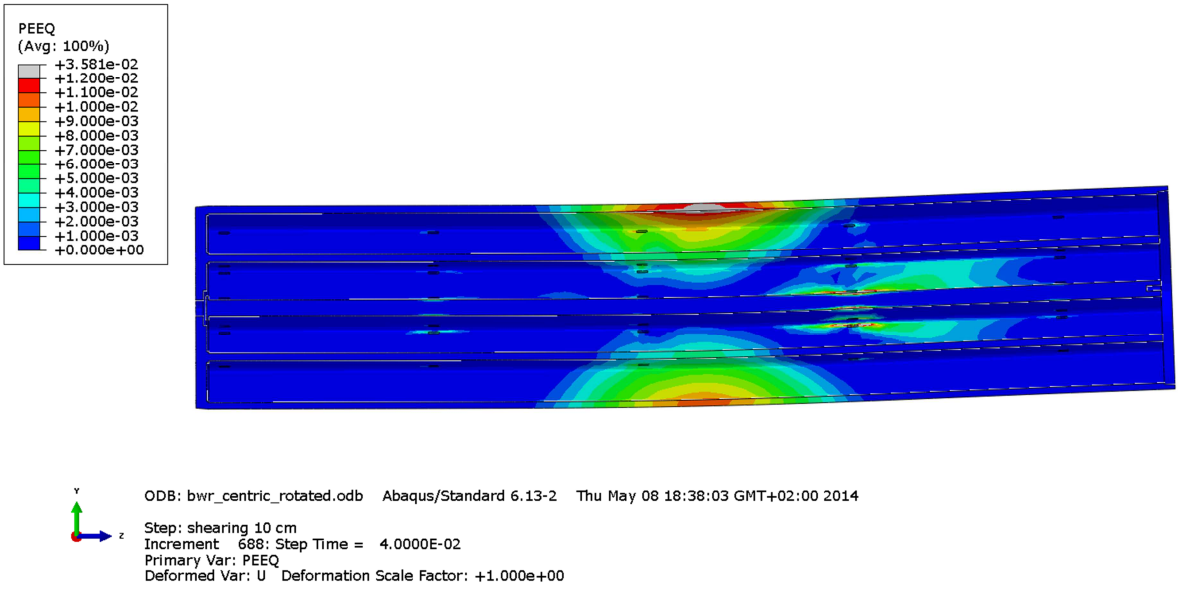

Figure A3-19 *Plot showing equivalent plastic strain (PEEQ) for the insert after 9 cm shearing.*

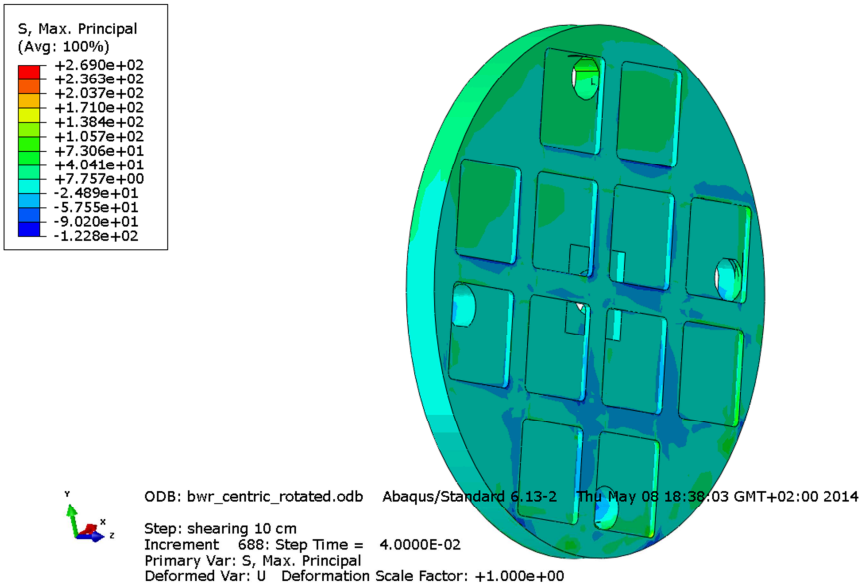

Figure A3-20 *Plot showing maximum principal stress [MPa] for the insert base after 8 cm shearing.*

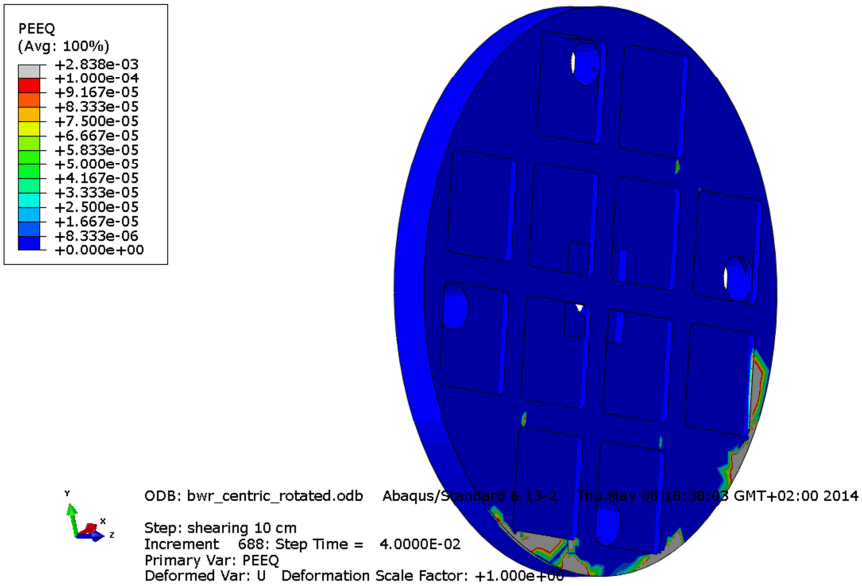

Figure A3-21 *Plot showing equivalent plastic strain (PEEQ) for the insert base after 9 cm shearing.*

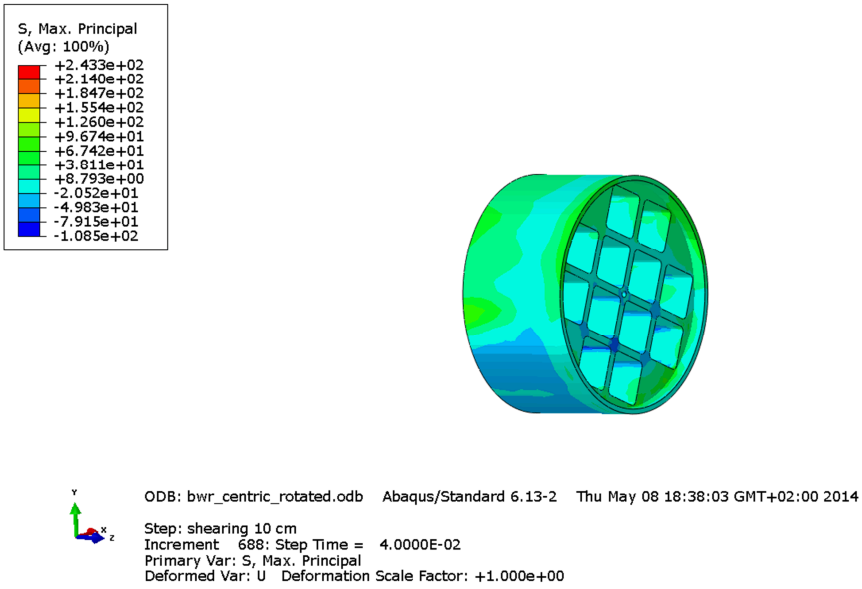

Figure A3-22 *Plot showing maximum principal stress [MPa] for the insert top after 9 cm shearing.*

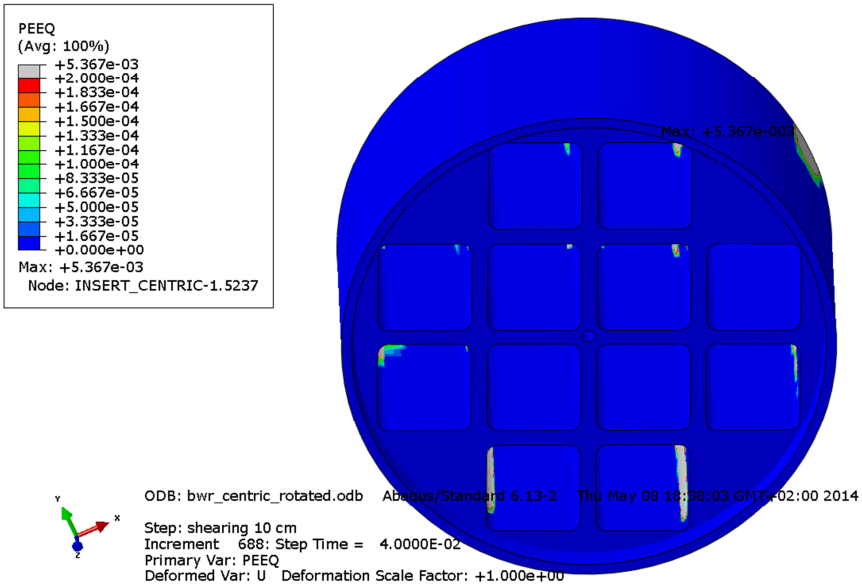

Figure A3-23 *Plot showing equivalent plastic strain (PEEQ) for the insert top after 9 cm shearing.*

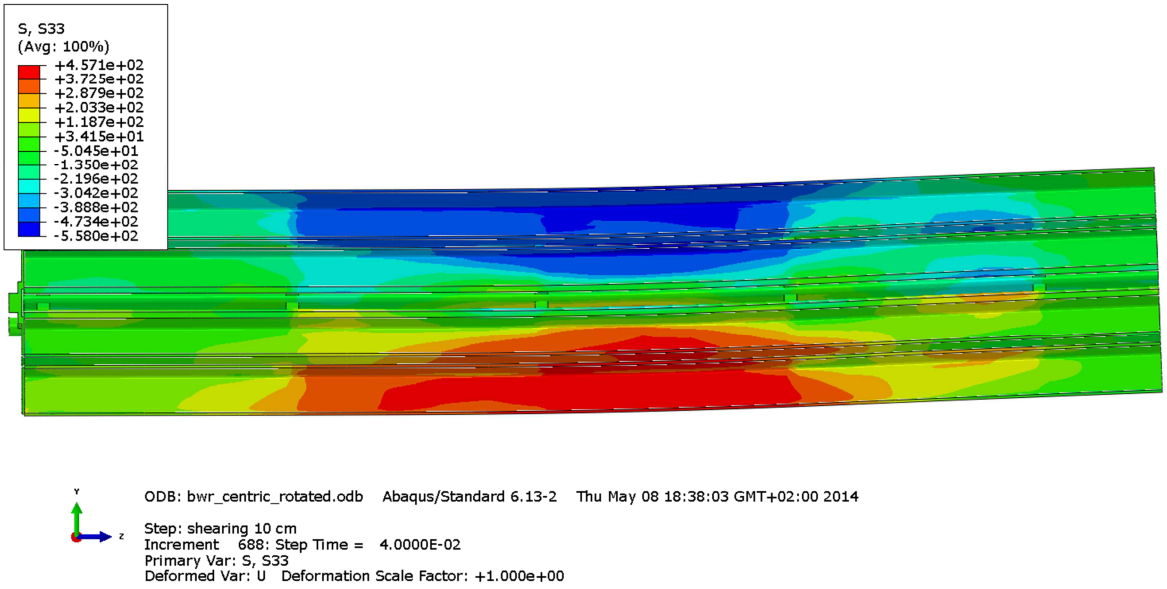

Figure A3-24 *Plot showing axial stress [MPa] for the steel channel tubes after 9 cm shearing.*

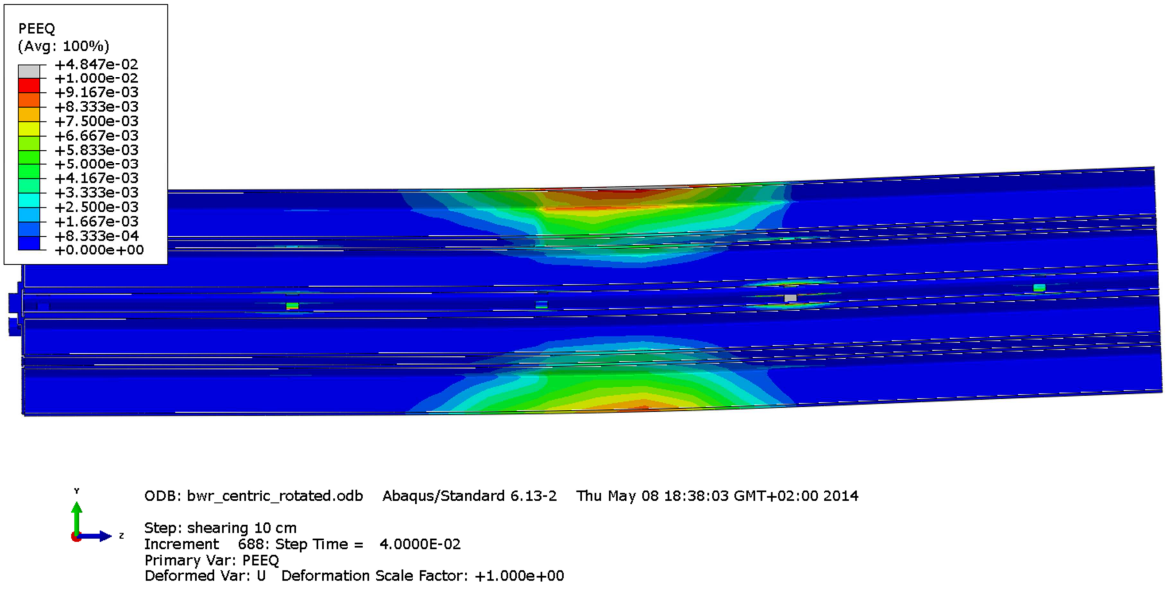

Figure A3-25 *Plot showing equivalent plastic strain (PEEQ) for the steel channel tubes after 9 cm shearing.*

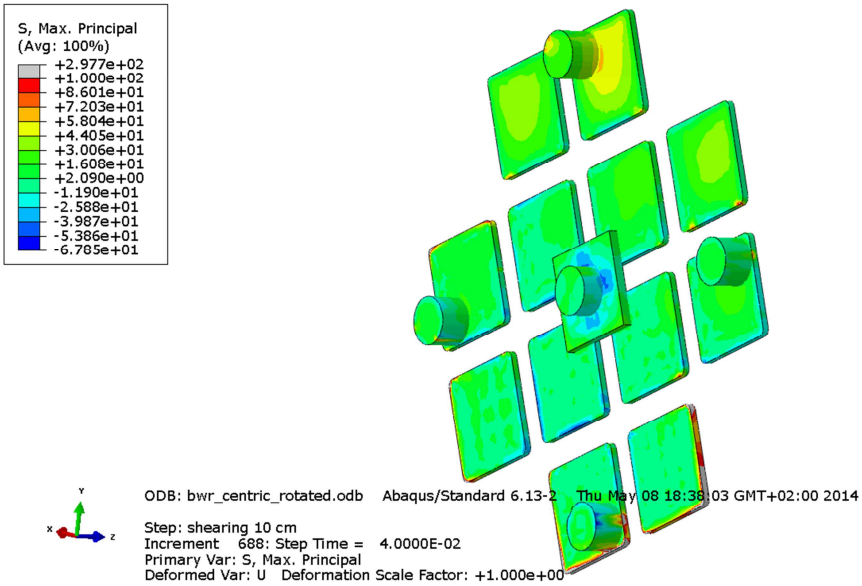

Figure A3-26 *Plot showing maximum principal stress [MPa] for the steel channel tubes base plates after 9 cm shearing.*

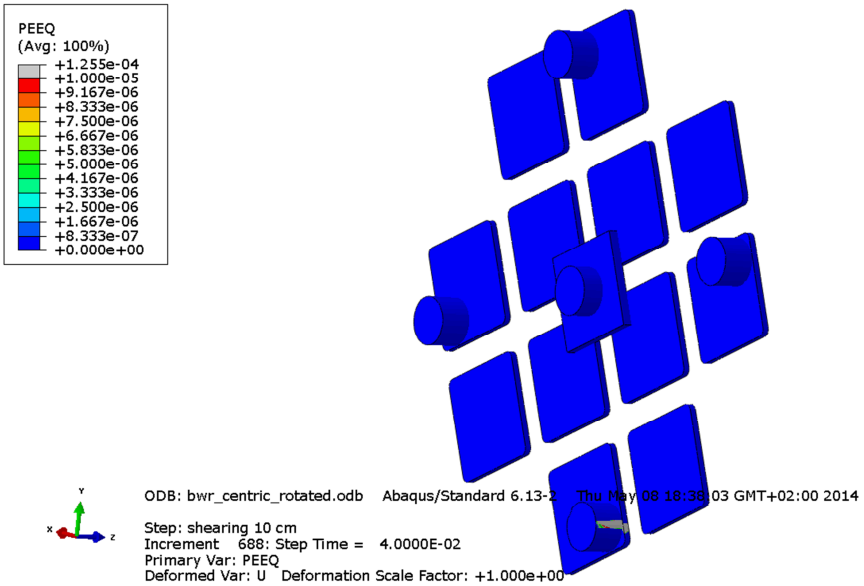

Figure A3-27 *Plot showing equivalent plastic strain (PEEQ) for the steel channel tubes base plates after 9 cm shearing.*

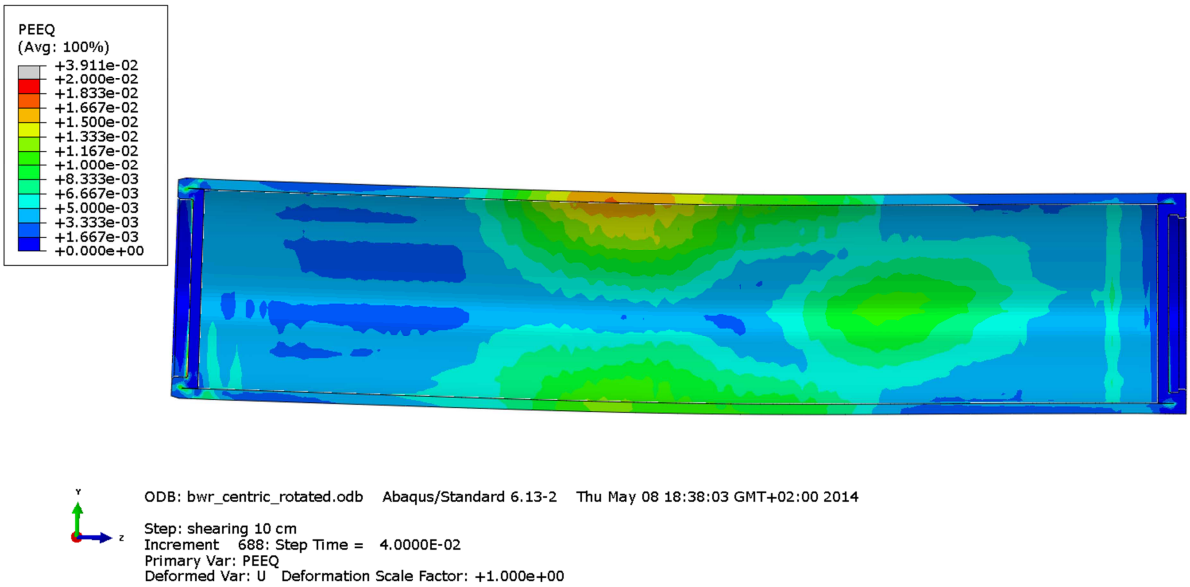

Figure A3-28 *Plot showing equivalent plastic strain (PEEQ) for the copper shell after 9 cm shearing.*

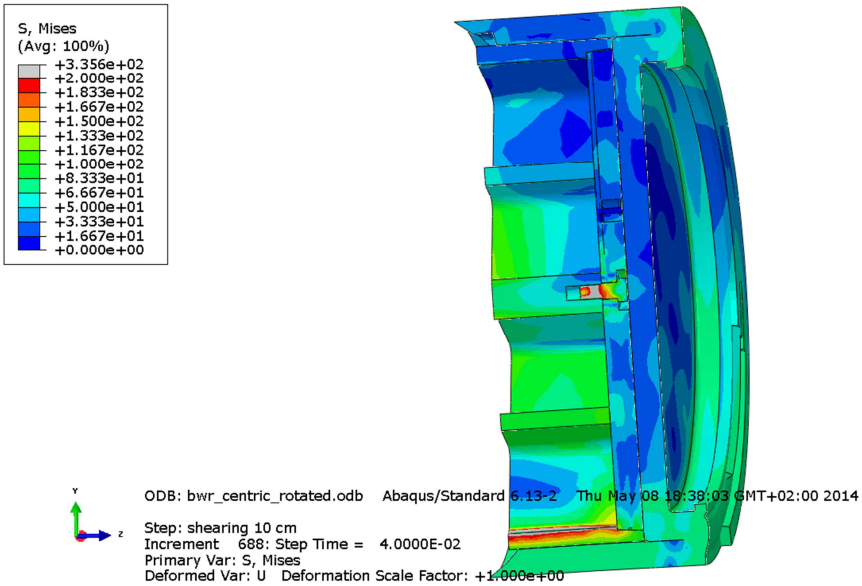

Figure A3-29 *Plot showing Mises stress [MPa] close to the insert lid fixing screw after 9 cm shearing.*

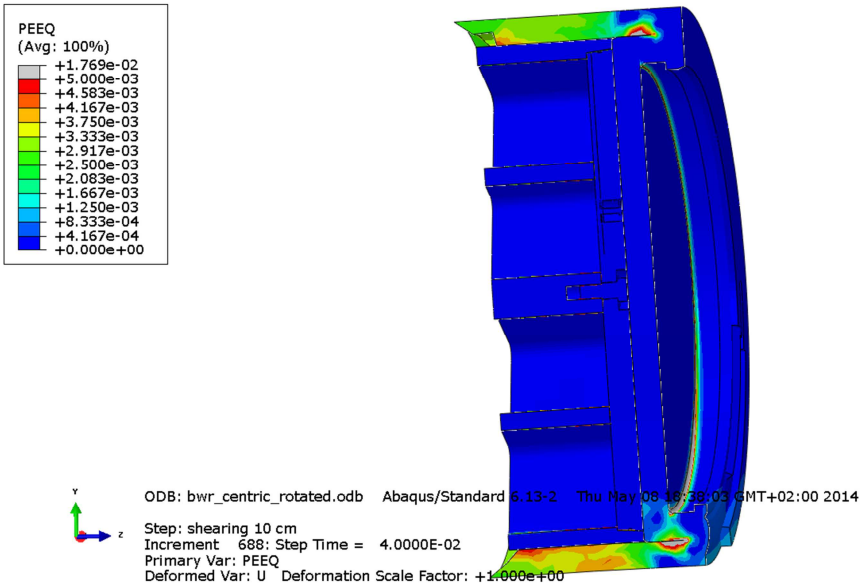

Figure A3-30 *Plot showing equivalent plastic strain (PEEQ) close to the insert lid fixing screw after 9 cm shearing.*

Appendix 4 – Plots for bwr_excentric_rotated

Plots showing deformed geometry as contour plots for all parts at shearing magnitude 5 and 8 cm for case bwr_eccentric_rotated (horizontal shearing at ¾-distance from the insert base) when the insert is placed eccentrically in respect to the rotated steel channel tubes taking tolerances into account. The view shows the symmetry plane and all deformations are scaled by a factor of two.

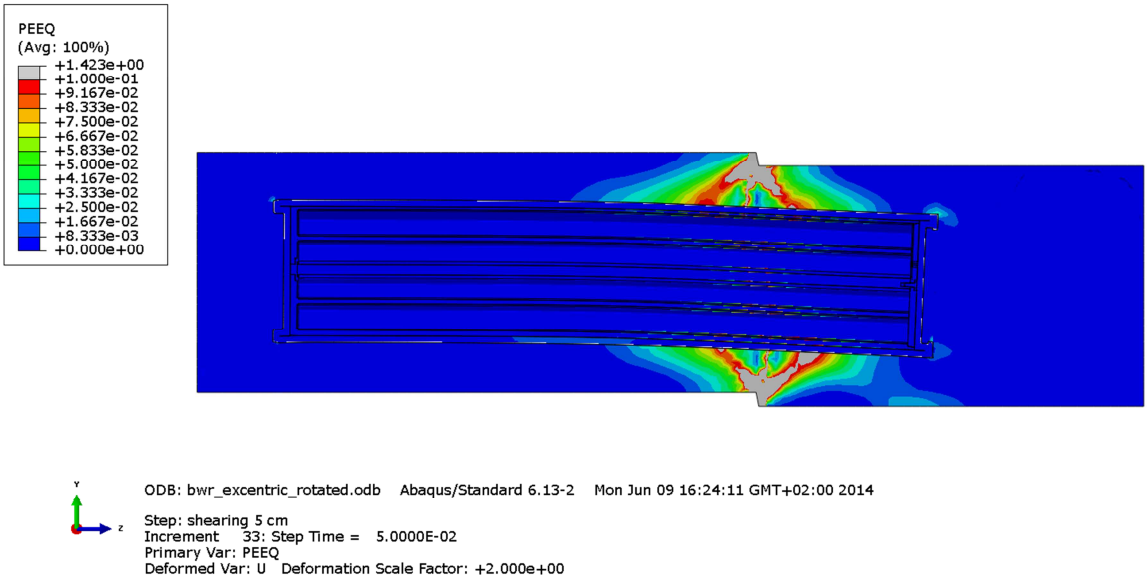

Figure A4-1 *Plot showing equivalent plastic strain (PEEQ) after 5 cm shearing.*

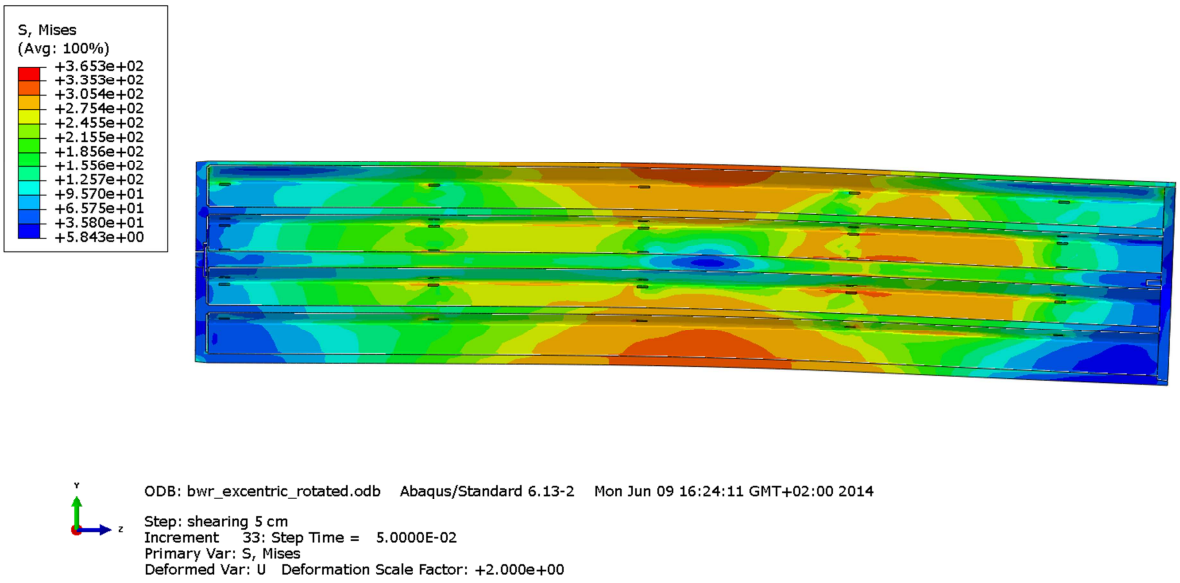

Figure A4-2 *Plot showing Mises stress [MPa] for the insert after 5 cm shearing.*

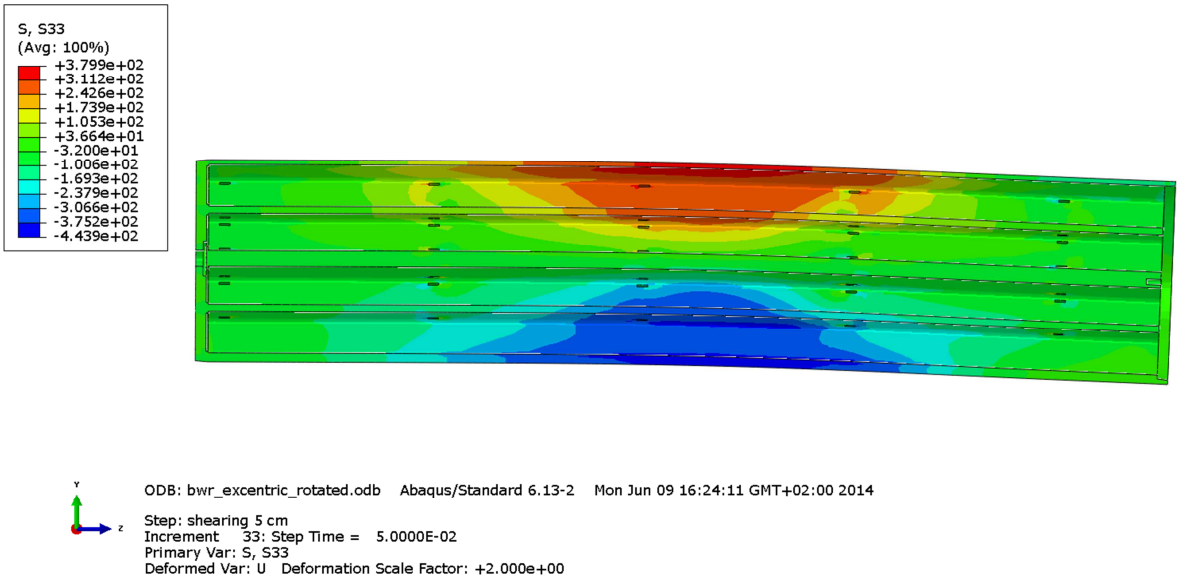

Figure A4-3 *Plot showing axial stress [MPa] for the insert after 5 cm shearing.*

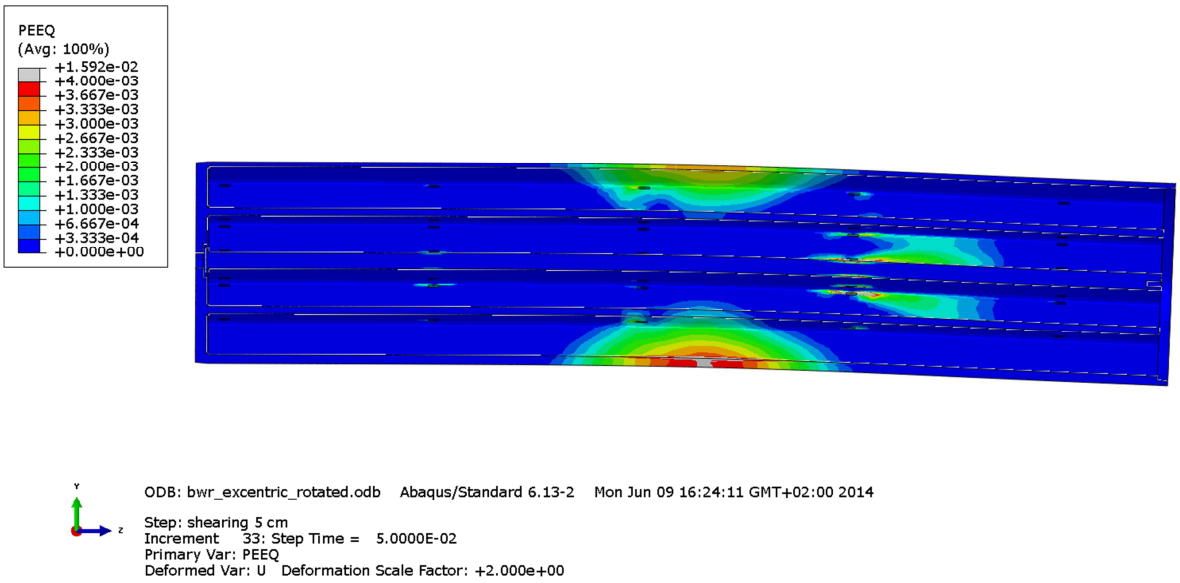

Figure A4-4 *Plot showing equivalent plastic strain (PEEQ) for the insert after 5 cm shearing.*

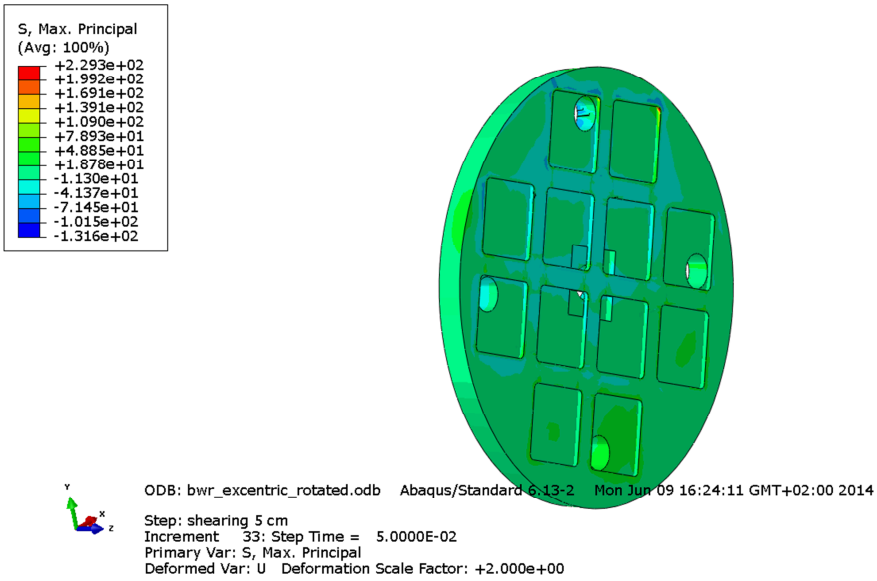

Figure A4-5 *Plot showing maximum principal stress [MPa] for the insert base after 5 cm shearing.*

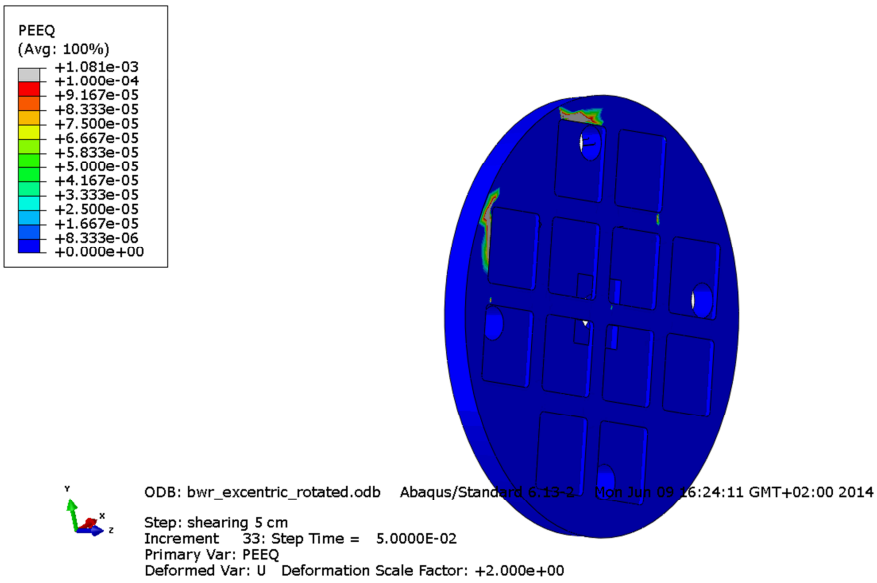

Figure A4-6 *Plot showing equivalent plastic strain (PEEQ) for the insert base after 5 cm shearing.*

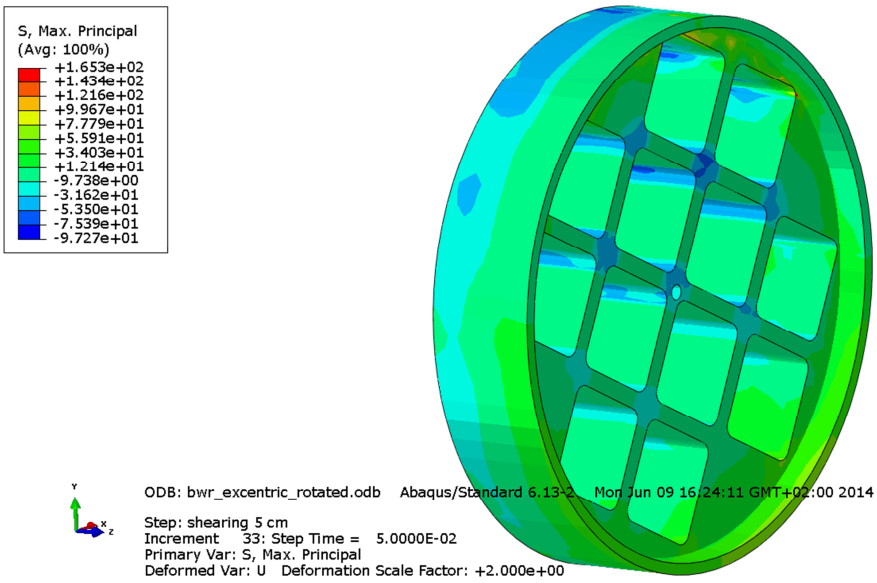

Figure A4-7 *Plot showing maximum principal stress [MPa] for the insert top after 5 cm shearing.*

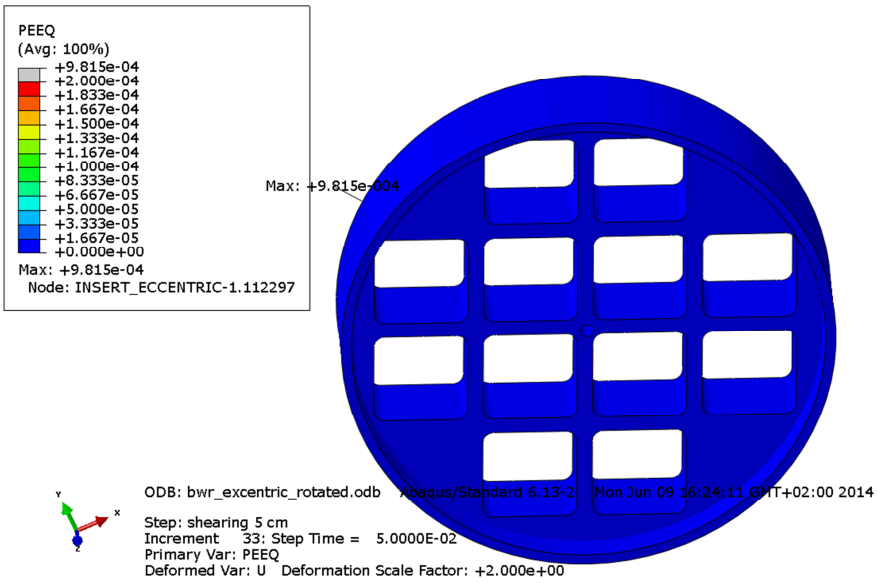

Figure A4-8 *Plot showing equivalent plastic strain (PEEQ) for the insert top after 5 cm shearing.*

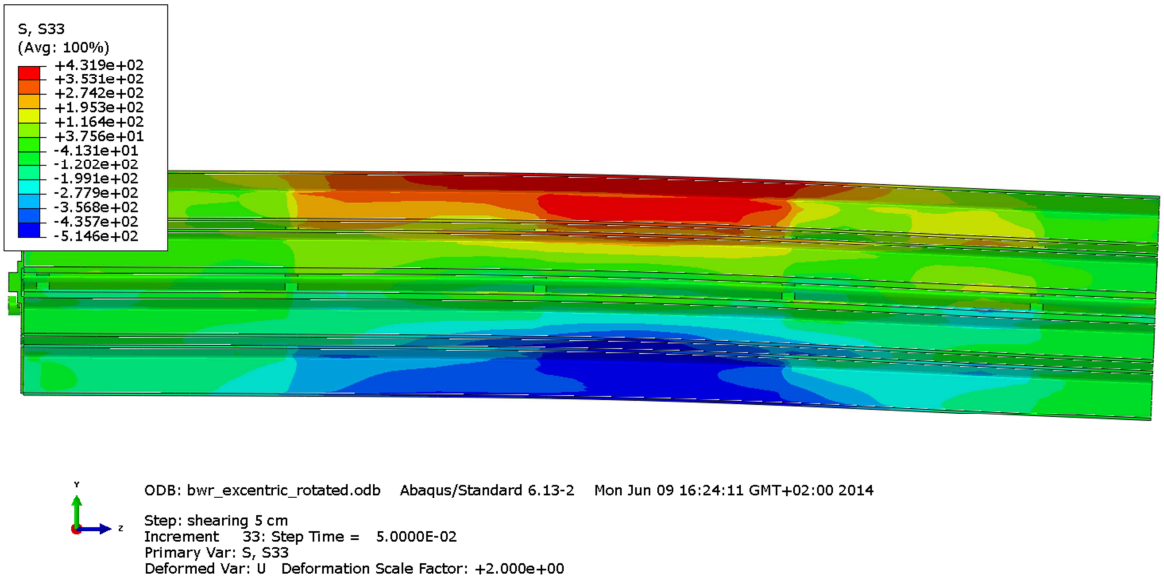

Figure A4-9 *Plot showing axial stress [MPa] for the steel channel tubes after 5 cm shearing.*

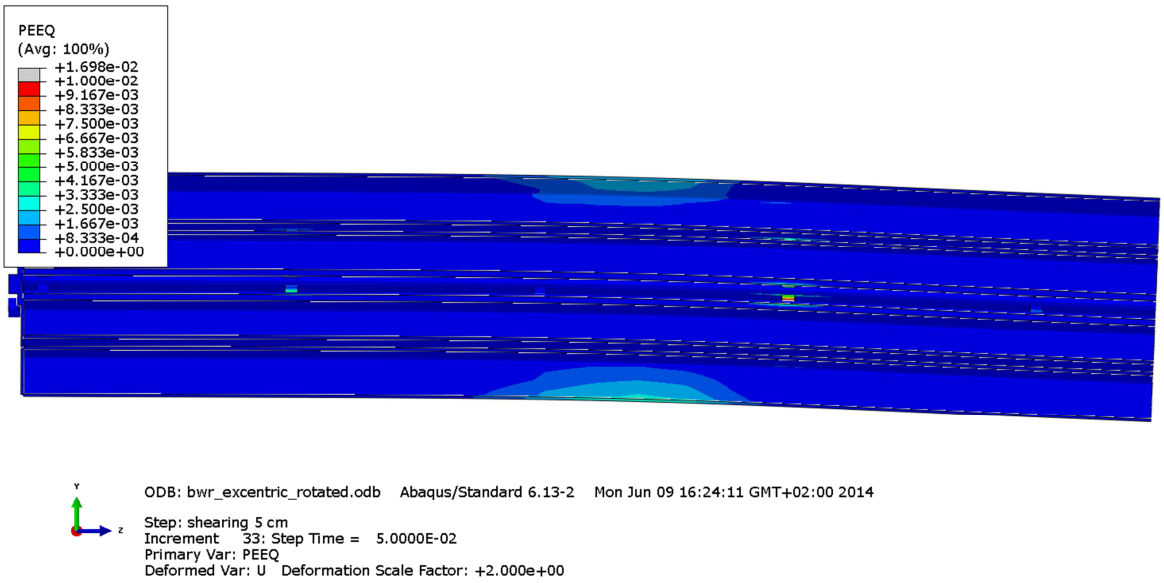

Figure A4-10 *Plot showing equivalent plastic strain (PEEQ) for the steel channel tubes after 5 cm shearing.*

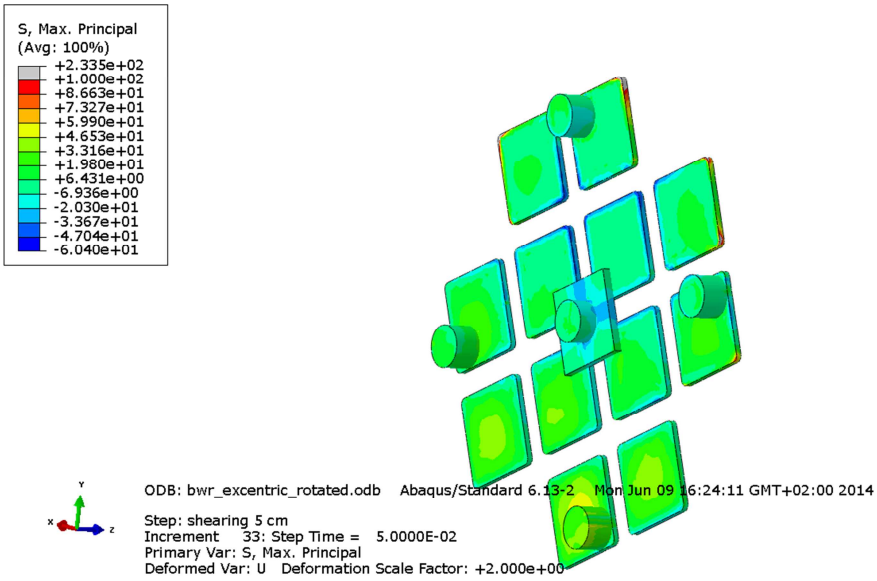

Figure A4-11 *Plot showing maximum principal stress [MPa] for the steel channel tubes base plates after 5 cm shearing.*

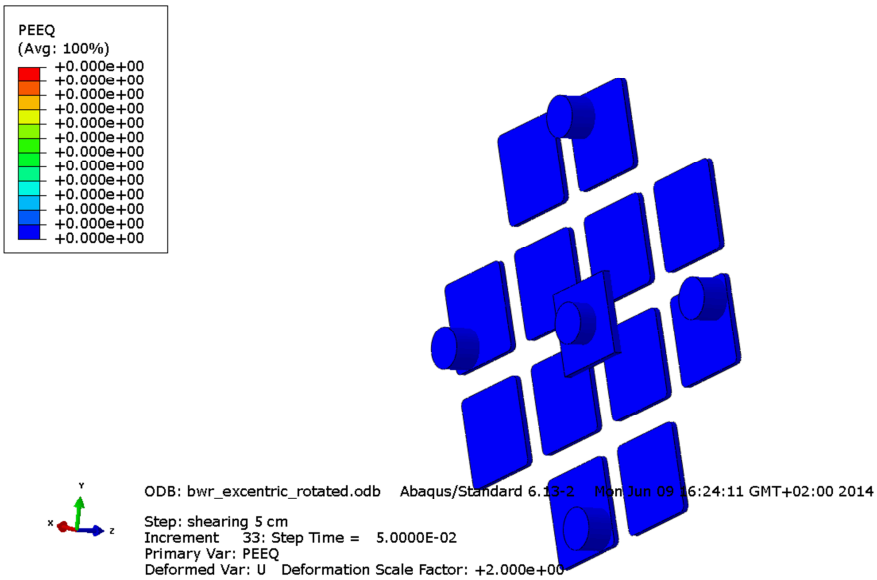

Figure A4-12 *Plot showing equivalent plastic strain (PEEQ) for the steel channel tubes base plates after 5 cm shearing.*

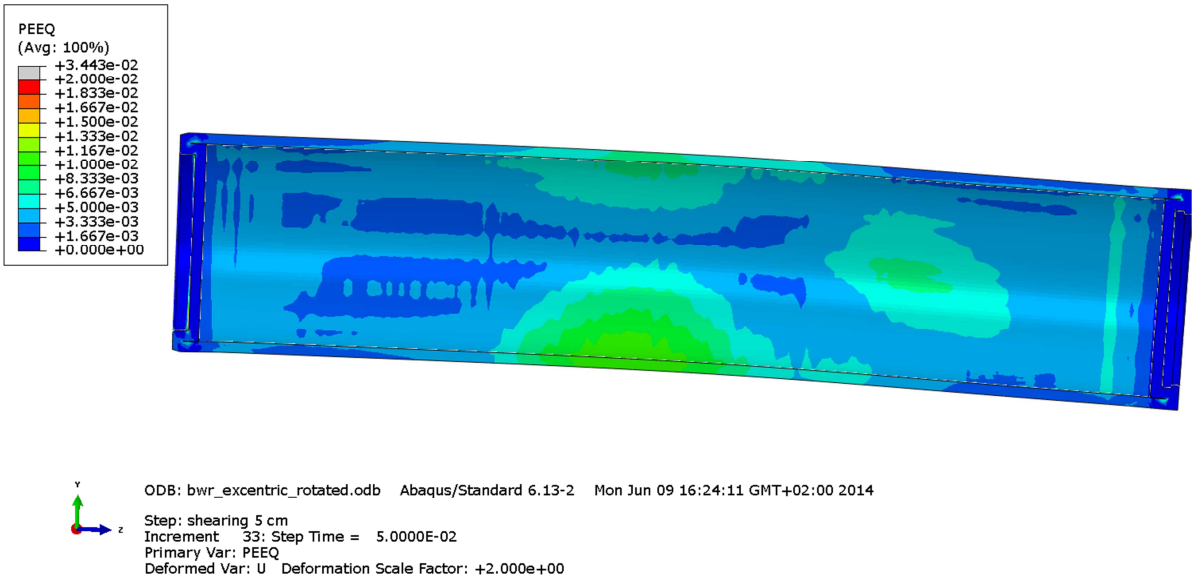

Figure A4-13 *Plot showing equivalent plastic strain (PEEQ) for the copper shell after 5 cm shearing.*

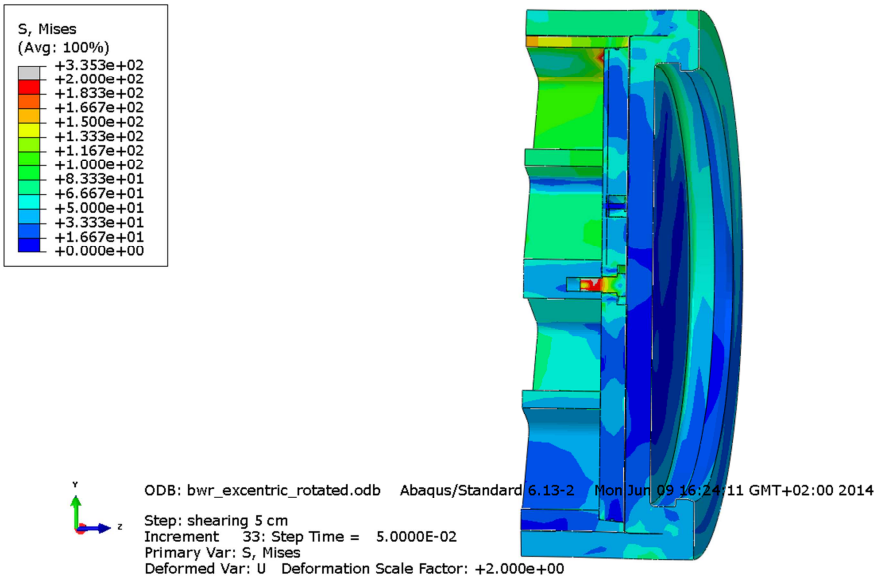

Figure A4-14 *Plot showing Mises stress [MPa] close to the insert lid fixing screw after 5 cm shearing.*

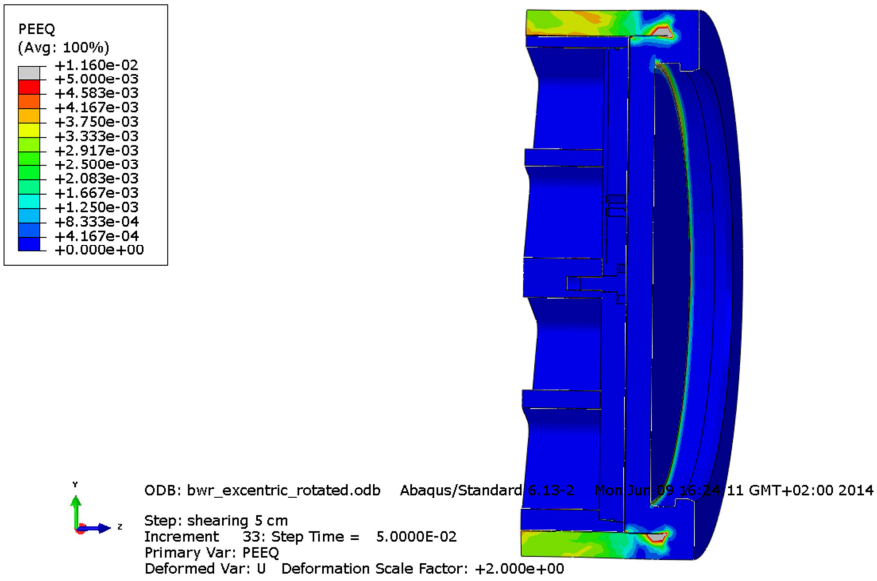

Figure A4-15 *Plot showing equivalent plastic strain (PEEQ) close to the insert lid fixing screw after 5 cm shearing.*

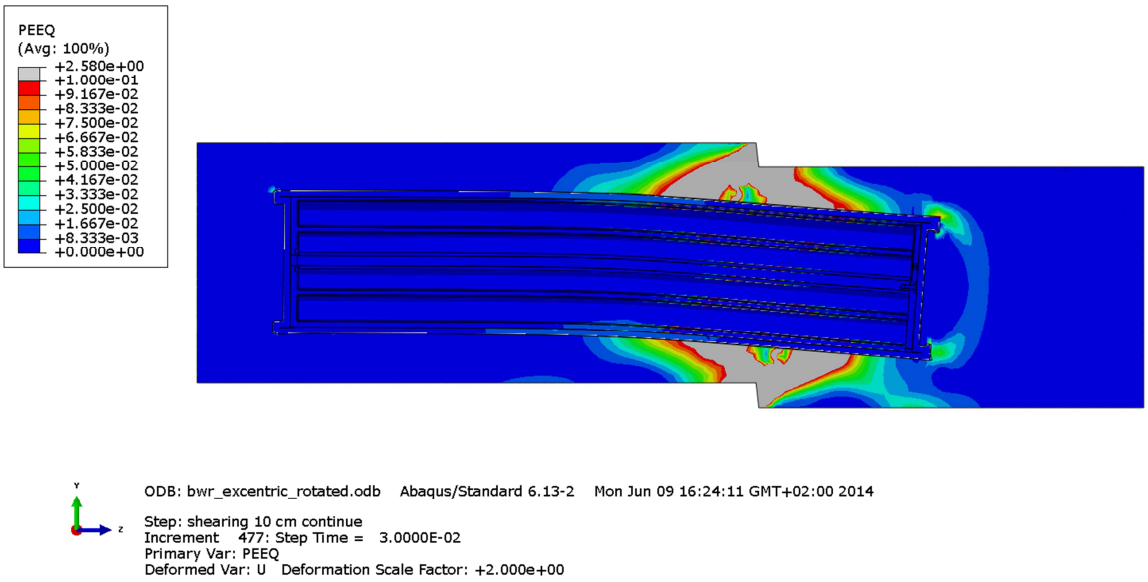

Figure A4-16 *Plot showing equivalent plastic strain (PEEQ) after 9 cm shearing.*

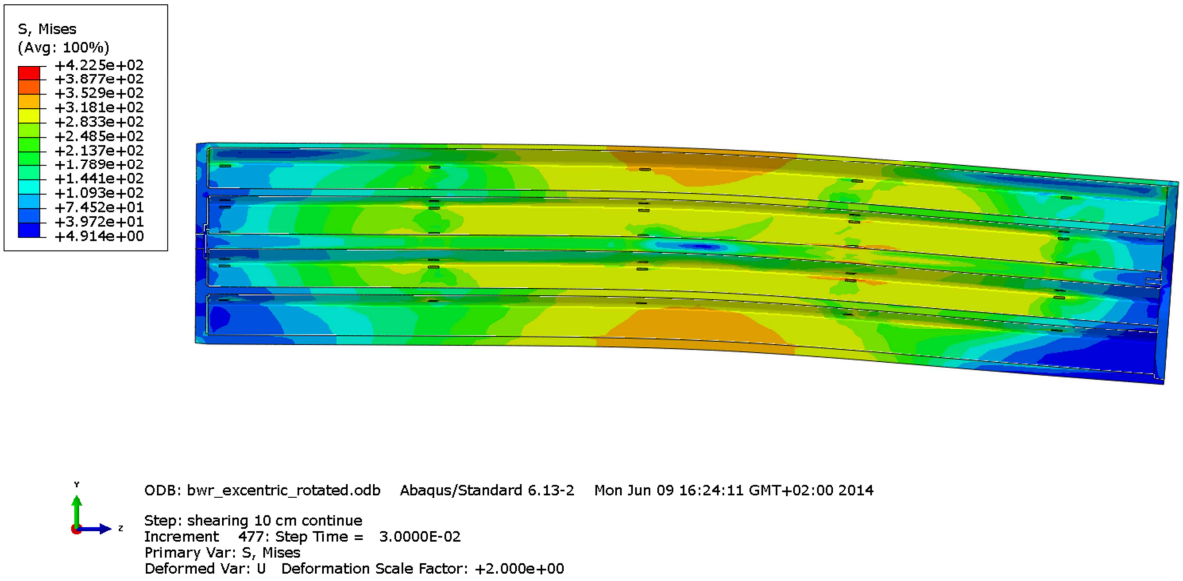

Figure A4-17 *Plot showing Mises stress [MPa] for the insert after 9 cm shearing.*

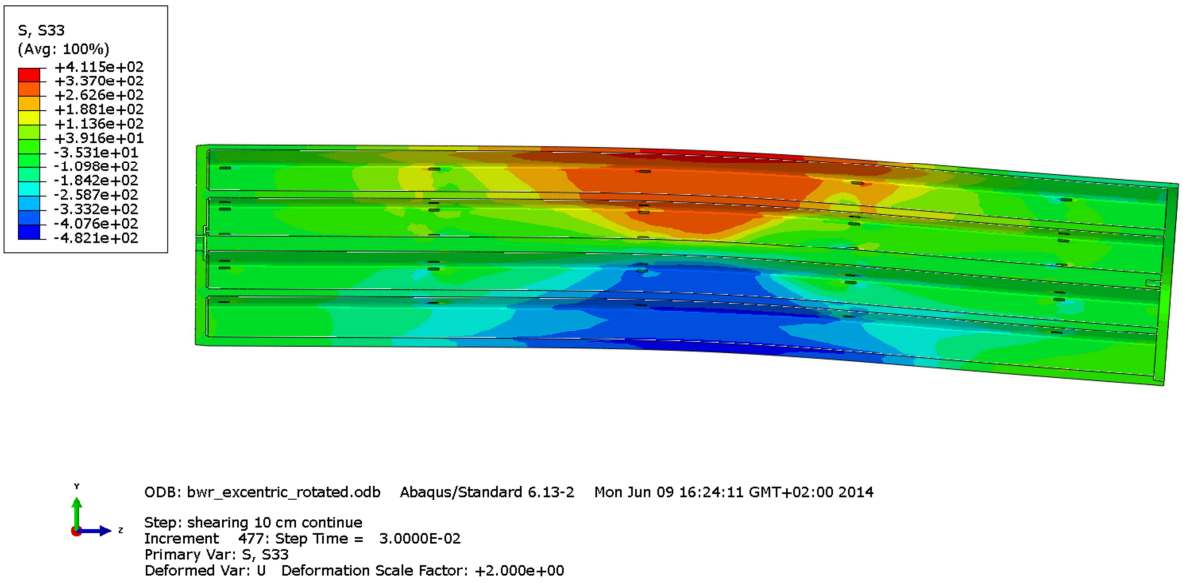

Figure A4-18 *Plot showing axial stress [MPa] for the insert after 9 cm shearing.*

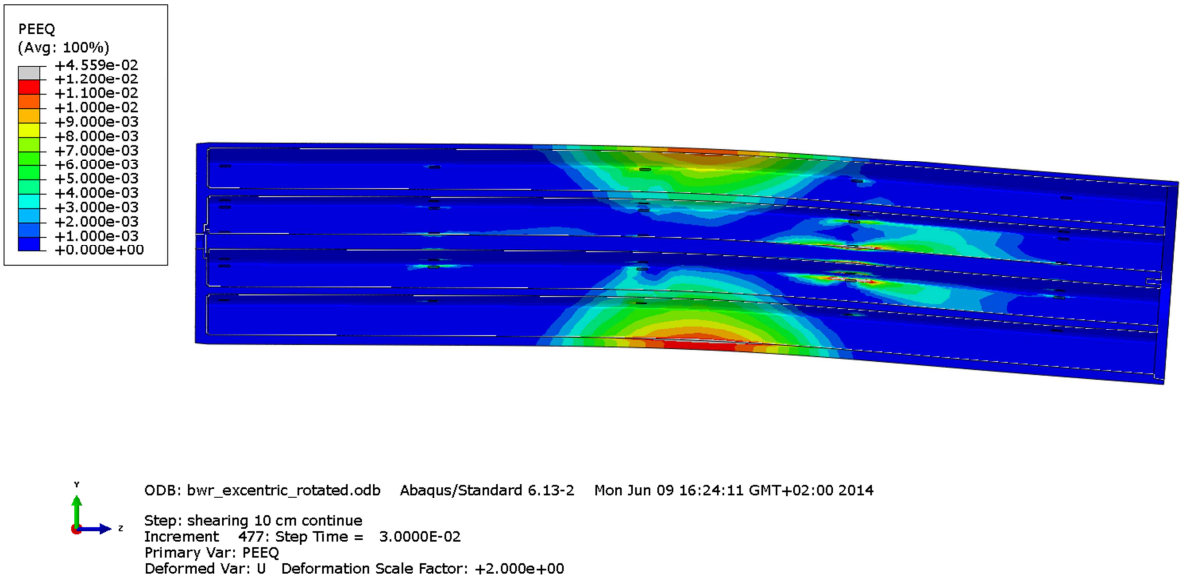

Figure A4-19 *Plot showing equivalent plastic strain (PEEQ) for the insert after 9 cm shearing.*

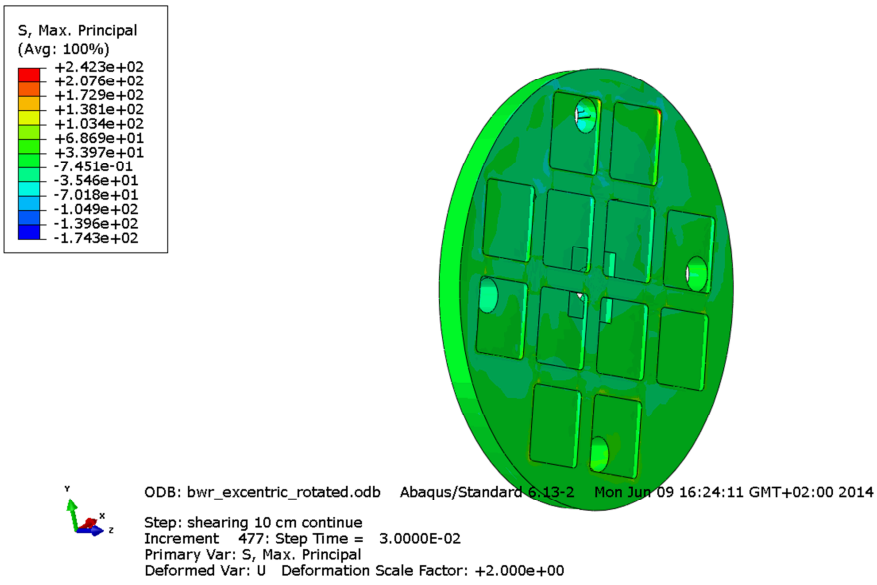

Figure A4-20 *Plot showing maximum principal stress [MPa] for the insert base after 9 cm shearing.*

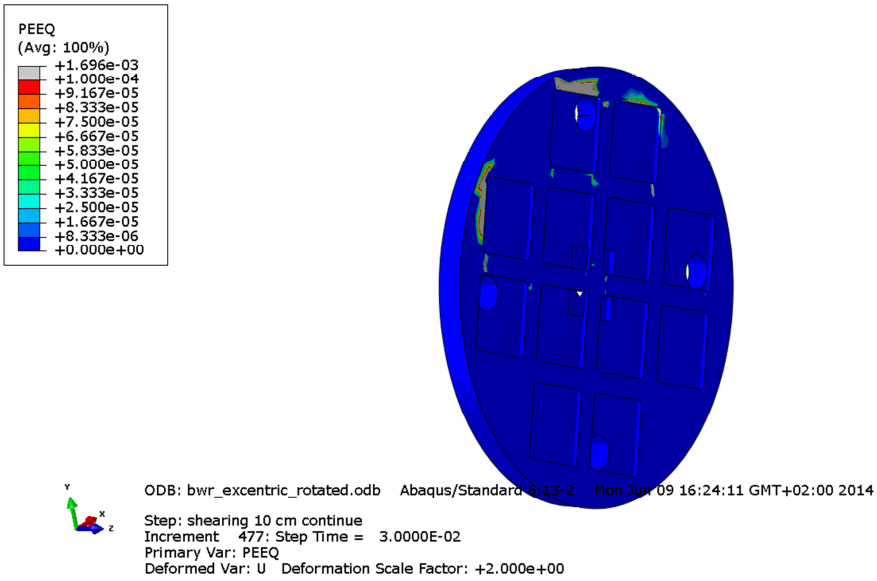

Figure A4-21 *Plot showing equivalent plastic strain (PEEQ) for the insert base after 9 cm shearing.*

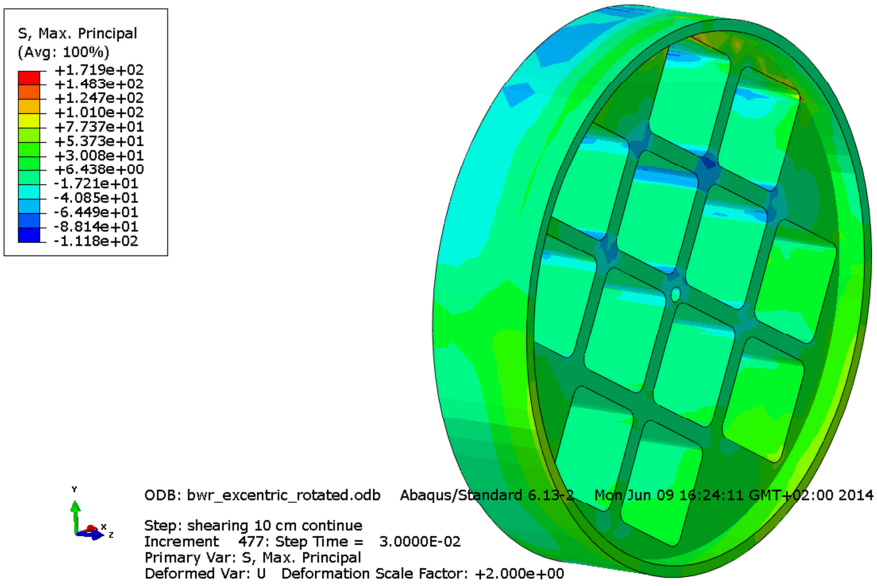

Figure A4-22 *Plot showing maximum principal stress [MPa] for the insert top after 9 cm shearing.*

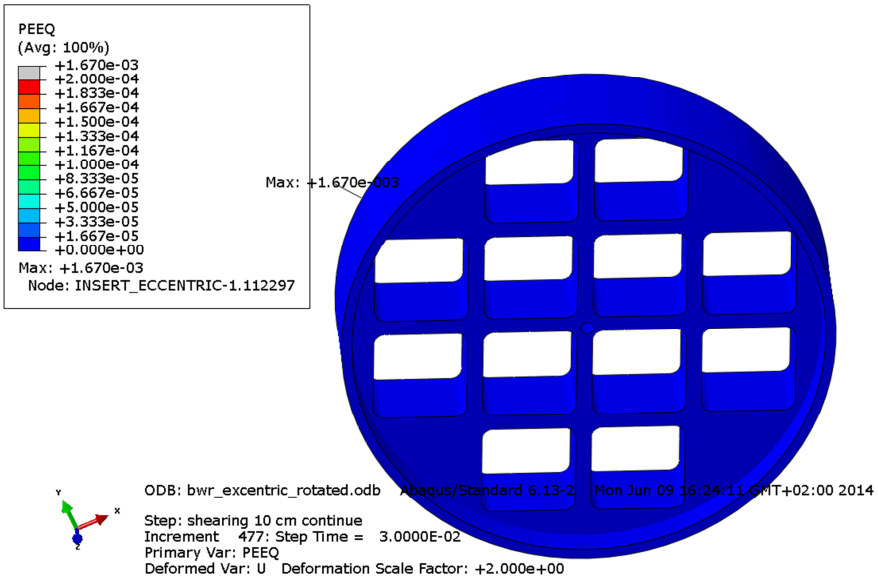

Figure A4-23 *Plot showing equivalent plastic strain (PEEQ) for the insert top after 9 cm shearing.*

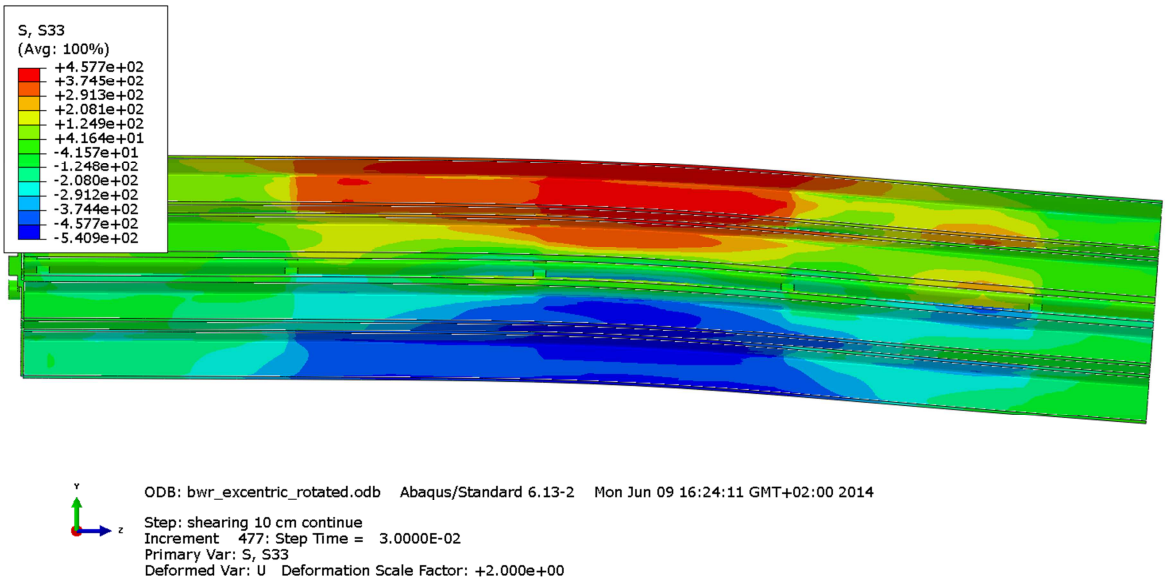

Figure A4-24 Plot showing axial stress [MPa] for the steel channel tubes after 9 cm shearing.

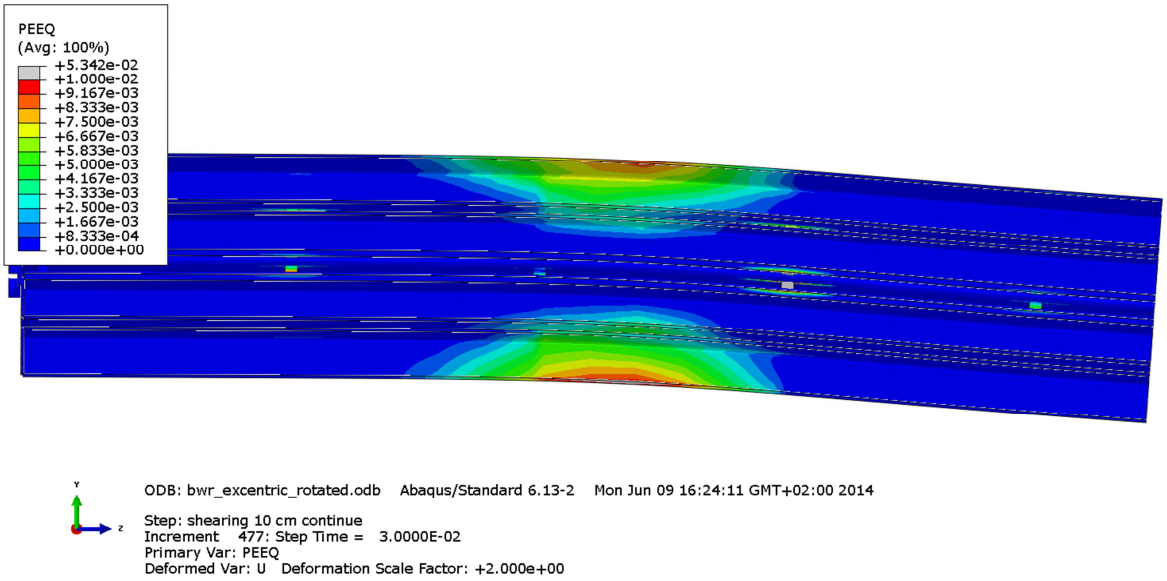

Figure A4-25 *Plot showing equivalent plastic strain (PEEQ) for the steel channel tubes after 9 cm shearing.*

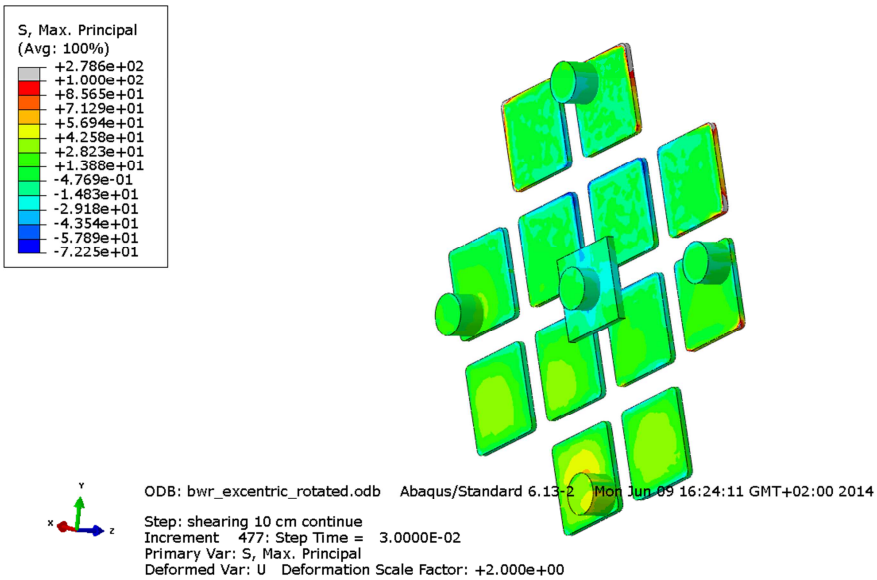

Figure A4-26 *Plot showing maximum principal stress [MPa] for the steel channel tubes base plates after 9 cm shearing.*

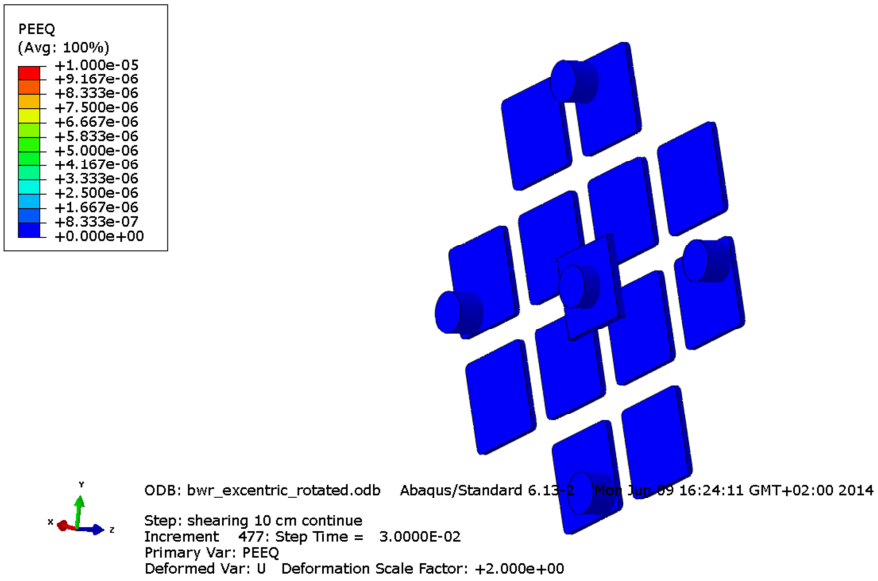

Figure A4-27 *Plot showing equivalent plastic strain (PEEQ) for the steel channel tubes base plates after 9 cm shearing.*

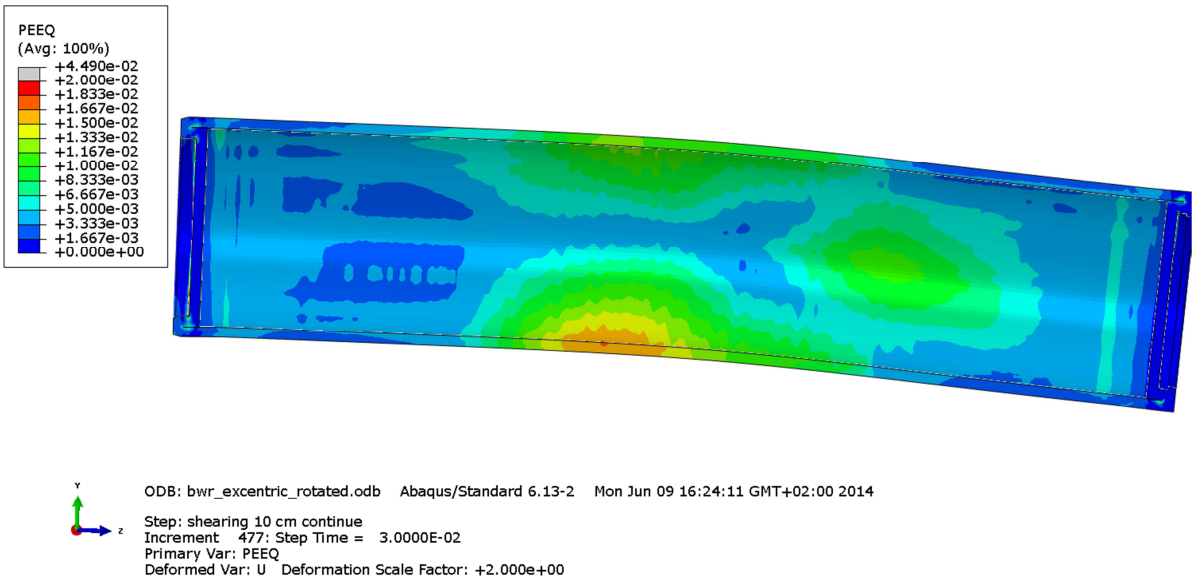

Figure A4-28 *Plot showing equivalent plastic strain (PEEQ) for the copper shell after 9 cm shearing.*

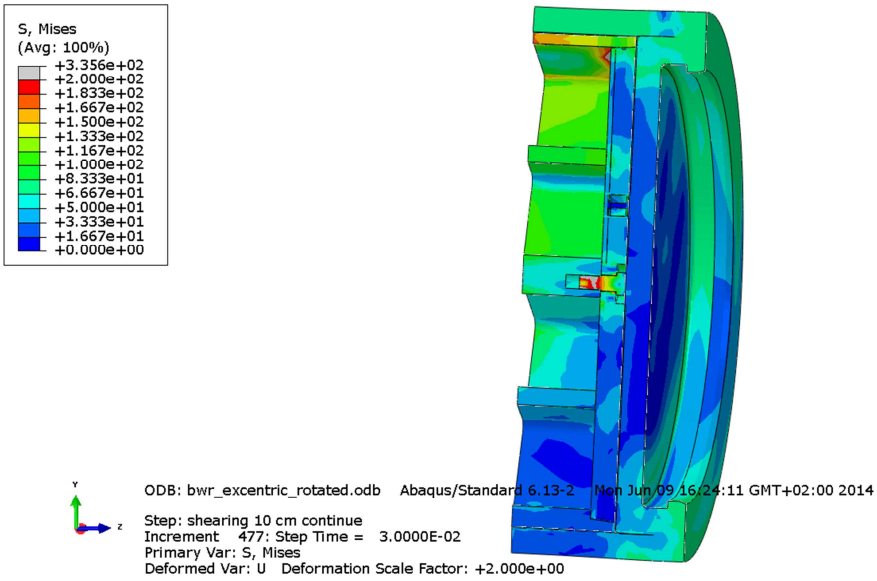

Figure A4-29 *Plot showing Mises stress [MPa] close to the insert lid fixing screw after 9 cm shearing.*

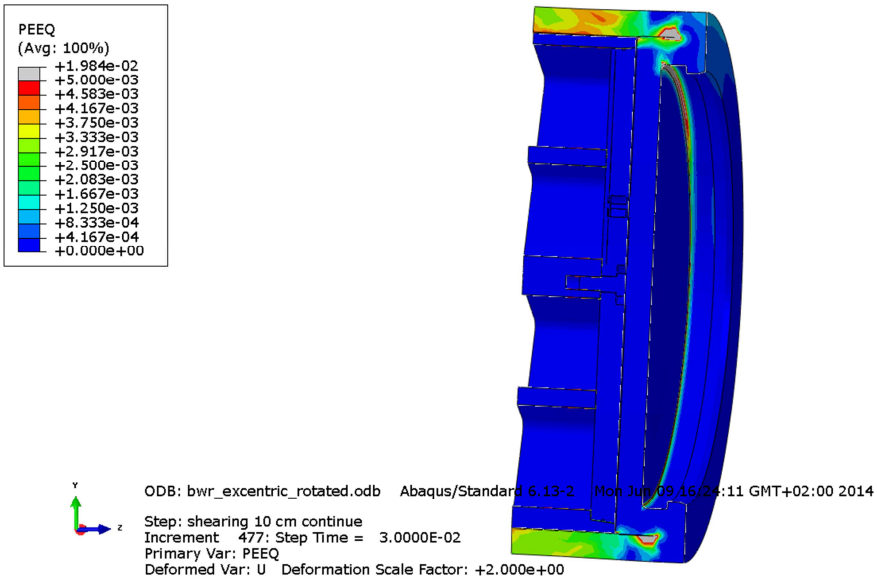

Figure A4-30 *Plot showing equivalent plastic strain (PEEQ) close to the insert lid fixing screw after 9 cm shearing.*

Appendix 5 – Comparison for all cases after 8 cm shearing at 75% distance from the insert base

Plots showing comparison between detailed modelling and the reference case at shearing magnitude 8 cm (horizontal shearing at ¾ distance from insert base). The view shows the symmetry plane and all deformations are scaled by a factor of two. The following cases are shown:

- bwr_eccentric_half, upper left plot
- bwr_centric_rotated, upper mid plot
- bwr_excentric_rotated, upper right plot
- bwr_eccentric_lock, lower left plot
- model6g_normal_quarter_2050, lower mid plot
- bwr_eccentric_1, 6 cm shearing, lower right plot

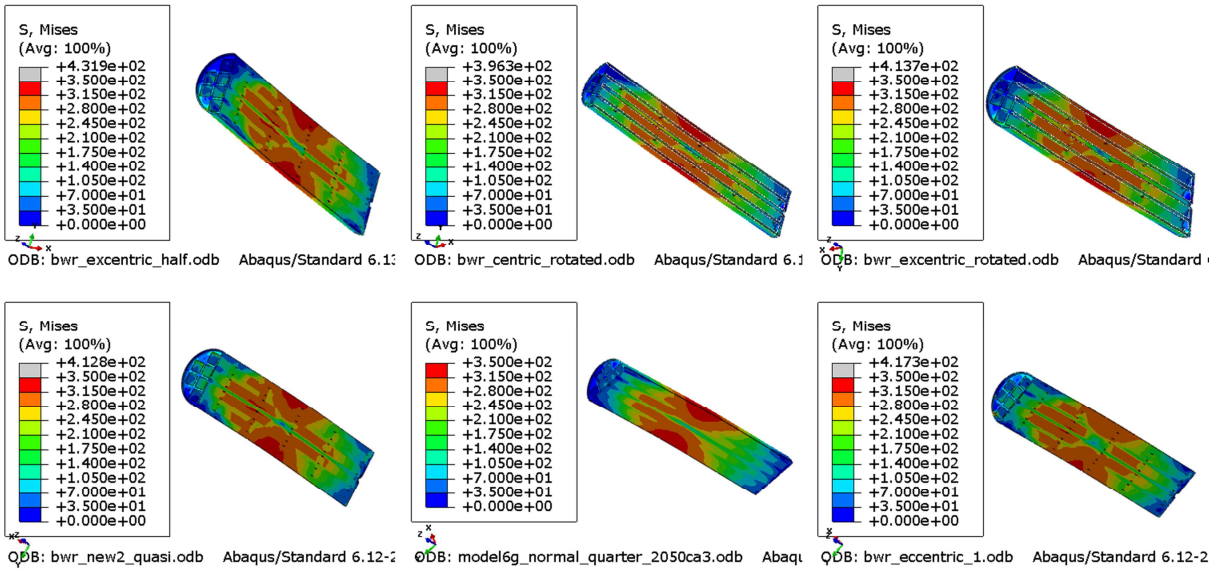

Figure A5-1 *Plot showing Mises stress [MPa] after 8 cm shearing for BWR-insert.*

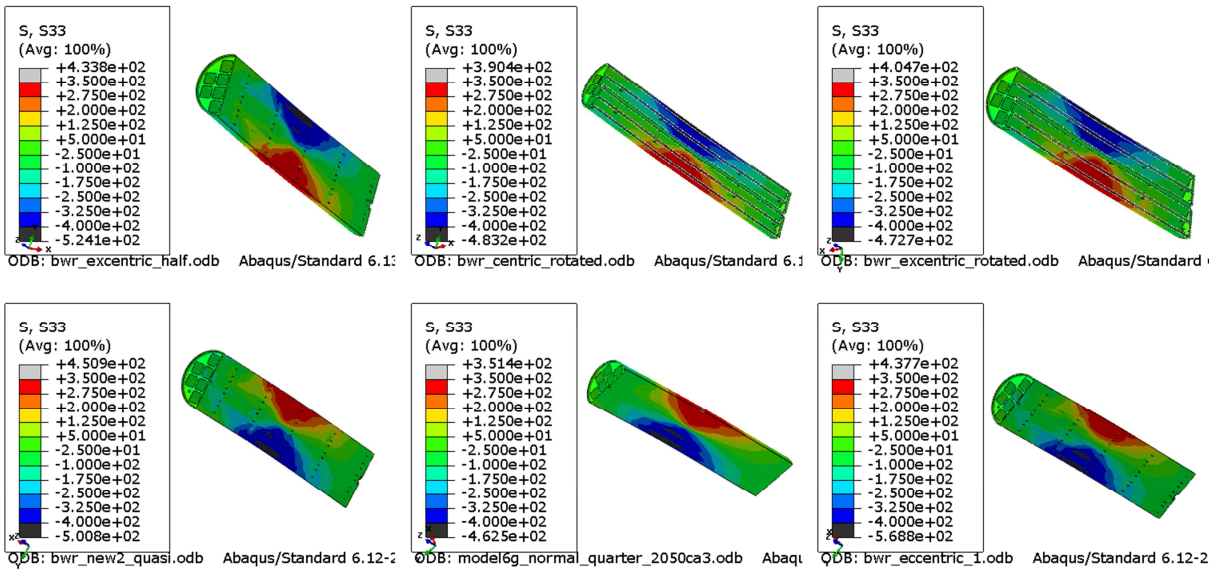

Figure A5-2 *Plot showing axial stress, S33, [MPa] after 8 cm shearing for BWR-insert.*

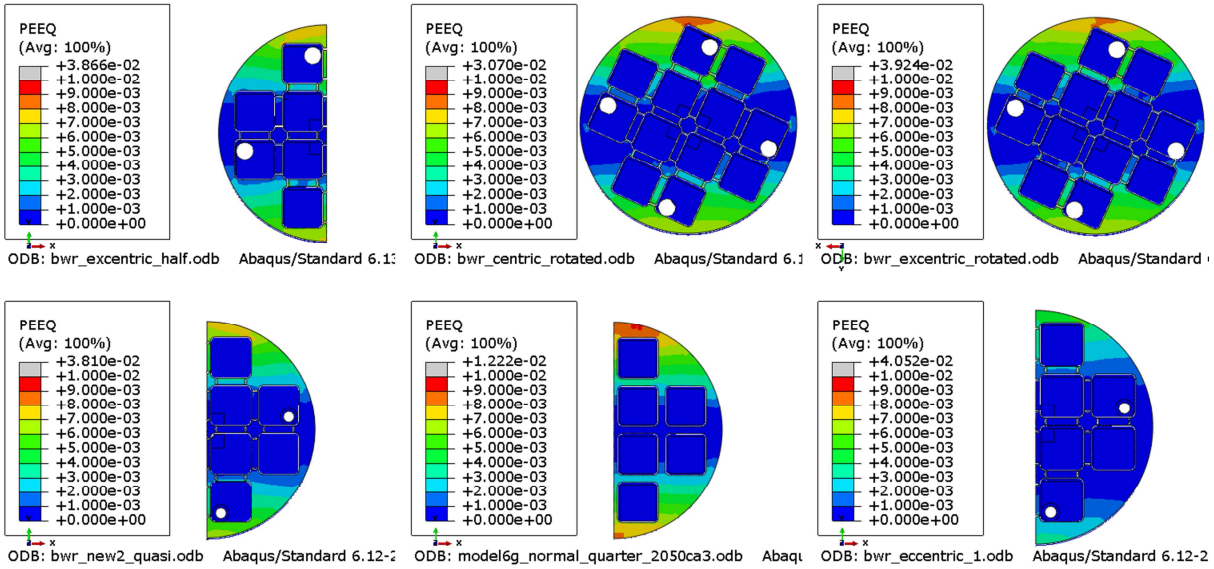

Figure A5-3 *Plot showing plastic equivalent strain (PEEQ) after 8 cm shearing for BWR-insert.*

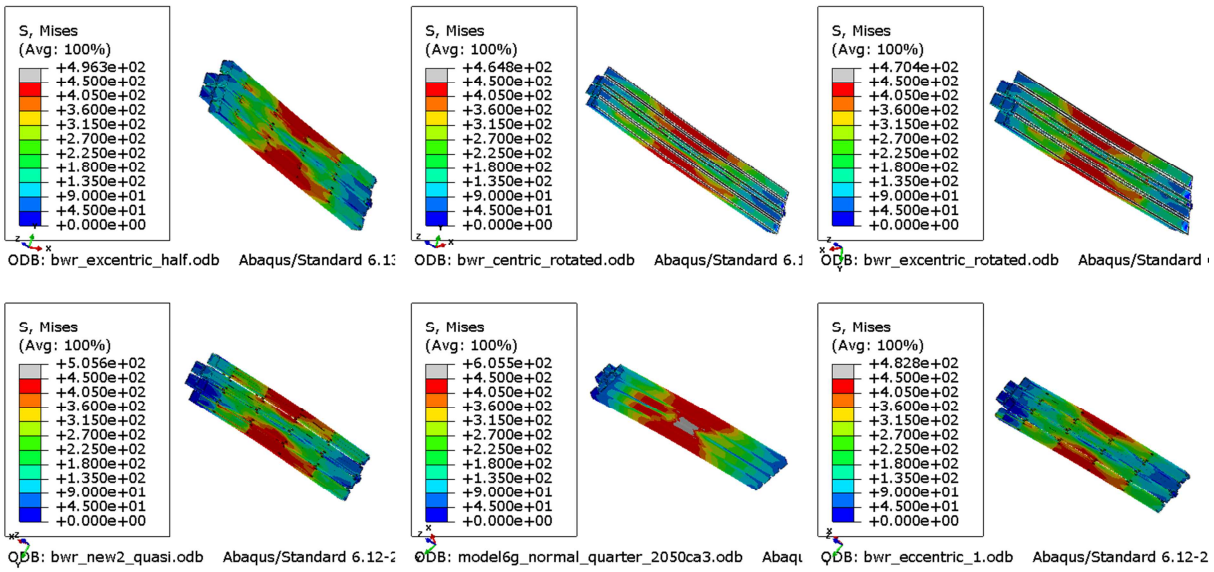

Figure A5-4 *Plot showing Mises stress [MPa] after 8 cm shearing for BWR channel tubes.*

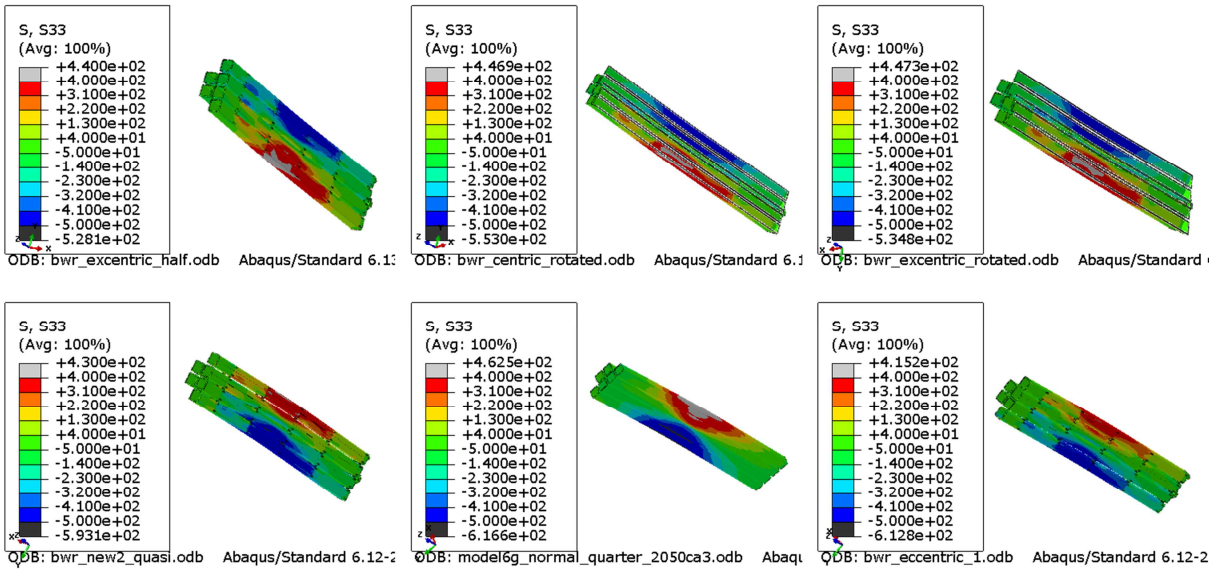

Figure A5-5 *Plot showing axial stress [MPa] after 8 cm shearing for BWR channel tubes.*

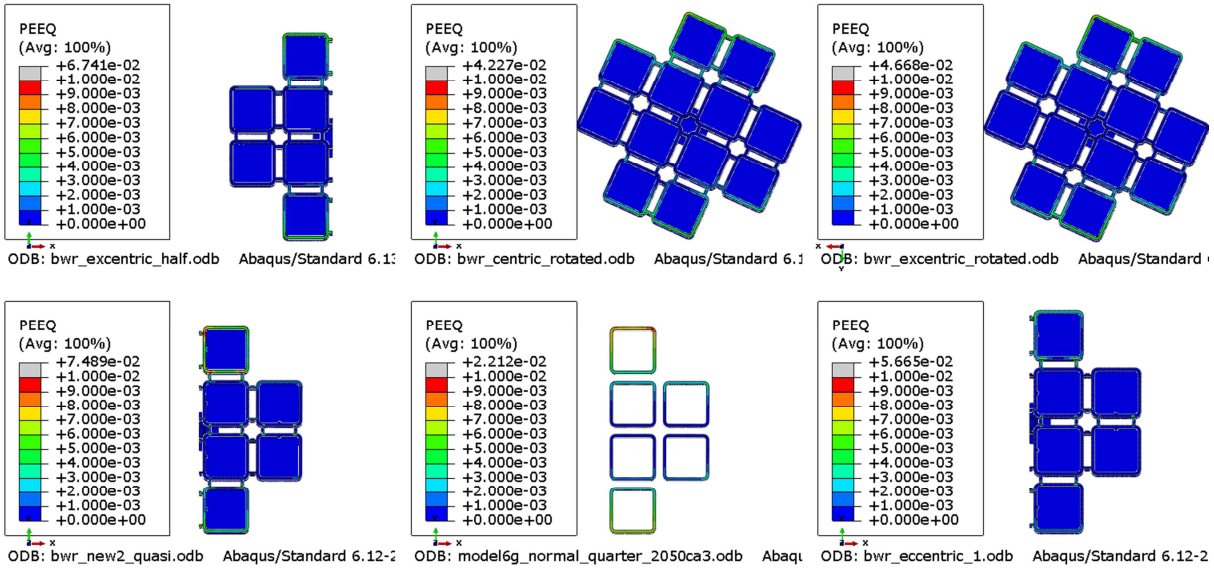

Figure A5-6 *Plot showing plastic equivalent plastic strain (PEEQ) after 8 cm shearing for BWR channel tubes.*

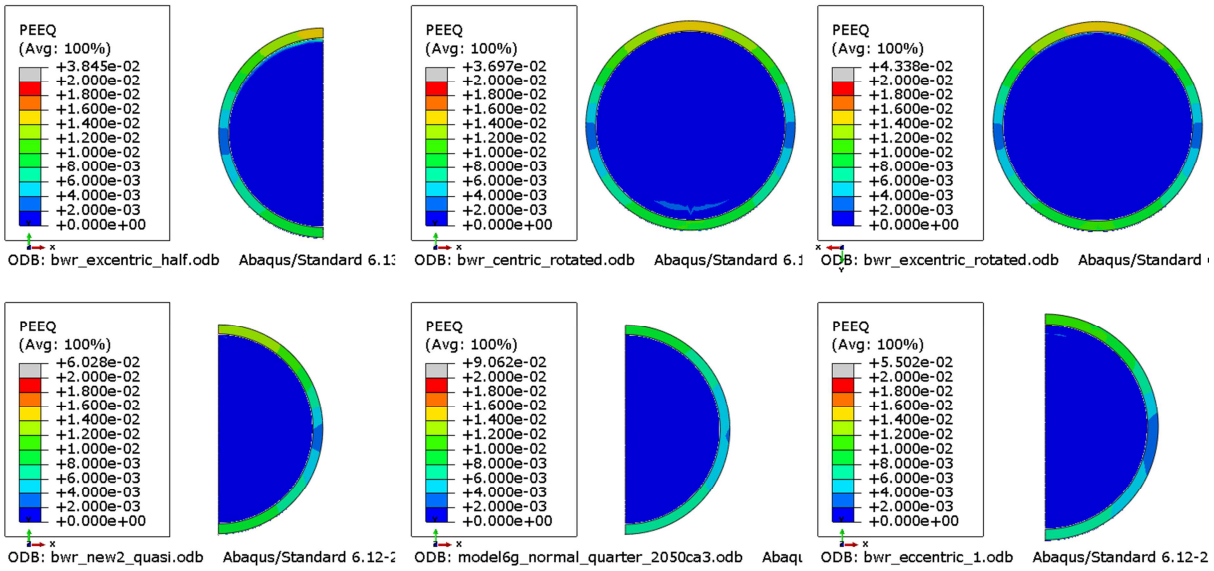

Figure A5-7 *Plot showing plastic equivalent strain (PEEQ) for the BWR copper shell after 8 cm shearing.*

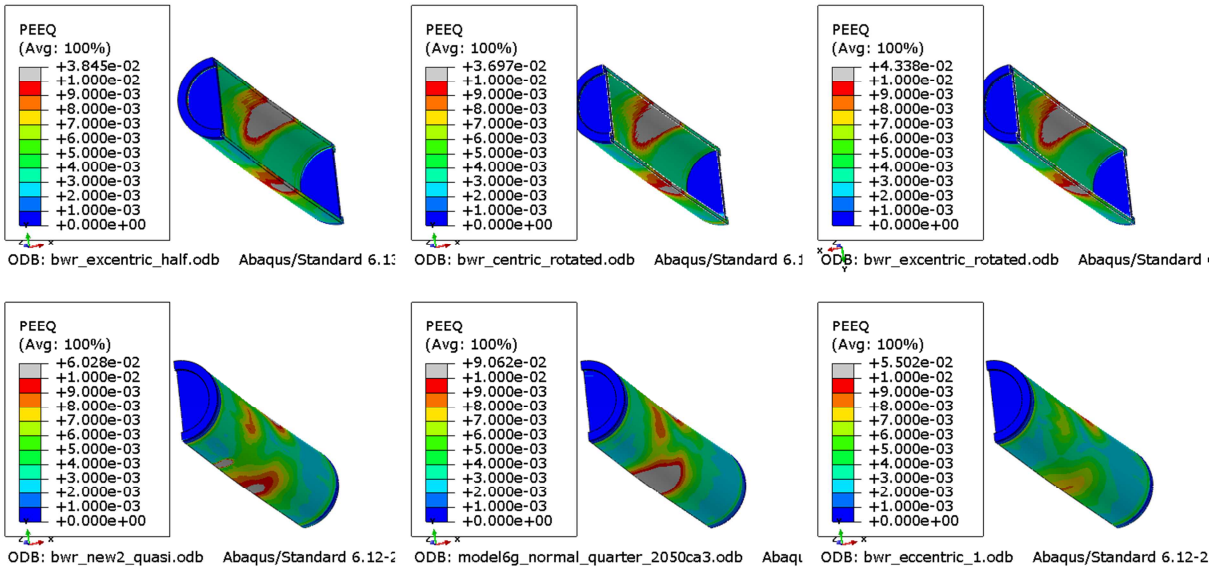

Figure A5-8 *Plot showing plastic equivalent strain (PEEQ) for the BWR copper shell after 8 cm shearing.*

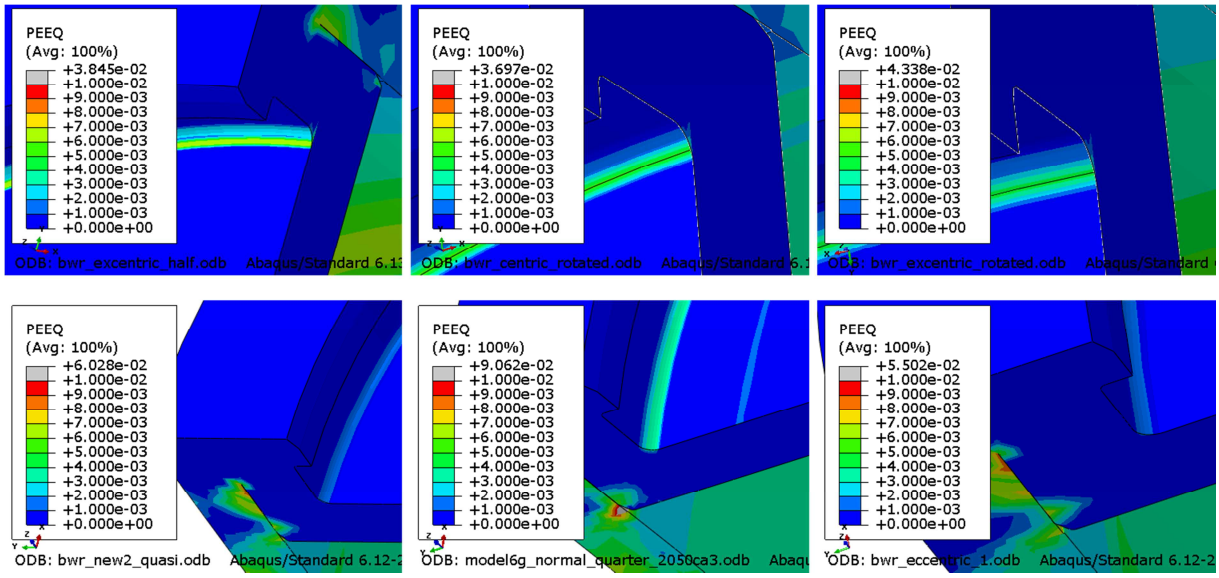

Figure A5-9 *Plot showing plastic equivalent strain (PEEQ) for the BWR copper shell top corner after 8 cm shearing.*

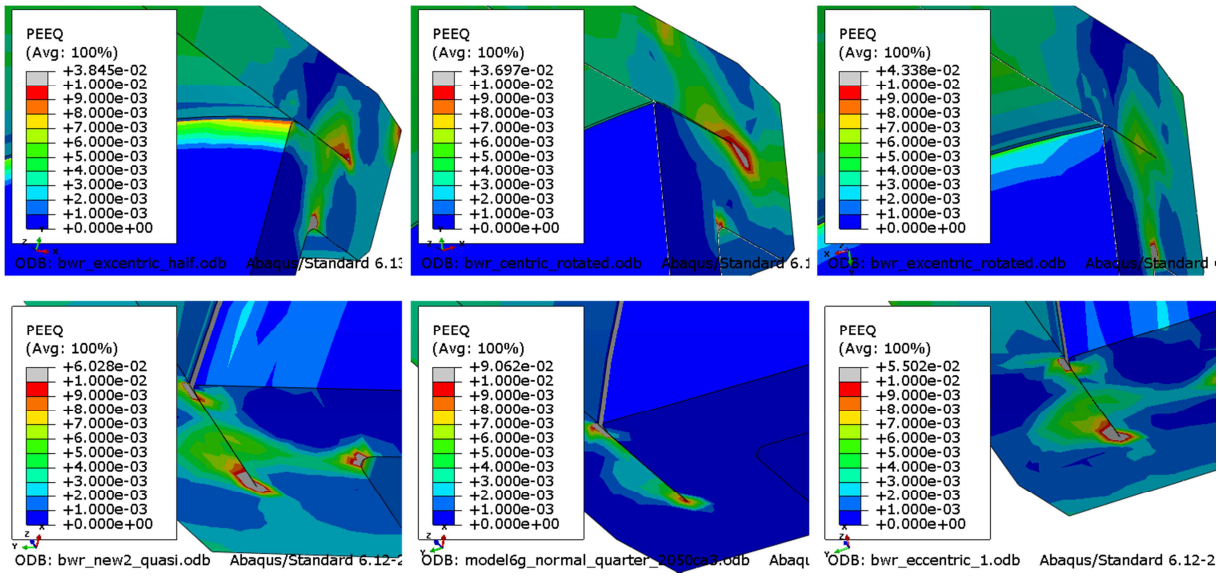

Figure A5-10 *Plot showing plastic equivalent strain (PEEQ) for the BWR copper shell bottom corner after 8 cm shearing .*

Appendix 6 – Plots for bwr_eccentric_lock

Plots showing deformed geometry as contour plots for all parts at shearing magnitude 5 and 6 cm for case bwr_eccentric_lock (horizontal shearing at the steel_lid). The view shows the symmetry plane and all deformations are scaled by a factor of two. Note! The analysis failed to converge for shearing displacement > 6 cm.

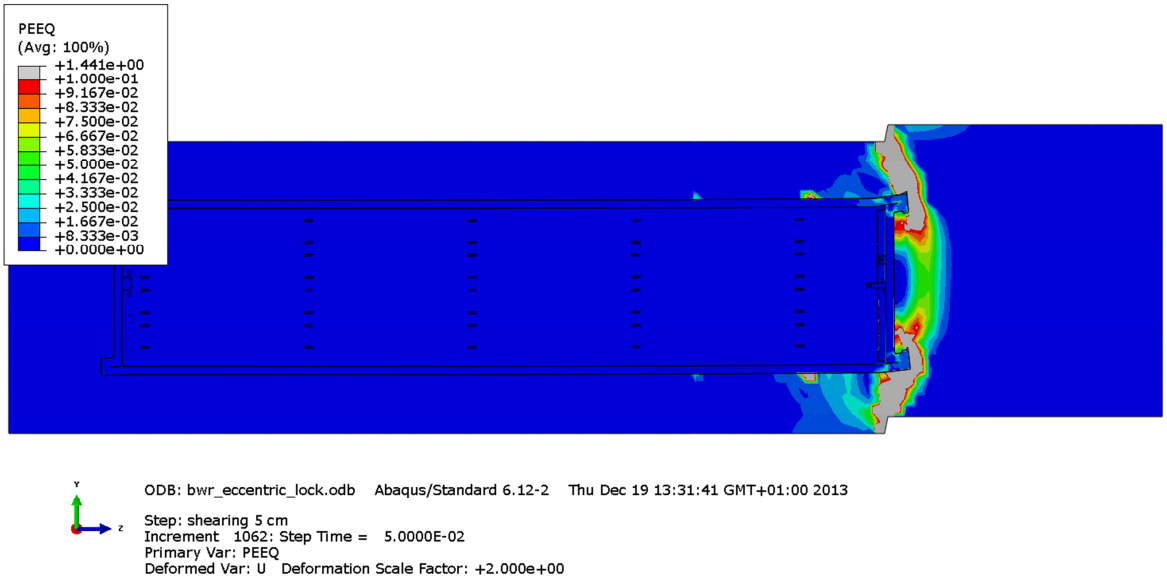

Figure A6-1 *Plot showing equivalent plastic strain (PEEQ) after 5 cm shearing.*

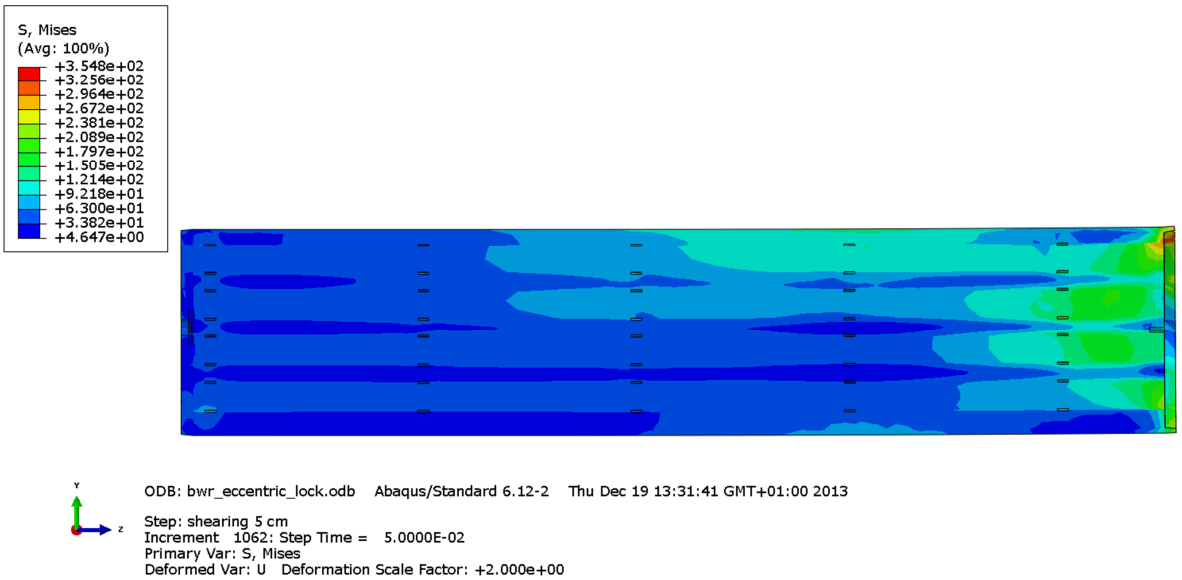

Figure A6-2 *Plot showing Mises stress [MPa] for the insert after 5 cm shearing.*

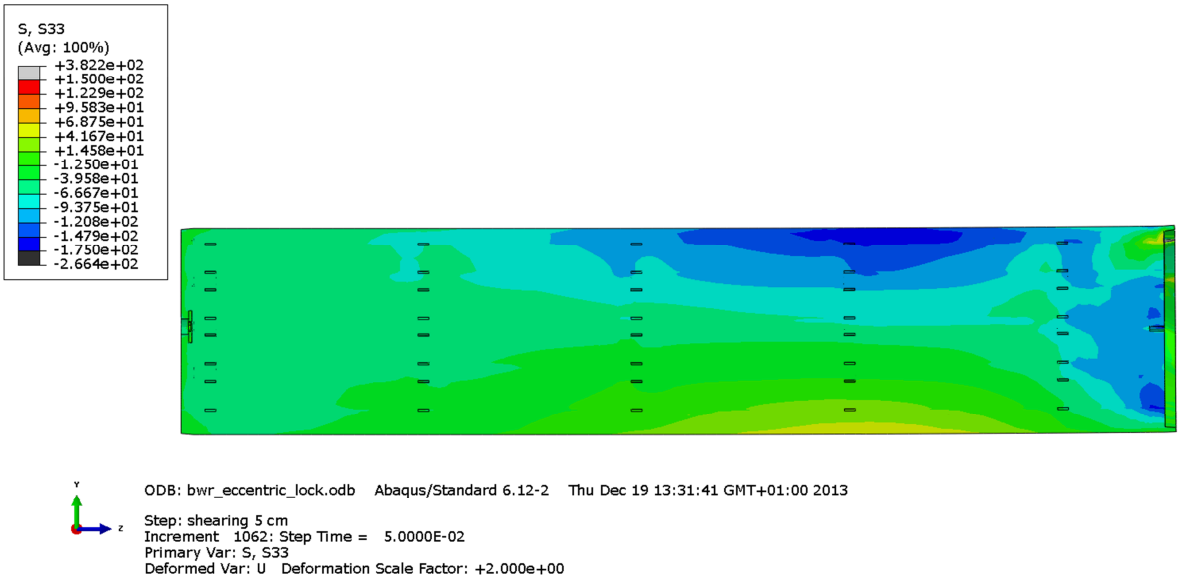

Figure A6-3 *Plot showing axial stress [MPa] for the insert after 5 cm shearing.*

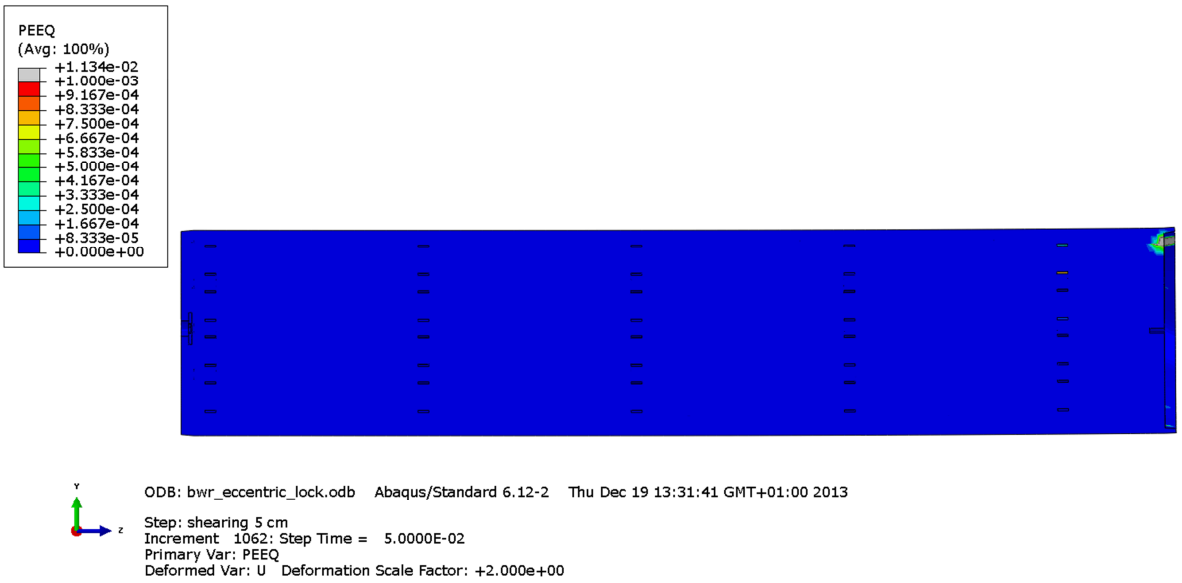

Figure A6-4 *Plot showing equivalent plastic strain (PEEQ) for the insert after 5 cm shearing.*

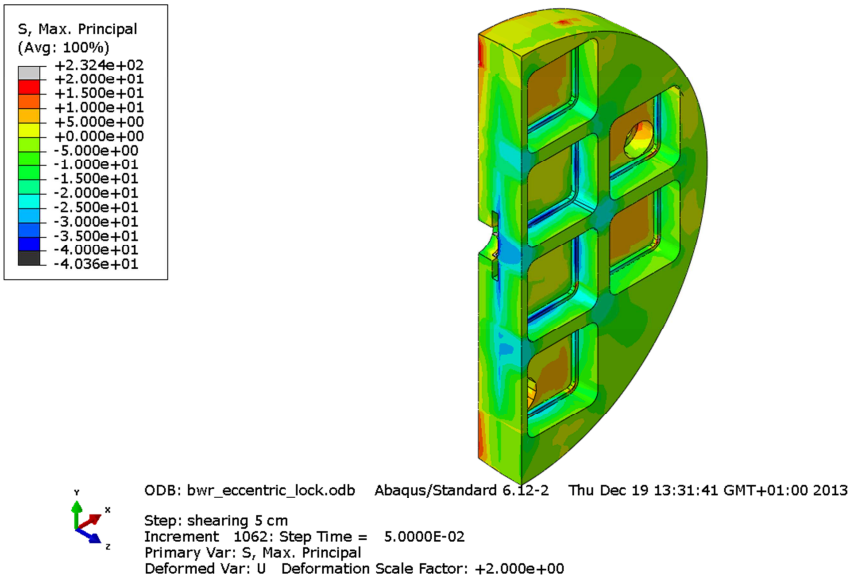

Figure A6-5 *Plot showing maximum principal stress [MPa] for the insert base after 5 cm shearing.*

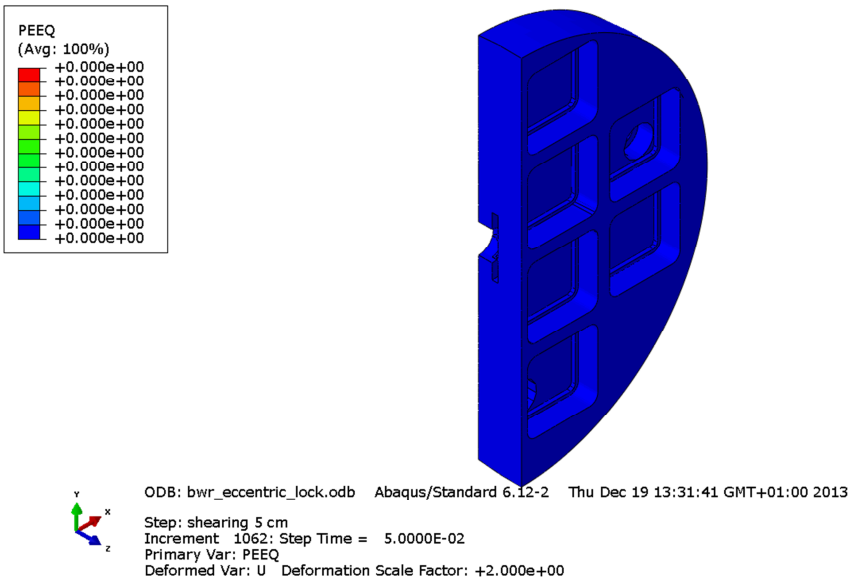

Figure A6-6 *Plot showing equivalent plastic strain (PEEQ) for the insert base after 5 cm shearing.*

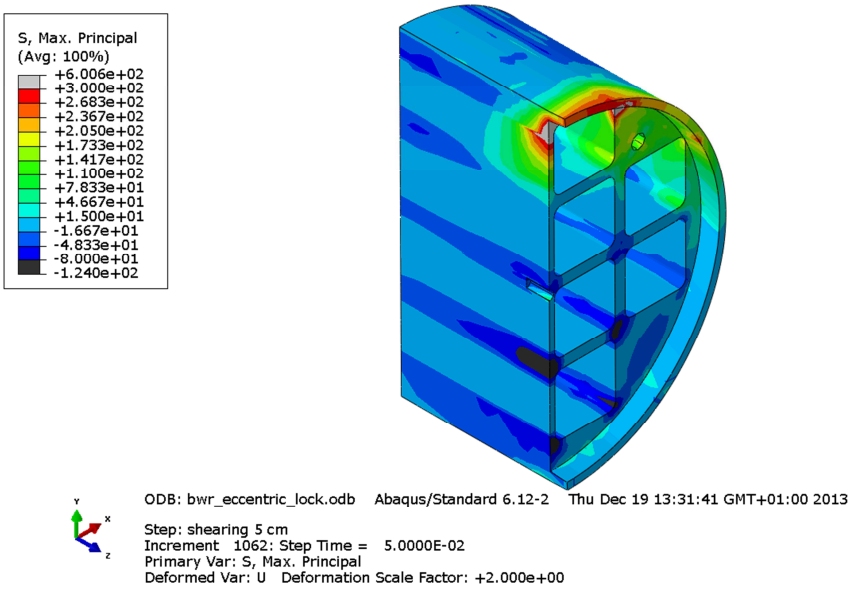

Figure A6-7 *Plot showing maximum principal stress [MPa] for the insert top after 5 cm shearing.*

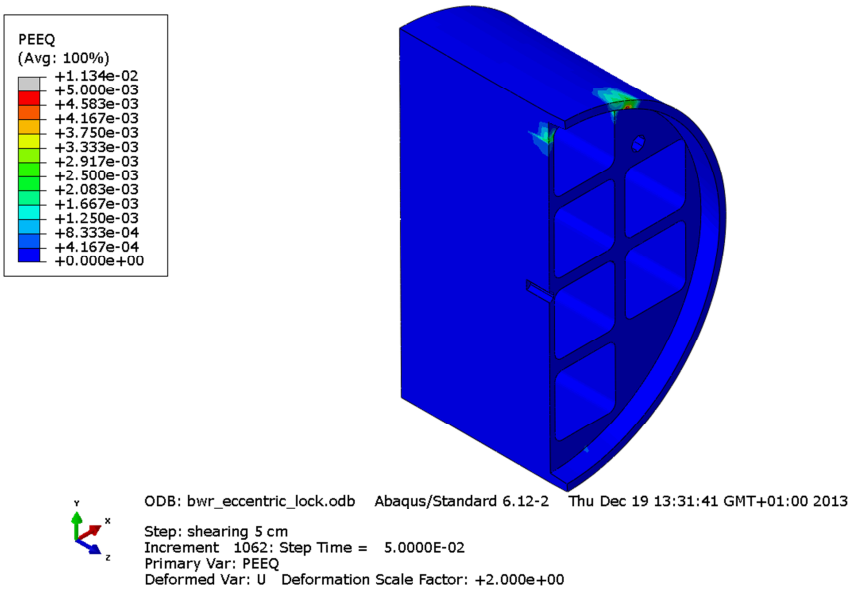

Figure A6-8 *Plot showing equivalent plastic strain (PEEQ) for the insert top after 5 cm shearing.*

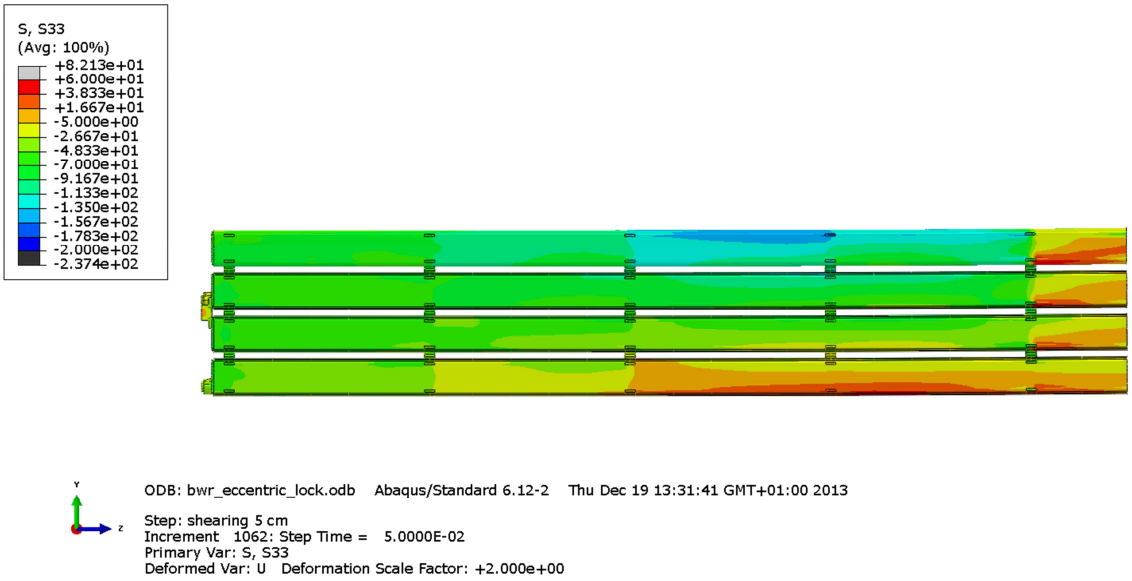

Figure A6-9 *Plot showing axial stress [MPa] for the steel channel tubes after 5 cm shearing.*

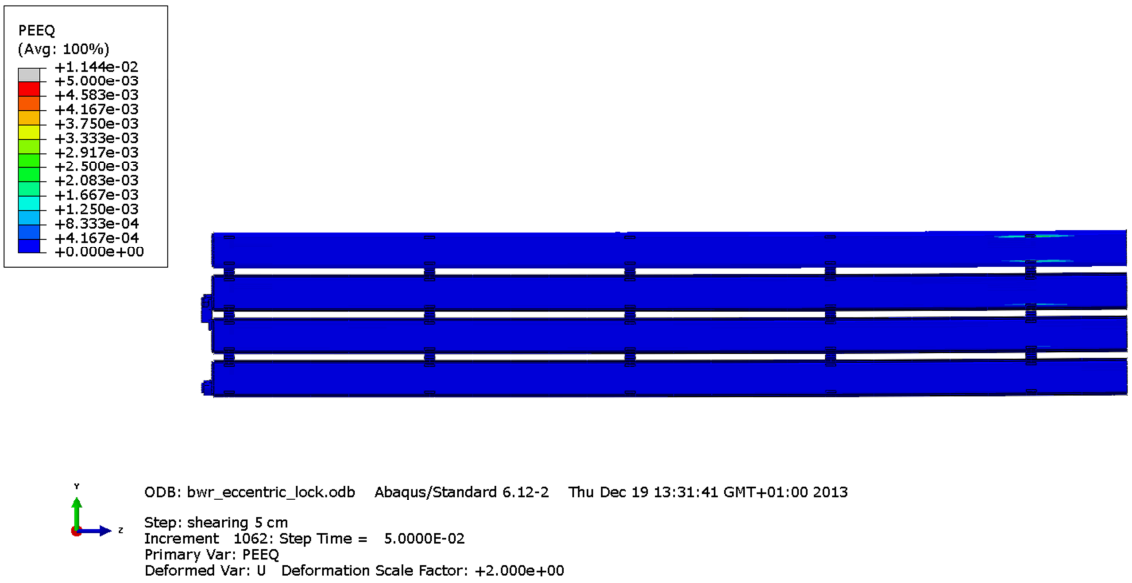

Figure A6-10 *Plot showing equivalent plastic strain (PEEQ) for the steel channel tubes after 5 cm shearing.*

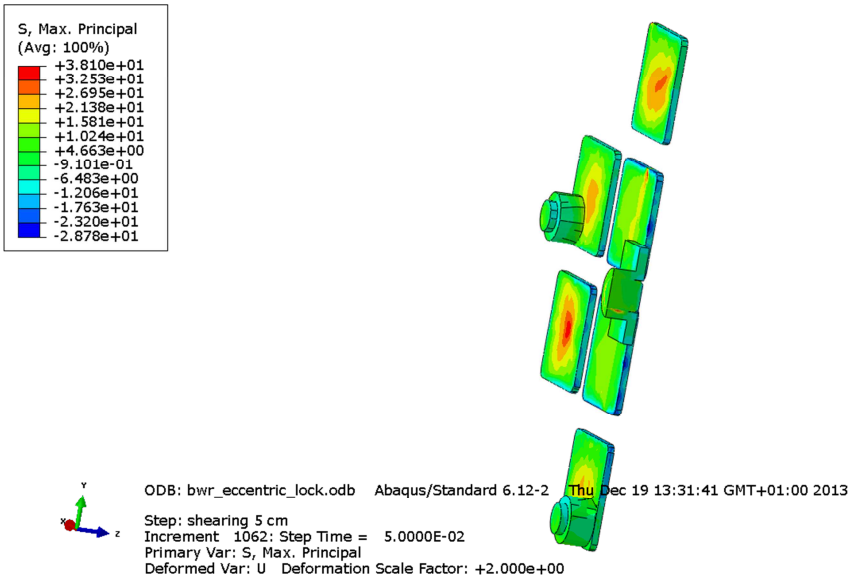

Figure A6-11 *Plot showing maximum principal stress [MPa] for the steel channel tubes base plates after 5 cm shearing.*

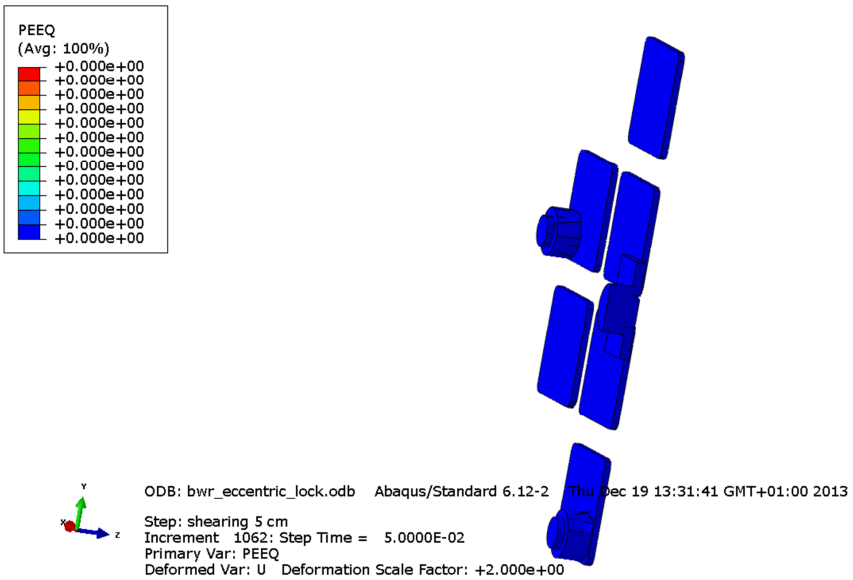

Figure A6-12 *Plot showing equivalent plastic strain (PEEQ) for the steel channel tubes base plates after 5 cm shearing.*

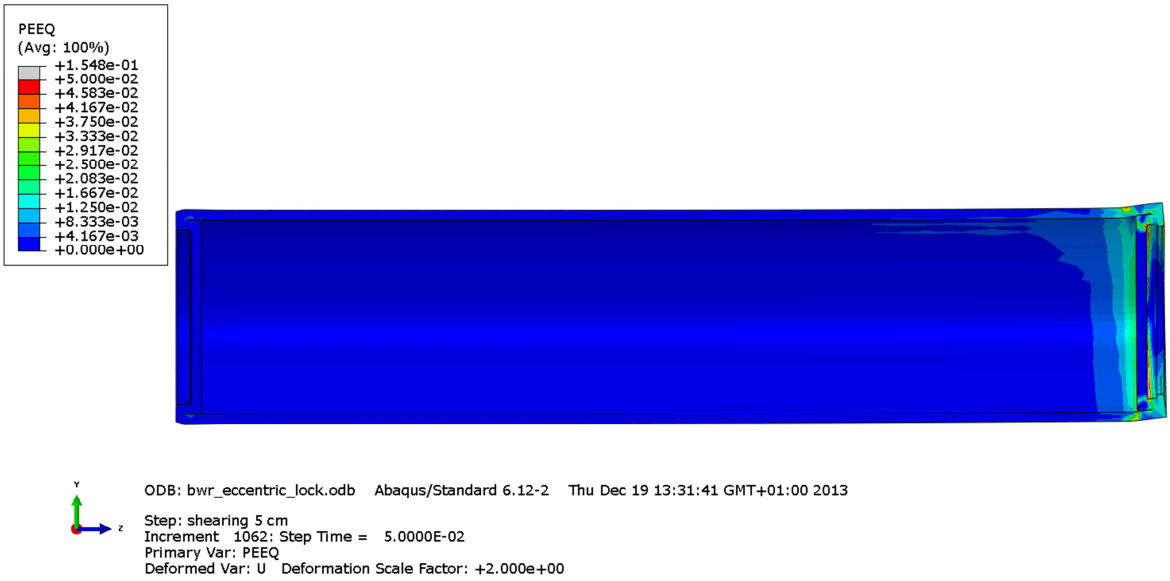

Figure A6-13 *Plot showing equivalent plastic strain (PEEQ) for the copper shell after 5 cm shearing.*

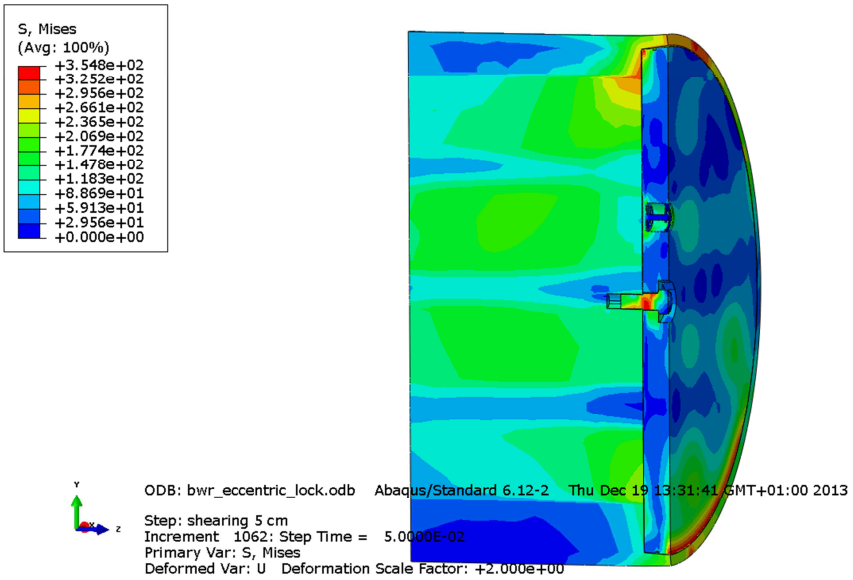

Figure A6-14 *Plot showing Mises stress [MPa] close to the insert lid fixing screw after 5 cm shearing.*

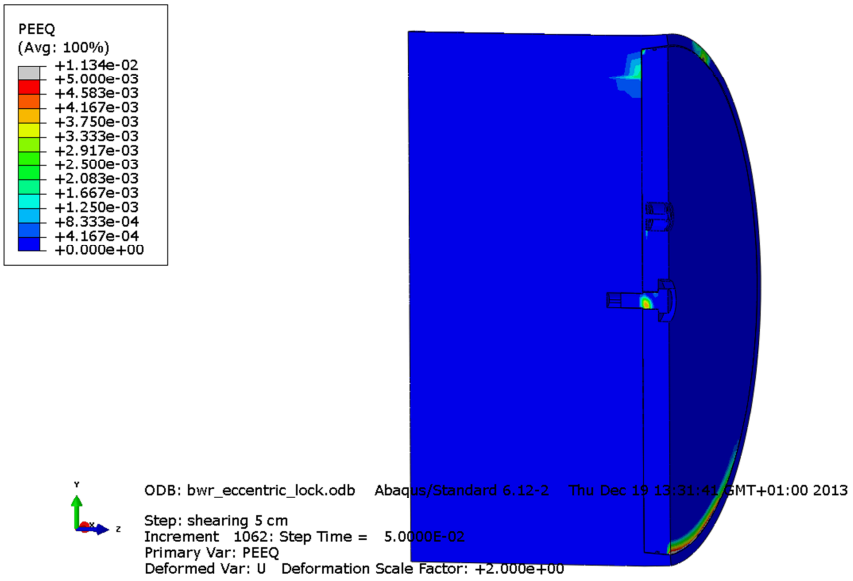

Figure A6-15 *Plot showing equivalent plastic strain (PEEQ) close to the insert lid fixing screw after 5 cm shearing.*

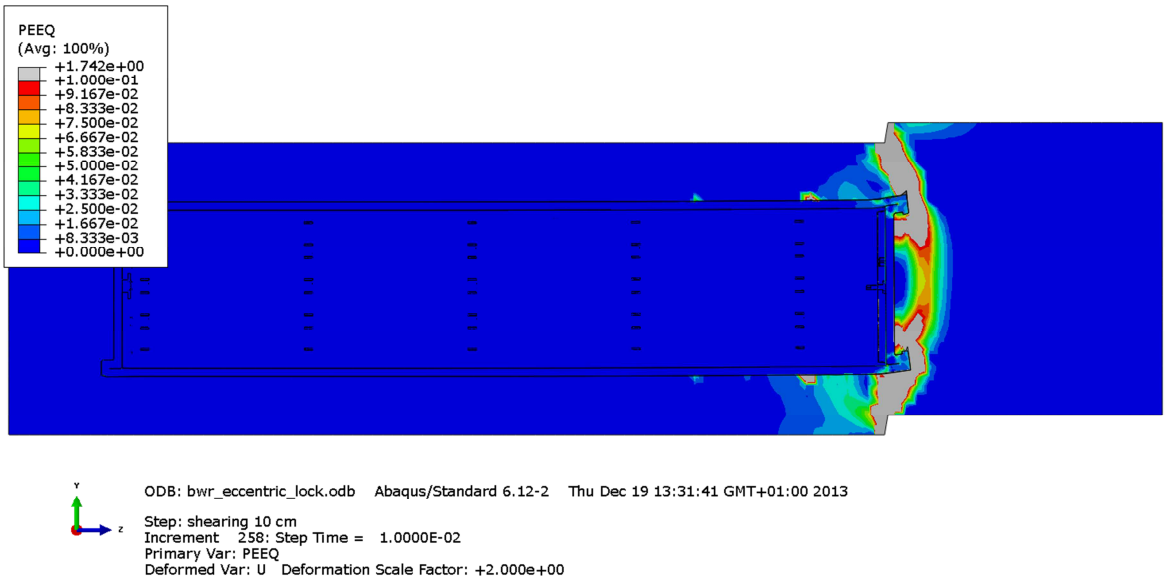

Figure A6-16 *Plot showing equivalent plastic strain (PEEQ) after 6 cm shearing.*

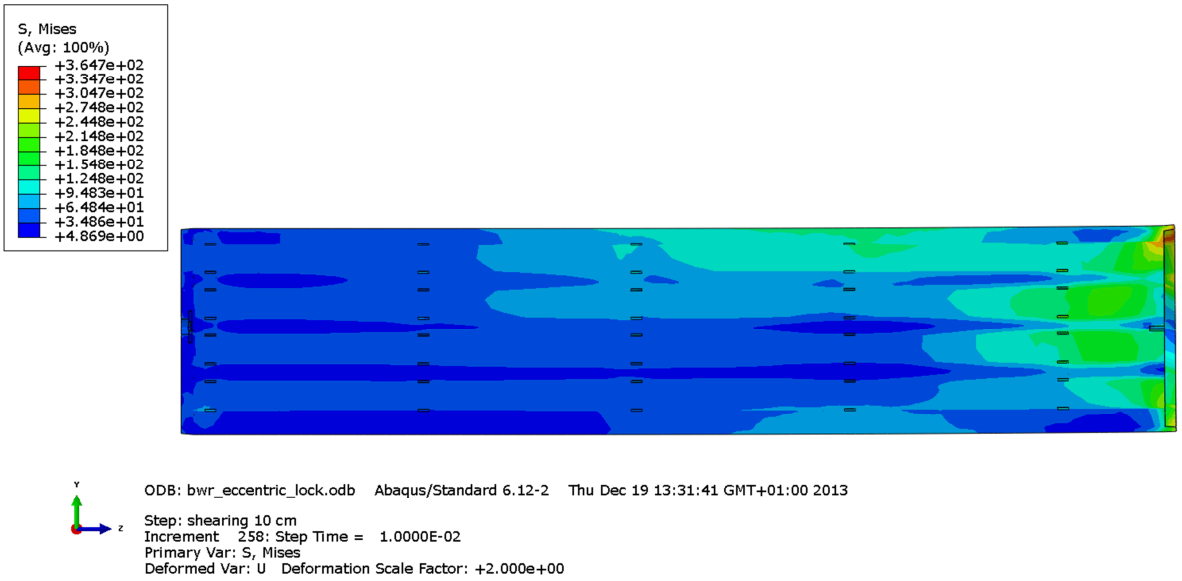

Figure A6-17 *Plot showing Mises stress [MPa] for the insert after 6 cm shearing.*

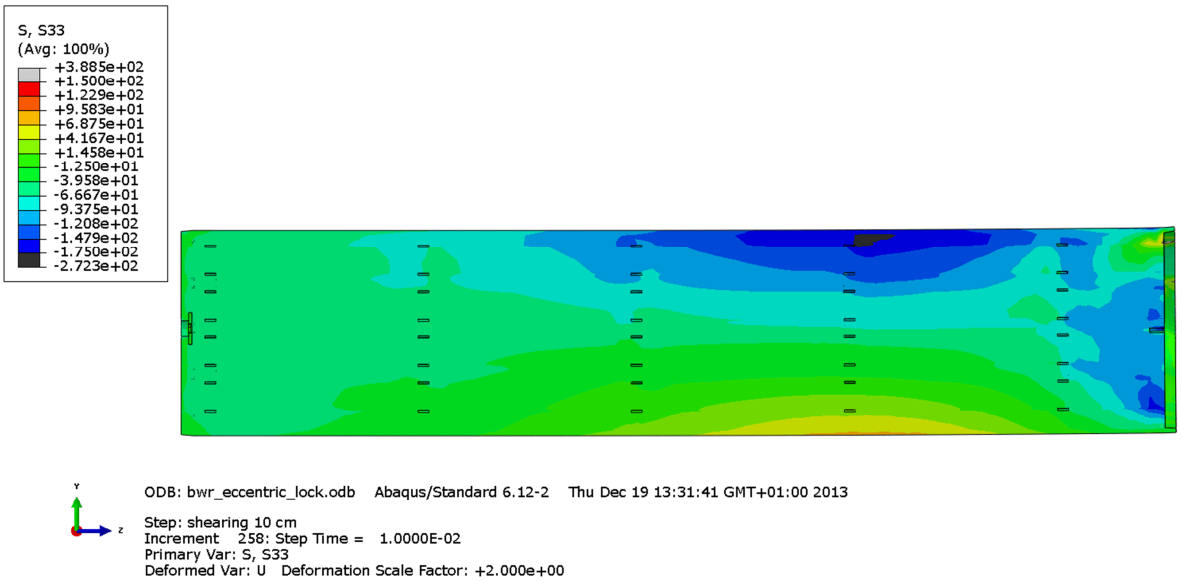

Figure A6-18 *Plot showing axial stress [MPa] for the insert after 6 cm shearing.*

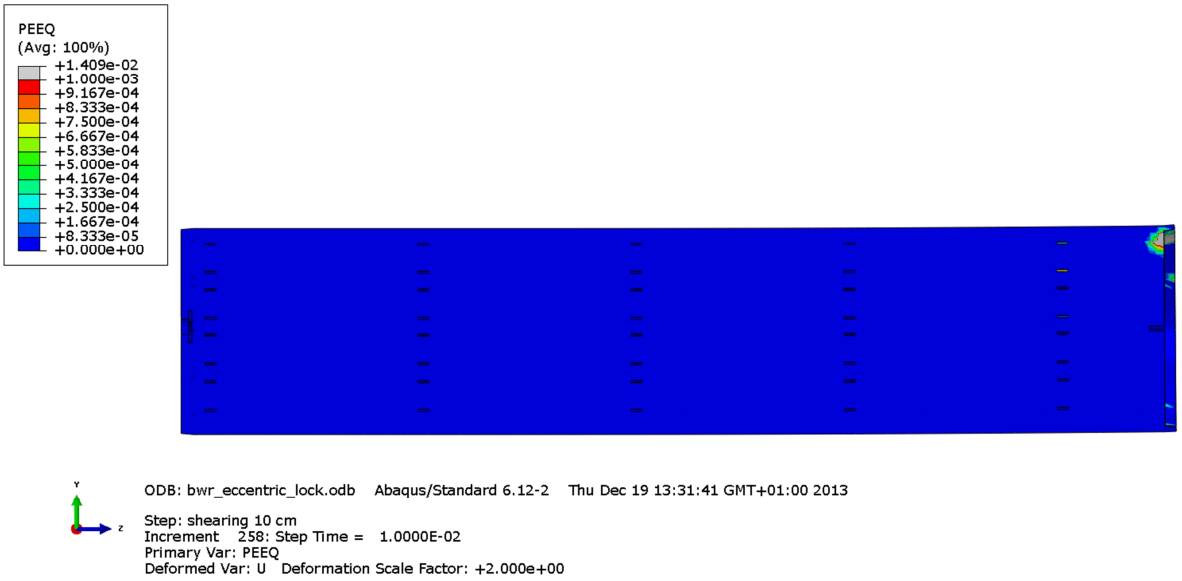

Figure A6-19 *Plot showing equivalent plastic strain (PEEQ) for the insert after 6 cm shearing.*

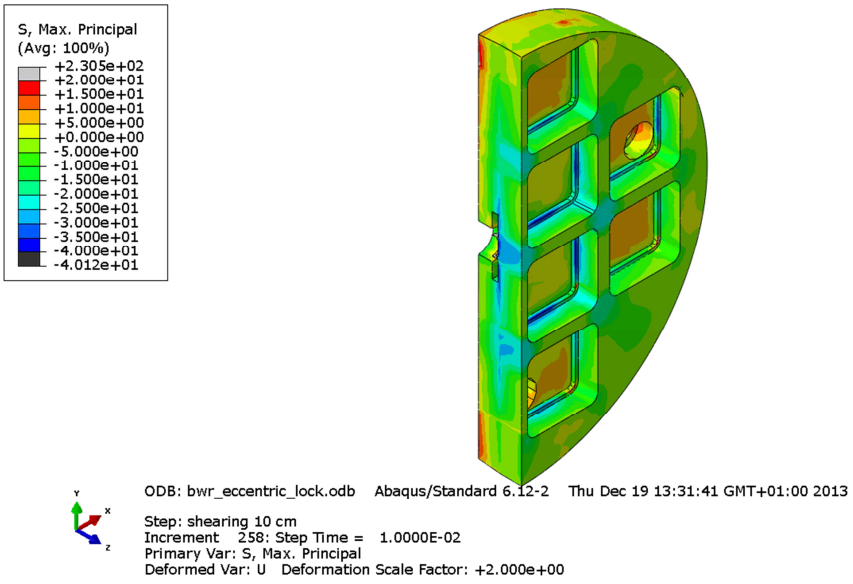

Figure A6-20 *Plot showing maximum principal stress [MPa] for the insert base after 6 cm shearing.*

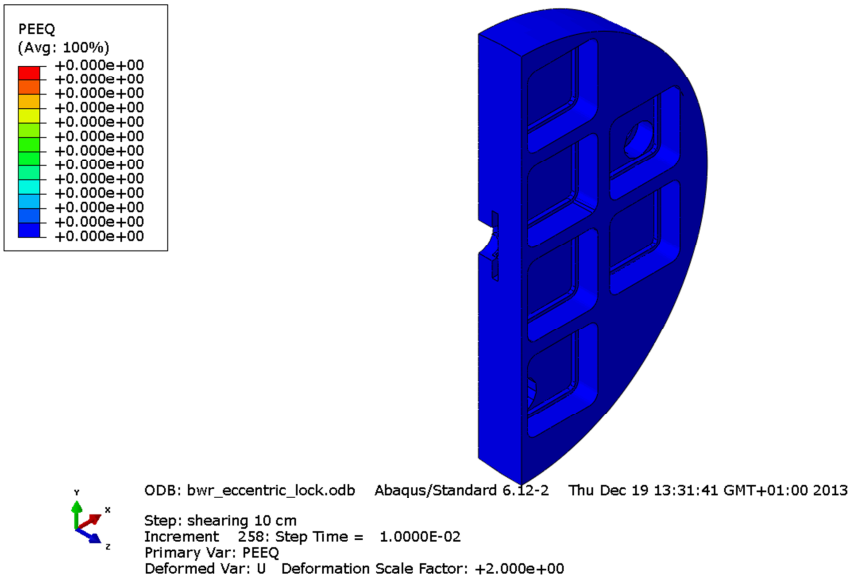

Figure A6-21 *Plot showing equivalent plastic strain (PEEQ) for the insert base after 6 cm shearing.*

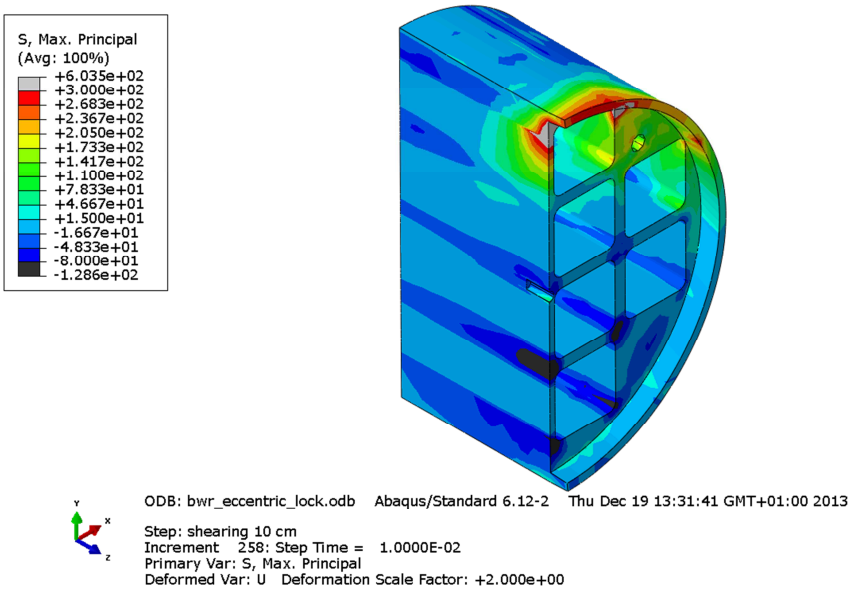

Figure A6-22 *Plot showing maximum principal stress [MPa] for the insert top after 6 cm shearing.*

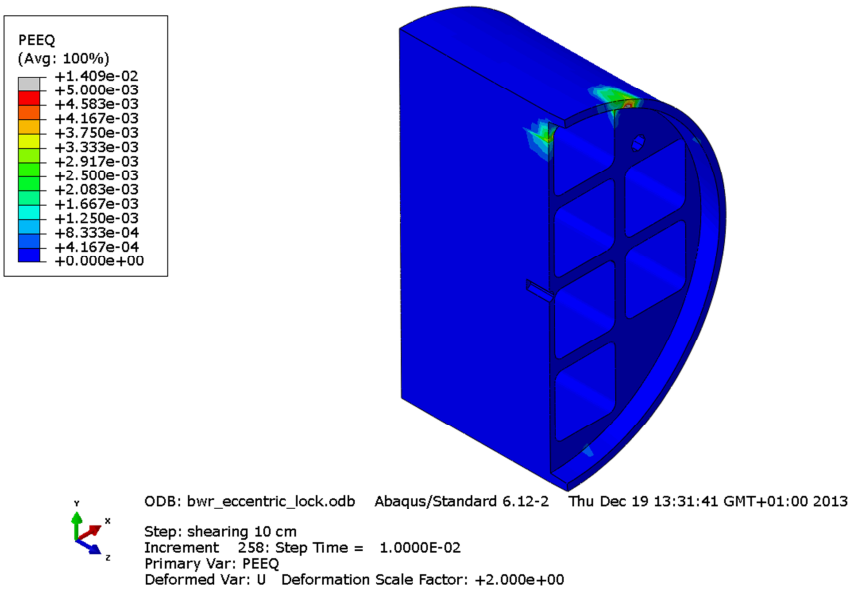

Figure A6-23 *Plot showing equivalent plastic strain (PEEQ) for the insert top after 6 cm shearing.*

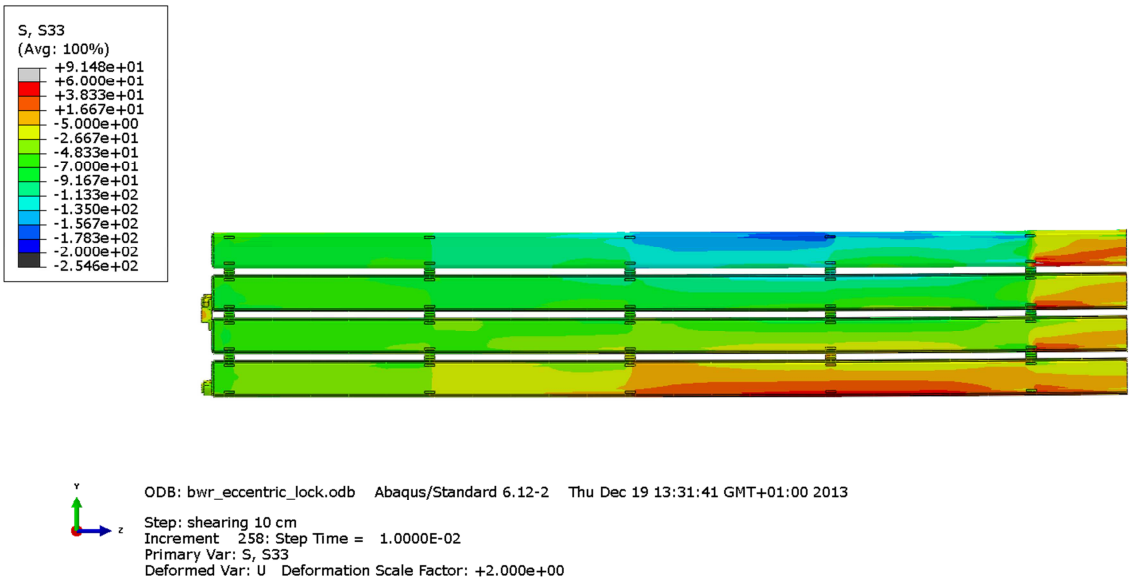

Figure A6-24 *Plot showing axial stress [MPa] for the steel channel tubes after 6 cm shearing.*

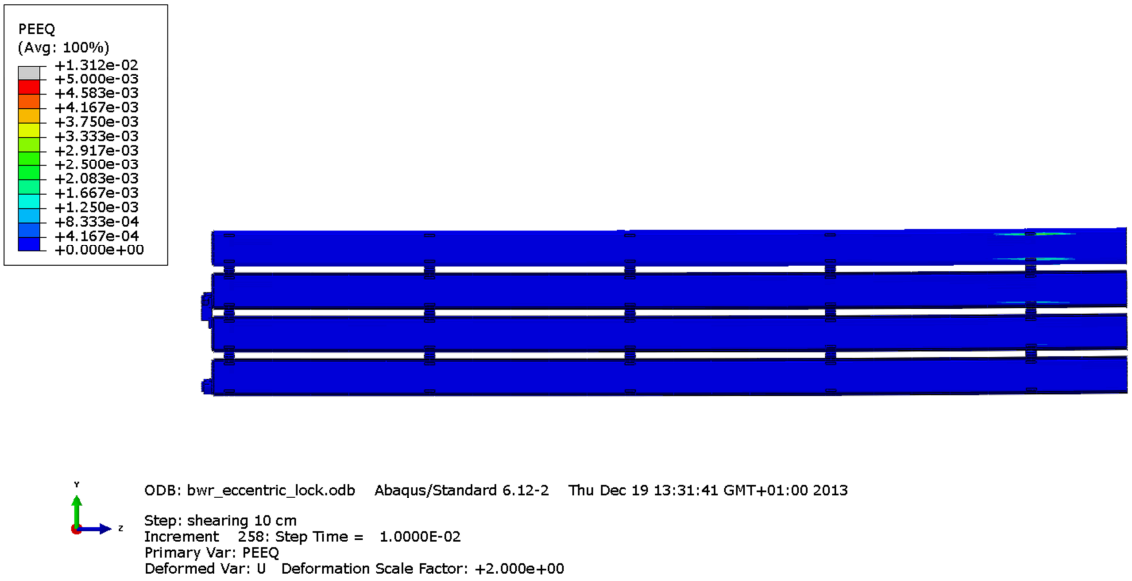

Figure A6-25 *Plot showing equivalent plastic strain (PEEQ) for the steel channel tubes after 6 cm shearing.*

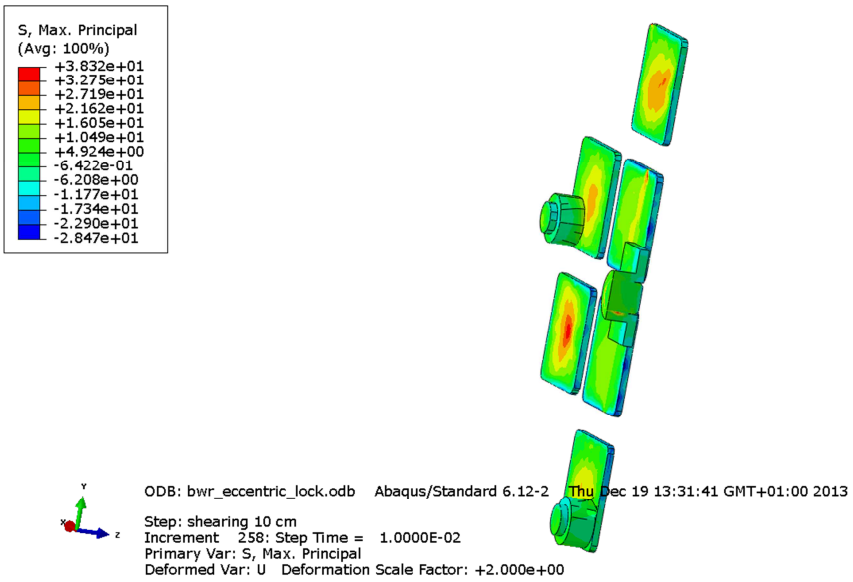

Figure A6-26 *Plot showing maximum principal stress [MPa] for the steel channel tubes base plates after 6 cm shearing.*

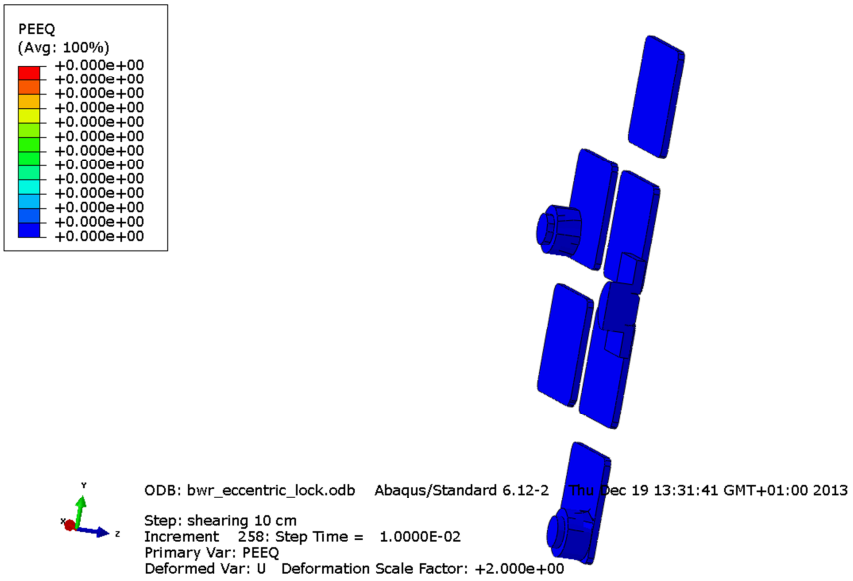

Figure A6-27 *Plot showing equivalent plastic strain (PEEQ) for the steel channel tubes base plates after 6 cm shearing.*

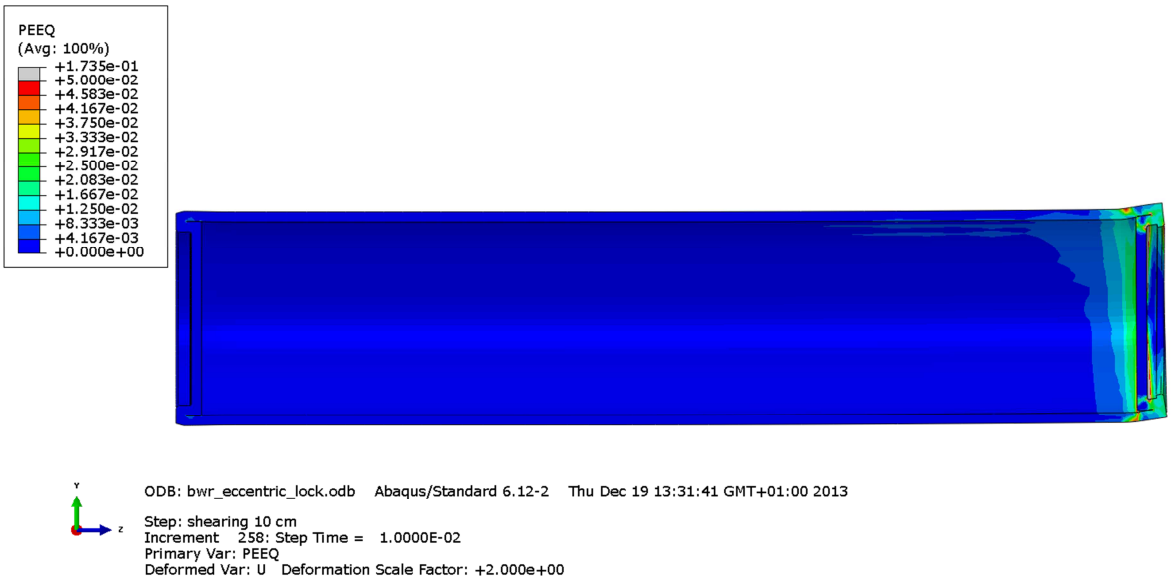

Figure A6-28 *Plot showing equivalent plastic strain (PEEQ) for the copper shell after 6 cm shearing.*

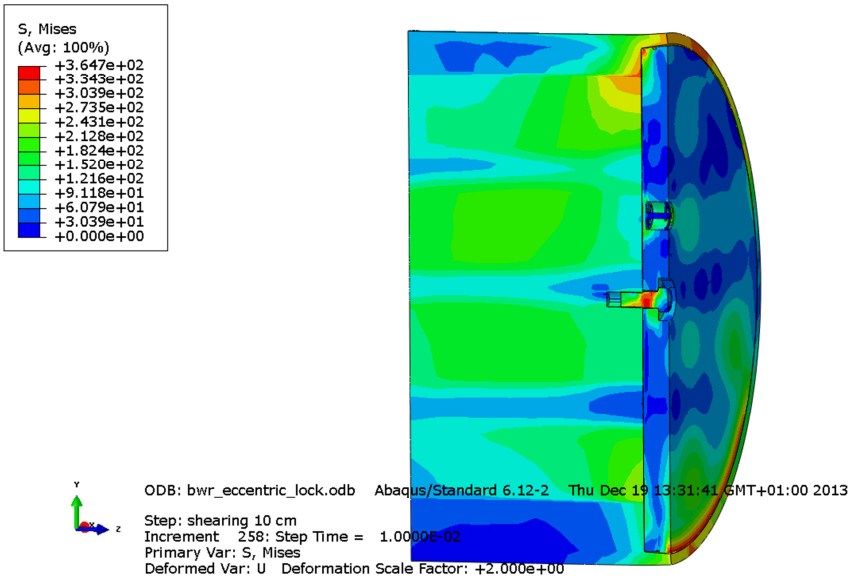

Figure A6-29 *Plot showing Mises stress [MPa] close to the insert lid fixing screw after 6 cm shearing.*

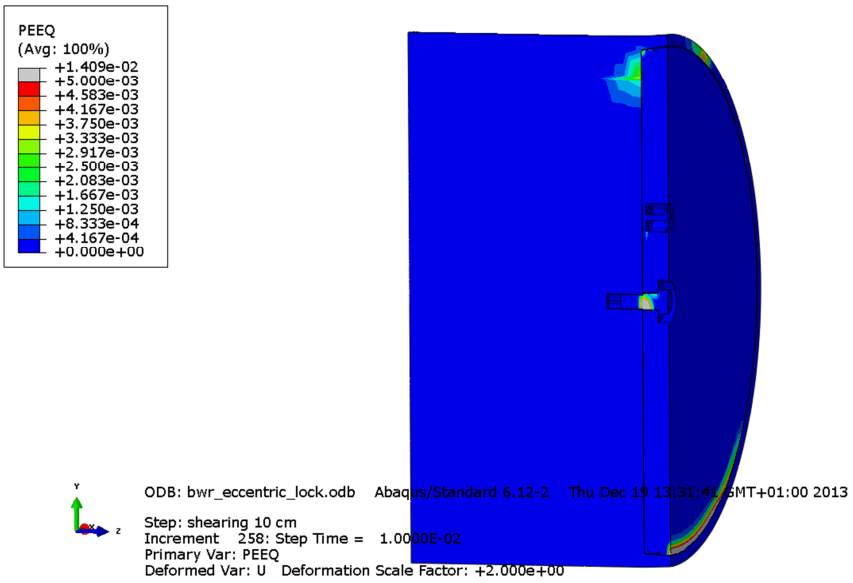

Figure A6-30 *Plot showing equivalent plastic strain (PEEQ) close to the insert lid fixing screw after 6 cm shearing.*

Appendix 7 – comparisons at last converged solutions

Figures A7-1 –A7-15 show comparisons between the reference case (model6g_normal quarter_2050ca3 and the corresponding detailed model (bwr_eccentric_lock) after 8 cm shearing at ¾-distance from the insert base.

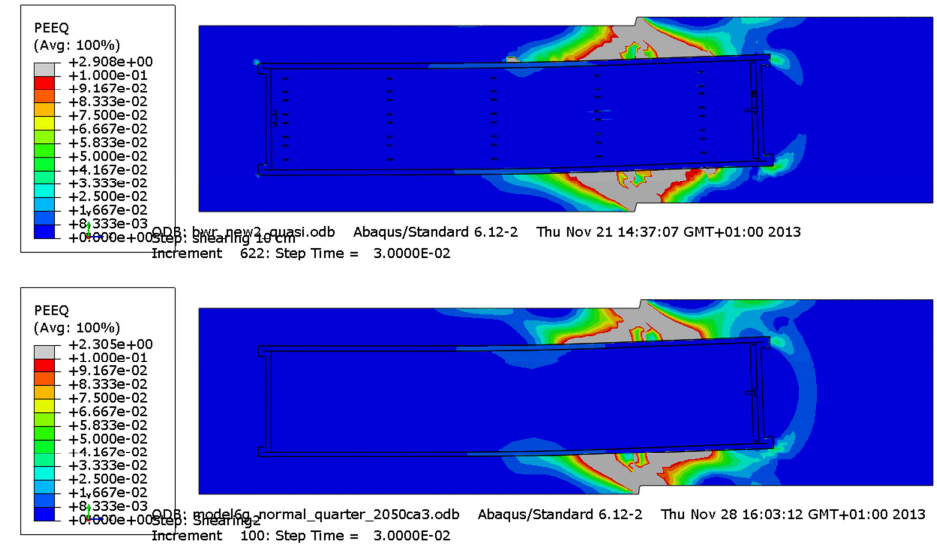

Figure A7-1. *Plot showing equivalent plastic strain (PEEQ) after 8 cm shearing for detailed BWR model (upper) and the reference BWR model (lower). Symmetrically positioned channel tubes.*

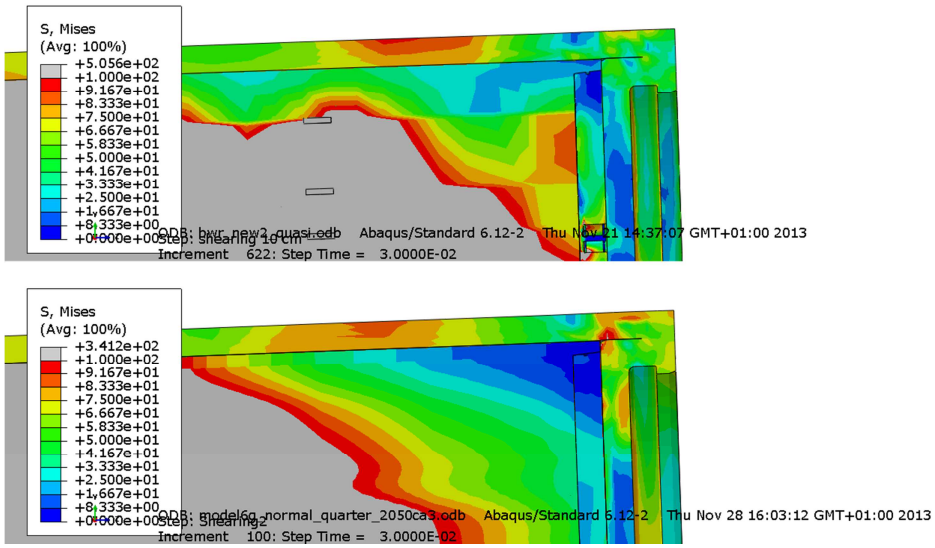

Figure A7-2. *Plot showing Mises stress at the left top corner after 8 cm shearing for detailed BWR model (upper) and the reference BWR model (lower). Symmetrically positioned channel tubes.*

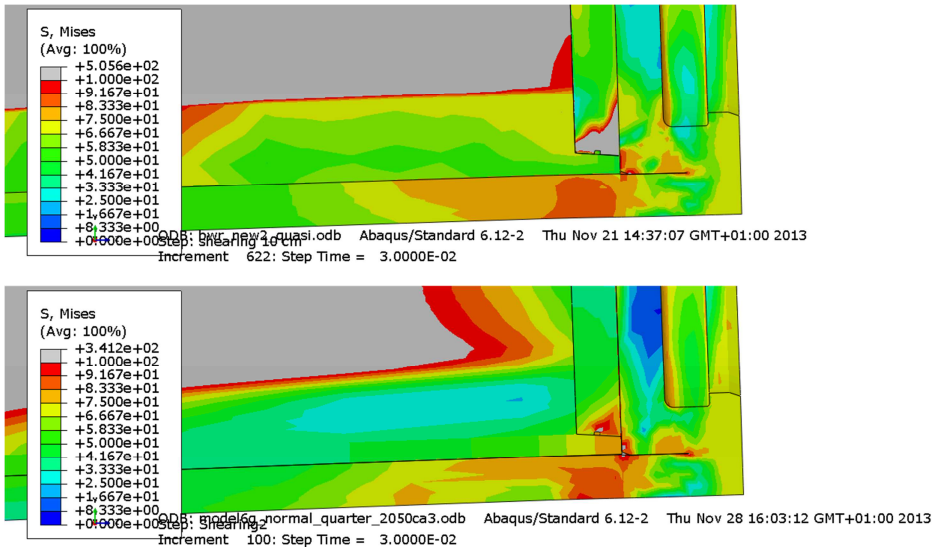

Figure A7-3. *Plot showing Mises stress at the right top corner after 8 cm shearing for detailed BWR model (upper) and the reference BWR model (lower). Symmetrically positioned channel tubes.*

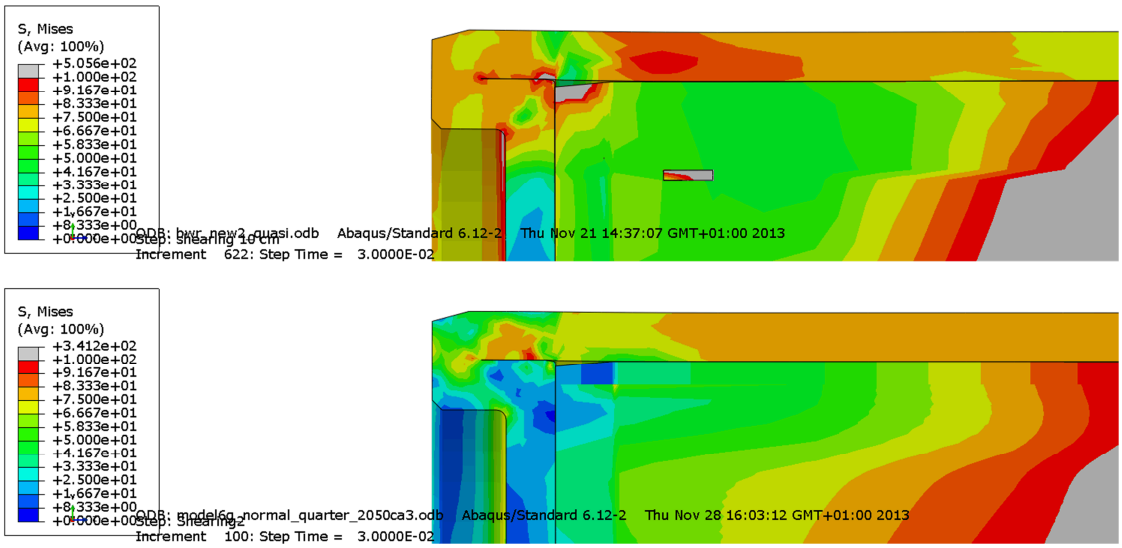

Figure A7-4. *Plot showing Mises stress at the left bottom corner after 8 cm shearing for detailed BWR model (upper) and the reference BWR model (lower). Symmetrically positioned channel tubes.*

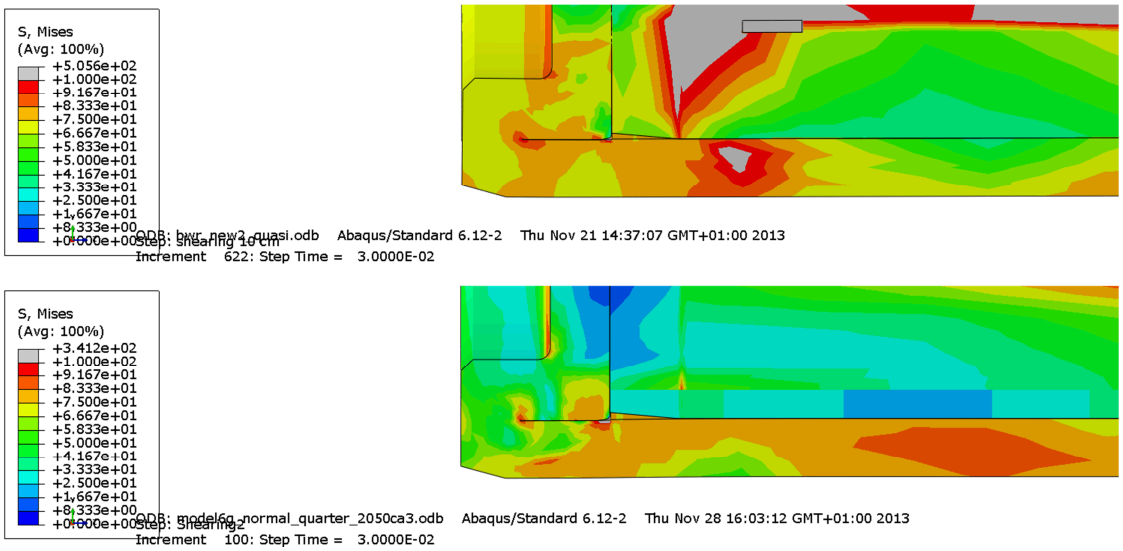

Figure A7-5. *Plot showing Mises stress at the right top corner after 8 cm shearing for detailed BWR model (upper) and the reference BWR model (lower). Symmetrically positioned channel tubes.*

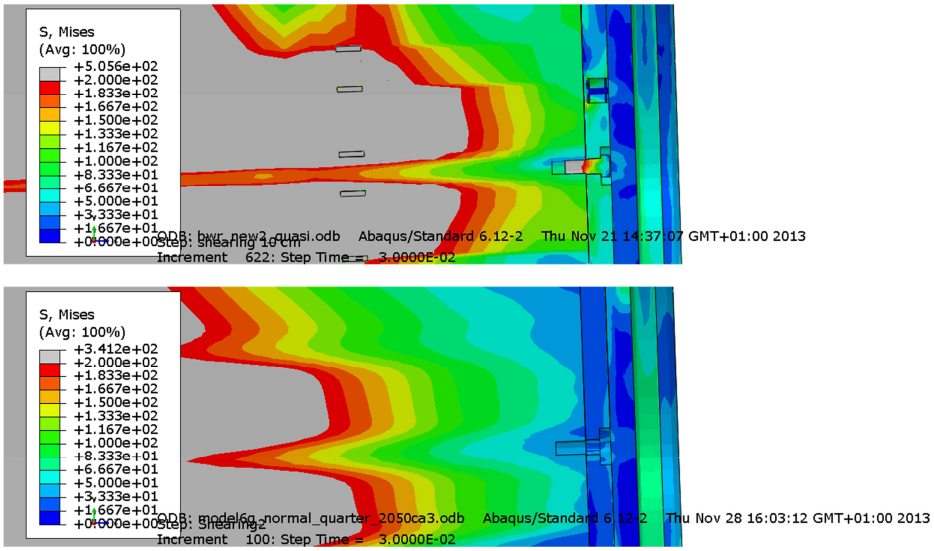

Figure A7-6. *Plot showing Mises stress at the top close to the screw after 8 cm shearing for detailed BWR model (upper) and the reference BWR model (lower). Symmetrically positioned channel tubes.*

Copper shell

Figures A7-7 – A7-8 show rather small differences between the detailed BWR-model (bwr_eccentric_lock) and the reference model (model6g_normal_quarter_2050ca3) for the copper shell. Highest values are for the reference model even though the global response shows higher values for the detailed BWR-model. The global values are acceptable and the local peak values occur in areas mainly in compression and where the model has discontinuities.

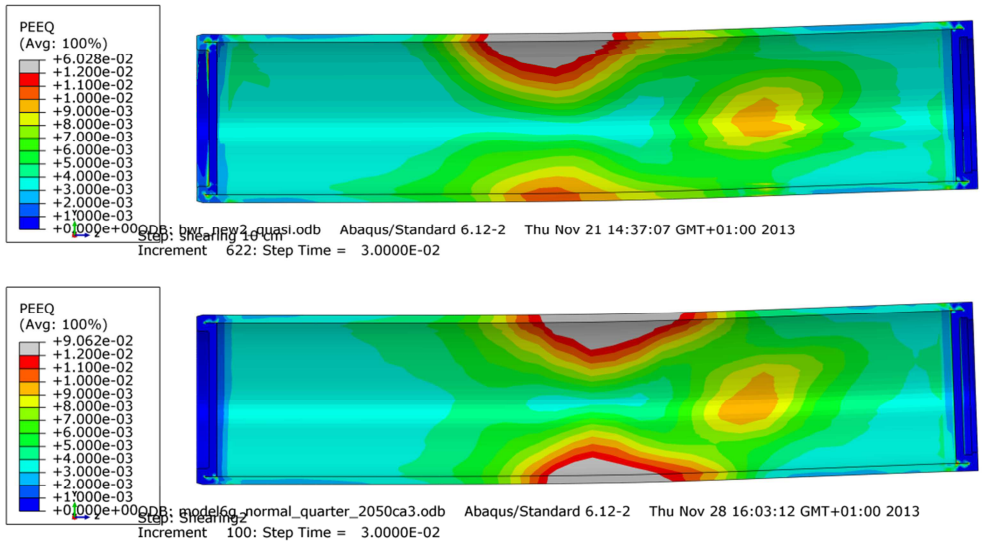

Figure A7-7. *Plot showing equivalent plastic strain (PEEQ) for the copper shell after 8 cm shearing for detailed BWR model (upper) and the reference BWR model (lower). Symmetrically positioned channel tubes.*

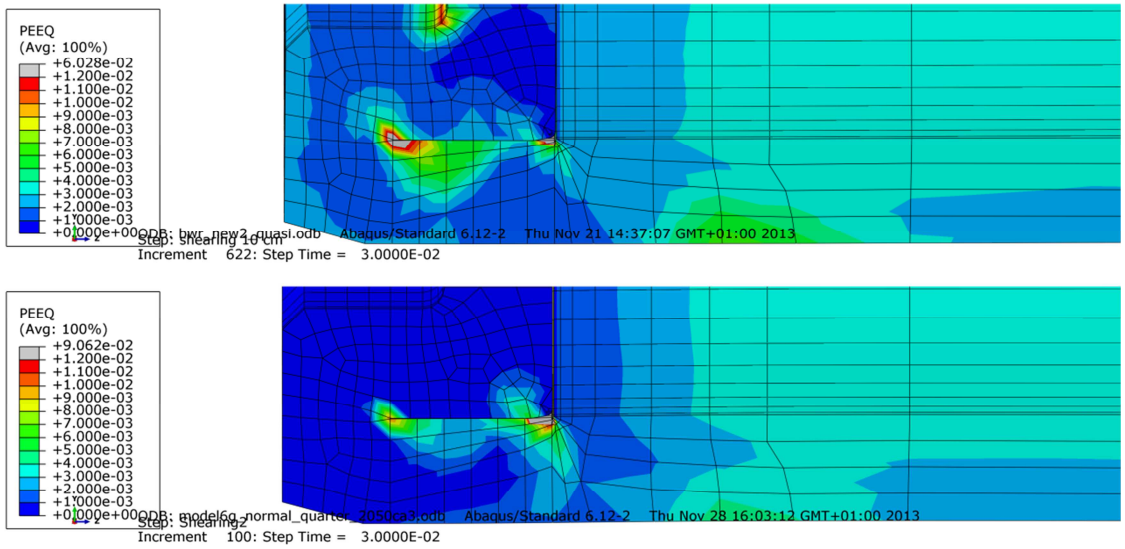

Figure A7-8. *Plot showing equivalent plastic strain (PEEQ) for the copper shell after 8 cm shearing for detailed BWR model (upper) and the reference BWR model (lower). Symmetrically positioned channel tubes.*

Nodular cast iron insert

Figures A7-9 and A7-10 show similar results for detailed BWR-model (bwr_eccentric_lock) and the reference model (model6g_normal_quarter_2050ca3) for the equivalent plastic strain except at the corner radius for the steel channel tubes.

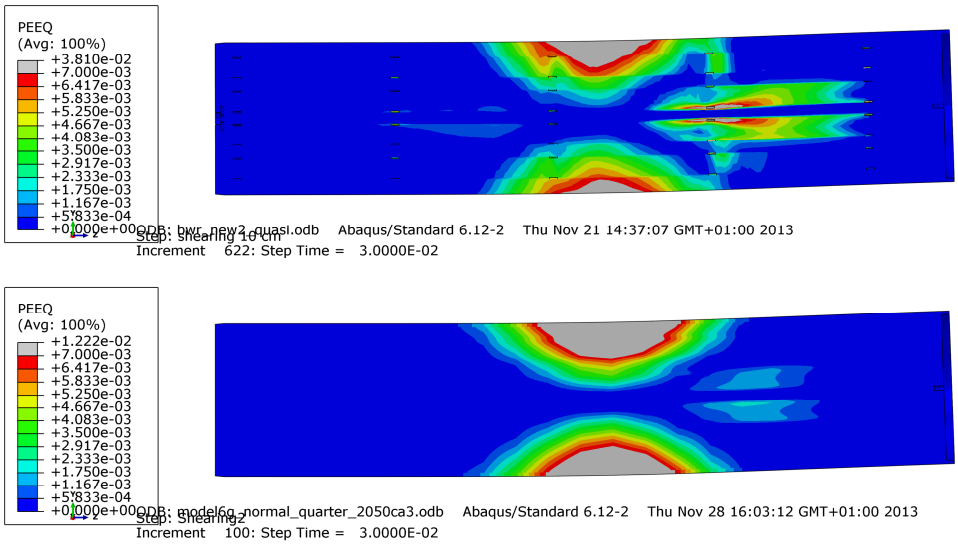

Figure A7-9. *Plots showing plastic equivalent strain (PEEQ) for the insert after 8 cm shearing for detailed BWR model (upper) and the reference BWR model (lower). Symmetrically positioned channel tubes.*

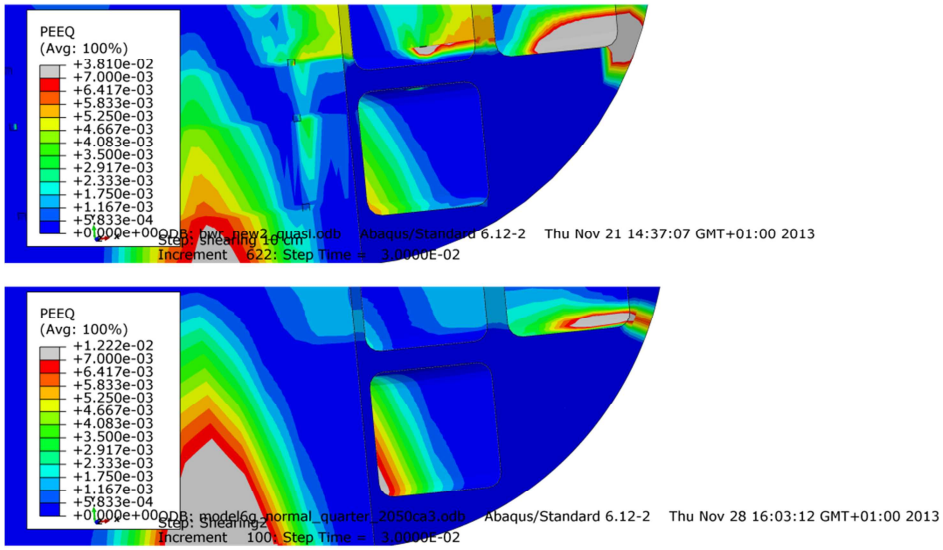

Figure A7-10. *Plots showing plastic equivalent strain (PEEQ) for the insert after 8 cm shearing for detailed BWR model (upper) and the reference BWR model (lower). Symmetrically positioned channel tubes.*

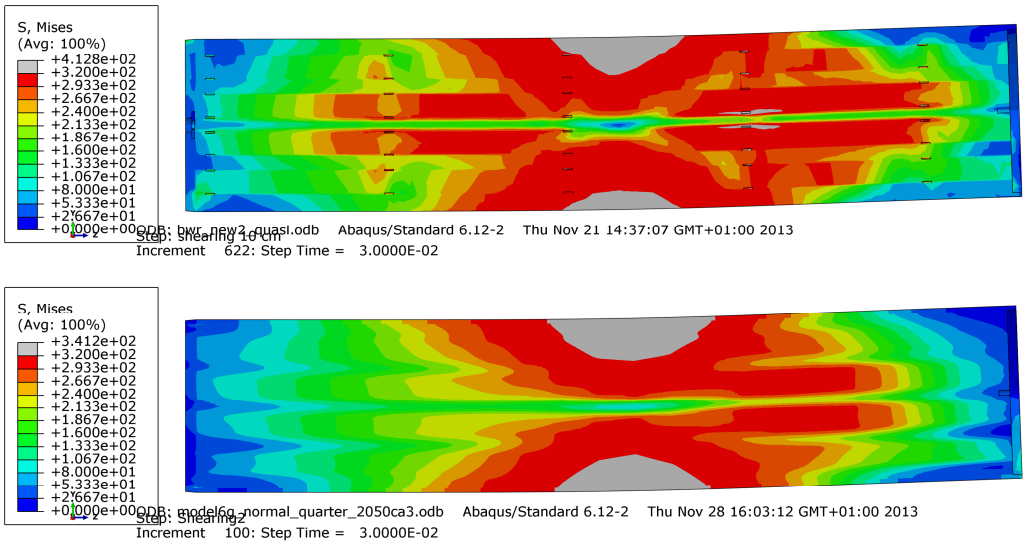

Figure A7-11. *Plots showing Mises stress for the insert after 8 cm shearing for detailed BWR model (upper) and the reference BWR model (lower). Symmetrically positioned channel tubes.*

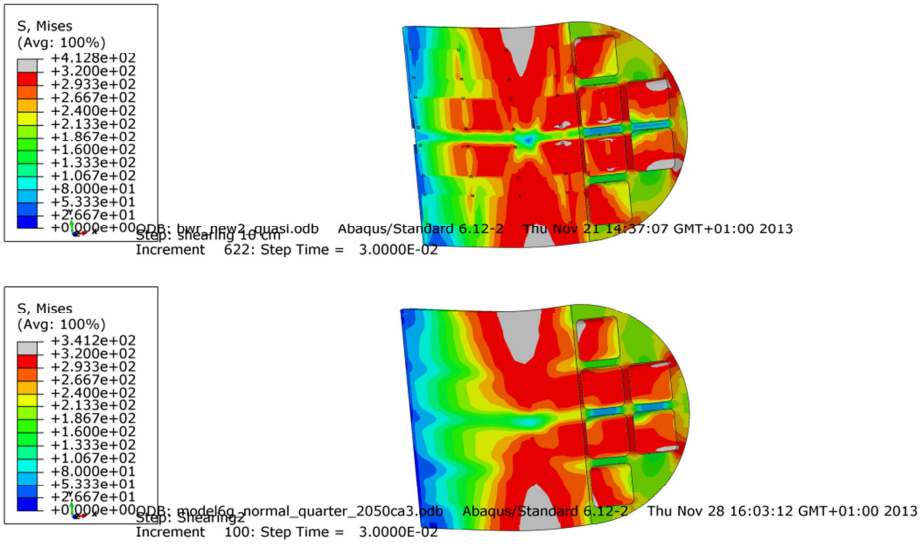

Figure A7-12. *Plots showing Mises stress for the insert after 8 cm shearing for detailed BWR model (upper) and the reference BWR model (lower). Symmetrically positioned channel tubes.*

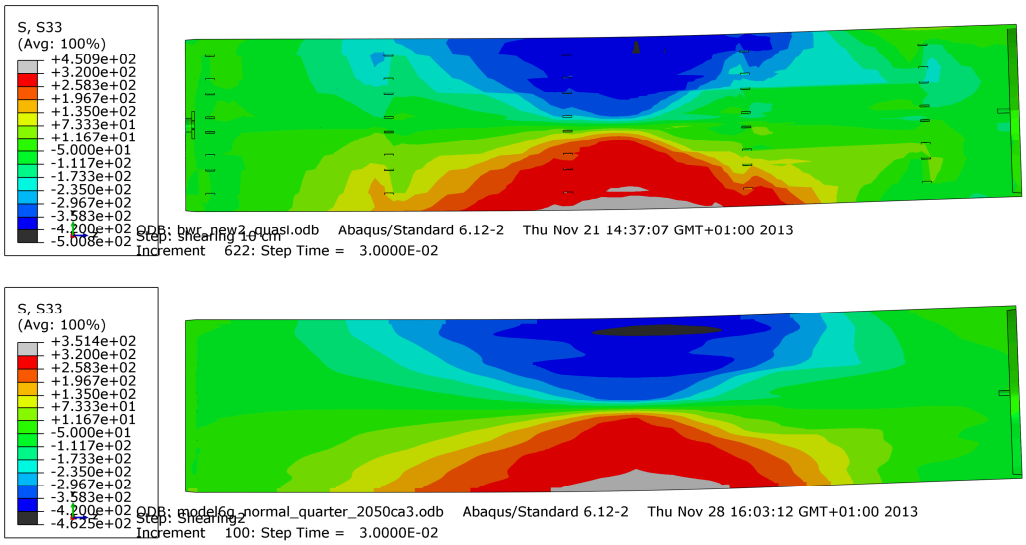

Figure A7-13. *Plots showing axial stress (S33) for the insert after 8 cm shearing for detailed BWR model (upper) and the reference BWR model (lower). Symmetrically positioned channel tubes.*

Steel channel tubes

Figures A7-14 to A7-15 show differences between the detailed BWR-model (bwr_eccentric_lock) and the reference model (model6g_normal_quarter_2050ca3). One observation is that the global stress level is lower for the detailed model even though the maximum value is higher. The reason for the decreased stress level could be explained by the support plates which increase the bending stiffness.

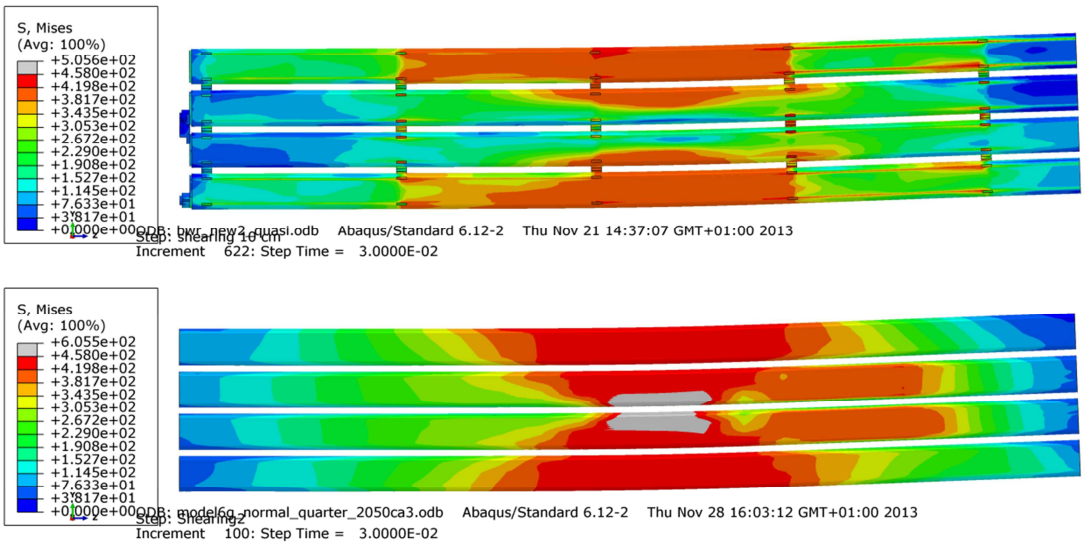

Figure A7-14. *Plots showing Mises stress for the steel channel tubes after 8 cm shearing for detailed BWR model (upper) and the reference BWR model (lower). Symmetrically positioned channel tubes.*

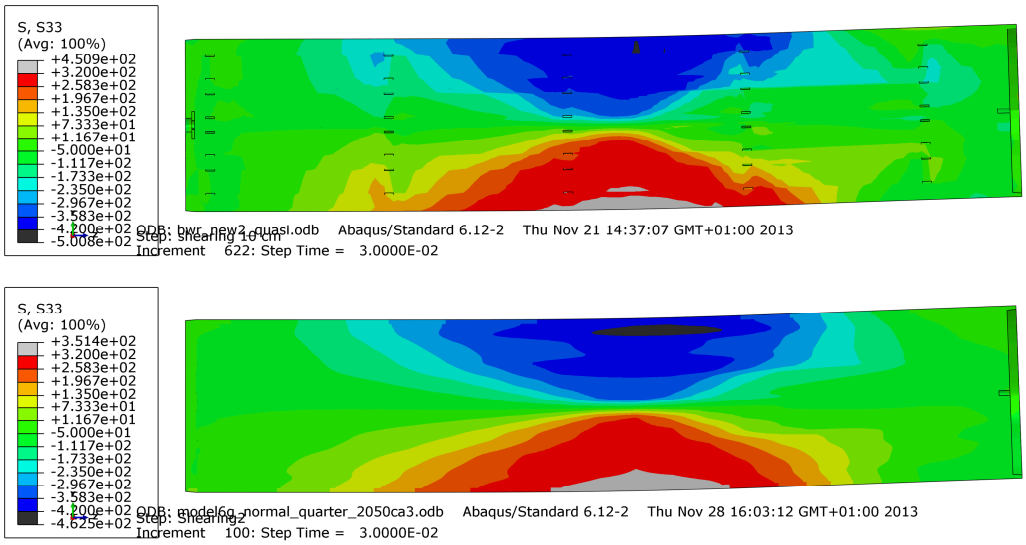

Figure A7-15. *Plots showing axial stress (S33) for the steel channel tubes after 8 cm shearing for detailed BWR model (upper) and the reference BWR model (lower). Symmetrically positioned channel tubes.*

Eccentric positioning of the steel channel tubes for the BWR insert. Symmetrically positioned channel tubes.

Figures A7-16 – A7-21 compares results using the detailed model for centric and eccentric positioning of the steel channel tubes when a horizontal shearing is applied at ¾-distance from the insert base. Figure A7-16 shows positioning of steel channel tubes with and without tolerances. Figures A7-17 – A7-18 show comparison of the Mises stress and equivalent plastic strain (PEEQ) where a slightly increase could be observed when eccentric positioning. The peak value for Mises stress increases from 473 to 483 MPa and plastic equivalent strain increases from 5.5 to 5.7%. However, visual inspection of the plots shows very similar contours. Figures A7-19 – A7-20 show similar observation for the steel channel tubes. The peak value for axial stress (S33) decreases from 417 to 415 MPa. The largest difference is for the equivalent plastic strain (PEEQ), 2.2 respectively 4.1%, at the corner radius of the insert for the thinnest wall thickness, Figure A7-21.
Note! Even though the eccentricity is modelled as 20 mm instead of the correct value of 10 mm the increase of equivalent plastic strain is rather small.

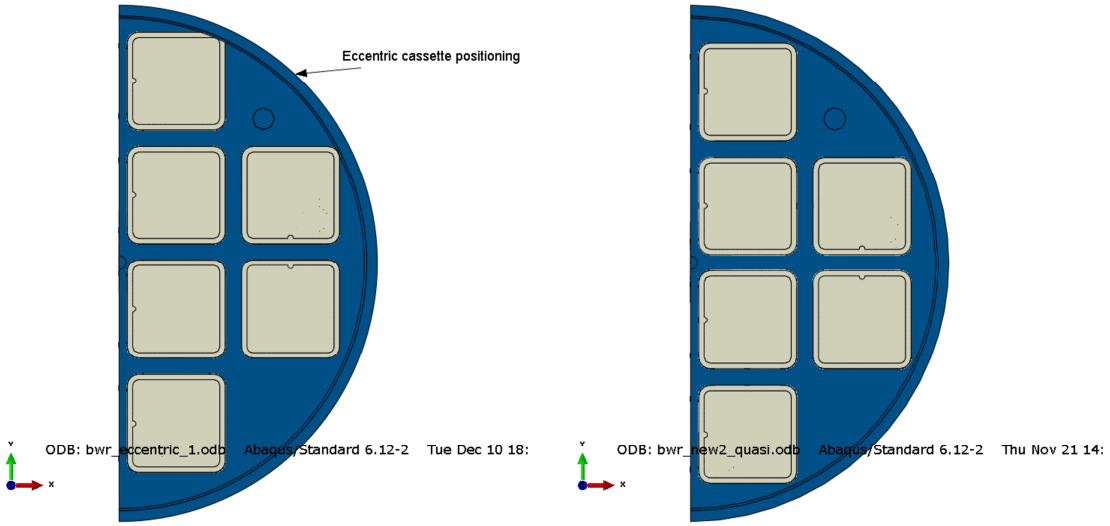

Figure A7-16 *Plots showing positioning of steel channel tubes, first case eccentric (left) and centric (right).*

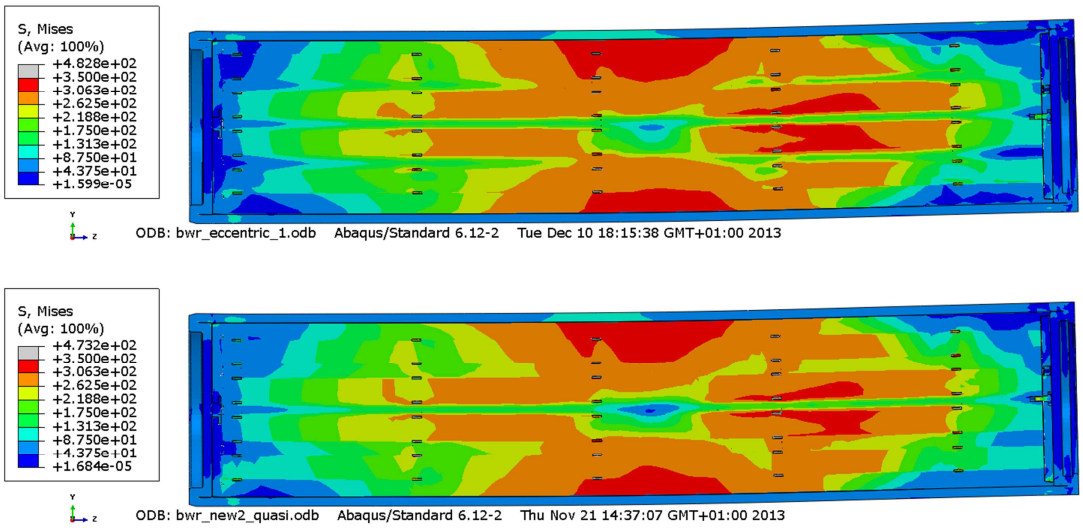

Figure A7-17 *Plots showing Mises stress after 6 cm shearing for first case eccentric BWR model (upper) and the centric BWR model (lower).*

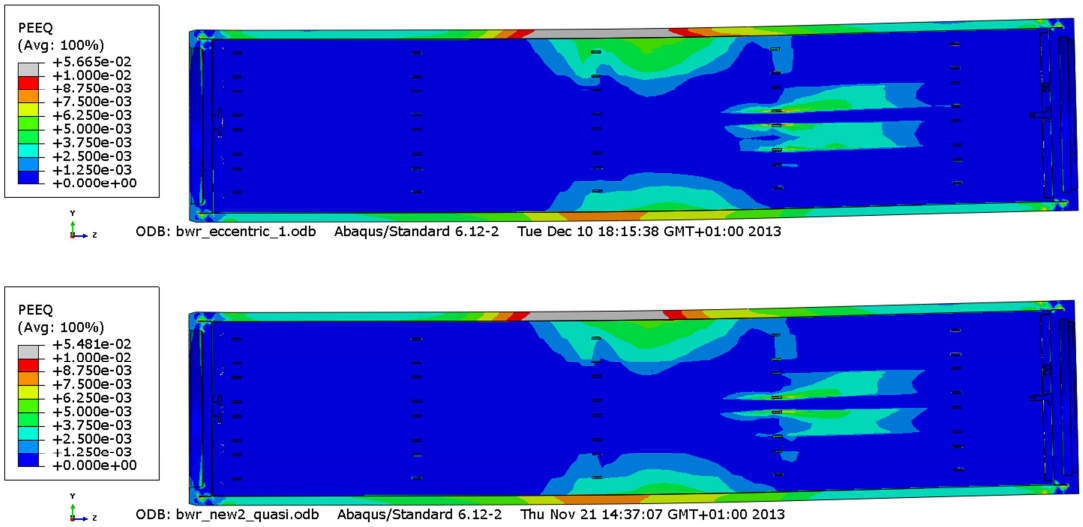

Figure A7-18 *Plots showing equivalent plastic strain (PEEQ) after 6 cm shearing for first case eccentric BWR model (upper) and the centric BWR model (lower).*

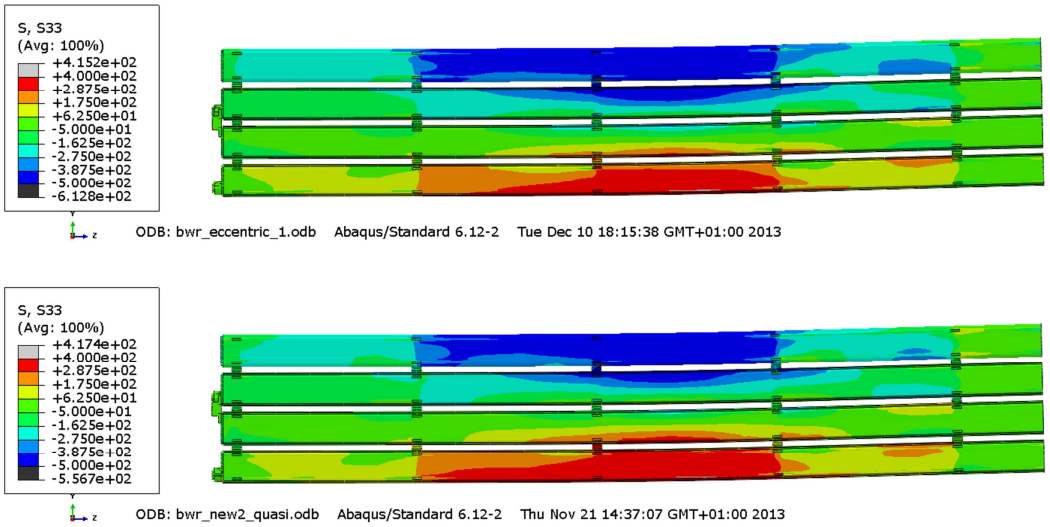

Figure A7-19 *Plots showing axial stress for the steel channel tubes after 6 cm shearing for first case eccentric BWR model (upper) and the centric BWR model (lower).*

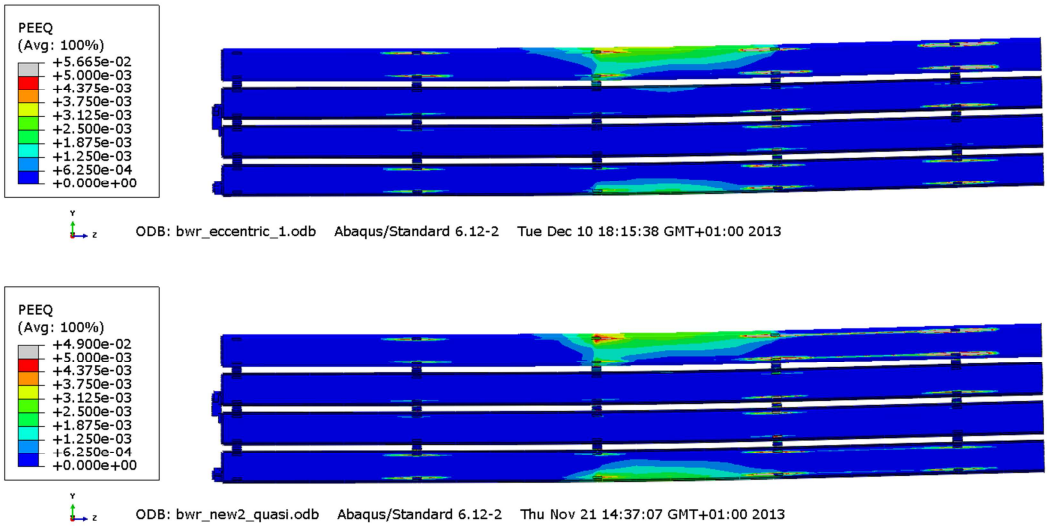

Figure A7-20 *Plots showing equivalent plastic strain (PEEQ) for the steel channel tubes after 6 cm shearing for first case eccentric BWR model (upper) and the centric BWR model (lower).*

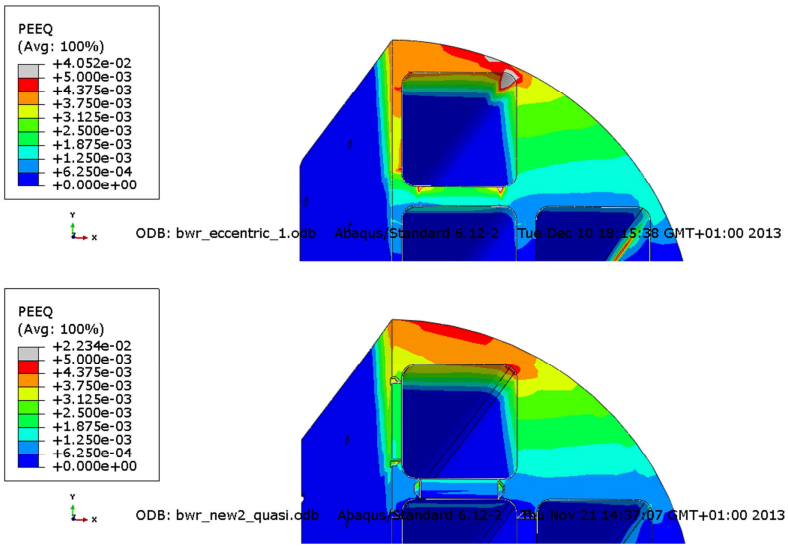

Figure A7-21 *Plots showing equivalent plastic strain (PEEQ) for the insert after 6 cm shearing for first case eccentric BWR model (upper) and the centric BWR model (lower).*

Figures A7-22 – A7-36 compare results for the first (bwr_eccentric_1 with 20 mm eccentricity and shearing such that the region with shortest distance between shell corner node and outer surface of the insert has compressive axial stress) and second case (bwr_eccentric_half with 10 mm eccentricity and shearing such that the region with shortest distance between shell corner node and outer surface of the insert has axial stress in tension) for eccentricity definitions after 10 cm shearing.
Figure A7-22 shows small difference between the axial stresses for the two cases which also imply similar results for the plastic equivalent strain (PEEQ), see Figure A7-23. For both cases the highest values for PEEQ occurs in the region with compressive stresses probably because the contribution to compressive stresses from the initial hydrostatic pressure. Figure A7-24 shows that the peak values for PEEQ occur at the second row of channel tubes and not where the distance between the channel tube corner and insert outer radius has its minimum.
Figures A7-26 – A7-28 show results for the channel tubes. Also for the channel tubes the stresses (axial and Mises) shows higher values for the second case and lower magnitude for plastic equivalent strain.

Figures A7-29 – A7-30 show results for the insert lid and the screw, Figure A7-30 shows that there are small plastic strains in the screw.
Figure A7-31 shows the plastic equivalent strain in the buffer and also the shearing direction is visible.
Figures A7-32 – A7-36 show plastic equivalent strain for the two cases with small differences except at the fillets where the second model has an improved mesh picking up the strains more accurate.

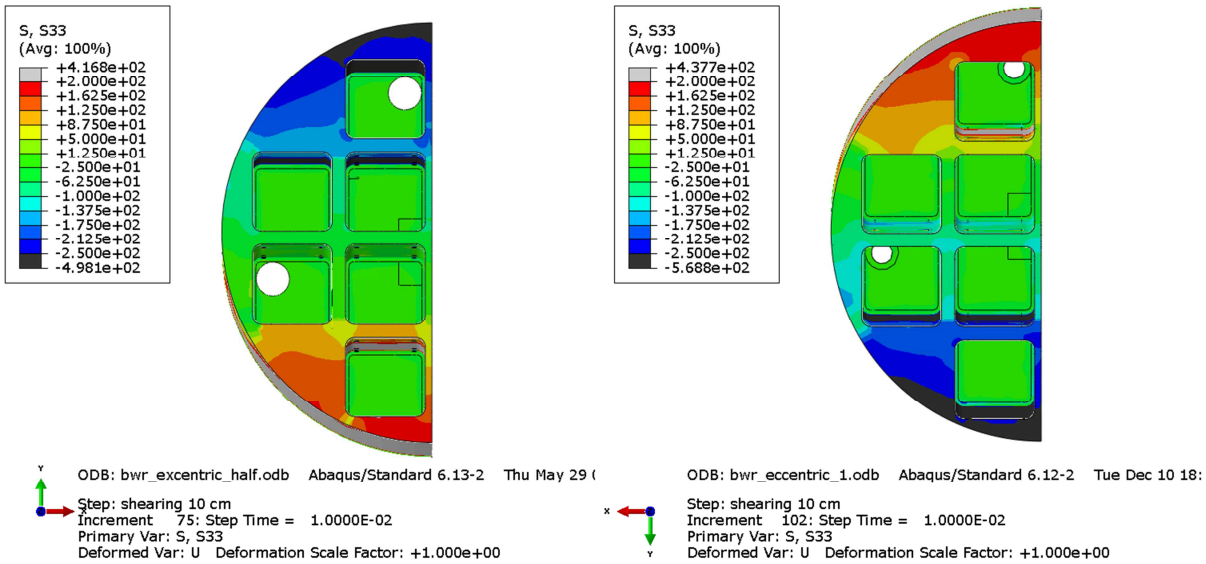

Figure A7-22 *Plots showing axial stress (S33 [MPa]) for the insert after 10 cm shearing for first (right) and second (left) case eccentric BWR model. Note the sign difference for the axial stress.*

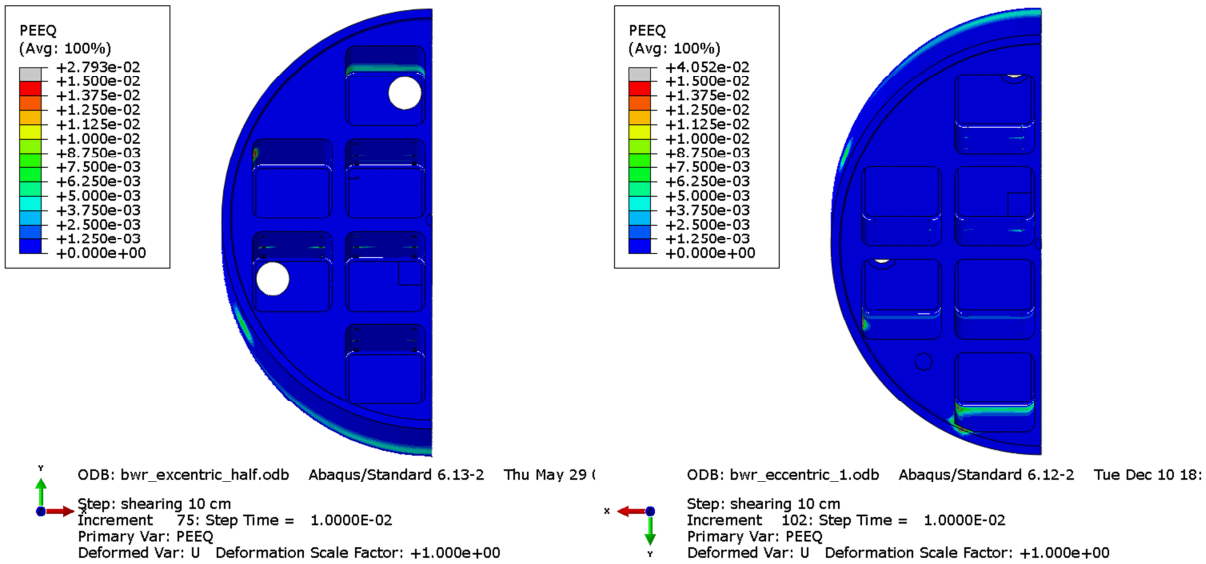

Figure A7-23 *Plots showing plastic equivalent strain (PEEQ) for the insert after 10 cm shearing for first (right) and second (left) case eccentric BWR model.*

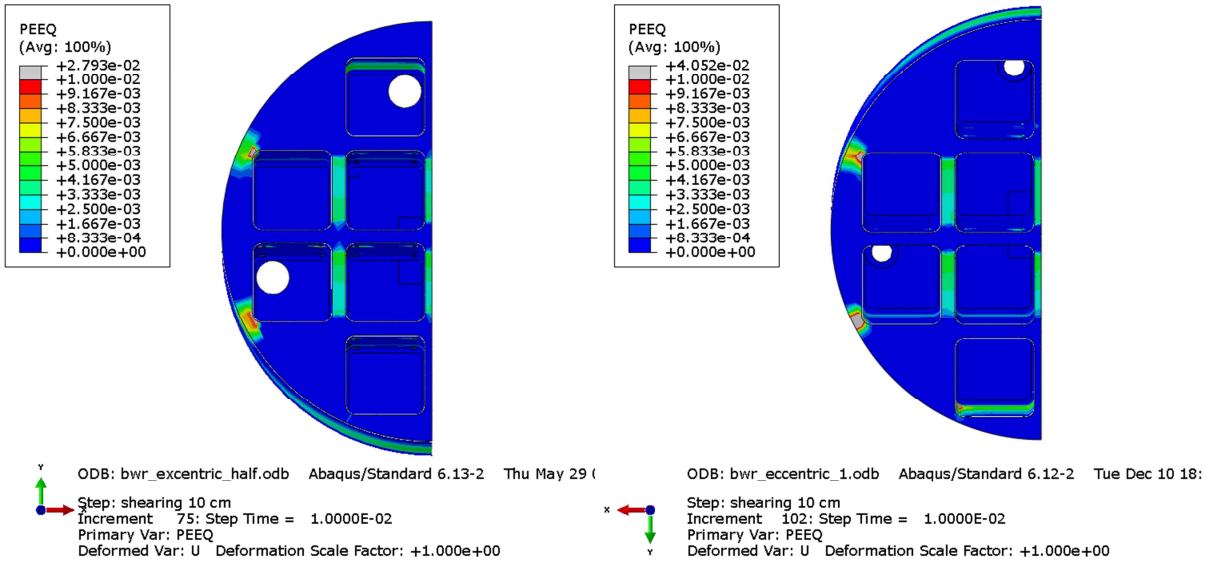

Figure A7-24 *Plots showing plastic equivalent strain (PEEQ) for the insert after 10 cm shearing for first (right) and second (left) case eccentric BWR model. Section at the highest magnitude of PEEQ.*

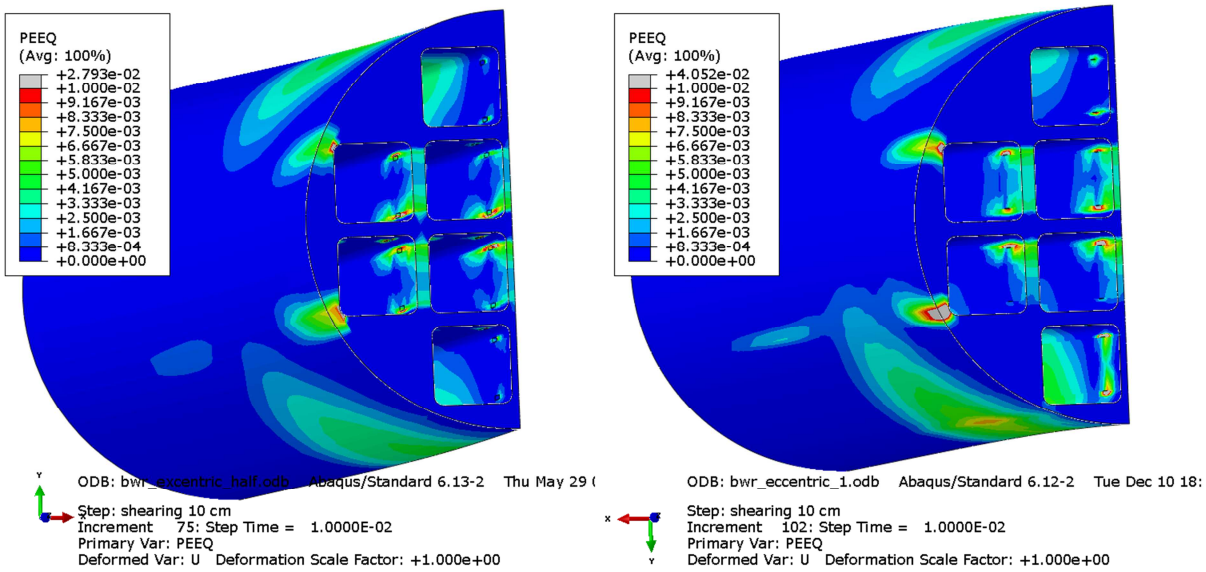

Figure A7-25 *Plots showing plastic equivalent strain (PEEQ) for the insert after 10 cm shearing for first (right) and second (left) case eccentric BWR model. Section at the largest magnitude of PEEQ.*

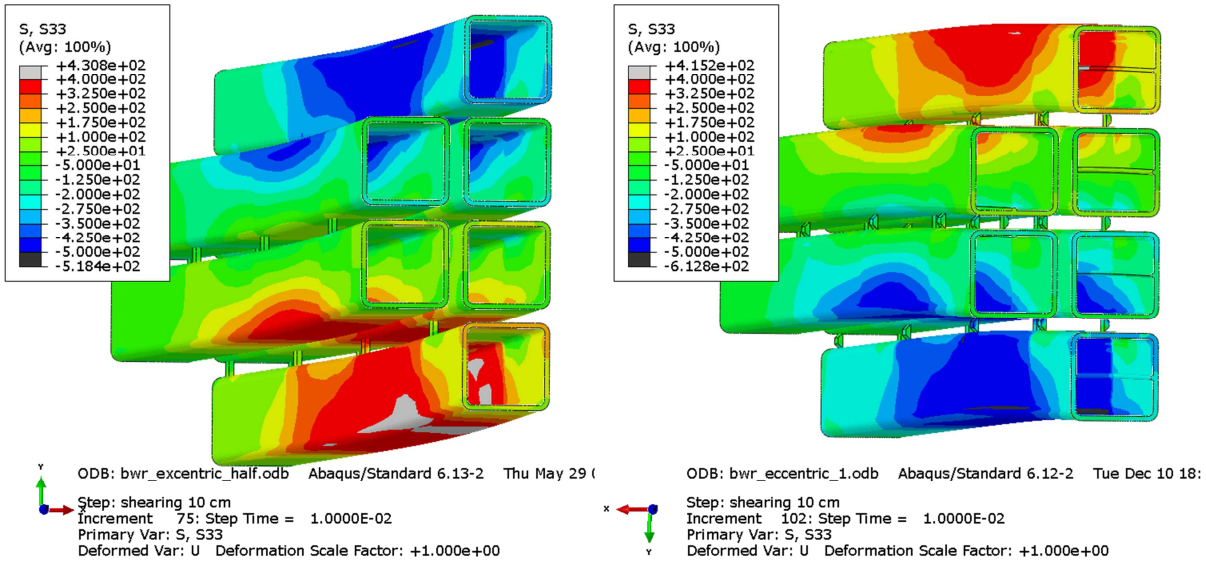

Figure A7-26 *Plots showing axial stress (S33 [MPa]) for the channel tubes after 10 cm shearing for first (right) and second (left) case eccentric BWR model.*

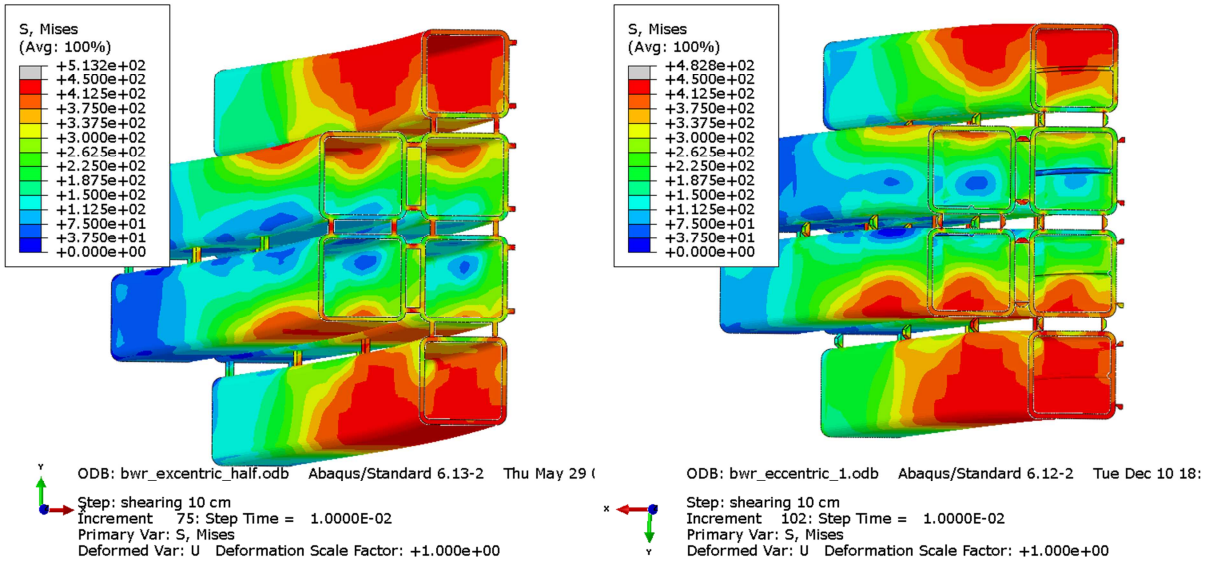

Figure A7-27 *Plots showing Mises stress [MPa] for the insert after 10 cm shearing for first (right) and second (left) case eccentric BWR model.*

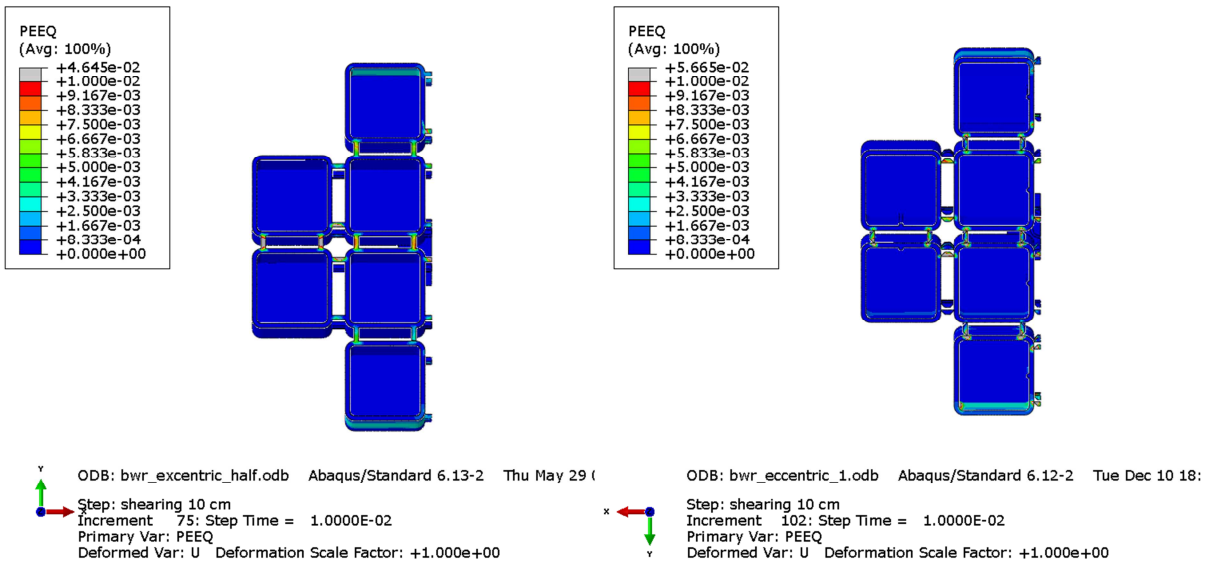

Figure A7-28 *Plots showing plastic equivalent strain (PEEQ) for the insert after 10 cm shearing for first (right) and second (left) case eccentric BWR model.*

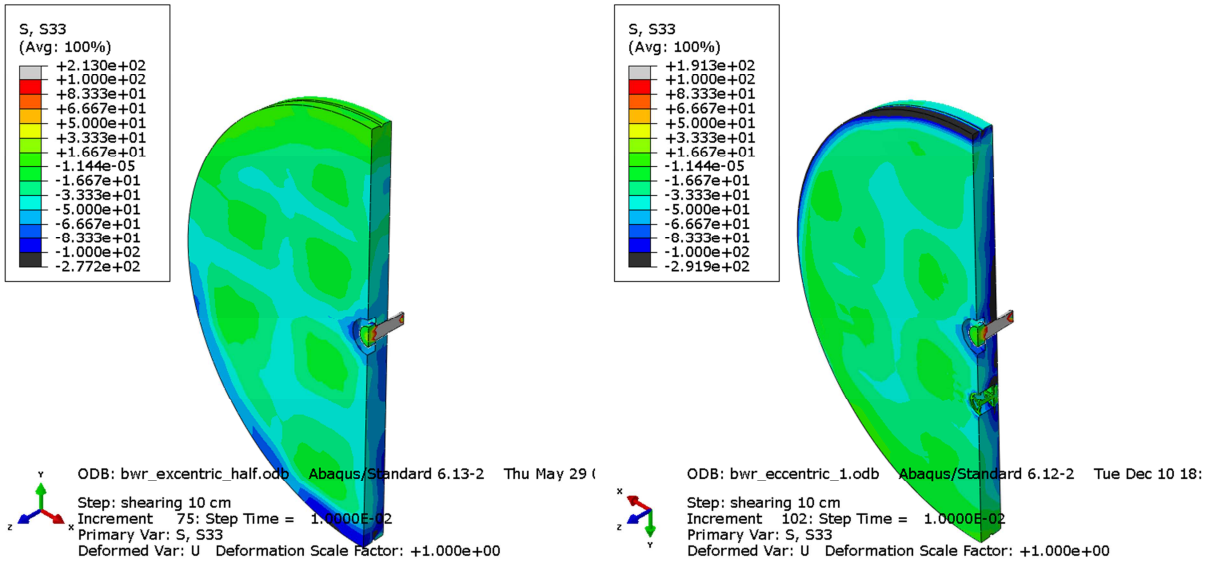

Figure A7-29 *Plots showing axial stress (S33 [MPa]) for the insert after 10 cm shearing for first (right) and second (left) case eccentric BWR model.*

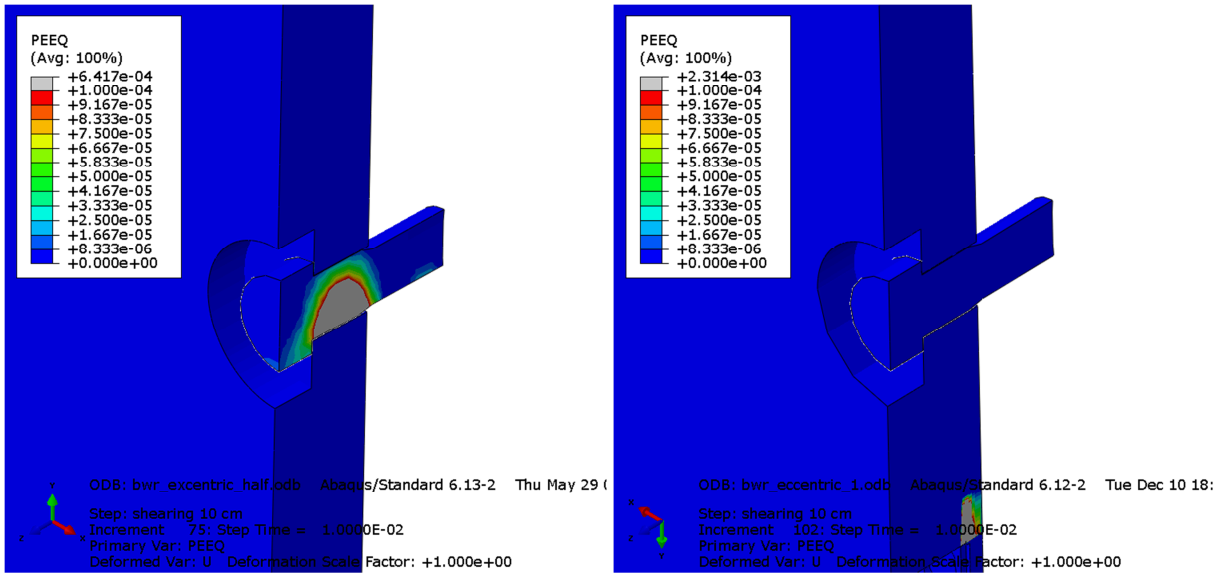

Figure A7-30 *Plots showing plastic equivalent strain (PEEQ) for the insert lid and centre screw after 10 cm shearing for first (right) and second (left) case eccentric BWR model.*

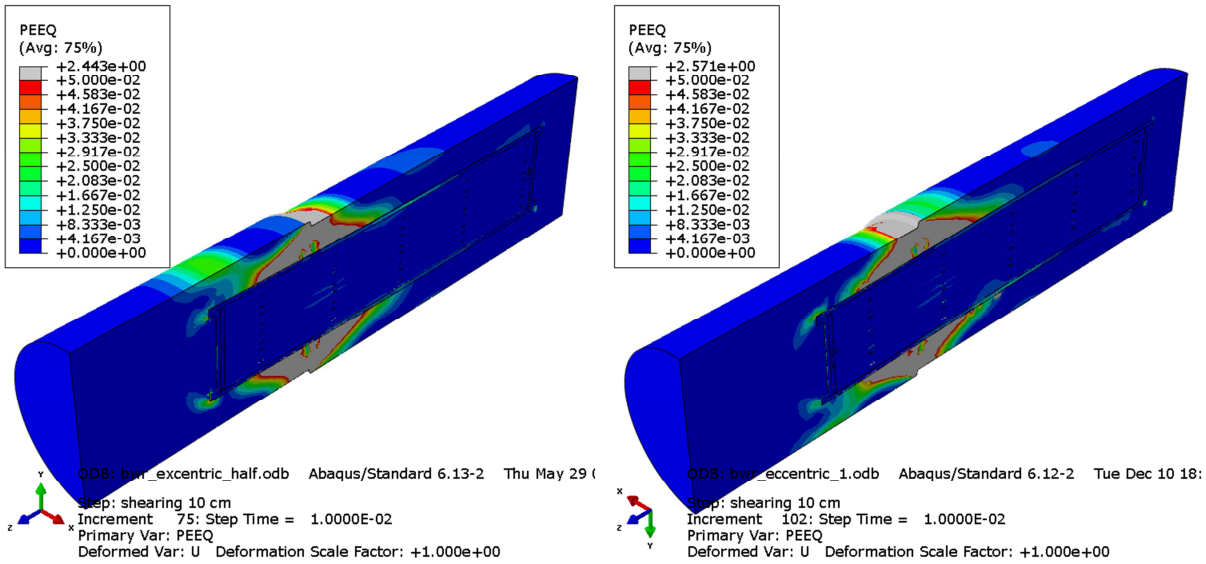

Figure A7-31 *Plots showing plastic equivalent strain (PEEQ) for the buffer after 10 cm shearing for first (right) and second (left) case eccentric BWR model.*

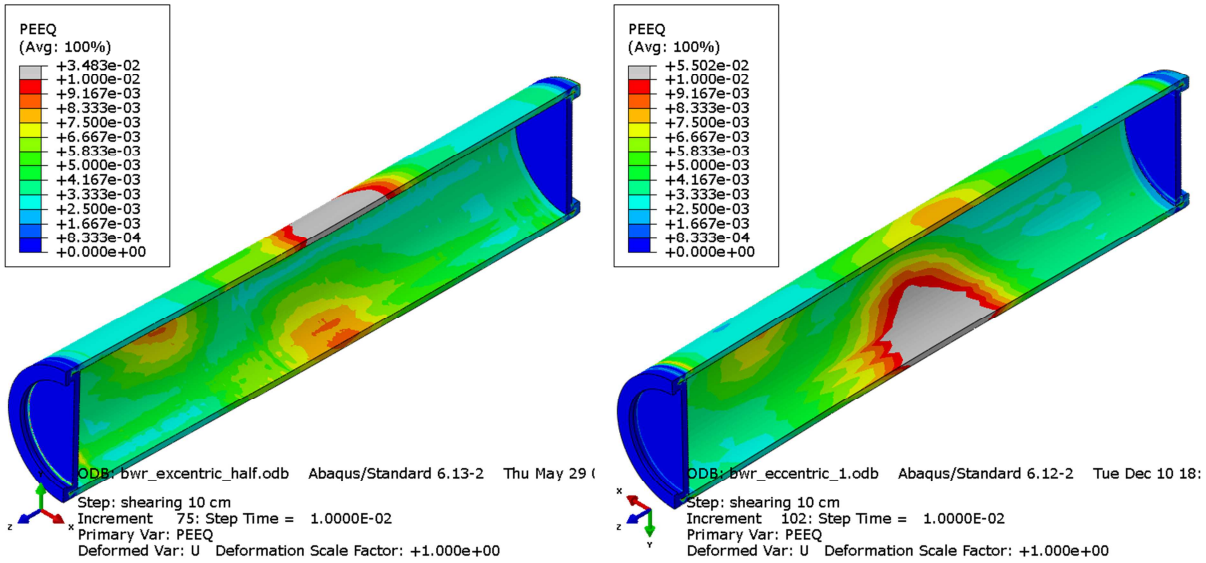

Figure A7-32 *Plots showing plastic equivalent strain (PEEQ) for the copper shell after 10 cm shearing for first (right) and second (left) case eccentric BWR model.*

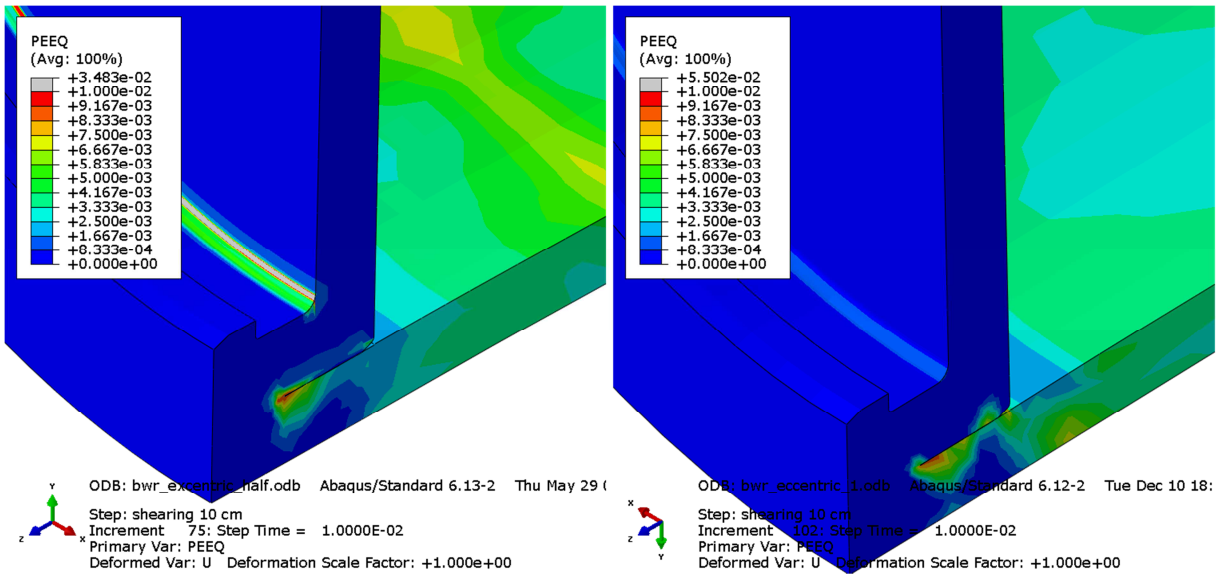

Figure A7-33 *Plots showing plastic equivalent strain (PEEQ) for the copper shell left top after 10 cm shearing for first (right) and second (left) cases eccentric BWR model.*

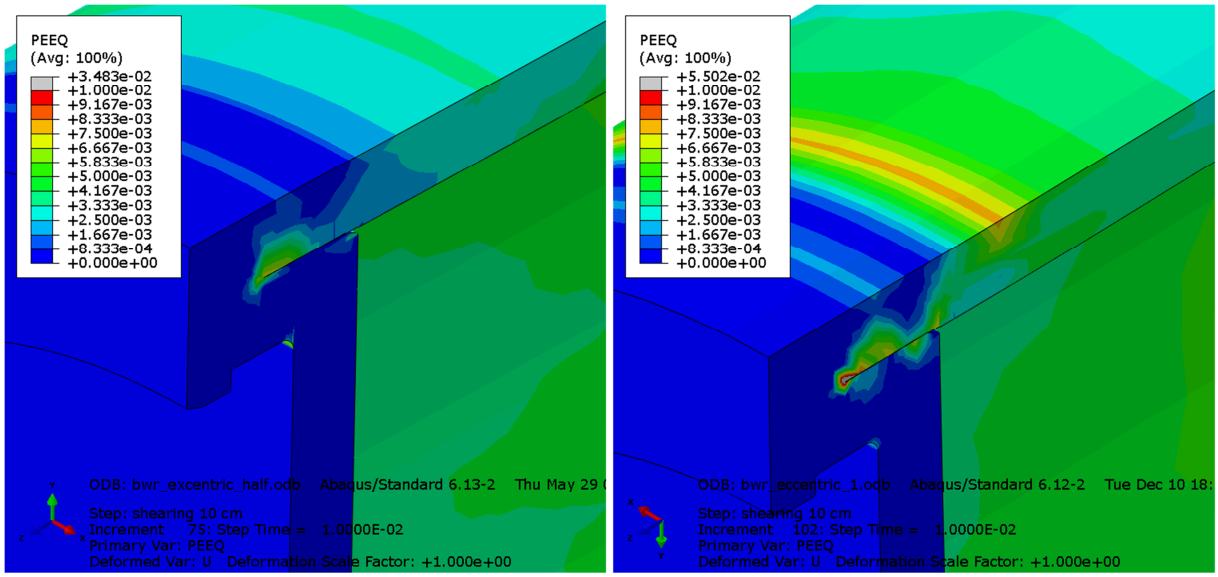

Figure A7-34 *Plots showing plastic equivalent strain (PEEQ) for the copper shell right top after 10 cm shearing for first (right) and second (left) cases eccentric BWR model.*

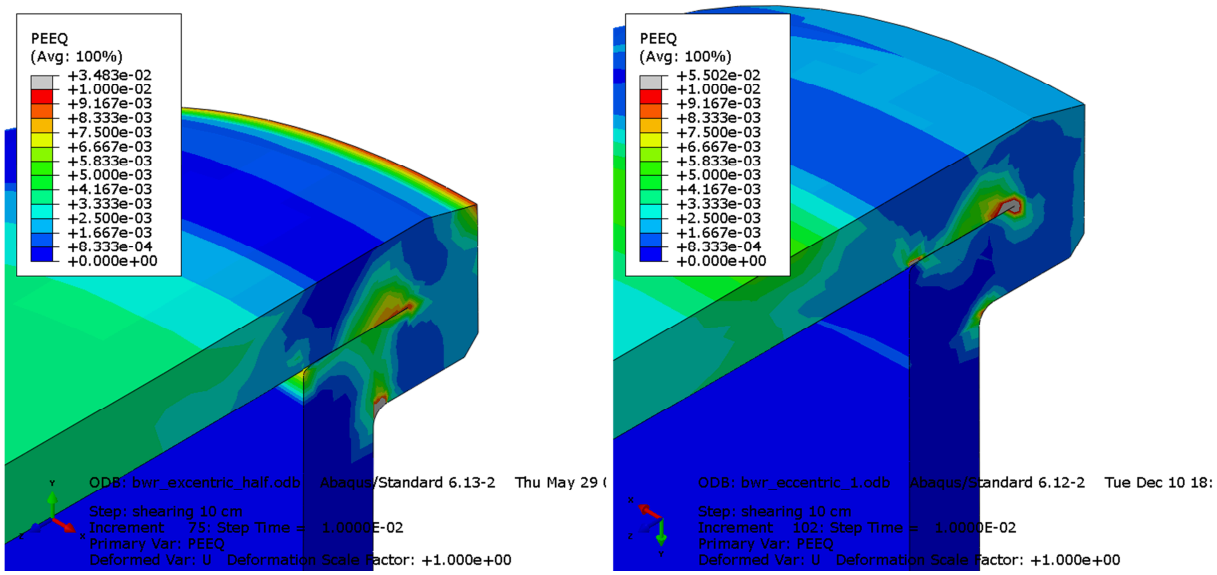

Figure A7-35 *Plots showing plastic equivalent strain (PEEQ) for the copper shell right bottom after 10 cm shearing for first (right) and second (left) case eccentric BWR model.*

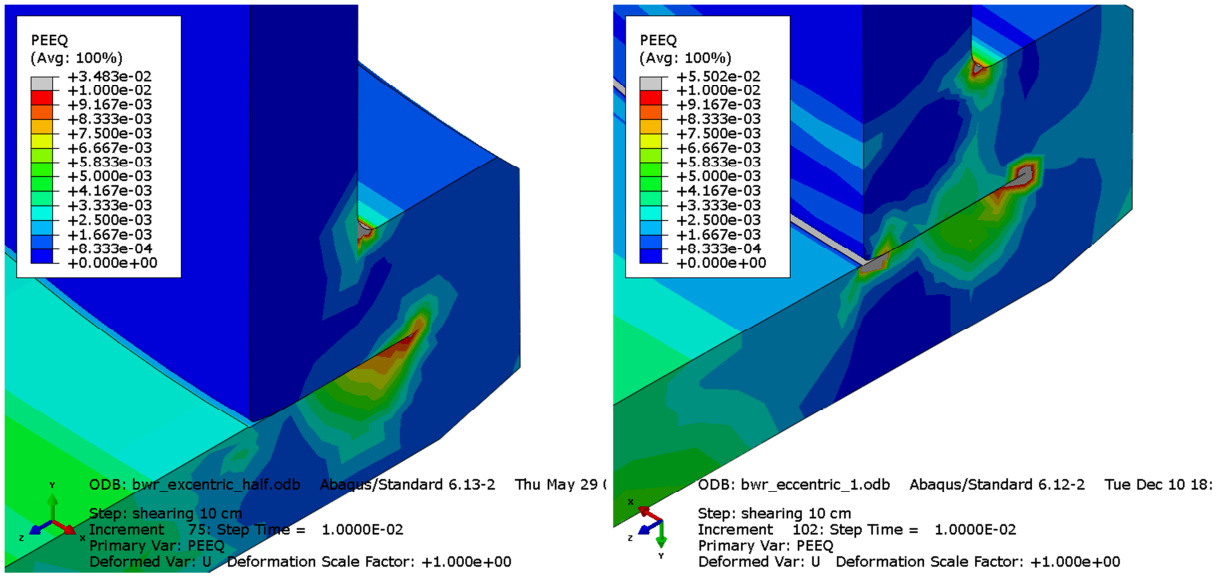

Figure A7-36 *Plots showing plastic equivalent strain (PEEQ) for the copper shell left bottom after 10 cm shearing for first (right) and second (left) cases eccentric BWR model.*

Steel channel tubes rotated for the BWR insert. Symmetrically and eccentrically positioned channel tubes.

Most analyses have been performed defining the shearing direction such that one symmetry plane exist which makes the analyses less demanding. However, there is a risk that defining the shearing direction to coincide with the direction where the distance between channel tube corner and the insert outer radius is shortest could imply larger stresses/strains. This could e.g. be achieved by rotating the channel tubes to have the shortest distance to the insert outer radius in the global y-direction. Two cases are studied:

- First (bwr_centric_rotated) case with the channel tubes positioned centric to the insert.
- Second case (bwr_eccentric_rotated) with the channel tubes positioned eccentrically (10 mm eccentricity).

Figures A7-37 – A7-47 show comparison of results for these two cases after 9 cm shearing.

The obtained results for stresses and strains show small differences between the two cases even though there are some findings:

- Maximum global stresses and strains are used by bending of the insert.
- Eccentric positioned channel tubes moves the bending axis which means that stresses/strains increase in the region with axial tensile stresses and decrease in the region with axial compressive stresses when comparing with centric positioned channel tubes, see e.g. Figures A7-38 – A7-39.
- Maximum plastic equivalent strain is however caused by shearing stress and occurs close to the bending axis.
- For the copper shell there are six regions with similar magnitude of maximum plastic equivalent strain (fillets at top and base, welds at top and base and also top and base of the outer shell), see Figures A7-43 – A7-47. However, the maximum magnitude of PEEQ is rather low 4.5% for the eccentric positioned channel tubes and 3.9% for the centric positioned channel tubes.

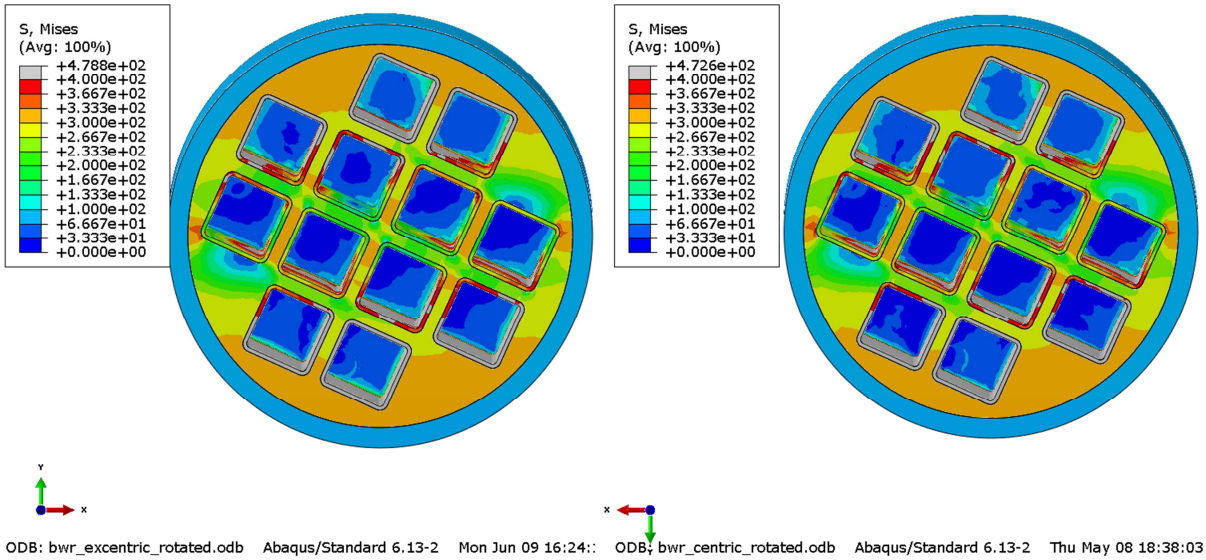

Figure A7-37 *Plots showing Mises stress [MPa] for the insert after 9 cm shearing with rotated channel tubes for eccentric(left) and centric (right) BWR model.*

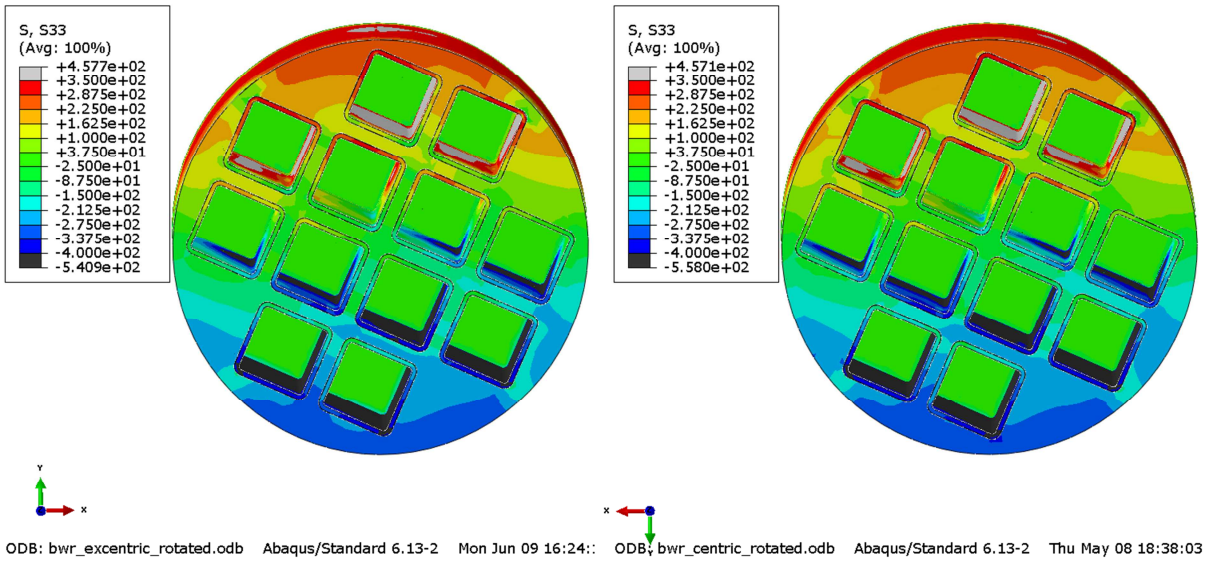

Figure A7-38 *Plots showing axial stress, S33, [MPa] for the insert after 9 cm shearing with rotated channel tubes for eccentric(left) and centric (right) BWR model.*

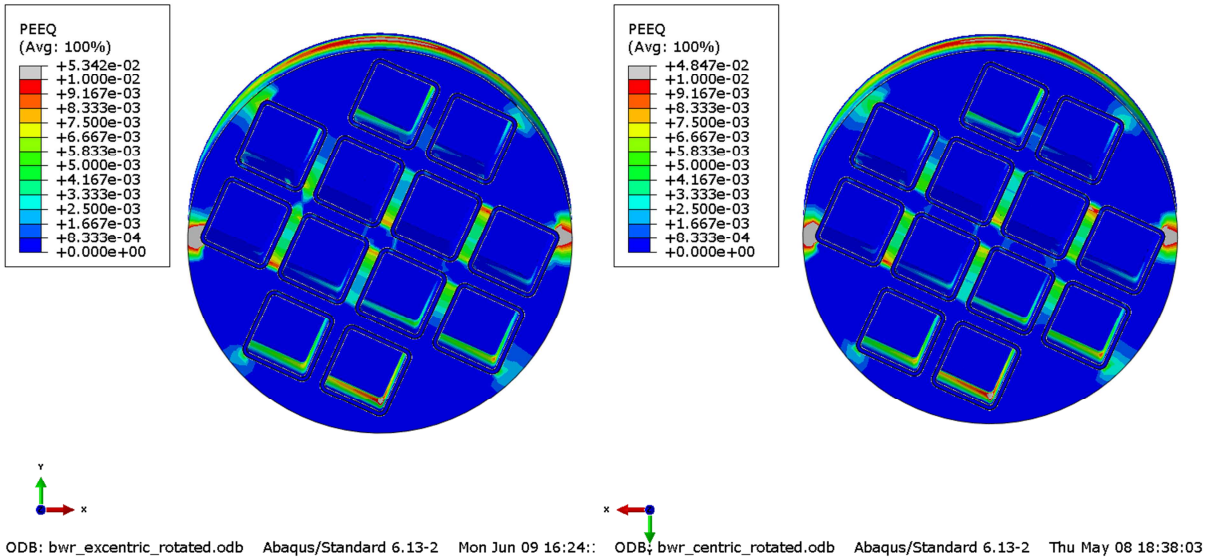

Figure A7-39 *Plots showing plastic equivalent strain (PEEQ)] for the insert after 9 cm shearing with rotated channel tubes for eccentric(left) and centric (right) BWR model.*

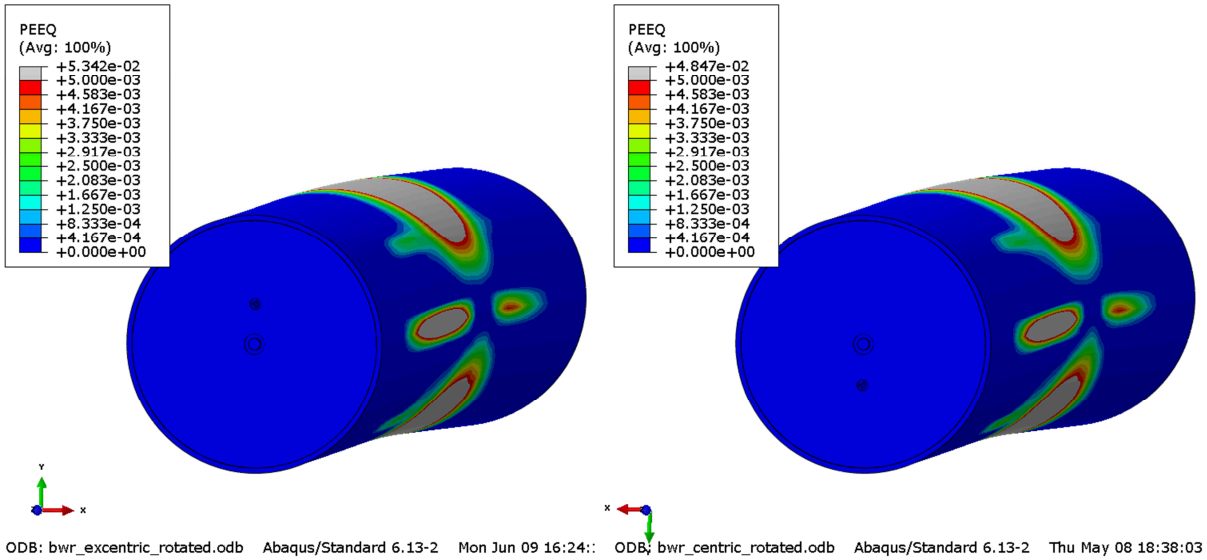

Figure A7-40 *Plots showing plastic equivalent strain (PEEQ) for the insert after 9 cm shearing with rotated channel tubes for eccentric(left) and centric (right) BWR model.*

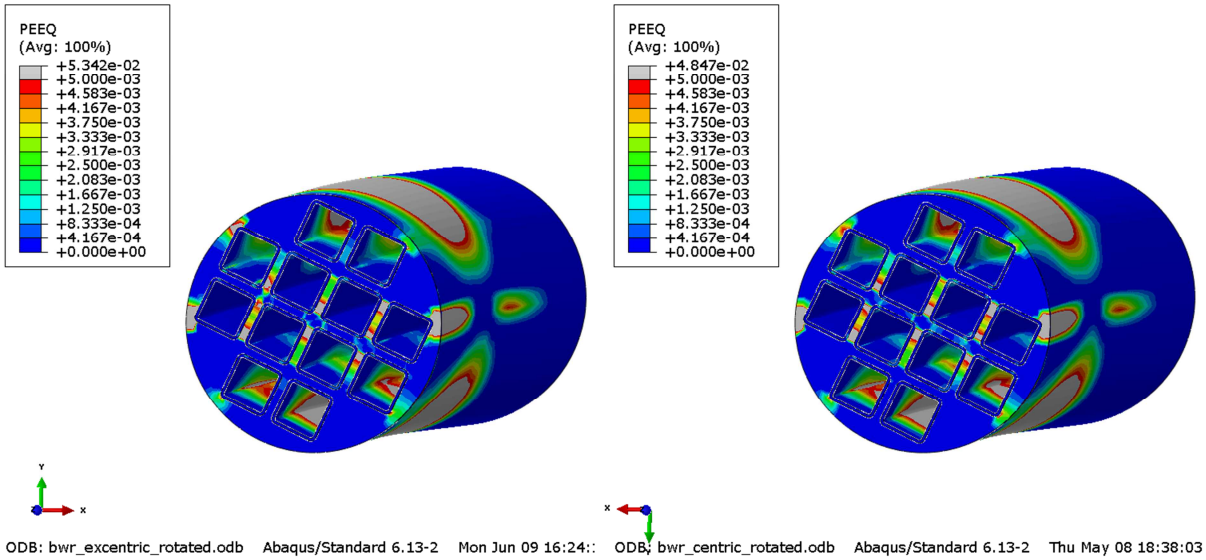

Figure A7-41 *Plots showing plastic equivalent strain (PEEQ) for the insert section with maximum magnitude after 9 cm shearing with rotated channel tubes for eccentric(left) and centric (right) BWR model.*

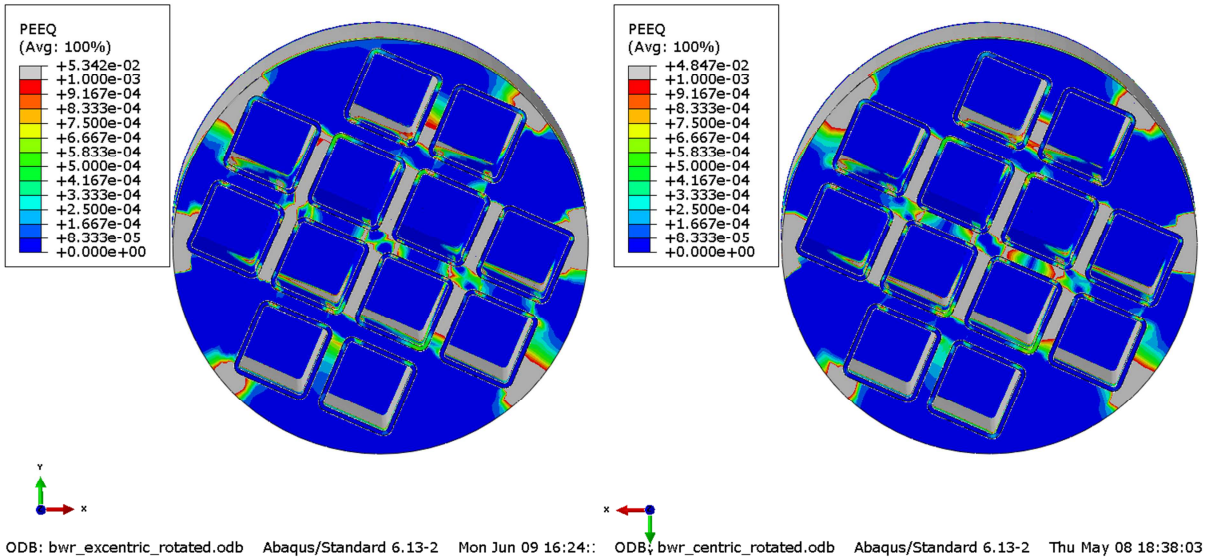

Figure A7-42 *Plots showing plastic equivalent strain (PEEQ) for the insert section with maximum magnitude after 9 cm shearing with rotated channel tubes for eccentric(left) and centric (right) BWR model.*

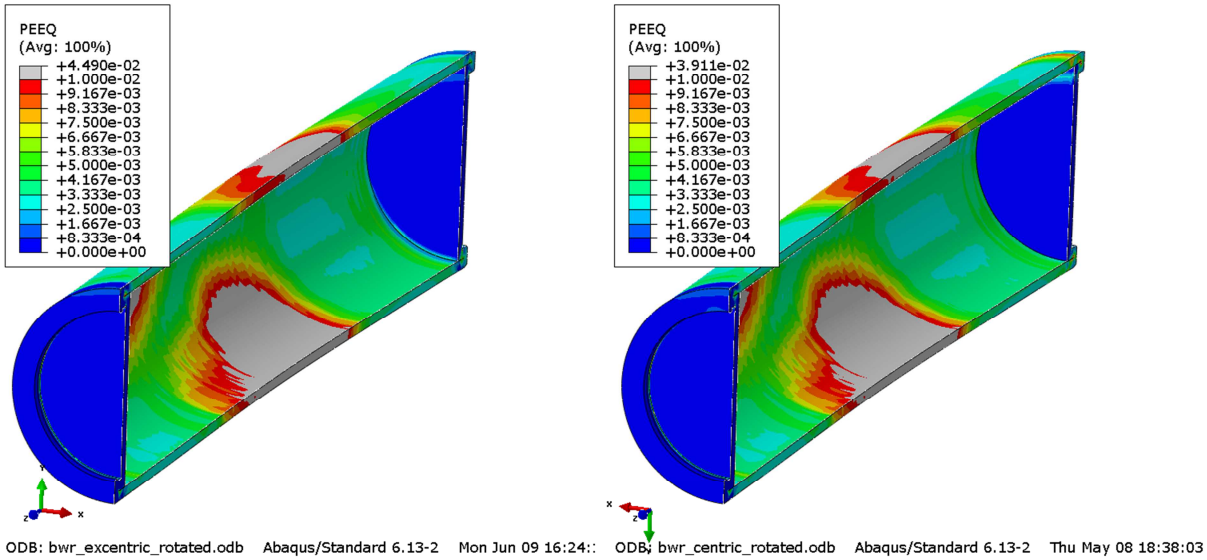

Figure A7-43 *Plots showing plastic equivalent strain (PEEQ) for the copper shell after 9 cm shearing with rotated channel tubes for eccentric(left) and centric (right) BWR model.*

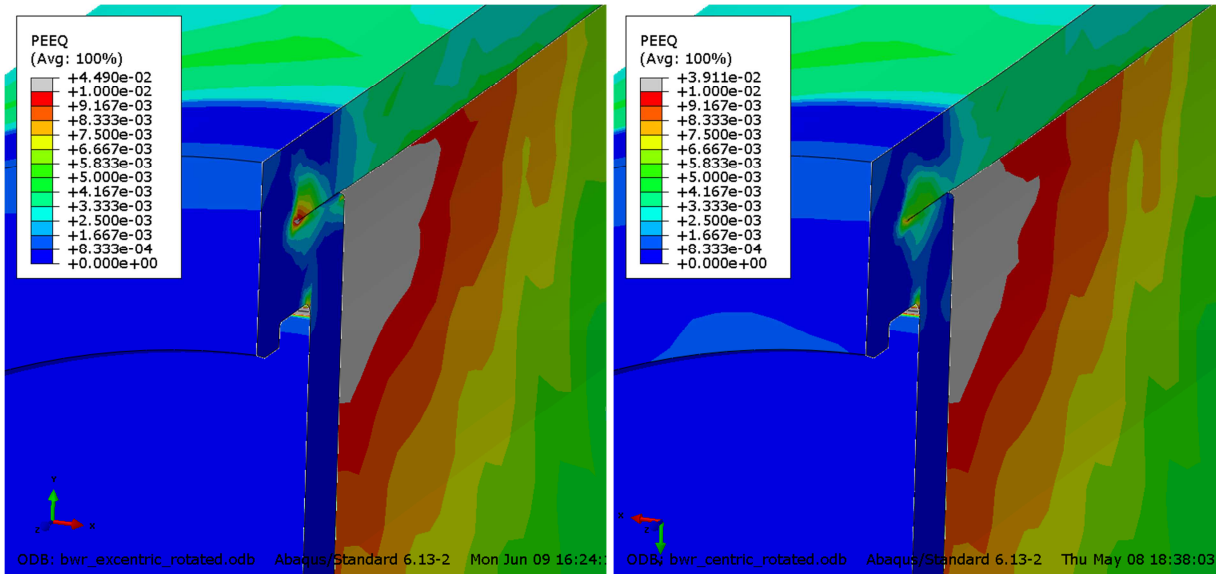

Figure A7-44 *Plots showing plastic equivalent strain (PEEQ) for the copper shell top upper corner after 9 cm shearing with rotated channel tubes for eccentric(left) and centric (right) BWR model.*

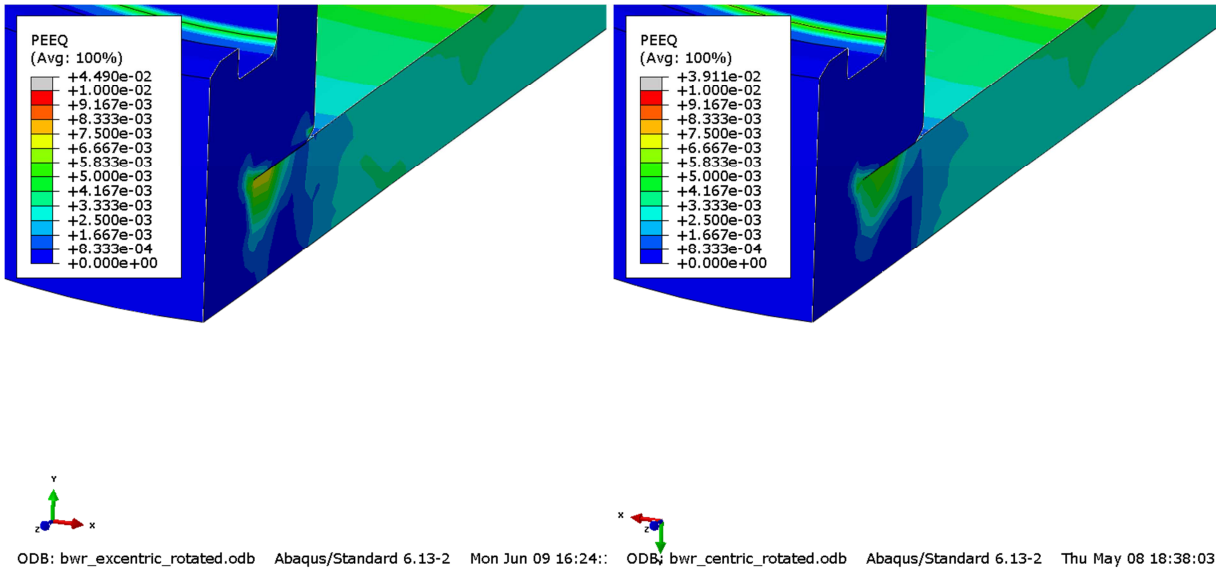

Figure A7-45 *Plots showing plastic equivalent strain (PEEQ) for the copper shell top lower corner after 9 cm shearing with rotated channel tubes for eccentric(left) and centric (right) BWR model.*

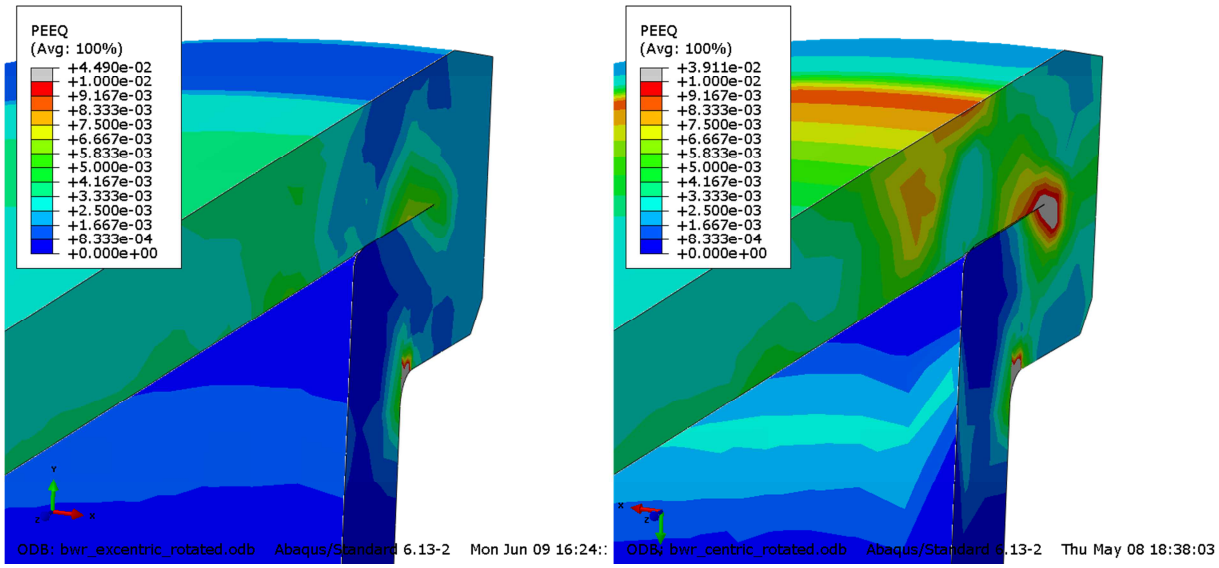

Figure A7-46 *Plots showing plastic equivalent strain (PEEQ) for the copper shell bottom upper corner after 9 cm shearing with rotated channel tubes for eccentric(left) and centric (right) BWR model.*

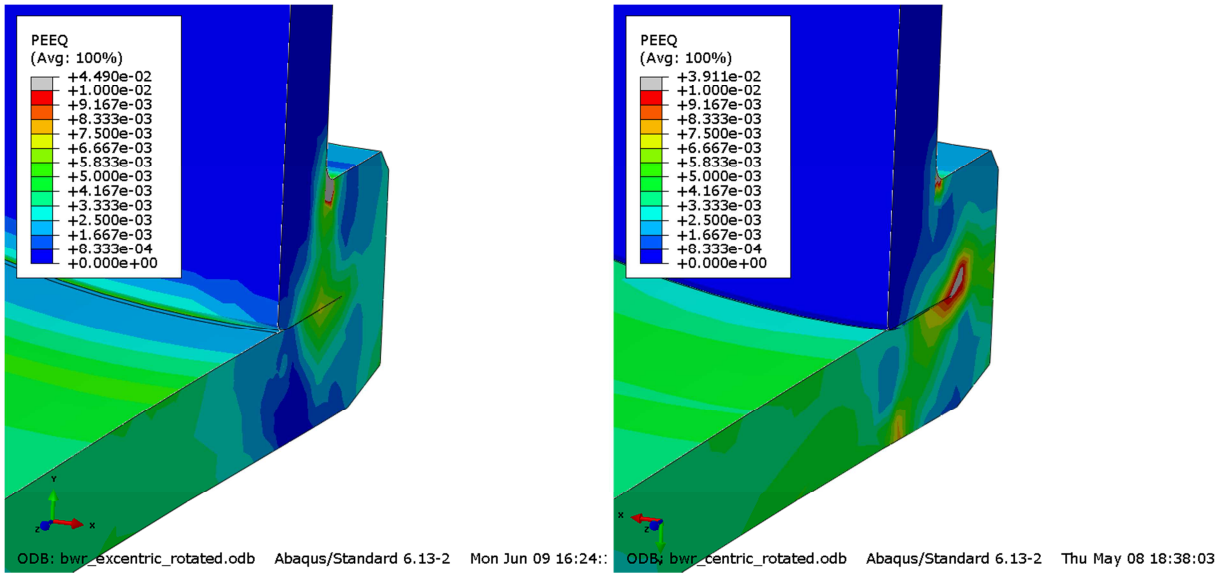

Figure A7-47 *Plots showing plastic equivalent strain (PEEQ) for the copper shell bottom lower corner after 9 cm shearing with rotated channel tubes for eccentric(left) and centric (right) BWR model.*

Appendix 8 – Storage of files

This report is based on the results from a lot of FE-simulations using ABAQUS which is a commercial available code and is thus not stored as part of the work. Below is a short description of files used in the project and directories for storage of these. These files are also stored at SKB.

The files are stored in directories as:

Geometry Input-files Plots Detailed models models for BWR-canisters for Earthquake induced rock shear.docx - this report Scripts

1 – Plot-files used in the report

Contents in C:\Users\jhd\mappar\skb\Detailed_PWR_BWR\bwr\Plots

Geometry plots

```
Fig2-1-shearing_planes.png
Fig2-2-detailes.png
Fig2-3-detailes_washer.png
Fig2-4-detailes_bottom.png
Fig3-1-buffer.png
Fig3-steel_lid.png
Fig3-screw.png
Fig3-washer.png
Fig3-bwr-insert1.png
Fig3-bwr-insert2.png
Fig3-bwr-insert3.png
Fig3-bwr-insert4.png
Fig3-bwr-insert5.png
Fig3-bwr-insert6.png
Fig3-bwr-channels1.png
Fig3-bwr-channels2.png
Fig3-bwr-channels3.png
```

Contents in C:\Users\jhd\mappar\skb\Detailed_PWR_BWR\bwr\Plots

Results – comparison

compare_5cm-bwr_eccentric_rotated-copper_peeq1.png
compare_5cm-bwr_eccentric_rotated-copper_peeq2.png
compare_5cm-bwr_eccentric_rotated-copper_peeq3.png
compare_5cm-bwr_eccentric_rotated-copper_peeq4.png
compare_5cm-bwr_eccentric_rotated-copper_peeq5.png
compare_5cm-bwr_eccentric_rotated-mises.png
compare_5cm-bwr_eccentric_rotated-peeq.png
compare_5cm-bwr_eccentric_rotated-peeq2.png
compare_5cm-bwr_eccentric_rotated-peeq3.png
compare_5cm-bwr_eccentric_rotated-peeq4.png
compare_5cm-bwr_eccentric_rotated-s33-2.png
compare_5cm-bwr_new-model6g-peeq.png
compare_5cm-bwr_new-model6g_channels-mises.png
compare_5cm-bwr_new-model6g_channels-s33.png
compare_5cm-bwr_new-model6g_copper-peeq.png
compare_5cm-bwr_new-model6g_copper-peeq_max.png
compare_5cm-bwr_new-model6g_detail_bot2_corner-mises.png
compare_5cm-bwr_new-model6g_detail_bot_corner-mises.png
compare_5cm-bwr_new-model6g_detail_screw-mises.png
compare_5cm-bwr_new-model6g_detail_top2_corner-mises.png
compare_5cm-bwr_new-model6g_detail_top_corner-mises.png
compare_5cm-bwr_new-model6g_insert-mises.png
compare_5cm-bwr_new-model6g_insert-mises2.png
compare_5cm-bwr_new-model6g_insert-peeq.png
compare_5cm-bwr_new-model6g_insert-peeq2.png
compare_5cm-bwr_new-model6g_insert-s33.png
compare_5cm-bwr_new-model6g_insert_outer-s33.png
compare_5cm_bwr_excentric_half-channels_mises.png
compare_5cm_bwr_excentric_half-channels_peeq.png
compare_5cm_bwr_excentric_half-channels_peeq2.png
compare_5cm_bwr_excentric_half-channels_s33-1.png
compare_5cm_bwr_excentric_half-channels_s33.png
compare_5cm_bwr_excentric_half-channels_undeformed-mesh.png
compare_5cm_bwr_excentric_half-channels_undeformed.png
compare_5cm_bwr_excentric_half-copper-peeq.png
compare_5cm_bwr_excentric_half-copper-peeq2.png
compare_5cm_bwr_excentric_half-copper-peeq3.png
compare_5cm_bwr_excentric_half-copper-peeq4.png
compare_5cm_bwr_excentric_half-copper-peeq5.png
compare_5cm_bwr_excentric_half-insert-peeq2.png
compare_5cm_bwr_excentric_half-insert_peeq.png
compare_5cm_bwr_excentric_half-insert_peeq2.png
compare_5cm_bwr_excentric_half-insert_peeq3.png
compare_5cm_bwr_excentric_half-insert_s33.png
compare_5cm_bwr_excentric_half-peeq.png
compare_5cm_bwr_excentric_half-peeq2.png
compare_5cm_bwr_excentric_half-steel_lid-peeq.png
compare_5cm_bwr_excentric_half-steel_lid-s33.png
compare_5cm_bwr_excentric_half-undeformed.png
compare_5cm_eccentric_bwr-channels_peeq.png
compare_5cm_eccentric_bwr-channels_s33.png
compare_5cm_eccentric_bwr-insert_peeq.png
compare_5cm_eccentric_bwr-insert_position.png
compare_5cm_eccentric_bwr-mises.png
compare_5cm_eccentric_bwr-peeq.png
compare_5cm_eccentric_bwr-top_left-peeq.png
compare_5cm_eccentric_bwr-top_left-s22.png
compare_5cm_eccentric_bwr-top_right-peeq.png
compare_5cm_eccentric_bwr-top_right-s22.png

Appendix 1

bwr_eccentric_lock 10cm peeq screw.png
bwr_eccentric_lock 10cm mises screw.png
bwr_eccentric_lock 10cm peeq channels_bot.png
bwr_eccentric_lock 10cm maxPrin channels_bot.png
bwr_eccentric_lock 10cm S33 channels.png
bwr_eccentric_lock 10cm peeq channels.png
bwr_eccentric_lock 10cm peeq insert_bot.png
bwr_eccentric_lock 10cm maxPrin insert_bot.png
bwr_eccentric_lock 10cm peeq insert_top.png
bwr_eccentric_lock 10cm maxPrin insert_top.png
bwr_eccentric_lock 10cm peeq insert.png
bwr_eccentric_lock 10cm S33 insert.png
bwr_eccentric_lock 10cm mises insert.png
bwr_eccentric_lock 10cm peeq.png
bwr_eccentric_lock 5cm peeq screw.png
bwr_eccentric_lock 5cm mises screw.png
bwr_eccentric_lock 5cm peeq channels_bot.png
bwr_eccentric_lock 5cm maxPrin channels_bot.png
bwr_eccentric_lock 5cm S33 channels.png
bwr_eccentric_lock 5cm peeq channels.png
bwr_eccentric_lock 5cm peeq insert_bot.png
bwr_eccentric_lock 5cm maxPrin insert_bot.png
bwr_eccentric_lock 5cm peeq insert_top.png
bwr_eccentric_lock 5cm maxPrin insert_top.png
bwr_eccentric_lock 5cm peeq insert.png
bwr_eccentric_lock 5cm S33 insert.png
bwr_eccentric_lock 5cm mises insert.png
bwr_eccentric_lock 5cm peeq.png

Appendix 2

```
bwr_excentric_half  5cm peeq channels_bot.png
bwr_excentric_half  5cm maxPrin channels_bot.png
bwr_excentric_half  5cm S33 channels.png
bwr_excentric_half  5cm peeq channels.png
bwr_excentric_half  5cm peeq insert_bot.png
bwr_excentric_half  5cm maxPrin insert_bot.png
bwr_excentric_half  5cm peeq insert_top.png
bwr_excentric_half  5cm maxPrin insert_top.png
bwr_excentric_half  5cm peeq insert.png
bwr_excentric_half  5cm S33 insert.png
bwr_excentric_half  5cm mises insert.png
bwr_excentric_half  5cm peeq.png
bwr_excentric_half  5cm peeq screw.png
bwr_excentric_half  5cm mises screw.png
bwr_excentric_half  10cm peeq screw.png
bwr_excentric_half  10cm mises screw.png
bwr_excentric_half  10cm peeq channels_bot.png
bwr_excentric_half  10cm maxPrin channels_bot.png
bwr_excentric_half  10cm S33 channels.png
bwr_excentric_half  10cm peeq channels.png
bwr_excentric_half  10cm peeq insert_bot.png
bwr_excentric_half  10cm maxPrin insert_bot.png
bwr_excentric_half  10cm peeq insert_top.png
bwr_excentric_half  10cm maxPrin insert_top.png
bwr_excentric_half  10cm peeq insert.png
bwr_excentric_half  10cm S33 insert.png
bwr_excentric_half  10cm mises insert.png
bwr_excentric_half  10cm peeq copper.png
bwr_excentric_half  10cm peeq.png
```

Appendix 3

```
bwr_centric_rotated  5cm peeq channels_bot.png
bwr_centric_rotated  5cm maxPrin channels_bot.png
bwr_centric_rotated  5cm S33 channels.png
bwr_centric_rotated  5cm peeq channels.png
bwr_centric_rotated  5cm peeq insert_bot.png
bwr_centric_rotated  5cm maxPrin insert_bot.png
bwr_centric_rotated  5cm peeq insert_top.png
bwr_centric_rotated  5cm maxPrin insert_top.png
bwr_centric_rotated  5cm peeq insert.png
bwr_centric_rotated  5cm S33 insert.png
bwr_centric_rotated  5cm mises insert.png
bwr_centric_rotated  5cm peeq.png
bwr_centric_rotated  5cm peeq screw.png
bwr_centric_rotated  5cm mises screw.png
bwr_centric_rotated  10cm peeq screw.png
bwr_centric_rotated  10cm mises screw.png
bwr_centric_rotated  10cm peeq channels_bot.png
bwr_centric_rotated  10cm maxPrin channels_bot.png
bwr_centric_rotated  10cm S33 channels.png
bwr_centric_rotated  10cm peeq channels.png
bwr_centric_rotated  10cm peeq insert_bot.png
bwr_centric_rotated  10cm maxPrin insert_bot.png
bwr_centric_rotated  10cm peeq insert_top.png
bwr_centric_rotated  10cm maxPrin insert_top.png
bwr_centric_rotated  10cm peeq insert.png
bwr_centric_rotated  10cm S33 insert.png
bwr_centric_rotated  10cm mises insert.png
bwr_centric_rotated  10cm peeq copper.png
bwr_centric_rotated  10cm peeq.png
```

Appendix 4

```
bwr_excentric_rotated  5cm peeq channels_bot.png
bwr_excentric_rotated  5cm maxPrin channels_bot.png
bwr_excentric_rotated  5cm S33 channels.png
bwr_excentric_rotated  5cm peeq channels.png
bwr_excentric_rotated  5cm peeq insert_bot.png
bwr_excentric_rotated  5cm maxPrin insert_bot.png
bwr_excentric_rotated  5cm peeq insert_top.png
bwr_excentric_rotated  5cm maxPrin insert_top.png
bwr_excentric_rotated  5cm peeq insert.png
bwr_excentric_rotated  5cm S33 insert.png
bwr_excentric_rotated  5cm mises insert.png
bwr_excentric_rotated  5cm peeq.png
bwr_excentric_rotated  5cm peeq screw.png
bwr_excentric_rotated  5cm mises screw.png
bwr_excentric_rotated  10cm peeq screw.png
bwr_excentric_rotated  10cm mises screw.png
bwr_excentric_rotated  10cm peeq channels_bot.png
bwr_excentric_rotated  10cm maxPrin channels_bot.png
bwr_excentric_rotated  10cm S33 channels.png
bwr_excentric_rotated  10cm peeq channels.png
bwr_excentric_rotated  10cm peeq insert_bot.png
bwr_excentric_rotated  10cm maxPrin insert_bot.png
bwr_excentric_rotated  10cm peeq insert_top.png
bwr_excentric_rotated  10cm maxPrin insert_top.png
bwr_excentric_rotated  10cm peeq insert.png
bwr_excentric_rotated  10cm S33 insert.png
bwr_excentric_rotated  10cm mises insert.png
bwr_excentric_rotated  10cm peeq copper.png
bwr_excentric_rotated  10cm peeq.png
```

Appendix 5

```
compare_all-mises_channels2.png
compare_all-mises_insert2.png
compare_all-peeq_channels.png
compare_all-peeq_copper.png
compare_all-peeq_copper2.png
compare_all-peeq_copper3.png
compare_all-peeq_copper4.png
compare_all-peeq_insert.png
compare_all-peeq_insert2.png
compare_all-s33_channels2.png
compare_all-s33_insert2.png
```

Appendix 6

```
bwr_eccentric_lock  5cm peeq channels_bot.png
bwr_eccentric_lock  5cm maxPrin channels_bot.png
bwr_eccentric_lock  5cm S33 channels.png
bwr_eccentric_lock  5cm peeq channels.png
bwr_eccentric_lock  5cm peeq insert_bot.png
bwr_eccentric_lock  5cm maxPrin insert_bot.png
bwr_eccentric_lock  5cm peeq insert_top.png
bwr_eccentric_lock  5cm maxPrin insert_top.png
bwr_eccentric_lock  5cm peeq insert.png
bwr_eccentric_lock  5cm S33 insert.png
bwr_eccentric_lock  5cm mises insert.png
bwr_eccentric_lock  5cm peeq.png
bwr_eccentric_lock  5cm peeq screw.png
bwr_eccentric_lock  5cm mises screw.png
bwr_eccentric_lock  6cm peeq screw.png
bwr_eccentric_lock  6cm mises screw.png
bwr_eccentric_lock  6cm peeq channels_bot.png
bwr_eccentric_lock  6cm maxPrin channels_bot.png
bwr_eccentric_lock  6cm S33 channels.png
bwr_eccentric_lock  6cm peeq channels.png
bwr_eccentric_lock  6cm peeq insert_bot.png
bwr_eccentric_lock  6cm maxPrin insert_bot.png
bwr_eccentric_lock  6cm peeq insert_top.png
bwr_eccentric_lock  6cm maxPrin insert_top.png
bwr_eccentric_lock  6cm peeq insert.png
bwr_eccentric_lock  6cm S33 insert.png
bwr_eccentric_lock  6cm mises insert.png
bwr_eccentric_lock  6cm peeq copper.png
bwr_eccentric_lock  6cm peeq.png
```

Appendix 7

compare_bwr_eccentric_rotated-copper_peeq1.png
compare_bwr_eccentric_rotated-copper_peeq2.png
compare_bwr_eccentric_rotated-copper_peeq3.png
compare_bwr_eccentric_rotated-copper_peeq4.png
compare_bwr_eccentric_rotated-copper_peeq5.png
compare_bwr_eccentric_rotated-mises.png
compare_bwr_eccentric_rotated-peeq.png
compare_bwr_eccentric_rotated-peeq2.png
compare_bwr_eccentric_rotated-peeq3.png
compare_bwr_eccentric_rotated-peeq4.png
compare_bwr_eccentric_rotated-s33-2.png
compare_bwr_new-model6g-peeq.png
compare_bwr_new-model6g_channels-mises.png
compare_bwr_new-model6g_channels-s33.png
compare_bwr_new-model6g_copper-peeq.png
compare_bwr_new-model6g_copper-peeq_max.png
compare_bwr_new-model6g_detail_bot2_corner-mises.png
compare_bwr_new-model6g_detail_bot_corner-mises.png
compare_bwr_new-model6g_detail_screw-mises.png
compare_bwr_new-model6g_detail_top2_corner-mises.png
compare_bwr_new-model6g_detail_top_corner-mises.png
compare_bwr_new-model6g_insert-mises.png
compare_bwr_new-model6g_insert-mises2.png
compare_bwr_new-model6g_insert-peeq.png
compare_bwr_new-model6g_insert-peeq2.png
compare_bwr_new-model6g_insert-s33.png
compare_bwr_new-model6g_insert_outer-s33.png
compare_bwr_excentric_half-channels_mises.png
compare_bwr_excentric_half-channels_peeq.png
compare_bwr_excentric_half-channels_peeq2.png
compare_bwr_excentric_half-channels_s33-1.png
compare_bwr_excentric_half-channels_s33.png
compare_bwr_excentric_half-channels_undeformed-mesh.png
compare_bwr_excentric_half-channels_undeformed.png
compare_bwr_excentric_half-copper-peeq.png
compare_bwr_excentric_half-copper-peeq2.png
compare_bwr_excentric_half-copper-peeq3.png
compare_bwr_excentric_half-copper-peeq4.png
compare_bwr_excentric_half-copper-peeq5.png
compare_bwr_excentric_half-insert-peeq2.png
compare_bwr_excentric_half-insert_peeq.png
compare_bwr_excentric_half-insert_peeq2.png
compare_bwr_excentric_half-insert_peeq3.png
compare_bwr_excentric_half-insert_s33.png
compare_bwr_excentric_half-peeq.png
compare_bwr_excentric_half-peeq2.png
compare_bwr_excentric_half-steel_lid-peeq.png
compare_bwr_excentric_half-steel_lid-s33.png
compare_bwr_excentric_half-undeformed.png
compare_eccentric_bwr-channels_peeq.png
compare_eccentric_bwr-channels_s33.png
compare_eccentric_bwr-insert_peeq.png
compare_eccentric_bwr-insert_position.png
compare_eccentric_bwr-mises.png
compare_eccentric_bwr-peeq.png
compare_eccentric_bwr-top_left-peeq.png
compare_eccentric_bwr-top_left-s22.png
compare_eccentric_bwr-top_right-peeq.png
compare_eccentric_bwr-top_right-s22.png

2 – Input files used for the simulations

Each analysis is started by abaqus job=input-file (w/o .inp).

Contents in C:\Users\jhd\mappar\skb\Detailed_PWR_BWR\bwr\Input-files

```
bwr_centric_rotated.inp
bwr_eccentric.incl
bwr_eccentric_1.inp
bwr_eccentric_lock.inp
bwr_excentric_half.inp
bwr_excentric_rotated.inp
bwr_new2_quasi.inp
contacts.incl
mater.incl
model6g_material.incl
model6g_normal_quarter_2050ca3.inp
```

4 – Scripts used for post-processing

Used inside ABAQUS/CAE or by abaqus cae startup=script.py after appropriate editing of job-name inside the script-file.

Contents in C:\Users\jhd\mappar\skb\Detailed_PWR_BWR\bwr\Scripts

```
contour2_plots_bwr.py          - script for contour plots
pictures_bwr.py                - script for geometry plots
compare_model6g_bwr.py         - script for comparison plots
bwr_detailed.py                - script for plotting details of results
bwr_detailed_geometry.py       - script for plotting details of the geometry
bwr_eccentric_lock.py          - scrip for contour plots of eccentric model
bwr_plates.py                  - script for plotting of support plates
colors.py                      - script with colours definition for contour plots
compare_all.py                 - script for comparison of all models
compare_bwr_eccentric_half.py  - script for comparison of symmetric models
compare_bwr_rotated_eccentric.py - script for comparing eccentric/centric models
contour3_plots_bwr.py          - script for contour plots
shear_eccentric_bwr.py         - script for comparison
```

5 – Geometry definitions

Contents in C:\Users\jhd\mappar\skb\Detailed_PWR_BWR\bwr\Geometry

```
bwr.cae bwr.jnl       - ABAQUS/CAE-database and journal files (BWR-insert)
bwr_corrected_test.cae bwr_corrected_test.jnl – CAE and journal files (detailed models
```

CAD-geometries received from SKB:

```
IDE-00015.pdf
IDE-00015.stp
IDE-00015-001.pdf
IDE-00015-21.pdf
IDE-00015-211.pdf
IDE-00015-001.stp
IDE-00015-21.stp
IDE-00015-211.stp
IDE-00025-131.stp
IDE-00025-13.stp
IDE-00015-121.stp
```